Microbes and Environments

DIGEST

JAPANESE SOCIETY OF MICROBIAL ECOLOGY
JAPANESE SOCIETY OF SOIL MICROBIOLOGY
TAIWAN SOCIETY OF MICROBIAL ECOLOGY
JAPANESE SOCIETY OF PLANT MICROBE INTERACTIONS
JAPANESE SOCIETY FOR EXTREMOPHILES

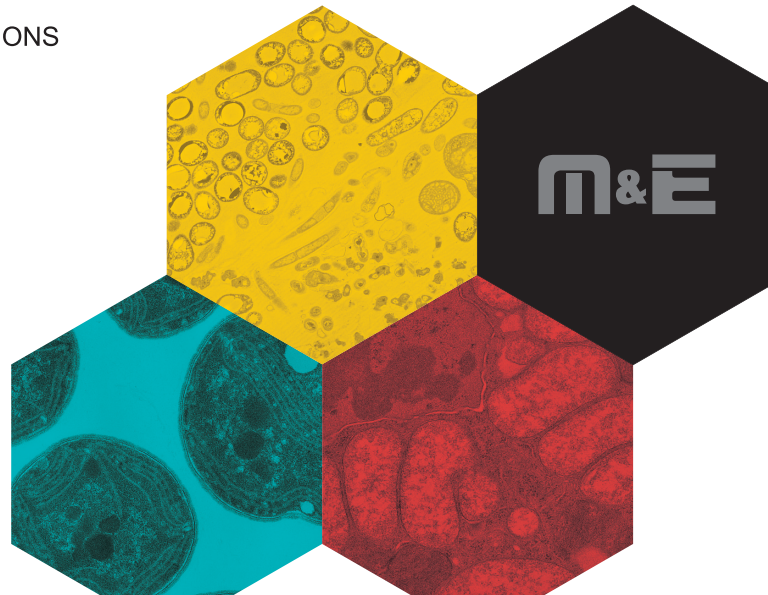

September 2022

Microbes and Environments
digest 2022

CONTENTS

*Times cited at the end of 2021

About Microbes and Environments

Microbes and Environments (M&E) is an international, peer-reviewed, open access journal devoted to the publication of original and review articles regarding all aspects of research on microbial ecology and environmental microbiology. It is published quarterly in a printed and an electronic version by Japanese Society of Microbial Ecology (JSME), Japanese Society of Soil Microbiology (JSSM), Taiwan Society of Microbial Ecology (TSME), Japanese Society of Plant Microbe Interactions (JSPMI) and Japanese Society for Extremophiles (JSE).

Benefits for Authors

- Open access policy for electric publication in PubMed, PubMed Central, and J-Stage
- Included in Web of Science® by Clarivate Analytics
- Page charges: ¥60,000/article for JSME/JSSM/TSME/JSPMI/JSE members
  ¥140,000/article for non-members

Interest of the Journal

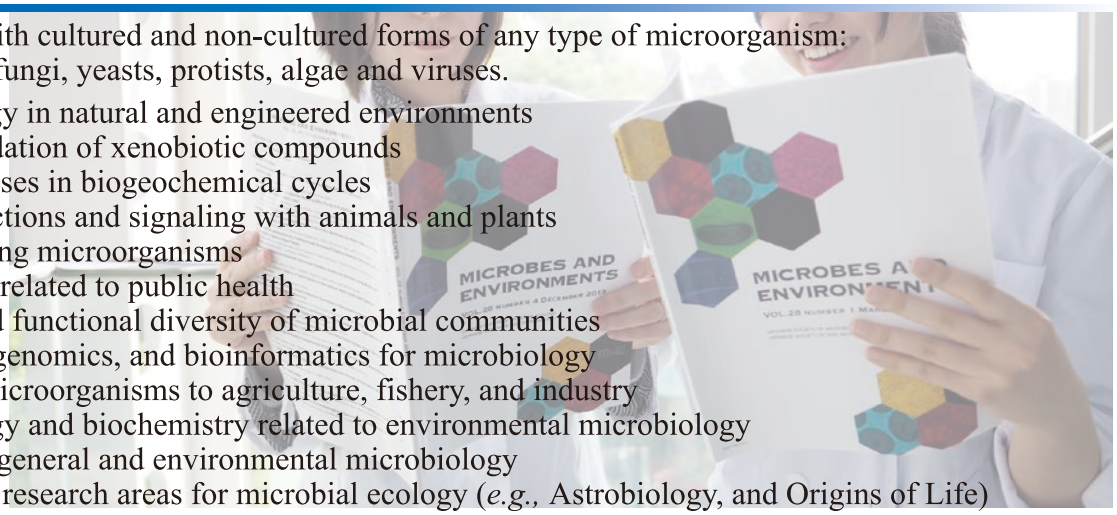

Articles can deal with cultured and non-cultured forms of any type of microorganism: Bacteria, Archaea, fungi, yeasts, protists, algae and viruses.

· Microbial ecology in natural and engineered environments
· Microbial degradation of xenobiotic compounds
· Microbial processes in biogeochemical cycles
· Microbial interactions and signaling with animals and plants
· Interactions among microorganisms
· Microorganisms related to public health
· Phylogenetic and functional diversity of microbial communities
· Genomics, metagenomics, and bioinformatics for microbiology
· Application of microorganisms to agriculture, fishery, and industry
· Molecular biology and biochemistry related to environmental microbiology
· Methodology in general and environmental microbiology
· Interdisciplinary research areas for microbial ecology (*e.g.,* Astrobiology, and Origins of Life)
· Taxonomic description of novel microorganisms with ecological perspective
· Physiology and metabolisms of microorganisms
· Evolution of genes and microorganisms
· Genome report of microorganisms with ecological perspective
· Life in extreme environments

Message from Editor-in-Chief

Microbes and Environments is now becoming one of the important journals for microbial ecology. The journal is being edited by five academic societies but the submission is open to all of the researchers including non-members. In fact, we are receiving manuscripts from non-members all over the world. Microbes and Environments is an open access and freely available online journal. Once the manuscript is accepted, it will be published immediately after proof corrections so that readers can see and read the paper in a timely fashion. Different from commercial journals, we are providing the publication opportunity with an affordable price. We look forward to receiving your high quality manuscripts.

Ken Takai
Japan Agency for Marine-Earth Science and Technology (JAMSTEC), Yokosuka, Japan

Submit Your Manuscript

http://www.microbes-and-environments.jp/

Microbes Environ. 35(3), 2020
https://www.jstage.jst.go.jp/browse/jsme2 doi:10.1264/jsme2.ME20049

MOST VALUABLE PAPER OF THE YEAR 2020

Mechanisms of Rice Endophytic Bradyrhizobial Cell Differentiation and Its Role in Nitrogen Fixation

Teerana Greetatorn[1], Shun Hashimoto[3], Taro Maeda[4], Mitsutaka Fukudome[3], Pongdet Piromyou[1], Kamonluck Teamtisong[2], Panlada Tittabutr[1], Nantakorn Boonkerd[1], Masayoshi Kawaguchi[4], Toshiki Uchiumi[3†], and Neung Teaumroong[1*†]

[1]*School of Biotechnology, Institute of Agricultural Technology, Suranaree University of Technology, Nakhon Ratchasima 30000, Thailand;* [2]*The Center for Scientific and Technological Equipment, Suranaree University of Technology, Nakhon Ratchasima 30000, Thailand;* [3]*Graduate School of Science and Engineering, Kagoshima University, 890–0065 Kagoshima, Japan; and* [4]*National Institute for Basic Biology, Nishigonaka 38, Myodaiji, Okazaki 444–8585 Aichi, Japan*

(Received April 16, 2020—Accepted June 23, 2020—Published online July 29, 2020)

Bradyrhizobium sp. strain SUTN9-2 is a symbiotic and endophytic diazotrophic bacterium found in legume and rice plants and has the potential to promote growth. The present results revealed that SUTN9-2 underwent cell enlargement, increased its DNA content, and efficiently performed nitrogen fixation in response to rice extract. Some factors in rice extract induced the expression of cell cycle and nitrogen fixation genes. According to differentially expressed genes (DEGs) from the transcriptomic analysis, SUTN9-2 was affected by rice extract and the deletion of the *bclA* gene. The up-regulated DEGs encoding a class of oxidoreductases, which act with oxygen atoms and may have a role in controlling oxygen at an appropriate level for nitrogenase activity, followed by GroESL chaperonins are required for the function of nitrogenase. These results indicate that following its exposure to rice extract, nitrogen fixation by SUTN9-2 is induced by the collective effects of GroESL and oxidoreductases. The expression of the sensitivity to antimicrobial peptides transporter (*sapDF*) was also up-regulated, resulting in cell differentiation, even when *bclA* (*sapDF*) was mutated. This result implies similarities in the production of defensin-like antimicrobial peptides (DEFs) by rice and nodule-specific cysteine-rich (NCR) peptides in legume plants, which affect bacterial cell differentiation.

Key words: rice, endophyte, *Bradyrhizobium*, cell differentiation, nitrogen fixation

Bradyrhizobium spp. from symbiotic and endophytic relationships with legumes and non-legumes, such as rice, namely, *Oryza breviligulata* (Chaintreuil *et al.*, 2000) and *Oryza sativa* L. ssp. *indica* (Teamtisong *et al.*, 2014) and *japonica* (Piromyou *et al.*, 2015a, 2015b). *Bradyrhizobium* sp. strain SUTN9-2 is capable of forming symbiotic and endophytic relationships with legume and rice plants (Piromyou *et al.*, 2017; Greetatorn *et al.*, 2019). Biological nitrogen fixation (BNF) by endophytic bradyrhizobia in rice may be caused by the activity of nitrogenase enzyme, encoded by the gene *nifH* (the nitrogenase structural component) (Teamtisong *et al.*, 2014; Okubo *et al.*, 2016). Another gene, *nifV*, is involved in the biosynthesis of homocitrate synthase, which activates the nitrogenase Fe protein in free-living diazotrophs (Howard and Rees, 1994) and *Bradyrhizobium* sp. (Pagan *et al.*, 1975; Okubo *et al.*, 2016). The *nifV* gene was also found in *Bradyrhizobium* sp. SUTN9-2 (Noisangiam *et al.*, 2012; Hashimoto *et al.*, 2019). This gene is mostly absent in *Rhizobium* sp. that efficiently perform nitrogen fixation only in symbiosis with legumes (Hakoyama *et al.*, 2009). This finding indicates its potential as a candidate for use as a biofertilizer or bioinoculant. However, there is currently no information on the rice endophytic molecular mechanisms that play important roles in plant colonization and growth promotion.

Elongated SUTN9-2 cells were recently observed in rice tissues at 7 days post-inoculation (dpi) by scanning electron microscopy (SEM). The elongation of these cells occurred between 3 (≅1–2 micrometer [μm]) and 7 (≅3 μm) dpi (Piromyou *et al.*, 2017). Based on this finding, we hypothesize that interactions between rice plants and bacterial factors may contribute to cell size enlargements and increases in nitrogen fixation efficiency by SUTN9-2 in rice plants, similar to bacteroid differentiation in legume plants. The responses of endophytic *Burkholderia kururiensis* M130 to rice macerate have been investigated using a transcriptomic analysis. The findings obtained revealed 27.7% of differentially expressed genes (DEGs) of its open reading frames in the presence of rice macerate. These genes were involved in membrane transporter and secretion systems, motility, chemotaxis, and adhesion, indicating the importance of the exchange of molecules for bacterial endophytic growth and adaptation to rice plants (Coutinho *et al.*, 2015).

The terminal bacteroid differentiation (TBD) of *Rhizobium* and *Bradyrhizobium* spp. has been extensively examined, particularly in an Inverted Repeat-Lacking Clade (IRLC) producing elongated polyploid bacterial cells that switch their cell cycle towards endoreduplication (Mergaert *et al.*, 2006; Kondorosi *et al.*, 2013; Alunni and Gourion,

* Corresponding author. E-mail: neung@sut.ac.th;
Tel: +66–4422–4153; Fax: +66–4422–4150.
† These authors contributed equally to this work.

Citation: Greetatorn, T., Hashimoto, S., Maeda, T., Fukudome, M., Piromyou, P., Teamtisong, K., et al. (2020) Mechanisms of Rice Endophytic Bradyrhizobial Cell Differentiation and Its Role in Nitrogen Fixation. *Microbes Environ* **35**: ME20049.
https://doi.org/10.1264/jsme2.ME20049

2016). TBD is assessed by host plant factors, including defensin-like antimicrobial peptides (DEFs) consisting of nodule-specific cysteine-rich (NCR) peptides, which are produced in large families of IRLC and Delbergioid legume clades, together with the BacA transporter protein in microbes (Mergaert *et al.*, 2006; Alunni and Gourion, 2016). NCR peptides and the BacA transporter protein have been shown to mediate the polyploidy of *Sinorhizobium meliloti* in *Medicago* nodules by altering the processes involved in sequential changes in the expression of cell cycle genes and cell size enlargements (De Nisco *et al.*, 2014; Penterman *et al.*, 2014). The BacA-like transporter of *Bradyrhizobium* sp. strain ORS285 also provides protection against the antimicrobial activity of NCR peptides in *Aeschynomene* spp. nodules. The BacA-like transporter has been identified in ORS285, carrying three genes (BRAO285v1_1320006, BRAO285v1_250005, and BRAO285v1_950010). These genes are characterized by the presence of the transmembrane domain pfam06472 (ABC_membrane_2) or pfam05992 (SbmA_BacA). However, only BRAO285v1_1320006 plays a key role in the symbiotic phenotype in host plants, providing protection against the antimicrobial activity of NCR peptides in *Aeschynomene* spp. nodules. The mutant produced small nodules, undifferentiated bacteroids, reduced nitrogen fixation activity in *Aeschynomene indica* and *Aeschynomene afraspera*, and some dead cells were observed in *A. indica* nodules. The other two genes formed normal symbiosis nodules, differentiated bacteroids, and nitrogen fixation, indicating that these genes are not important for ORS285 in *Aeschynomene* spp. symbiosis (Guefrachi *et al.*, 2015). These findings suggested that BacA-like proteins in ORS285 were encoded by BRAO285v1_1320006. However, *Bradyrhizobium* BacA-like (BclA), named according to BacA or the *Escherichia coli* homolog SbmA, differs from *Bradyrhizobium* proteins due to the presence of a C-terminal cytosolic ATPase domain typical for canonical ABC transporters (Guefrachi *et al.*, 2015). Furthermore, a correlation was observed between cell differentiation and nitrogen fixation activity in alfalfa (*Medicago sativa*) nodules (Vasse *et al.*, 1990). The small bacteroid size (1–2.5 µm) with a low nucleic acid content also exhibited weak acetylene reduction activity. On the other hand, the enlarged bacteroid size (5–7 µm) had a high nucleic acid content and very strong acetylene reduction activity (Paau and Cowles, 1978). This finding indicated a correlation between cell size and nitrogen fixation activity. Thus, the effects of DEFs from rice plants and the BclA of SUTN9-2 on cell size enlargement and nitrogen fixation efficiency, occurring during the interaction between SUTN9-2 and rice extract, were analyzed. The results obtained provide a better understanding of the mechanisms and factors involved in cell differentiation and nitrogen fixation in this model.

Materials and Methods

Plants and the bacterial strain

The rice plants *O. sativa* L. ssp. *indica* cv. Pathum Thani 1 and *O. sativa* L. ssp. *japonica* cv. Nipponbare were used in the present study. *Bradyrhizobium* sp. strain SUTN9-2 WT (LAXE00000000) was isolated from the root and stem nodules of *A. americana*, grown in rice field areas in Thailand (Noisangiam *et al.*, 2012). SUTN9-2 DsRed-tagged (Piromyou *et al.*, 2015b), Δ*nifV*, and Δ*bclA* were also used in the present study. SUTN9-2 WT and mutants were cultured at 30±2°C in yeast extract-mannitol (YEM) broth medium (Somasegaran and Hoben, 2012) for further analyses. The medium was supplemented with 200 µg mL^{-1} of streptomycin and spectinomycin for SUTN9-2 DsRed-tagged, 20 µg mL^{-1} of cefotaxime for Δ*nifV*, and 200 µg mL^{-1} of streptomycin for Δ*bclA*.

Rice growth and rice extract preparation

Rice seeds (*O. sativa* L. ssp. *indica* cv. Pathum Thani 1 and *O. sativa* L. ssp. *japonica* cv. Nipponbare) were dehulled and surface sterilized with 70% ethanol for 3 min, twice with 10% hydrogen peroxide for 10 min, with 3% sodium hypochlorite for 1 h, and then washed 3 times with sterilized water (Greetatorn *et al.*, 2019). To obtain a small emerging root, surface-disinfected rice seeds were germinated on 0.85% agar with YEM medium at 37°C for 1 day in the dark. Three germinated seeds (no contamination on YEM) were transplanted into glass test tubes (22×200 mm) containing a sterilized aluminum net and N-free rice nutrient solution ([mmol L^{-1}]: $NaH_2PO_4 \cdot 2H_2O$, 0.6; K_2SO_4, 0.3; $CaCl_2 \cdot 2H_2O$, 0.3; $MgCl_2 \cdot 6H_2O$, 0.6; EDTA-Fe, 0.045; H_3BO_3, 0.05; $MnSO_4 \cdot 5H_2O$, 0.009; $CuSO_4 \cdot 5H_2O$, 0.0003; $ZnSO_4 \cdot 7H_2O$, 0.0007; and $Na_2MoO_4 \cdot 2H_2O$, 0.0001) and pH adjusted to 6.8 (Mae and Ohira, 1981). Rice plants were grown for 14 days under controlled environmental conditions at 28±2°C and 70% relative humidity on a 16:8-h day:night cycle (full light, 639 microeinsteins [µE] m^{-2} S^{-1}).

Whole rice samples (root+shoot; 0.5 g $plant^{-1}$) were harvested at 14 dpi, sterilized and macerated separately with a sterilized mortar and pestle in sterilized buffered nodulation medium B (BNM-B) minimal medium, and kept at 4°C for no more than 3 days for further analyses. BNM-B is a synthetic plant growth medium (Ehrhardt *et al.*, 1992) supplemented with succinate, glutamate, and a cocktail of vitamins (Renier *et al.*, 2011). The rice extract was used by supplementing BNM-B medium (20–25 g of rice extract 400 mL^{-1} in BNM-B). The homogenate was passed through three layers comprising a miracloth (22–25 µm), membrane filter (8 µm), and syringe filter (0.2 µm) to discard plant debris and the rice extract obtained was further incubated with 10^8 SUTN9-2 cells in a 10-mL test tube with a tight cap and stable stage.

Construction of SUTN9-2 bclA *and* nifV *mutants*

The *bclA* deletion mutant (SUTN9-2Δ*bclA*) was constructed and standard molecular techniques were used in the present study. The 700-bp upstream and downstream fragments of the *bclA* gene were amplified by PCR and the primers used are listed in Table S1. The two regions were merged by overlap extension PCR and then digested by *EcoR*I/*Xba*I and cloned into the plasmid pNPTS129. This plasmid cannot replicate in *Bradyrhizobium* strains and carries *sacB* and the kanamycin resistance gene, which confer sensitivity to sucrose, thereby inducing bacterial death (Tsai and Alley, 2000). The spectinomycin and streptomycin cartridge from pHP45Ω was digested by *BamH*I and introduced into the upstream and downstream regions previously cloned in the pNPTS129 plasmid. The plasmid was then transferred into SUTN9-2 by triparental conjugation with the helper plasmid pRK2013 (Tamura *et al.*, 2011). Single recombinant clones were obtained by antibiotic selection, followed by double recombinant clones by growth on sucrose with spectinomycin and streptomycin, but not kanamycin. Candidate clones were checked for the loss of kanamycin resistance from the pNPTS129 plasmid, and the deletion of the *bclA* gene was verified by PCR. The mutation of the *nifV* gene was constructed as described by Hashimoto *et al.* (2019).

Confocal laser scanning microscopy

SUTN9-2 DsRed-tagged was treated with BNM-B and BNM-B supplemented with rice extract (*O. sativa* L. ssp. *Indica* cv. Pathum Thani) for 7, 14, 21, and 28 days. SUTN9-2 WT, Δ*nifV*, and Δ*bclA*

were treated with rice extract BNM-B and BNM-B supplemented with rice extract from *indica* and *japonica* for 7, 14, 21, and 28 days, and were then collected and stained with 30 μg mL^{-1} DAPI and 15 μg mL^{-1} FM4-64. Cell size, DNA content, and the cell membrane were observed in all treated cells under a confocal laser scanning microscope (Nikon Model Ni-E; *Nikon* Instech). The mean DNA content area was calculated from each cell (μm^2) using an ImageJ analysis (Collins, 2007), and the average enlarged cell size in each treatment was calculated from 20 cells in each replication for 3 replications.

Flow cytometry analysis

SUTN9-2 WT and DsRed-tagged cells were treated with BNM-B and BNM-B supplemented with rice extract (*O. sativa* L. ssp. *Indica* cv. Pathum Thani 1) for 7, 14, and 28 days. SUTN9-2 WT-treated cells were fixed at 4°C overnight in 70% ethanol, the fixed sample was digested with RNase (DNase free), and then stained with 50 μg mL^{-1} propidium iodide (PI) to analyze the DNA content (Deitch *et al.*, 1982). The size of SUTN9-2 DsRed-tagged cells treated as described above was assessed. The analysis of cell size and DNA content was conducted using a flow cytometer (BD FACSCalibur, BD Bioscience) with Cyflowgic software.

Acetylene reduction assay (ARA)

The effects of rice extract on the nitrogen fixation efficiency of SUTN9-2 WT (DsRed-tagged), Δ*nifV*, and Δ*bclA* cells treated with rice extract were investigated using ARA (Chaintreuil *et al.*, 2000). The reactions were performed in a 10-mL test tube containing 2 mL each of BNM-B medium and BNM-B medium supplemented with rice extract (*O. sativa* L. ssp. *indica* cv. Pathum Thani 1 and *japonica* cv. Nipponbare) as described previously. The reaction was incubated at 28±2°C for 7, 14, 21, and 28 days. Acetylene was injected to reach a final concentration of 10% (v/v) of the gas phase in the headspace (Somasegaran and Hoben, 2012). After the incubation, gas from the vessel was injected into a gas chromatograph (6′×1/8″ S.S. Hayesep T column; Valco Instruments). Ethylene gas production was analyzed, as described by Renier *et al.* (2011). Total concentrations in the cell suspension were evaluated using a plate count of colony-forming units (CFU) on YEM medium. The medium was supplemented with 200 μg mL^{-1} of streptomycin and spectinomycin for SUTN9-2 DsRed-tagged cells, 20 μg mL^{-1} of cefotaxime for Δ*nifV*, and 200 μg mL^{-1} of streptomycin for Δ*bclA*.

Rice cultivation and growth promotion

The rice seeds of *O. sativa* L. ssp. *indica* cv. Pathum Thani 1 were surface sterilized and germinated as described above. Germinated seeds were soaked overnight in YEM broth containing SUTN9-2 WT, Δ*nifV*, and Δ*bclA* (10^8 CFU mL^{-1}), and three germinated seeds were then transplanted into glass test tubes (22×200 mm) containing a sterilized aluminum net with N-free rice nutrient solution and N-free supplemented with 1 mmol L^{-1} ammonium nitrate under controlled environmental conditions, as previously described. Rice plants were grown and harvested at 7, 14, 21, and 28 dpi, whole rice samples were then dried in an oven at 65°C for 72 h, and dry weights were measured.

RNA preparation for qRT-PCR

RNA was isolated from three independent cultures of SUTN9-2 WT, Δ*bclA*, and Δ*nifV* incubated in BNM-B medium or BNM-B medium supplemented with rice extract (*indica*). The cultures were incubated in a 10-mL test tube with a tight cap at 28±2°C for 21 days. RNA was isolated from 10^8 cells using Plant RNA extraction kits (Qiagen). RNAs from rice plant samples (shoot+root) were harvested at 21 dpi, sterilized, and macerated (Greetatorn *et al.*, 2019). Total RNA extraction was performed according to the manufacturer's procedure. RNAs were treated with DNaseI (Qiagen) at 28±2°C for 30 min to prevent the contamination of genomic DNA. The purity of RNA was assessed by PCR on total RNA (250 ng) with GoTaq polymerase (Promega) using *dnaK*_SUNT9-2 primers and *EF-1*∝_rice plants (Table S1). The quality and concentration of RNA were assessed by Nanodrop (Thermo Scientific) and agarose gel electrophoresis.

qRT-PCR and analysis

Transcription levels were measured by qRT–PCR using Applied Biosystem, QuantStudio Design (Waltham). Primers for the amplification of genes involved in the cell cycle (*dnaK*, *gcrA*, *ctrA*, *dnaA*, and *GcrM*), nitrogen fixation (*nifH* and *nifV*), and rice hemoglobin (*EF-1*∝, *hb1*, and *hb5*) are listed in Table S1. PCR amplification was performed under the following cycling conditions: an initial denaturation step at 95°C for two min, 35 cycles at 95°C for 2 min and at the annealing temperature of all genes (50°C) for 30 s, followed by a final 5-min extension at 72°C. Relative gene expression was analyzed by the comparative Ct method (-ΔΔCT) normalized to the endogenous housekeeping gene, *dnaK* for bacterial SUTN9-2 and *EF-1*∝ for rice plants. Three biological replicates were pooled and analyzed.

RNA preparation for the RNAseq analysis

RNA was isolated from three independent cultures of SUTN9-2 WT and Δ*bclA* incubated in BNM-B medium and BNM-B medium supplemented with rice extract (*indica*). Cultures were incubated in a 50-mL test tube with a tight cap at 28±2°C for 21 days. RNA was isolated from 3×10^8 cells using Plant RNA extraction kits (Qiagen). Total RNA was extracted according to the manufacturer's procedure. The purity of RNA was assessed as described above.

RNA sequencing and analysis

To identify the bacterial genes that respond to rice extract, we used a comparative RNAseq analysis of SUTN9-2. RNA-Seq libraries were constructed from the RNA sample incubated with or without rice extract (20–25 g of rice extract 400 mL^{-1} in BNM-B) for SUTN9-2 WT and the Δ*bclA* mutant. Three biological replicates were prepared for each treatment. RNA samples were extracted following the same protocol for qRT-PCR. Eukaryotic rRNA from the samples was removed using the Ribo-Zero Magnetic Kit (Illumina) and stranded RNA-Seq libraries were constructed with the TruSeq Stranded mRNA kit (Illumina). Paired-end sequencing (150 bp) of the libraries was performed by the NovaSeq platform (Illumina). The libraries were constructed and sequenced at Novogene.

In the gene expression analysis, we adapted the mapping of the transcriptomic data obtained to the previously reported SUTN9-2 genome. A total of 865M reads (R1+R2) were obtained from the 12 libraries (Table S3). Adapter sequences and low-quality sequences were removed from raw single-end reads using fastp (v0.20.0) (fastp: an ultra-fast all-in-one FASTQ preprocessor [Chen *et al.*, 2018]). The trimmed paired-end reads were mapped to the SUTN9-2 genome (INSDC ID ASM312264v1) and calculated the TPM-normalized mapped read numbers by RSEM (v1.3.1) (RSEM: accurate transcript quantification from RNA-Seq data with or without a reference genome, [Li and Dewey, 2011]) with the --bowtie2 option (bowtie2 version 2.3.5.1) (Fast gapped-read alignment with Bowtie 2, [Langmead and Salzberg, 2012]). The mapped reads were counted based on the gene models of SUTN9-2 (LAXE01000000) predicted by Piromyou *et al.* (2015b). Differentially expressed genes (DEGs) were detected based on the false discovery rate (FDR) (<0.1) and log fold change (logFC) (>0.1 or <–0.1) from the RSEM analysis. In the enrichment analysis, the public gene models from LAXE01000000 were annotated with interproscan (v5.36-75) with --goterms option (for gene ontology annotation) and with KofamKOALA (downloaded on 13th Aug. 2019) (KofamKOALA: KEGG Ortholog assignment based on the profile HMM and adaptive score threshold [Aramaki *et al.*, 2020] for KEGG Orthologs annotation). Enrichment analyses were performed by goseq (v1.38.0) on R (v3.6.1) (gene ontology analysis for RNA-seq: accounting for selection bias, [Young *et al.*, 2010]).

qRT-PCR validation

To validate the results of the transcriptome analysis, significant DEGs were selected to compare their expression in SUTN9-2 WT in BNM-B with rice extract and SUTN9-2 WT in BNM-B alone, including biphenyl-2,3-diol 1,2-dioxygenase (*hpaD*), 3-(3-hydroxyphenyl) propanoate hydroxylase (*mhpA*), chaperonin GroEL (*groEL*), chaperonin GroES (*groES*), ABC transporter ATP-binding protein (*sapDF*), ABC transporter substrate-binding protein (*sapA*), and RND family efflux transporter (*cusF*). Primers for the amplification of these genes are listed in Table S1. RNA preparation, qRT-PCR, and analyses were performed as described above.

SbmA_BacA domain proteins and phylogenetic analysis

The identified protein sequences of the SbmA_BacA domain, including the BacA, *Bradyrhizobium* homologous, ExsX, and *Mycobacterium* BacA clades, were obtained from Guefrachi *et al.* (2015). The BacA-related protein sequences of SUTN9-2 (BclA; PWE81210.1, SapA; PWE77331.1, and SapDF; PWE82048.1) were obtained from the National Center for Biotechnology Information (NCBI) database. Protein sequences were aligned using the ClustalW program. The phylogenetic tree was constructed using the neighbor-joining method with confidence levels for 500 replicates using the MEGAX package (Saitou and Nei, 1987; Kumar *et al.*, 2008).

Statistical analysis

The statistical analysis of data sets was performed with SPSS software (SPSS 16.0 for Windows; SPSS) on data from three independent samples (each with three technical replicates). Experimental data were statistically analyzed according to Steel and Torrie (1980), and means were compared by Duncan's multiple range test ($P \leq 0.05$) (Duncan, 1955).

Results

*Cell size enlargement by SUTN9-2 in rice (*indica*) plants*

To confirm whether SUTN9-2 cell size enlargement occurs within rice plants, the red fluorescent-tagged SUTN9-2 strain (DsRed) was extracted from rice plant tissues (*indica*) at 21 and 28 dpi and visualized using confocal laser scanning microscopy. The cells of SUTN9-2 were longer, with average sizes of 5.6 and 5.8 μm at 21 and 28 dpi, respectively, than free-living SUTN9-2 cells (2.8 μm) (Fig. S1). These results revealed that SUTN9-2 cell size increased within rice plants. However, small numbers of SUTN9-2 cells were extracted from rice plant tissues. Therefore, rice extract was prepared and subsequent experiments were performed by incubating SUTN9-2 cells with the extract to investigate the influence of rice and its derived molecules on the differentiation of SUTN9-2 cells.

*SUTN9-2 increases its cell size and DNA content in response to the rice extract (*indica*) treatment*

Increases in cell size and DNA content in SUTN9-2 cells in response to the rice extract (*indica*) treatment were examined using a flow cytometer. The sizes of treated SUTN9-2 DsRed-tagged cells in BNM-B minimal medium and BNM-B supplemented with rice extract were analyzed. The forward scatter (FS) of a treated cell is related to its size. BNM-B with rice extract-treated cells had a higher FS than BNM-B-treated cells at 7, 14, and 28 days (Fig. 1A). Furthermore, the DNA content of treated SUTN9-2 WT cells was assessed by the fluorescent staining of nuclei using PI. The DNA content of BNM-B with rice extract-treated SUTN9-2 cells was higher than that in BNM-B-treated cells. The DNA content of BNM-B-treated cells was 1 to 2 genome complement (1C to 2C), similar to the ploidy level of free-growing cells (1C to 2C) (Czernic *et al.*, 2015), whereas BNM-B with rice extract-treated cells reached 2C to 7C ploidy levels, similar to the ploidy level of bacteroid cells (7C to 16C) (Czernic *et al.*, 2015; Guefrachi *et al.*, 2015) (Fig. 1A). These results confirmed that differentiated SUTN9-2 cells affected rice plants.

*SUTN9-2 cells increase their size and nitrogen fixation activity in response to rice extract (*indica*)*

To investigate whether an enlarged cell size increases nitrogen fixation activity in response to rice extract, SUTN9-2 DsRed-tagged cells treated with deionized water (DI), BNM-B, and BNM-B with rice extract (*indica*) were analyzed. Cell size was larger in the BNM-B with rice extract group than in the BNM-B alone and DI groups. The average sizes of BNM-B with rice extract-treated cells at 7, 14, 21, and 28 days were 2.76, 3.18, 3.38, and 3.79 μm, respectively (Fig. 1B), and average nitrogenase activities were 0.01, 0.02, 0.09, and 0.30 nmol C_2H_4 $\log_{10}^{-1}$ CFU, respectively (Fig. 1C). The average sizes of BNM-B alone-treated cells at 7, 14, 21, and 28 days were with 2.52, 2.74, 2.42, and 2.64 μm, respectively (Fig. 1B). Average nitrogenase activities in this group were 0.01 nmol C_2H_4 $\log_{10}^{-1}$ CFU at 7, 14, and 21 days and 0.02 nmol C_2H_4 $\log_{10}^{-1}$ CFU at 28 days (Fig. 1C). The average sizes of DI-treated cells at 7, 14, 21, and 28 days were 1.86, 2.04, 1.36, and 1.37 μm, respectively (Fig. 1B), and these cells only exhibited nitrogenase activity of 0.01 nmol C_2H_4 $\log_{10}^{-1}$ CFU at 14 days (Fig. 1C). These results demonstrated the influence of rice extract on the cell size and nitrogen fixation efficiency of SUTN9-2 cells. Time-dependent increases were observed in elongated cells in the BNM-B with rice extract group, but not in the BNM-B alone or DI group (Fig. 1B and C).

*SUTN9-2 WT and mutants show increases in cell size, DNA content, and nitrogen fixation activity in the presence of rice extract (*indica *and* japonica*)*

To clarify the effects of rice species variations and *bclA* and *nifV* genes on cell differentiation and nitrogen fixation, SUTN9-2 WT, Δ*bclA*, and Δ*nifV* were treated with rice extract from 2 different species of rice (*indica* and *japonica*). Cell size, DNA content, and nitrogenase activity were increased in the BNM-B with rice extract (*indica*) group at 28 days with average cell sizes of 3.28, 3.22, and 3.03 μm (Fig. 1D, E, and F), mean DNA content areas of 0.43, 0.33, and 0.32 μm^2 (Fig. S2 and S3), and nitrogenase activities of 0.28, 0.07, and 0.00 nmol C_2H_4 $\log_{10}^{-1}$ CFU in SUTN9-2 WT, Δ*bclA*, and Δ*nifV*, respectively (Fig. 1D, E, and F). The BNM-B with rice extract (*japonica*) group showed average cell sizes of 2.66, 2.56, and 2.60 μm (Fig. 1D, E, and F), mean DNA content areas of 0.32, 0.33, and 0.28 μm^2 (Fig. S2 and S3), and nitrogenase activities of 0.06, 0.03, and 0.00 nmol C_2H_4 $\log_{10}^{-1}$ CFU for SUTN9-2 WT, Δ*bclA*, and Δ*nifV*, respectively (Fig. 1D, E, and F). Average cell sizes at 28 days in BNM-B-treated cells were

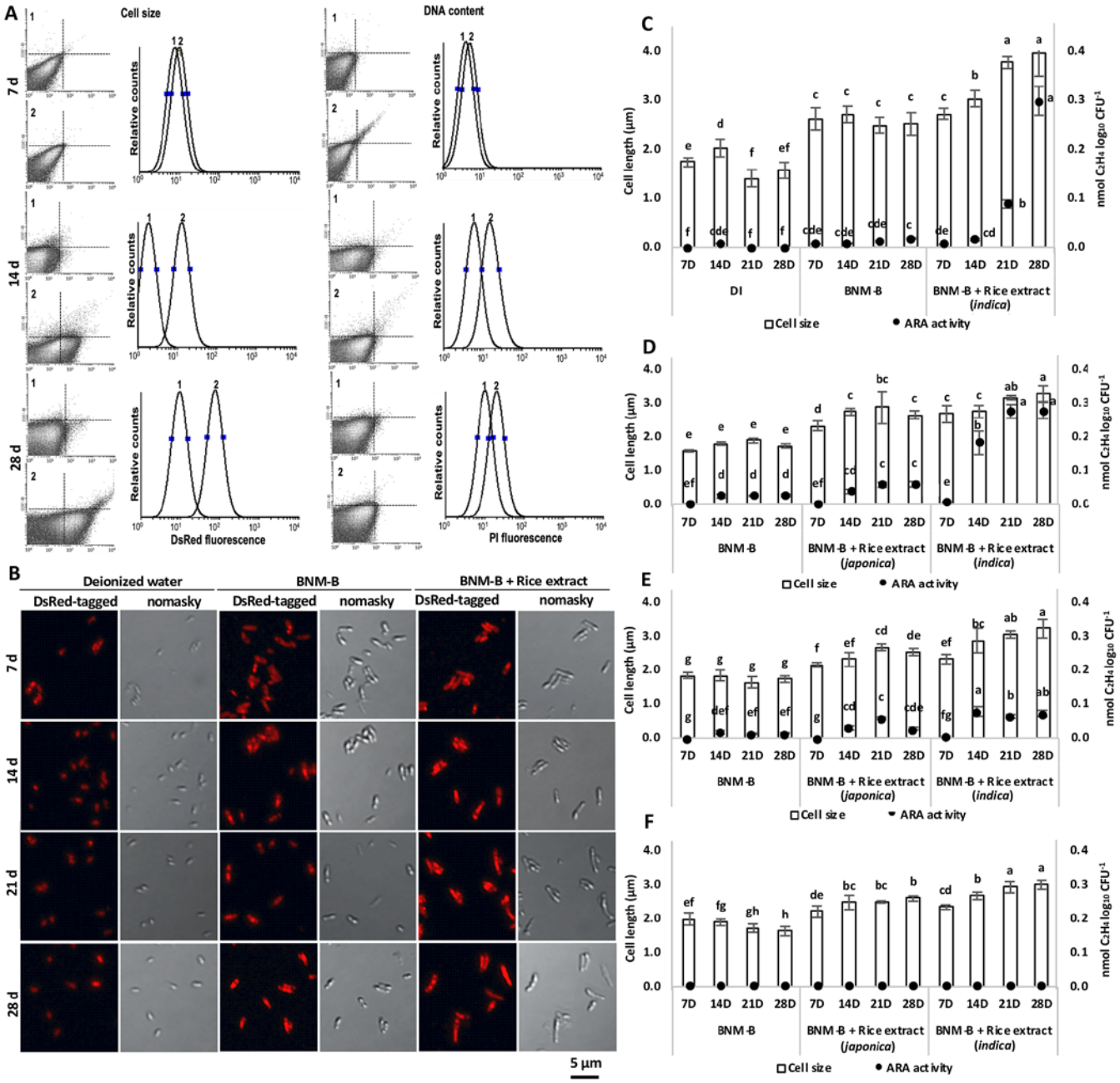

Fig. 1. Cell size, DNA content, and nitrogenase activity of SUTN9-2 in response to rice extract (*indica*). Cell size, enlarged DsRed-tagged cells, and propidium iodide (PI)-stained DNA content were analyzed by flow cytometry (1 represents free growing, and 2 represents cells treated with rice extract) (A). Cell size and enlarged DsRed-tagged cells by confocal laser scanning microscope (B). Observation of cell size by a confocal laser scanning microscope and nitrogenase activity by the acetylene reduction assay of SUTN9-2 WT cells treated with DI, BNM-B, and BNM-B +rice extract (*indica*) (C), and SUTN9-2 WT (D), Δ*bclA* (E), and Δ*nifV* (F) with BNM-B, BNM-B+rice extract (*japonica*), and BNM-B+rice extract (*indica*) at 7, 14, 21, and 28 days. Significance at $P \leq 0.05$ is indicated by the mean±standard deviation (n=3).

1.73, 1.73, and 1.63 µm (Fig. 1D, E, and F), mean DNA content areas of 0.11, 0.15, and 0.15 µm^2 (Fig. S2 and S3), and nitrogenase activities of 0.05, 0.01, and 0.00, nmol C_2H_4 log_{10}^{-1} CFU in SUTN9-2 WT, Δ*bclA*, and Δ*nifV*, respectively (Fig. 1D, E, and F). Similar results were obtained at 7, 14, and 21 days (Fig. 1D, E, and F). The effects of rice extract and Δ*bclA* and Δ*nifV* on cell sizes were observed under a transmission electron microscope (TEM). The cells of SUTN9-2 WT, Δ*bclA*, and Δ*nifV* elongated in response to the rice extract (*indica*) treatment (Fig. S4).

These results demonstrated that rice extract (*indica*) exerted stronger effects on cell elongation and nitrogen fixation activity than rice extract (*japonica*) in WT and mutant SUTN9-2 cells. Increases in cell size and nitrogenase activity were smaller in Δ*bclA* than in the WT strain. Furthermore, nitrogenase activity was not detected in Δ*nifV* and their cell size was smaller than those of WT and Δ*bclA* following the treatment with both rice extracts. These results also revealed the effects of *bclA* and *nifV* genes on cell size enlargement and nitrogen fixation activity in response to different rice varieties.

*Effects of WT and mutant SUTN9-2 on rice (*indica*) plant growth*

SUTN9-2 has been reported to promote rice (*indica*) growth at the early seedling stage (Greetatorn *et al.*, 2019). Consistent results were obtained in the present study; SUTN9-2 WT, Δ*bclA*, and Δ*nifV* increased rice dry weight more than the non-inoculated control, particularly at 7 and 14 dpi, in N-free medium and ammonium nitrate-supplemented medium (Fig. S5). The significant difference observed at 7 and 14 dpi between rice plants inoculated with SUTN9-2 WT, Δ*bclA*, and Δ*nifV* and the non-inoculated control was not detected at 21 or 28 dpi (Fig. S5). However, rice dry weight did not show a significant difference between rice plants inoculated with SUTN9-2 WT, Δ*bclA*, and Δ*nifV* at 7, 14, 21, and 28 dpi (Fig. S5). These results clearly demonstrated that SUTN9-2 promoted rice plant growth at the early stage at 7 and 14 dpi under the presence or absence of supplementation with a nitrogen source. However, the effects of *bclA* and *nifV* genes on rice plant growth remain unclear.

*Expression of cell cycle genes in WT and mutant SUTN9-2 in response to rice extract (*indica*)*

SUTN9-2 cell differentiation-related genes, including *gcrA*, *ctrA*, *ccrM*, and *dnaA*, were selected based on their role in the master cell cycle. Similar results were obtained for the expression of all genes between SUTN9-2 WT and Δ*bclA*. However, Δ*bclA* showed the down-regulated expression of the genes listed above. The expression levels of *gcrA* and *ctrA* were lower in the BNM-B with rice extract (*indica*) group than in the BNM-B alone group, with 0.01- and 0.09-fold differences in WT and 0.008- and 0.01-fold differences in Δ*bclA*, respectively (Fig. 2A). However, no significant difference was noted in *gcrA* expression between the BNM-B alone and BNM-B with rice extract groups. In contrast, the expression levels of *ccrM* and *dnaA* were higher in the BNM-B with rice extract group than in the BNM-B alone group, with 0.20- and 0.22-fold differences for WT and 0.10- and 0.10-fold differences for Δ*bclA*, respectively (Fig. 2A). In spite of this result, the expression of all genes in Δ*nifV* was several-fold lower in the BNM-B with rice extract group than in the BNM-B alone group (Fig. 2A). These results suggested that cell size enlargements may also be affected by the *nifV* gene, supporting the observation of cell enlargement under the microscope. They also indicated that the *bclA* gene was disrupted, whereas other *bclA*-associated genes were still active and required for cell enlargement, showing a similar pattern of gene expression to WT. Collectively, these results demonstrated that some factors from rice extract may affect master cell-cycle regulators.

*Nitrogen fixation and BclA transporter gene expression in WT and mutant SUTN9-2 in response to rice extract (*indica*)*

To examine the effects of rice extract on BclA transporter and nitrogen fixation-related gene expression in SUTN9-2, their relative expression levels were measured in SUTN9-2 WT, Δ*bclA*, and Δ*nifV*. The expression levels of the *nifH*, *nifV*, and *bclA* genes were significantly increased in WT (0.12-, 0.12-, and 0.11-fold, respectively) and Δ*bclA* (*nifH*; 0.14-, and *nifV*; 0.14-fold) in the presence of rice extract (Fig. 2B). In contrast, the expression levels of these genes were significantly decreased in Δ*nifV* (*nifH*; 0.06-, *bclA*; 0.008-fold) in the presence of rice extract (Fig. 2B). However, the expression of the *bclA* and *nifV* genes was not detected in SUTN9-2 mutants lacking *bclA* and *nifV*, respectively (Fig. 2B). The results demonstrated that rice extract affected BclA transporter and nitrogen fixation-related gene expression, indicating the effect of Δ*nifV* on *nifH* and *bclA* gene expression.

*Expression of rice (*indica*) hemoglobin genes in response to WT and mutant SUTN9-2*

To assess the relationship between hemoglobin gene expression and nitrogen fixation efficiency by SUTN9-2 in rice plants, *hb1* and *hb5* gene expression levels were assessed in rice plants inoculated with SUTN9-2 WT, Δ*bclA*, and Δ*nifV*. The results obtained showed that *hb1* and *hb5* expression was more strongly induced in rice inoculated with SUTN9-2 WT (0.2- and 0.03-fold), Δ*bclA* (0.02- and 0.007-fold), and Δ*nifV* (0.06- and 0.01-fold) than with the non-inoculated control (Fig. 2C). The expression of these genes was suppressed in Δ*bclA*- and Δ*nifV*-inoculated rice, with the expression level of the *hb5* gene being lower than that of the *hb1* gene (Fig. 2C). These results indicated that the activity of hemoglobin in rice plants may be induced in response to the SUTN9-2 inoculation and may function as an oxygen scavenger or oxygen stock to facilitate nitrogen fixation in the endophytic state of SUTN9-2.

*SUTN9-2 transcriptome in response to rice extract (*indica*)*

To analyze the RNAseq transcriptome, total RNA was purified from SUTN9-2 incubated in BNM-B medium in the presence or absence of rice extract. The main reason for performing the transcriptome analysis was to elucidate the mechanisms and factors involved in cell differentiation and nitrogen fixation by endophytic SUTN9-2 in rice plants. The results obtained showed that the expression of a large number of genes was significantly altered (FDR value ≤0.1) in response to rice extract, with the differential expression of 365 genes being significant, representing 63.8% of DEGs (Fig. 3A). The percentage of DEGs was higher (42.1%) in BNM-B with rice extract-treated SUTN9-2 WT cells than in BNM-B-treated cells (Fig. 3A). The effects of Δ*bclA* in rice extract were also demonstrated because 42.1% of genes were differentially regulated in treated WT SUTN9-2 cells in the BNM-B with rice extract group compared to Δ*bclA* in the BNM-B with rice extract group (Fig. 3A). These results revealed the influence of rice extract and the *bclA* gene on the expression of genes in SUTN9-2.

The highest differentially up-regulated genes in SUTN9-2 WT in response to rice extract were biphenyl-2,3-diol 1,2-dioxygenase (PWE78131.1; 2.33 logFC) followed by 3-(3-hydroxyphenyl) propanoate hydroxylase (PWE78129.1; 1.85 logFC) (Fig. 3D and E). Both of these genes belong to the class of oxidoreductase catalytic enzymes involved in the degradation of plant-related compounds and interact with oxygen atoms, which are incorporated into the substrate. The third and fifth highest differentially up-regulated

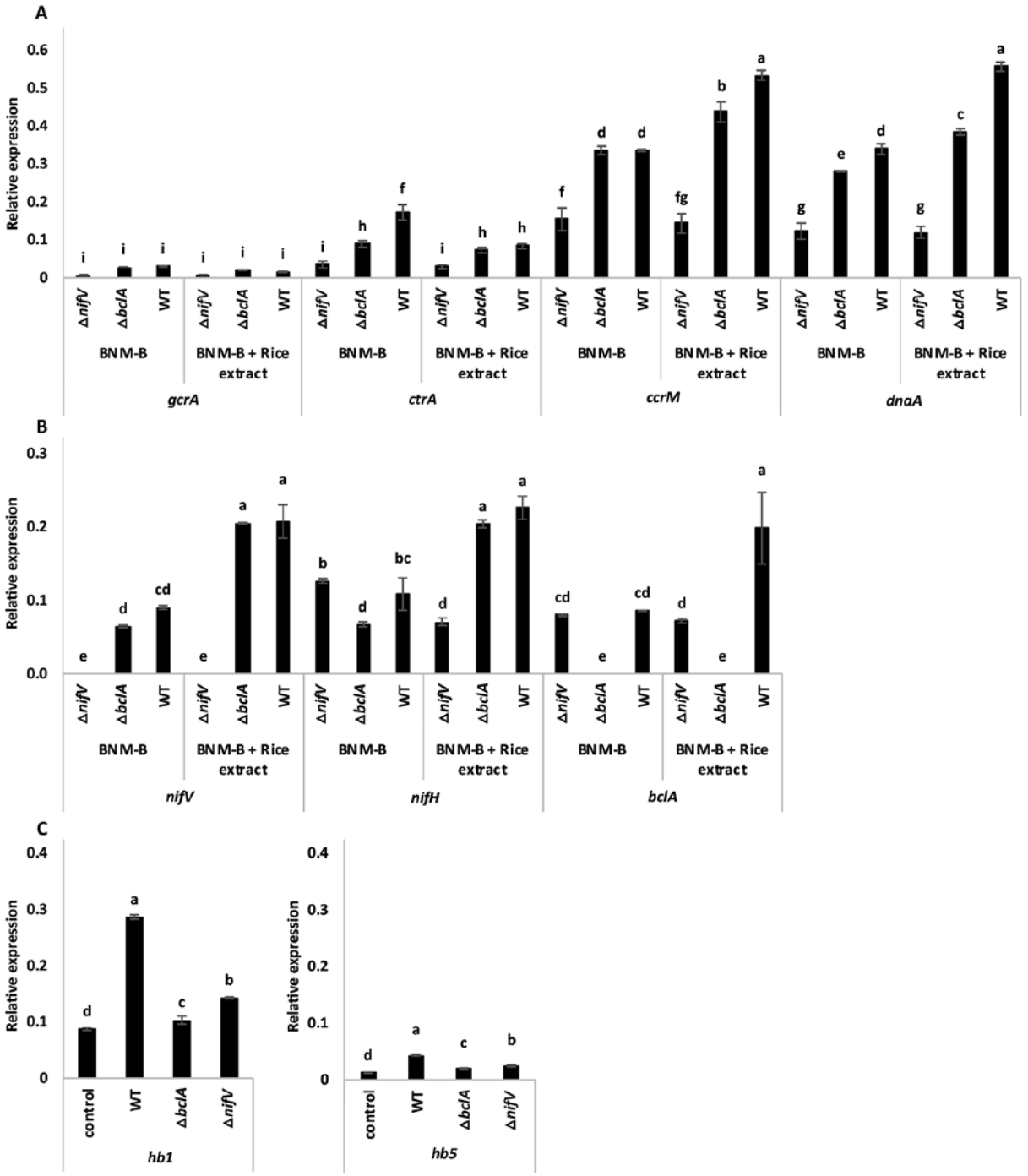

Fig. 2. Relative expression of genes involved in the master cell cycle (A), nitrogen fixation and BclA transporter (B) of SUTN9-2 Δ*nifV*, Δ*bclA*, and WT in response to rice extract (*indica*) at 21 days. Relative expression of the rice hemoglobin gene (*hb1* and *hb5*) in response to SUTN9-2 Δ*nifV*, Δ*bclA*, and WT at 21 dpi (C). Significance at $P \leq 0.05$ was indicated by the mean standard deviation ($n=3$).

genes were the molecular chaperones sGroEL (PWE76243.1; 1.42 logFC) and GroES (PWE81524.1; 1.34 logFC), which are required for the proper folding of many proteins and the function of the nitrogen fixation regulatory protein NifA. The results from the RNAseq analysis indicated that the differential expression of genes involved in nitrogen fixation and nitrogen metabolism in response to rice extract was not significant (Fig. 3E), whereas qRT-PCR results showed that nitrogen fixation genes (*nifH* and *nifV*) were up-regulated (Fig. 2B) because their expression was detected in rice plants (Piromyou *et al.*, 2017; Greetatorn *et al.*, 2019). However, a key difference between the two experiments needs to be considered. The experimental set-up for the transcriptome analysis was performed on a bigger scale than that for qRT-PCR in order to obtain a sufficiently large number of SUTN9-2 cells in rice extract for RNA purification and the transcriptome analysis. This may have been affected by the different oxygen levels in the two

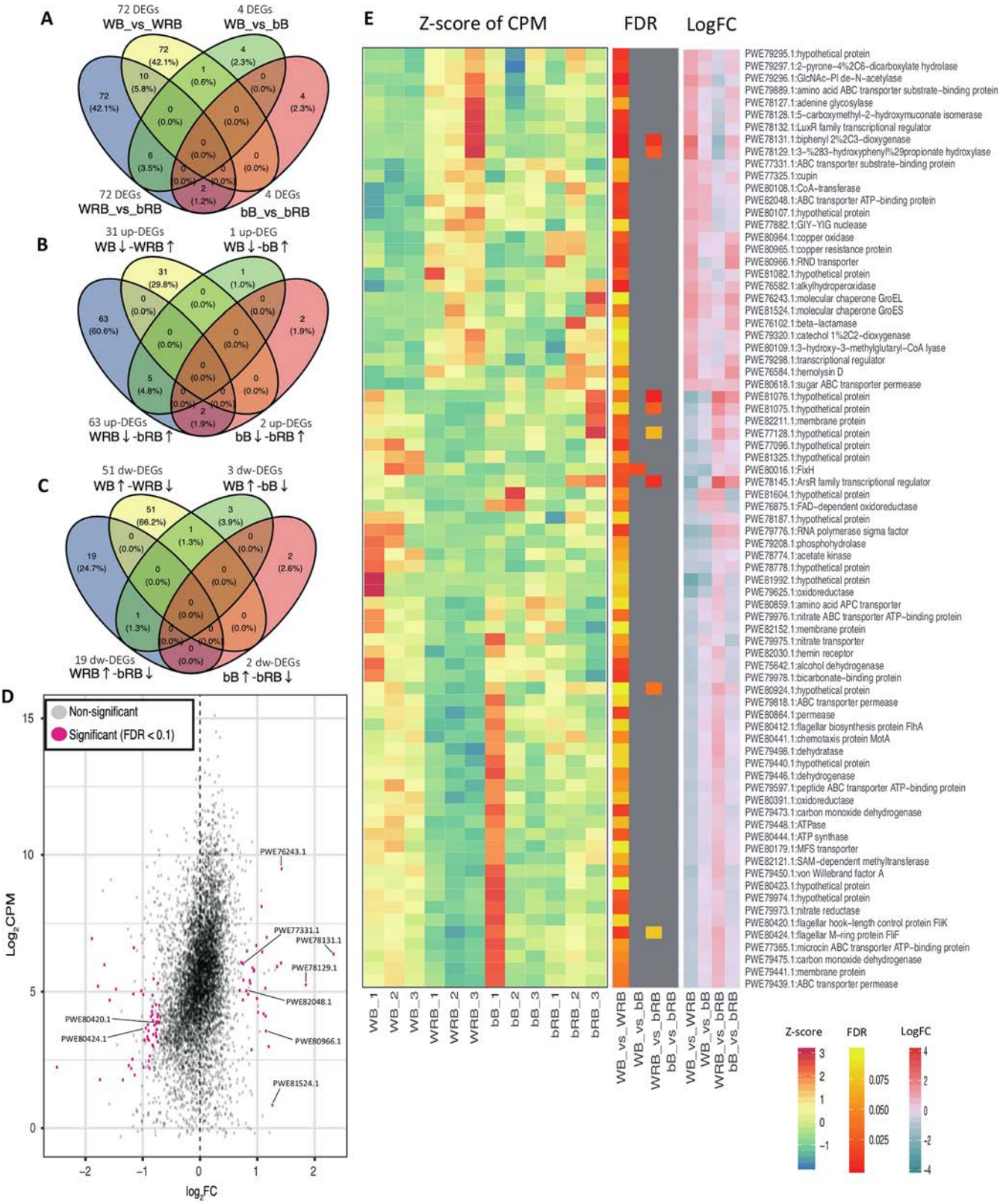

Fig. 3. Differentially expressed genes (DEGs) of SUTN9-2 WT versus Δ*bclA* in response to BNM-B (WB and bB) and BNM-B+rice extract (*indica*) (WRB and bRB). Venn diagram of all DEGs of WB_vs_WRB, WB_vs_bB, WRB_vs_bRB, and bB_vs_bRB (A), showing up-regulated genes (B), and down-regulated genes (C). MA plot of up- and down-regulated DEGs of WB_vs_WRB and genes of interest were labeled (D). Expression pattern of DEGs of WB, bB, WRB, and bRB. FDR (≤0.1) and logFC of DEGs of WB_vs_WRB, WB_vs_bB, WRB_vs_bRB, and bB_vs_bRB. The color scale bars are for normalized expression (E).

experimental set-ups, which perturbed *nif* gene expression in the transcriptome experiment.

DEGs in response to rice extract were also found to code for a protein involved in the cationic peptide transport system ATP-binding process. These DEGs include genes involved in the ABC transporter ATP-binding protein (PWE82048.1; 0.84 logFC) and ABC transporter substrate-binding protein (PWE77331.1; 7.5 logFC). The gene coding for efflux pumps was also found to be differentially up-regulated in the presence of rice extract (Fig. 3D and E). This gene belongs to the resistance nodulation and cell division family (RND) efflux system (PWE80966.1; 1.15 logFC), which may be involved in bacterial defenses against toxic plant metabolites. These results suggested the presence of cationic antimicrobial peptide (CAMP) in rice plants, which is toxic and affects bacterial cell differentiation. The significantly down-regulated DEGs of SUTN9-2 WT in the response to rice extract were related to flagella (PWE80412.1, PWE80420.1, and PWE80424.1) (Fig. 3E). In contrast, these genes were up-regulated in SUTN9-2 Δ*bclA* (PWE80424.1) in response to rice extract (Fig. 3D), indicating the influence of rice extract and Δ*bclA* on cell motility.

qRT-PCR validation

qRT-PCR was performed for DEGs, including *hpaD*, *mhpA*, *groEL*, *groES*, *sapDF*, *sapA*, and *cusF* in SUTN9-2 WT that significantly differed between the BNM-B with rice extract (*indica*) group and BNM-B alone group. The results obtained showed that the majority of genes were up-regulated in response to rice extract, which were similar to those from the transcriptome analysis. The expression of *mhpA* appeared to be more strongly up-regulated in response to rice extract (0.09-fold), followed by *sapDF* (0.07-fold), *cusF* (0.07-fold), *groEL* (0.06-fold), *hpaD* (0.05-foid), *sapA* (0.04-fold), and *groES* (0.01-fold), respectively (Fig. 4).

Discussion

The present results indicate that SUTN9-2 undergoes major changes in cell size and nitrogen fixation efficiency in response to rice extract (Fig. 1). The significant increase observed in the elongated cell size of SUTN9-2 was associated with more efficient nitrogen fixation. Similarly, a TBD process occurs before effective nitrogen fixation is established. These bacteroids are enlarged and polyploid and have lost their capacity to produce progeny (Mergaert *et al.*, 2006; Alunni and Gourion, 2016). The small bacteroid size (1–2.5 μm) in alfalfa (*Medicago sativa*) nodules had a low nucleic acid content and did not exhibit acetylene reduction activity (4.9 μmol C_2H_2 reduced $[10^{10}]^{-1}$ bacteroids). The enlarged bacteroid size (5–7 μm) had a high nucleic acid content and was very active for acetylene reduction (83.3 μmol C_2H_2 reduced $[10^{10}]^{-1}$ bacteroids) (Paau and Cowles, 1978). The bacteroids of bradyrhizobia in *A. afraspera* and *A. indica* exhibit differentiation along with a high DNA content, such that the mean DNA content of free-growing *Bradyrhizobium* sp. ORS285 was 1 to 2 genome complement (1C to 2C) and that of the bacteroid was 7C to 16C ploidy levels (Czernic *et al.*, 2015; Guefrachi *et al.*, 2015).

Cell differentiation by *Bradyrhizobium* bacteroids occurred in the interaction with defensin-like antimicrobial peptides (DEFs), which are found in the IRLC and Dalbergioids legume families with the action of BclA transporters (Guefrachi *et al.*, 2015). Based on a phylogenetic tree of SbmA_bacA domain proteins, three genes of *Bradyrhizobium* sp. strain ORS285 were revealed. Two genes (BRAO285v1_250005 and BRAO285v1_950010) are in the *Bradyrhizobium* homologous clade and one (BRAO285v1_1320006) in the BclA clade (Guefrachi *et al.*, 2015). However, only the mutant in gene BRAO285v1_1320006 had abnormal (undifferentiated) bacteroid cells, and exhibited markedly reduced nitrogen fixation activity in the host plants of *Aeschynomene* spp. (Guefrachi *et al.*, 2015). Similarly, SUTN9-2 Δ*bclA* in the present study belonged to the BclA clade. This gene was disrupted according to high homology with the BclA of ORS285 (Fig. S6). Based on the KO (KEGG [Kyoto Encyclopedia of Genes and Genomes] Orthology) annotation in the reconstruction pathway, the ABC transporter involving the CAMP resistance of SUTN9-2 Δ*bclA* was perturbed by the deletion of the ABC transporter ATP-binding domain (*bclA*; PWE81210.1) belonging to SapDF (Lopez-Solanilla *et al.*, 1998). However, the transcriptomic analysis showed that the ABC transporter substrate-binding protein consisting of SapA (PWE77331.1) and ABC transporter

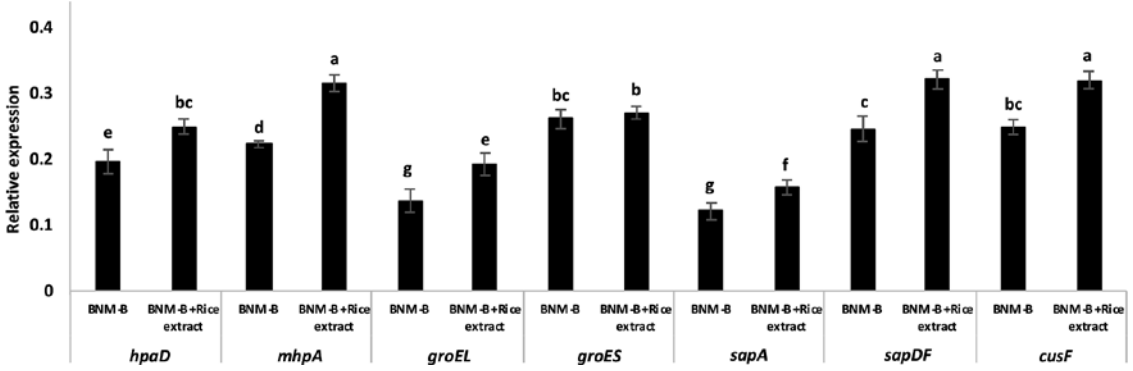

Fig. 4. qRT-PCR analysis data for significant DEGs in SUTN9-2 WT between BNM-B alone and BNM-B with rice extract (*indica*). Significance at $P \leq 0.05$ is indicated by the mean±standard deviation (n=3).

ATP-binding protein consisting of SapDF (PWE82048.1) were significantly and differentially up-regulated in response to rice extract (Fig. 3D and E, Table S2). A phylogenetic analysis based on the sequences of SbmA_BacA domain proteins showed that SapA (PWE77331.1) and SapDF (PWE82048.1) identified in SUTN9-2 were distant from the BclA and *Bradyrhizobium* homologous clades identified in *Bradyrhizobium* spp. However, both of these genes showed 97% similarity to these clades (Fig. S6) (Guefrachi *et al.*, 2015). These results indicate that SapA (PWE77331.1) and SapDF (PWE82048.1) play an important role together with SUTN9-2 Δ*bclA* (PWE81210.1; data not shown) for cell differentiation, nitrogen fixation in symbiosis, and responses to rice extract because the cell differentiation of SUTN9-2 Δ*bclA* was still maintained in both systems of bacteroids in legume plants (data not shown) and bacteria in response to rice extract (Fig. S2 and S4). However, decreases were also observed in the elongated cell sizes and nitrogen fixation activities of Δ*bclA* and Δ*nifV*. These results indicated the effects of *bclA* and *nifV* genes on the cell size and nitrogen fixation activity of SUTN9-2 cells in response to rice extract. The *sap* mutant pathogenic bacterium *Erwinia chrysanthemi* was sensitive to killing by antimicrobial peptides (AMPs) (wheat α-thionin and snaking-1) from potato tubers (Lopez-Solanilla *et al.*, 1998). The Sap transporter consists of SapABCDFZ, which shares homology to the 'ATP-binding cassette' (ABC) family of transporters that show diverse substrate binding and uptake (Hiles *et al.*, 1987; Abouhamad *et al.*, 1991; Parra-Lopez *et al.*, 1993). SapA is predicted to function as a periplasmic solute-binding protein; SapB and SapC as inner membrane permease proteins; SapD and SapF as ATPase subunits; whereas the function of SapZ remains unknown (Mason *et al.*, 2006). Moreover, previous studies identified several genes encoding cysteine-rich peptides (CRPs), also suggesting several uncharacterized AMPs in rice plants (Silverstein *et al.*, 2007), and genes encoding DEFs were also detected in rice plants (Tantong *et al.*, 2016; Li *et al.*, 2017). These results implied the production of DEFs in rice plants interacting with the Sap transporter of SUTN9-2, which affected enlarged cell sizes and high DNA contents in SUTN9-2 in response to rice extract (Fig. 5), similar to the cell differentiation and polyploidy of bacteroids in legume plants affected by NCR peptides.

Moreover, the gene coding for RND transporter efflux pumps (PWE80966.1) was differentially up-regulated in SUTN9-2 WT exposed to rice extract (Fig. 3D and E). Efflux pumps are transport proteins involved in the extrusion of toxic substrates into the external environment (Coutinho *et al.*, 2015). The RND efflux system has been recognized to play an important role in the successful colonization of the apple tree by the phytopathogen *Erwinia amylovora* (Burse *et al.*, 2004). RND efflux systems are strongly up-regulated in *B. kururiensis* M130 in the pres-

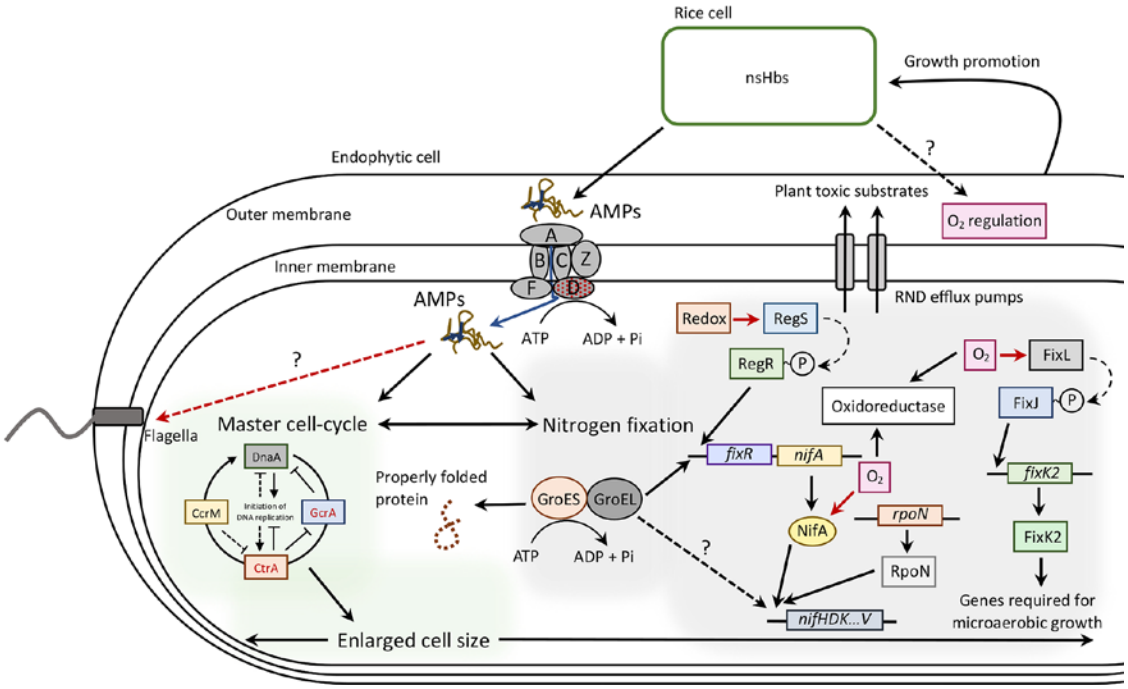

Fig. 5. Working model of cell differentiation and nitrogen fixation by SUTN9-2 exposed to rice extract. The currently implied AMPs from rice plants are predictably recognized by BclA ABC transporters belonging to Sap ABC transporter family-like AMP recognition receptors. AMPs are targeted to the cell membrane of bradyrhizobia, localizing the BclA or Sap transporter, promoting the import of AMPs and providing protection against the antimicrobial activity of these peptides. AMPs affect master cell cycle regulators by reducing GcrA activity and the CtrA autoregulation pathway, but promoting DnaA and CcrM for the initiation of DNA replication, resulting in an increase in DNA content and enlarged cell size. A defect in flagellar activity during cell differentiation was observed. This was followed by increased nitrogen fixation activity, which correlated with an enlarged cell size. Excess oxygen perturbs the nitrogen regulatory protein NifA and reduces nitrogen fixation activity. Oxidoreductase may play a role in controlling oxygen to an appropriate level for nitrogenase activity. GroESL co-regulated with the nitrogen regulatory gene *nifA* and *rpoN* RNA polymerase for the formation of a functional nitrogenase. The successful colonization of bradyrhizobia in rice plants is triggered by the RND efflux system and induced rice nsHbs then regulate low oxygen partial pressure and facilitate nitrogen-fixing endophytic cells.

ence of rice extract (Coutinho *et al.*, 2015). This type of efflux system may be important in bacterial survival defenses against toxic-plant metabolites, including DEFs (Fig. 5).

Flagellar biosynthesis is mostly down-regulated in symbiotic bacteroid cells. The transcriptome analysis of *Mesorhizobium loti* revealed that genes for flagellar formation were strongly repressed under the symbiotic condition because rhizobia under this condition do not need to be motile (Uchiumi *et al.*, 2004; Tatsukami *et al.*, 2013). In addition, the relative expression level of the SUTN9-2 flagella biosynthetic protein (*fliP*) in response to rice root exudate was lower than that without rice root exudate. The expression level of *fliP* also slightly decreased with an increase in plant age (Piromyou *et al.*, 2015b). Similarly, the differentially down-regulated expressed genes of SUTN9-2 WT were related to flagellar biosynthesis (PWE80412.1, PWE80420.1, and PWE80424.1) in response to rice extract. In contrast, these genes were up-regulated in Δ*bclA* (PWE80424.1) in response to rice extract (Fig. 3D). This up-regulation has also been observed in transcriptome experiments with *B. kururiensis* in response to rice extract and allows bacteria to escape host defense responses (Coutinho *et al.*, 2015). Therefore, the down-regulation of flagellar biosynthesis appears to be supporting the cell differentiation of SUTN9-2 in response to rice extract, similar to bacteroids in the symbiotic condition. In contrast, Δ*bclA* lacking some parts of the transporter against plant AMPs up-regulate genes for flagellar biosynthesis, thereby allowing bacteria to move faster in the plant environment in order to escape host defense responses (Fig. 5).

Rice extract (*O. sativa* L. ssp. *indica* cv. Pathum Thani 1) affected cell elongation and nitrogen fixation activity in SUTN9-2 more strongly than rice extract (*O. sativa* L. *japonica* cv. Nipponbare) in all treated SUTN9-2 WT, Δ*bclA*, and Δ*nifV* (Fig. 1D, E, F, and S2). Elongated cell size was smaller in Δ*nifV* than in WT and Δ*bclA* SUTN9-2, and also in Δ*bclA* than in WT SUTN9-2 (Fig. 1D, E, and S2). When SUTN9-2 WT was inoculated into the Thai rice cultivar Pathum Thani 1 (*indica*) and Japanese rice cultivar Nipponbare (*japonica*), the number of SUTN9-2 WT cells at 30 dpi was higher in Thai rice root tissues (*indica*) than in Japanese rice (*japonica*), with 10^3 and 10^1 CFU g^{-1} root fresh weight, respectively (Piromyou *et al.*, 2015b). The population density of SUTN 9-2 was larger in Thai rice (*indica*) than in Japanese rice (*japonica*). In addition, Thai bradyrhizobial strain SUTN9-2 was suggested to promote the total dry weight of rice (*indica*) more effectively than Japanese bradyrhizobial strains (Piromyou *et al.*, 2015a). On the other hand, rice (*indica*) responded positively only to putative Thai rice endophytic bradyrhizobia, while this phenomenon was not observed in Japanese rice (*japonica*) (Piromyou *et al.*, 2015a, 2015b). In addition, the type III secretion system (T3SS) of SUTN9-2 is involved in bradyrhizobial infections in rice plants. The density of the SUTN9-2 T3SS mutant in Thai rice (*indica)* was significantly lower than that of SUTN9-2 WT, and this property was not detected in Japanese rice (*japonica*), indicating SUTN9-2 had the ability to overcome native host rice defense responses through the function of T3SS and also that rice developed a system to protect itself from non-native soil bacteria (Piromyou *et al.*, 2015b). These results imply that the rice cultivar and bacterial strain are important factors that control the compatibility of the rice-bacterium relationship, which may contribute to bradyrhizobia-host evolution (Piromyou *et al.*, 2015b). These results support the existence of a preferable host for SUTN9-2 in rice species, which may also contribute to greater increases in the cell size enlargement and nitrogen fixation activity of SUTN9-2 in response to rice extract from *indica* than to that from *japonica*.

The attenuated pattern of *ctrA* expression in NCR-treated cells during the cell cycle may be caused by reduced GcrA activity or by defects in the CtrA autoregulation pathway. DnaA appears to be necessary for repeated initiation rounds of DNA replication during endoreduplication *in vivo* (Collier, 2012). CcrM DNA methyltransferase is present and active for a short time and essential for methylation at the start of DNA replication (Collier, 2012). In the present study, the results obtained suggested that AMPs in rice extract affect master cell-cycle regulators by suppressing the expression of *ctrA* and promoting *dnaA* and *ccrM* expression, resulting in an increase in cell size and DNA content (Fig. 2A, 5, and S3). In addition, the *nifV* gene may affect cell size enlargement following exposure to rice extract. The expression of genes involved in the nitrogen fixation activity (*nifH* and *nifV*) of SUTN9-2 has been detected in the endophytic relationship with rice plants (Piromyou *et al.*, 2017; Greetatorn *et al.*, 2019). Furthermore, the expression of *nifH*, *nifV*, and *bclA* in WT and Δ*bclA* SUTN9-2 increased in response to rice extract. In contrast, the expression of these genes in SUTN9-2 Δ*nifV* decreased in response to rice extract (Fig. 2B). These results suggest similarities in the expression model between these genes and the genes involved in the master cell cycle following exposure to rice extract. Furthermore, the effects of the interaction between the rice extract and BclA transporter on cell differentiation and nitrogen fixation were implied based on the expression of cell cycle and *nif* genes in response to rice extract (Fig. 5). Non-symbiotic hemoglobins (nsHbs) have been detected in several monocot plants. Rice (*O. sativa*) contains five copies of the *nsHb* gene, namely, *hb1-hb5* (Lira-Ruan *et al.*, 2002). *hb1*, *hb2*, and *hb5* are expressed in rice embryonic organs and vegetative organs, and their appear to function as oxygen carriers or in some aspects of oxygen metabolism (Garrocho-Villegas *et al.*, 2008; Lira-Ruan *et al.*, 2011). Hormone and stress response promoters exist upstream of the rice *hb5* gene, which was transcribed in rice organs. The amino acid sequence and protein model structure of Hb5 differ from those of rice Hbs 1 to 4 (Garrocho-Villegas *et al.*, 2008), suggesting different expression levels between *hb1* and *hb5* (Fig. 2C). However, they are present at very low levels inside host rice cells. In addition, the physiological functions of rice nsHbs are not involved in oxygen transport, but more closely resemble known oxygen sensors (Goodman and Hargrove, 2001). This finding revealed that nsHbs in rice plants may function as a regulator to maintain low oxygen partial pressure for nitrogenase activity to facilitate nitrogen-fixing endophytic cells (Fig. 5).

The RNAseq experiment provided a global view of the gene expression profile in response to rice extract. RNAseq results indicated that SUTN9-2 endophytic cells were affected by rice extract and the Δ*bclA* mutation, which is consistent with the results for significant DEGs (Fig. 3A). The expression of genes involved in the cell cycle and nitrogen fixation was up-regulated when SUTN9-2 was exposed to rice extract. These results are in contrast to those obtained from the transcriptome analysis of SUTN9-2 in the presence of rice extract. These genes did not show significant DEGs in the response to rice extract. Bacteria capable of utilizing biphenyl and phenylpropanoid compounds as carbon and energy sources are widely distributed in natural environments, and may originate from the putrefaction of proteins in soil or as breakdown products of several constituents of plants, such as lignin, various oils, and resins (Ferrandez *et al.*, 1997; Díaz *et al.*, 1998; Wesche *et al.*, 2005). The highest up-regulated DEGs involved in biphenyl-2,3-diol 1,2-dioxygenase (PWE78131.1) and 3-(3-hydroxyphenyl) propanoate hydroxylase (PWE78129.1) were observed. These genes belong to the class of oxidoreductases acting on donors with oxygen and the incorporation of atoms of oxygen into the substrate (Díaz *et al.*, 1998; Wesche *et al.*, 2005), which may have a role in controlling oxygen to an appropriate level for nitrogenase activity (Fig. 3D and E). This result suggests excess oxygen in the experimental set-up for the transcriptome analysis (50-mL tube), which affects nitrogenase activity. A larger scale experiment (50-mL tube) was performed to obtain a large amount of SUTN9-2 cells in rice extract for the transcriptome analysis, more than the experimental set-up for qRT-PCR (10-mL tube). The nitrogenase enzyme complex is highly sensitive to molecular oxygen, which irreversibly inactivates the enzyme. The inhibition of *nif* gene expression by molecular oxygen at the nitrogen regulatory protein NifA post-transcriptional stage was detected in *B. japonicum* (Fischer and Hennecke, 1987; Kullik *et al.*, 1989). Therefore, the suppression of nitrogen fixation genes observed in the transcriptome analysis may be due to the effects of excess oxygen on nitrogenase sensitivity (Fig. 5).

The molecular chaperones GroEL (PWE76243.1) and GroES (PWE81524.1) were identified as significant differentially up-regulated genes in response to rice extract (Fig. 3D and E). GroESL chaperonins are required for the formation of a functional nitrogenase in *B. japonicum*, which is co-regulated together with the symbiotic nitrogen regulatory gene *nifA* and transcribed by σ^{54} RNA polymerase (Fischer *et al.*, 1993, 1999). However, the requirement of chaperonins for nitrogen fixation does not occur at the level of RegSR-NifA-σ^{54}- or FixLJ-FixK-dependent gene regulation (Fischer *et al.*, 1999). This finding indicated that the nitrogen fixation of SUTN9-2 in response to rice extract may be affected by GroESL chaperonins with or without Nif-dependent gene regulation. Collectively, these studies imply that the nitrogen fixation of SUTN9-2 was induced in response to rice extract because the differentially up-regulated genes of GroESL chaperonins were detected (Fig. 5).

Based on the results and transcriptomic findings reported herein, a proposed model for the cell differentiation and nitrogen fixation activity of SUTN9-2 in response to rice extract was shown (Fig. 5). Rice plants are predicted to produce AMPs that are recognized during interactions by AMP recognition receptors (Sap ABC transporter family), thereby promoting the import of AMPs and protecting SUTN9-2 cells against the antimicrobial activity of these peptides. Following the recognition and transduction of these AMPs, several DEGs are induced in SUTN9-2. These AMPs predictably modulate master cell cycle regulators, thereby causing cell differentiation. These interactions induced several processes, including oxidoreductase, GroESL chaperonin, the RND efflux system, and flagellar biosynthesis, which may promote cell size enlargement, nitrogen fixation, and, ultimately, rice growth (Fig. 5). These results imply similarities in the mechanisms and factors involved in cell differentiation and nitrogen fixation between endophytic cells in rice plants and symbiotic cells in legume plants, which are based on similar mechanisms from both the bacterial side (BclA-like transporters) and plant side (AMPs). It is important to understand the mechanisms underlying the regulation of the factors, molecules, and signals of the plant as well as the bacterial cells involved in inducing cell differentiation and nitrogen fixation in endophytic cells required for *in-planta* survival and plant growth promotion. The specialized legume plant genes involved in symbiotic interactions may have arisen from a pre-existing non-symbiotic plant gene, such as rice plants, suggesting convergent coevolution in these distant plant species.

Acknowledgements

This work was supported by Suranaree University of Technology, Kagoshima University, the National Institute for Basic Biology, the Office of the Higher Education Commission under NRU project of Thailand, the National Research Council of Thailand, the Japan Society for the Promotion of Science, the Thailand Science Research and Innovation, and the Royal Golden Jubilee Ph.D. program.

References

Abouhamad, W.N., Manson, M., Gibson, M.M., and Higgins, C.F. (1991) Peptide transport and chemotaxis in *Escherichia coli* and *Salmonella typhimurium*: characterization of the dipeptide permease (Dpp) and the dipeptide-binding protein. *Mol Microbiol* **5**: 1035–1047.

Alunni, B., and Gourion, B. (2016) Terminal bacteroid differentiation in the legume-*Rhizobium* symbiosis: nodule-specific cysteine-rich peptides and beyond. *New Phytol* **211**: 411–417.

Aramaki, T., Blanc-Mathieu, R., Endo, H., Ohkubo, K., Kanehisa, M., Goto, S., and Ogata, H. (2020) KofamKOALA: KEGG ortholog assignment based on profile HMM and adaptive score threshold. *Bioinformatics* **36**: 2251–2252.

Burse, A., Weingart, H., and Ullrich, M.S. (2004) The phytoalexin-inducible multidrug efflux pump AcrAB contributes to virulence in the fire blight pathogen, *Erwinia amylovora*. *Mol Plant Microbe Interact* **17**: 43–54.

Chaintreuil, C., Giraud, E., Prin, Y., Lorquin, J., Bâ, A., Gillis, M., *et al.* (2000) Photosynthetic bradyrhizobia are natural endophytes of the African wild rice *Oryza breviligulata*. *Appl Environ Microbiol* **66**: 5437–5447.

Chen, S., Zhou, Y., Chen, Y., and Gu, J. (2018) fastp: an ultra-fast all-in-one FASTQ preprocessor. *Bioinformatics* **34**: i884–i890.

Collier, J. (2012) Regulation of chromosomal replication in *Caulobacter crescentus*. *Plasmid* **67**: 76–87.

Collins, T.J. (2007) ImageJ for microscopy. *Biotechniques* **43**: S25–S30.

Coutinho, B.G., Licastro, D., Mendonça-Previato, L., Cámara, M., and Venturi, V. (2015) Plant-influenced gene expression in the rice endophyte *Burkholderia kururiensis* M130. *Mol Plant Microbe Interact* **28**: 10–21.

Czernic, P., Gully, D., Cartieaux, F., Moulin, L., Guefrachi, I., Patrel, D., *et al.* (2015) Convergent evolution of endosymbiont differentiation in Dalbergioid and Inverted Repeat-Lacking Clade legumes mediated by nodule-specific cysteine-rich peptides. *Plant Physiol* **169**: 1254–1265.

De Nisco, N.J., Abo, R.P., Wu, C.M., Penterman, J., and Walker, G.C. (2014) Global analysis of cell cycle gene expression of the legume symbiont *Sinorhizobium meliloti*. *Proc Natl Acad Sci U S A* **111**: 3217–3224.

Deitch, A.D., Law, H., and deVere White, R. (1982) A stable propidium iodide staining procedure for flow cytometry. *J Histochem Cytochem* **30**: 967–972.

Díaz, E., Ferrández, A., and García, J.L. (1998) Characterization of the hca Cluster encoding the dioxygenolytic pathway for initial catabolism of 3-phenylpropionic acid in *Escherichia coli* K-12. *J Bacteriol* **180**: 2915–2923.

Duncan, D.B. (1955) Multiple Range and Multiple F Tests. *Biometrics* **11**: 1–42.

Ehrhardt, D.W., Atkinson, E.M., and Long, S.R. (1992) Depolarization of alfalfa root hair membrane potential by *Rhizobium meliloti* Nod factors. *Science* **256**: 998–1000.

Ferrández, A., Garciá, J.L., and Díaz, E. (1997) Genetic characterization and expression in heterologous hosts of the 3-(3-hydroxyphenyl) propionate catabolic pathway of *Escherichia coli* K-12. *J Bacteriol* **179**: 2573–2581.

Fischer, H.M., and Hennecke, H. (1987) Direct response of *Bradyrhizobium japonicum nifA*-mediated *nif* gene regulation to cellular oxygen status. *Mol Gen Genet* **209**: 621–626.

Fischer, H.M., Babst, M., Kaspar, T., Acuña, G., Arigoni, F., and Hennecke, H. (1993) One member of a gro-ESL-like chaperonin multigene family in *Bradyrhizobium japonicum* is co-regulated with symbiotic nitrogen fixation genes. *EMBO J* **12**: 2901–2912.

Fischer, H.M., Schneider, K., Babst, M., and Hennecke, H. (1999) GroEL chaperonins are required for the formation of a functional nitrogenase in *Bradyrhizobium japonicum*. *Arch Microbiol* **171**: 279–289.

Garrocho-Villegas, V., Bustos-Rivera, G., Gough, J., Vinogradov, S.N., and Arredondo-Peter, R. (2008) Expression and in silico structural analysis of a rice (*Oryza sativa*) hemoglobin 5. *Plant Physiol Biochem (Issy-les-Moulineaux, Fr)* **46**: 855–859.

Goodman, M.D., and Hargrove, M.S. (2001) Quaternary structure of rice nonsymbiotic hemoglobin. *J Biol Chem* **276**: 6834–6839.

Greetatorn, T., Hashimoto, S., Sarapat, S., Tittabutr, P., Boonkerd, N., Uchiumi, T., and Teaumroong, N. (2019) Empowering rice seedling growth by endophytic *Bradyrhizobium* sp. SUTN 9-2. *Lett Appl Microbiol* **68**: 258–266.

Guefrachi, I., Pierre, O., Timchenko, T., Alunni, B., Barrière, Q., Czernic, P., *et al.* (2015) *Bradyrhizobium* BclA is a peptide transporter required for bacterial differentiation in symbiosis with *Aeschynomene* legumes. *Mol Plant Microbe Interact* **28**: 1155–1166.

Hakoyama, T., Niimi, K., Watanabe, H., Tabata, R., Matsubara, J., Sato, S., *et al.* (2009) Host plant genome overcomes the lack of a bacterial gene for symbiotic nitrogen fixation. *Nature* **462**: 514–517.

Hashimoto, S., Wongdee, J., Songwattana, P., Greetatorn, T., Goto, K., Tittabutr, P., *et al.* (2019) Homocitrate synthase genes of two wide-host-range *Bradyrhizobium* strains are differently required for symbiosis depending on host plants. *Microbes Environ* **34**: 393–401.

Hiles, I.D., Gallagher, M.P., Jamieson, D.J., and Higgins, C.F. (1987) Molecular characterization of the oligopeptide permease of *Salmonella typhimurium*. *J Mol Biol* **195**: 125–142.

Howard, J.B., and Rees, D.C. (1994) Nitrogenase: a nucleotide-dependent molecular switch. *Annu Rev Biochem* **63**: 235–264.

Kondorosi, E., Mergaert, P., and Kereszt, A. (2013) A paradigm for endosymbiotic life: cell differentiation of *Rhizobium* bacteria provoked by host plant factors. *Annu Rev Microbiol* **67**: 611–628.

Kullik, I., Hennecke, H., and Fischer, H.-M. (1989) Inhibition of *Bradyrhizobium japonicum nifA*-dependent *nif* gene activation by oxygen occurs at the NifA protein level and is irreversible. *Arch Microbiol* **151**: 191–197.

Kumar, S., Nei, M., Dudley, J., and Tamura, K. (2008) MEGA: a biologist-centric software for evolutionary analysis of DNA and protein sequences. *Briefings Bioinf* **9**: 299–306.

Langmead, B., and Salzberg, S.L. (2012) Fast gapped-read alignment with Bowtie 2. *Nat Methods* **9**: 357–359.

Li, B., and Dewey, C.N. (2011) RSEM: accurate transcript quantification from RNA-Seq data with or without a reference genome. *BMC Bioinformatics* **12**: 323.

Li, X.M., Han, H.P., Chen, M., Yang, W., Liu, L., Li, N., *et al.* (2017) Overexpression of OsDT11, which encodes a novel cysteine-rich peptide, enhances drought tolerance and increases ABA concentration in rice. *Plant Mol Biol* **93**: 21–34.

Lira-Ruan, V., Ross, E.J.H., Sarath, G., Klucas, R.V., and Arredondo-Peter, R. (2002) Mapping and analysis of a hemoglobin gene family from *Oryza sativa*. *Plant Physiol Biochem (Issy-les-Moulineaux, Fr)* **40**: 199–202.

Lira-Ruan, V., Ruiz-Kubli, M., and Arredondo-Peter, R. (2011) Expression of non-symbiotic hemoglobin 1 and 2 genes in rice (*Oryza sativa*) embryonic organs. *Commun Integr Biol* **4**: 457–458.

López-Solanilla, E., García-Olmedo, F., and Rodríguez-Palenzuela, P. (1998) Inactivation of the *sapA* to *sapF* locus of *Erwinia chrysanthemi* reveals common features in plant and animal bacterial pathogenesis. *Plant Cell* **10**: 917–924.

Mae, T., and Ohira, K. (1981) The remobilization of nitrogen related to leaf growth and senescence in rice plants (*Oryza sativa* L.). *Plant Cell Physiol* **22**: 1067–1074.

Mason, K.M., Bruggeman, M.E., Munson, R.S., and Bakaletz, L.O. (2006) The non-typeable *Haemophilus influenzae* Sap transporter provides a mechanism of antimicrobial peptide resistance and SapD-dependent potassium acquisition. *Mol Microbiol* **62**: 1357–1372.

Mergaert, P., Uchiumi, T., Alunni, B., Evanno, G., Cheron, A., Catrice, O., *et al.* (2006) Eukaryotic control on bacterial cell cycle and differentiation in the *Rhizobium*-legume symbiosis. *Proc Natl Acad Sci U S A* **103**: 5230–5235.

Noisangiam, R., Teamtisong, K., Tittabutr, P., Boonkerd, N., Toshiki, U., Minamisawa, K., and Teaumroong, N. (2012) Genetic diversity, symbiotic evolution, and proposed infection process of *Bradyrhizobium* strains isolated from root nodules of *Aeschynomene americana* L. in Thailand. *Appl Environ Microbiol* **78**: 6236–6250.

Okubo, T., Piromyou, P., Tittabutr, P., Teaumroong, N., and Minamisawa, K. (2016) Origin and evolution of nitrogen fixation genes on symbiosis islands and plasmid in *Bradyrhizobium*. *Microbes Environ* **31**: 260–267.

Paau, A.S., and Cowles, J.R. (1978) Development of bacteroids in alfalfa (*Medicago sativa*) nodules. *Plant Physiol* **62**: 526–530.

Pagan, J., Child, J., Scowcroft, W., and Gibson, A. (1975) Nitrogen fixation by *Rhizobium* cultured on a defined medium. *Nature* **256**: 406–407.

Parra-Lopez, C., Baer, M.T., and Groisman, E.A. (1993) Molecular genetic analysis of a locus required for resistance to antimicrobial peptides in *Salmonella typhimurium*. *EMBO J* **12**: 4053–4062.

Penterman, J., Abo, R.P., De Nisco, N.J., Arnold, M.F., Longhi, R., Zanda, M., and Walker, G.C. (2014) Host plant peptides elicit a transcriptional response to control the *Sinorhizobium meliloti* cell cycle during symbiosis. *Proc Natl Acad Sci U S A* **111**: 3561–3566.

Piromyou, P., Greetatorn, T., Teamtisong, K., Okubo, T., Shinoda, R., Nuntakij, A., *et al.* (2015a) Preferential association of endophytic bradyrhizobia with different rice cultivars and its implications for rice endophyte evolution. *Appl Environ Microbiol* **81**: 3049–3061.

Piromyou, P., Songwattana, P., Greetatorn, T., Okubo, T., Kakizaki, K.C., Prakamhang, J., *et al.* (2015b) The type III secretion system (T3SS) is a determinant for rice-endophyte colonization by non-photosynthetic *Bradyrhizobium*. *Microbes Environ* **30**: 291–300.

Piromyou, P., Greetatorn, T., Teamtisong, K., Tittabutr, P., Boonkerd, N., and Teaumroong, N. (2017) Potential of rice stubble as a reservoir of bradyrhizobial inoculum in rice-legume crop rotation. *Appl Environ Microbiol* **83**: e01488-01417.

Renier, A., Maillet, F., Fardoux, J., Poinsot, V., Giraud, E., and Nouwen, N. (2011) Photosynthetic *Bradyrhizobium* sp. strain ORS285 synthesizes 2-O-methylfucosylated lipochitooligosaccharides for nod gene-dependent interaction with *Aeschynomene* plants. *Mol Plant Microbe Interact* **24**: 1440–1447.

Saitou, N., and Nei, M. (1987) The neighbor-joining method: a new method for reconstructing phylogenetic trees. *Mol Biol Evol* **4**: 406–425.

Silverstein, K.A., Moskal Jr, W.A., Wu, H.C., Underwood, B.A., Graham, M.A., Town, C.D., and VandenBosch, K.A. (2007) Small cysteine-rich peptides resembling antimicrobial peptides have been under-predicted in plants. *Plant J* **51**: 262–280.

Somasegaran, P., and Hoben, H.J. (2012) *Handbook for Rhizobia: Methods in Legume*-Rhizobium *Technology*. New York, NY: Springer.

Steel, R.G., and Torrie, J.H. (1980) *Principles and Procedures of Statistics*. New York, NY: McGraw-Hill.

Tamura, K., Peterson, D., Peterson, N., Stecher, G., Nei, M., and Kumar, S. (2011) MEGA5: Molecular evolutionary genetics analysis using maximum likelihood, evolutionary distance, and maximum parsimony methods. *Mol Biol Evol* **28**: 2731–2739.

Tantong, S., Pringsulaka, O., Weerawanich, K., Meeprasert, A., Rungrotmongkol, T., Sarnthima, R., *et al.* (2016) Two novel antimicrobial defensins from rice identified by gene coexpression network analyses. *Peptides (N Y, NY, U S)* **84**: 7–16.

Tatsukami, Y., Nambu, M., Morisaka, H., Kuroda, K., and Ueda, M. (2013) Disclosure of the differences of *Mesorhizobium loti* under the free-living and symbiotic conditions by comparative proteome analysis without bacteroid isolation. *BMC Microbiol* **13**: 180.

Teamtisong, K., Songwattana, P., Noisangiam, R., Piromyou, P., Boonkerd, N., Tittabutr, P., *et al.* (2014) Divergent nod-containing *Bradyrhizobium* sp. DOA9 with a megaplasmid and its host range. *Microbes Environ* **29**: 370–376.

Tsai, J.-W., and Alley, M. (2000) Proteolysis of the McpA chemoreceptor does not require the *Caulobacter* major chemotaxis operon. *J Bacteriol* **182**: 504–507.

Uchiumi, T., Ohwada, T., Itakura, M., Mitsui, H., Nukui, N., Dawadi, P., *et al.* (2004) Expression islands clustered on the symbiosis island of the *Mesorhizobium loti* genome. *J Bacteriol* **186**: 2439–2448.

Vasse, J., De Billy, F., Camut, S., and Truchet, G. (1990) Correlation between ultrastructural differentiation of bacteroids and nitrogen fixation in alfalfa nodules. *J Bacteriol* **172**: 4295–4306.

Wesche, J., Hammer, E., Becher, D., Burchhardt, G., and Schauer, F. (2005) The *bphC* gene-encoded 2, 3-dihydroxybiphenyl-1, 2-dioxygenase is involved in complete degradation of dibenzofuran by the biphenyl-degrading bacterium *Ralstonia* sp. SBUG 290. *J Appl Microbiol* **98**: 635–645.

Young, M.D., Wakefield, M.J., Smyth, G.K., and Oshlack, A. (2010) Gene ontology analysis for RNA-seq: accounting for selection bias. *Genome Biol* **11**: R14.

Microbes Environ. 36(2), 2021
https://www.jstage.jst.go.jp/browse/jsme2 doi:10.1264/jsme2.ME21007

MOST VALUABLE PAPER OF THE YEAR 2021

Bioelectrical Methane Production with an Ammonium Oxidative Reaction under the No Organic Substance Condition

Ha T.T Dinh[1,2], Hiromi Kambara[1], Yoshiki Harada[1], Shuji Matsushita[1,3], Yoshiteru Aoi[4], Tomonori Kindaichi[1], Noriatsu Ozaki[1], and Akiyoshi Ohashi[1]*

[1]*Department of Civil and Environmental Engineering, Graduate School of Advanced Science and Engineering, Hiroshima University, 1–4–1, Kagamiyama, Higashi-Hiroshima, Hiroshima 739–8527, Japan;* [2]*Faculty of Environment, Ho Chi Minh City University of Natural Resources and Environment, 236 Le Van Sy, 1 Ward, Tan Binh District, Ho Chi Minh City, Vietnam;* [3]*Agricultural Technology Research Center, Hiroshima Prefectural Technology Research Institute, 6869, Hara, Hachihonmatsu, Higashi-Hiroshima, Hiroshima 739–0151, Japan; and* [4]*Program of Biotechnology, Graduate School of Integrated Sciences for Life, Hiroshima University, 1–3–1, Kagamiyama, Higashi-Hiroshima, Hiroshima 739–8530, Japan*

(Received January 25, 2021—Accepted May 1, 2021—Published online June 17, 2021)

The present study investigated bioelectrical methane production from CO_2 without organic substances. Even though microbial methane production has been reported at relatively high electric voltages, the amount of voltage required and the organisms contributing to the process currently remain unknown. Methane production using a biocathode was investigated in a microbial electrolysis cell coupled with an NH_4^+ oxidative reaction at an anode coated with platinum powder under a wide range of applied voltages and anaerobic conditions. A microbial community analysis revealed that methane production simultaneously occurred with biological denitrification at the biocathode. During denitrification, NO_3^- was produced by chemical NH_4^+ oxidation at the anode and was provided to the biocathode chamber. H_2 was produced at the biocathode by the hydrogen-producing bacteria *Petrimonas* through the acceptance of electrons and protons. The H_2 produced was biologically consumed by hydrogenotrophic methanogens of *Methanobacterium* and *Methanobrevibacter* with CO_2 uptake and by hydrogenotrophic denitrifiers of *Azonexus*. This microbial community suggests that methane is indirectly produced without the use of electrons by methanogens. Furthermore, bioelectrical methane production occurred under experimental conditions even at a very low voltage of 0.05 V coupled with NH_4^+ oxidation, which was thermodynamically feasible.

Key words: ammonia oxidation, bio-electricity, denitrification, methane production, microbial community

Methane is the prime component of natural gas and is widely utilized as an energy source worldwide. It is mainly produced by biological and physical actions that collectively contribute to 20–80% of natural gas reserves (Rice and Claypool, 1981). Methane is physically produced through the thermal decomposition of organic matter in association with the formation of coal, gas, and oil (Schoell, 1988). Conversely, biological methane formation is primarily performed by methanogenic microbes (methanogens) in anaerobic environments (Whiticar *et al.*, 1986; Whiticar, 1999). Only methanogenic archaea are known to act as methanogens and use substrates produced from organic matter during fermentation, such as acetate, formate, and hydrogen gas. This methane fermentation occurs in nature, but has also been applied as an eco-friendly wastewater treatment technology (Onodera, 2013; Townsend-Small *et al.*, 2016). Artificially produced biogas may be utilized as an energy source after purification.

It is possible to generate electricity from organic substances. Microbial fuel cell (MFC) technology and its application to wastewater treatment have been extensively examined (Logan *et al.*, 2006; Sarmin *et al.*, 2019; Wang *et al.*, 2020). Conversely, in microbial electrosynthesis systems (MESs), methane is produced by providing electricity (Rabaey and Rozendal, 2010; Eerten-Jansen *et al.*, 2012). High methane production is expected when MESs are applied to wastewater treatment because of the combination of methane fermentation using organic substances and the conversion of CO_2 to methane by microbes through electricity (Clauwaert *et al.*, 2008; Clauwaert and Verstraete, 2009; Zhao *et al.*, 2016; Park *et al.*, 2018; Peng *et al.*, 2019). Ding *et al.* (2016) identified 0.8 V as the optimal applied voltage for appropriate wastewater treatment and maximum methane production using an MES.

In the MES, bioelectrical methane production is performed without organic substrates (Cheng *et al.*, 2009; Villano *et al.*, 2010; Zhen *et al.*, 2015). Cheng *et al.* (2009) reported that carbon dioxide was reduced to methane at a biocathode potential of <–0.7 V (vs. Ag/AgCl). At –1.0 V (vs. Ag/AgCl), the electron capture efficiency of methane production was 96%. Two mechanisms have been proposed for biological methane production using a biocathode. At high applied voltages, methane may be produced by hydrogenotrophic methanogens using abiotic H_2 formed in water oxidation (Wagner *et al.*, 2009; Eerten-Jansen *et al.*, 2012). In this case, H_2 is an important intermediate for methane production. The second mechanism is direct electrotrophic methane production. Cheng *et al.* (2009) reported that some

* Corresponding author. E-mail: ecoakiyo@hiroshima-u.ac.jp;
Tel: +81–82–424–7823; Fax: +81–82–424–7823.

Citation: Dinh, T. T H., Kambara, H., Harada, Y., Matsushita, S., Aoi, Y., Kindaichi, T., et al. (2021) Bioelectrical Methane Production with an Ammonium Oxidative Reaction under the No Organic Substance Condition. *Microbes Environ* **36**: ME21007.
https://doi.org/10.1264/jsme2.ME21007

methanogens must use electrons with CO_2 to directly produce methane, without hydrogen as an intermediary. Previous studies on extracellular electron transfer demonstrated that applied voltage may not be effective at promoting methane production, suggesting a pathway without H_2 (Rotaru *et al.*, 2013; Lohner *et al.*, 2014; Holmes *et al.*, 2017; Lee *et al.*, 2017). However, there are insufficient experimental data to prove direct electrotrophic methane production. It currently remains unclear whether bioelectrical methane production occurs via direct and/or indirect reaction(s) in MESs.

The CO_2 reduction potential to methane $E^{0'}_{cat}$ at the biocathode is –0.24 V (vs. SHE) under the standard condition at pH=7. When coupled with H_2O oxidation ($E^{0'}_{an}$=0.81 V vs SHE) at the anode, methane production in an MES occurs thermodynamically by applying more than 1.05 V under the standard condition. If the oxidation of inorganic compounds with a lower potential (such as NH_4^+ oxidation to NO_3^- and N_2: $E^{0'}_{an}$=0.36 V and –0.29 V vs. SHE, respectively) occurs instead of H_2O oxidation, methane may be produced at a lower applied voltage. However, MES studies have not provided sufficient information on the oxidation reaction at the anode, with experiments being conducted at relatively high voltages.

In the present study, we designed an MES experiment in which an organic substrate was not supplied, and NH_4^+ was added to the anode chamber to investigate whether methane production is possible even at very low applied voltages. Although the reaction of electrotrophic methane production with NH_4^+ oxidation to N_2 thermodynamically proceeded even without a supply of electricity, this is the first study to report coupling to the NH_4^+ oxidative reaction. In addition, the microbial community was analyzed to identify the organisms involved in bioelectrical methane production.

Materials and Methods

MES set-up

The MES used in the present study consisted of two glass chambers, each with an effective volume of 70 mL, which were connected by a 10-cm salt bridge containing 2% (w/w) agar (KF-30; Fujirika) and 20% (w/w) KCl (Fig. S1). The top of each chamber was connected to a 10-mL loss-of-resistance glass syringe to release the pressure generated in the chamber by the gas produced and also facilitate gas collection. A 9-cm^2 electrode of carbon cloth (Toyobo) was installed in both chambers. The biocathode and anode electrodes were connected to a DC power supply (Array 3600 Series; T&C Technology) using a platinum wire. A 100-Ω resistor was inserted between the power supply and biocathode electrode to estimate the electric current by measuring voltage using a digital multimeter (FlePow; Levin Japan). Even if the external resister was inserted, the effect on the actual applied voltage was negligible when the internal resistance of the MES was high. A small amount of anaerobic sludge taken from a laboratory-scale upflow anaerobic sludge blanket (UASB) reactor was inoculated on the surface of the cathode electrode. Platinum powder (10% by weight of platinum on carbon powder; E-TEK, C-1 10% Pt on Vulcan XC-72) was coated on the surface of the anode, as described in previous studies (Müller and Spitzer, 1905; Nutt and Kapur, 1968; De Vooys *et al.*, 2001; Bunce and Bejan, 2011; Li *et al.*, 2017).

MES operation

The MES was operated in the batch-processing mode at 30°C in a thermostatic chamber. The anodic and biocathodic chambers were filled with the same medium without organic substances and deoxidized through a nitrogen purge. The medium was composed of $NaHCO_3$ (200 mg L^{-1}), NH_4Cl (190 mg L^{-1}), NaH_2PO_4 (17 mg L^{-1}), and Na_2HPO_4 (124 mg L^{-1}), as well as trace elements, including $FeSO_4{\cdot}7H_2O$ (7 mg L^{-1}), $CoCl_2{\cdot}6H_2O$ (1.7 mg L^{-1}), $ZnSO_4{\cdot}7H_2O$ (1.5 mg L^{-1}), HBO_3 (0.6 mg L^{-1}), $MnCl_2{\cdot}4H_2O$ (4.2 mg·L^{-1}), $NiCl_2{\cdot}4H_2O$ (0.4 mg L^{-1}), $CuCl_2{\cdot}2H_2O$ (0.27 mg L^{-1}), and $Na_2MoO_2{\cdot}2H_2O$ (0.25 mg L^{-1}), at a pH of 7.5. The medium was completely replaced at intervals of 3, 5, 6, and 13 d, with the batch experiment being repeated 20 times over 110 d of operation. Each batch duration time was determined according to gas production for gas sampling. Each batch experiment was performed at a constant applied voltage in the range of 0.05–3.0 V to investigate whether methane production is possible even at low voltages. After setting up the MES, a voltage was immediately supplied to enhance microbial activity at the biocathode, and the anode was unsterilized.

Sampling and analyses

The volume of gas production in the respective chambers was measured using an airtight syringe. CH_4, N_2, CO_2, and H_2 concentrations were then measured using a gas chromatograph equipped with a thermal conductivity detector (GC-TCD; Shimadzu GC-8A). NH_4^+, NO_3^-, and NO_2^- concentrations in the medium were measured by ion chromatography (Shimadzu HPLC-20A) at the start and end of each batch operation. Dissolved CH_4 and N_2 concentrations were estimated using Henry's law.

Microbial community

The sludge sample at the biocathode was collected on day 110 of the last MES operation and washed with phosphate buffer. DNA was extracted using the FastDNA® SPIN Kit for Soil (MP Biomedicals), according to the manufacturer's instructions. PCR amplification of the 16S rRNA gene was performed using the primer sets 341'F (5′-CCTAHGGGRBGCAGCAG-3′) and 805R (5′-GACTACHVGGGTATCTAATCC-3′) with KAFA HiFi Hotstart ReadyMix (Kapa Biosystems). PCR conditions were as follows: the initial denaturation of DNA at 95°C for 3 min, followed by 25 cycles at 95°C for 30 s, at 55°C for 30 s, and at 72°C for 30 s, with a final extension at 72°C for 5 min. The PCR product was purified and sequenced by the emulsion method using Illumina/Miseq (Illumina) at Hokkaido System Science. The sequences obtained were analyzed using QIIME (v1.8.0) (Caporaso *et al.*, 2010). Operational taxonomic units (OTUs) were grouped based on a threshold value of 97% identity for DNA using the UCLUST algorithm (Edgar, 2010). These OTUs were classified using the Greengenes database (McDonald *et al.*, 2012; Werner *et al.*, 2012).

Sequence data were deposited in the DDBJ database under DDBJ/EMBL/GenBank accession number DRA011341.

Results

Performance of batch experiments

In MES batch operations, we initially attempted to apply a relatively high voltage of 2.0 V over 3 d. Once a higher current of approximately 0.18 mA was observed, it immediately decreased to 0.09 mA and gradually declined over time, as shown in Fig. 1. However, no gas bubbles were visible in either the biocathode or anode chambers, despite the sludge inoculation being expected to enable methane production activity. The 3-d batch experiment was then

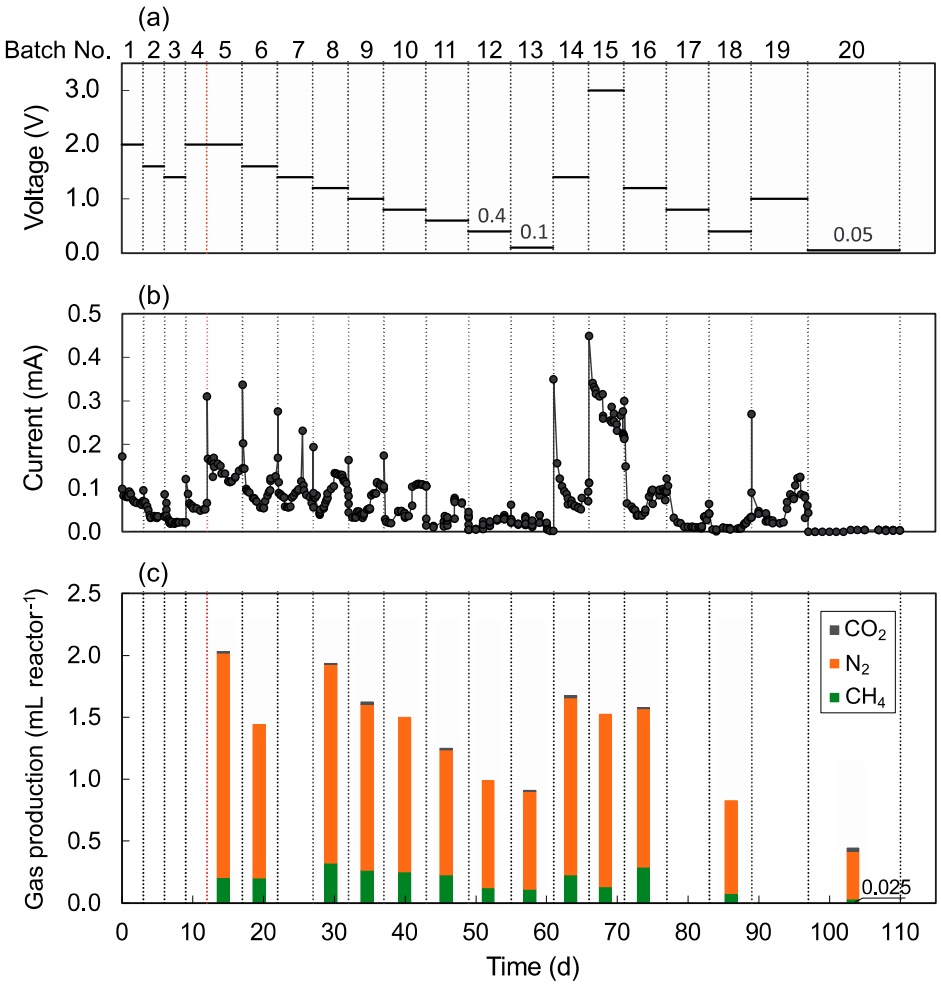

Fig. 1. Time courses of applied voltage (a), current (b), and gases (CH_4, N_2, and CO_2) produced (c) in batch experiments.

repeated with changes in bulk liquid, but at lower voltages of 1.6 V and 1.4 V, resulting in current behaviors that were the same as those at 2.0 V. Under these conditions, very few bubbles were observed in the biocathode chamber. In the next batch operation, bubbles were observed where the applied voltage was returned to 2.0 V. However, it was not possible to sample the gas produced because of its low volume.

Therefore, we changed the batch interval time from 3 to 5 d from day 12 onwards, except for some special batches. More bubbles were produced in the biocathode chamber and collected as a gas in the fifth batch operation at 2.0 V. The gas produced was approximately 2.0 mL on days 12–17 (Fig. 1). As expected, methane was detected, but its concentration was only 10.0%. The main component of the gas was N_2, with a very low concentration of CO_2. The current was markedly higher than that in the previous batch experiment at the same voltage. The current also decreased for approximately 3 d, but increased thereafter. A significant difference was observed in current behavior between the small and large gas production chambers. In control batch experiments without the inoculation, methane was not detected in the range of 1.0–2.0 V; however, hydrogen production was observed at an applied voltage higher than 1.2 V in the cathode chamber. Methane production is expected to be derived from inorganic carbon in the presence of microbes on the carbon cloth, the biological activity of which may be enhanced after 17 d of operation; however, no bubbles were observed in the anode chamber under any of the conditions used.

To investigate the effects of voltage on methane production, experiments were continuously performed while decreasing the applied voltage step-by-step down to 0.1 V until day 61 (Fig. 1). The current slightly decreased with voltage reductions; however, its pattern of behavior was similar in each batch period. Gas containing CH_4 and N_2 was produced at any voltage, except during days 22–27 when gas sampling failed.

Since high N_2 concentrations of approximately 75 to 90% were detected, we reconducted batch experiments under almost identical conditions over a range of 0.05–3.0 V on days 55–110 to reveal the source of N_2 yield by measuring ammonium, nitrate, and nitrite. In the last batch operation, we also attempted methane production at a very low voltage of 0.05 V. A small amount of gas containing 6.09% CH_4 was collected, even at the lowest voltage, particularly over a prolonged period of 13 d. NH_4^+ and NO_3^- concentrations decreased in both the biocathode and anode chambers (Fig. S2). Total nitrogen ions in the two chambers decreased in all batches, suggesting that the yield of N_2 was derived from

inorganic nitrogen ions. Regarding the nitrogen balance, a strong relationship was observed between the amount of consumed NH_4^+ plus NO_3^- and produced N_2 (Fig. S3). Cecconet *et al.* (2019) reported the accumulation of NO_2^- and N_2O in a biocathodic denitrification process for groundwater bioremediation. However, these intermediates in denitrification were not detected in this MES experiment. The lack of accumulation of intermediates may have been caused by the slow reaction.

Effects of voltage on gas production

Although a 100-Ω external resistor was inserted, the voltage supplied was nearly equal to the actual applied voltage between the biocathode and anode because the current versus supplied voltage was small throughout the experiment, as shown in Fig. 1. The gas production rate was significantly dependent on the applied voltage, as shown in Fig. 2. CH_4 production slightly increased in proportion to the voltage with 0.306 mL at 1.2 V, after which it decreased to 0.128 mL at 3.0 V. These results suggest that a very high voltage does not always enhance methane production and may have a negative effect on microbes. The N_2 production rate was similar to that of CH_4 with respect to the effects of voltage; however, large fluctuations were observed. This suggests that microbes also play a role in N_2 production. The retained microbes were expected to grow and increase with the operational time. However, they were slightly detached when bulk liquid was replaced as a result of changes in batch conditions. Therefore, the number of microbes was unstable, possibly contributing to fluctuations in gas production.

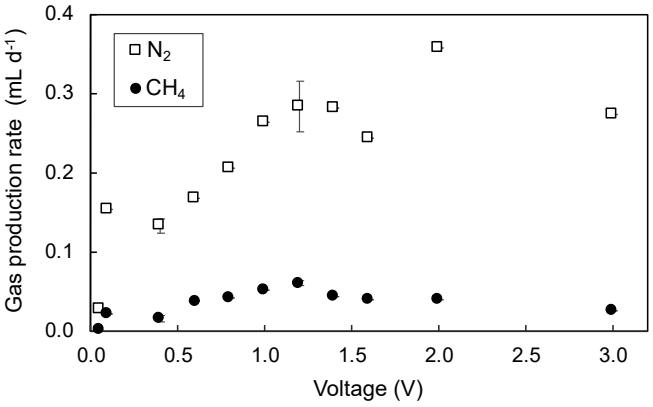

Fig. 2. Gas production rates at different applied voltages.

Microbial community

In the 16S rRNA gene sequencing of the biomass sample on day 110, more than 100,000 reads, including domain bacteria and archaea, were obtained, and the number of OTUs exceeded 1,200. Sequencing results revealed the presence of bacterial and archaeal communities (Fig. 3). Archaea comprised only 3.9% of the total reads.

The major families of bacteria were *Porphyromonadaceae*, *Rhodocyclaceae*, and *Geobacterceae*, accounting for 26.8, 11.4, and 10.7%, respectively. The three families made up approximately 45% of all microbes. Of the most dominant family *Porphyromonadaceae*, approximately 50% was the obligately anaerobic genus of *Petrimonas*, while 29.8% uncultured genera were detected (Fig. 3). *Petrimonas* consists of hydrogen-producing bacteria (Lu *et al.*, 2012; Sun *et al.*, 2015; Liu *et al.*, 2016), suggesting that hydrogen is pro-

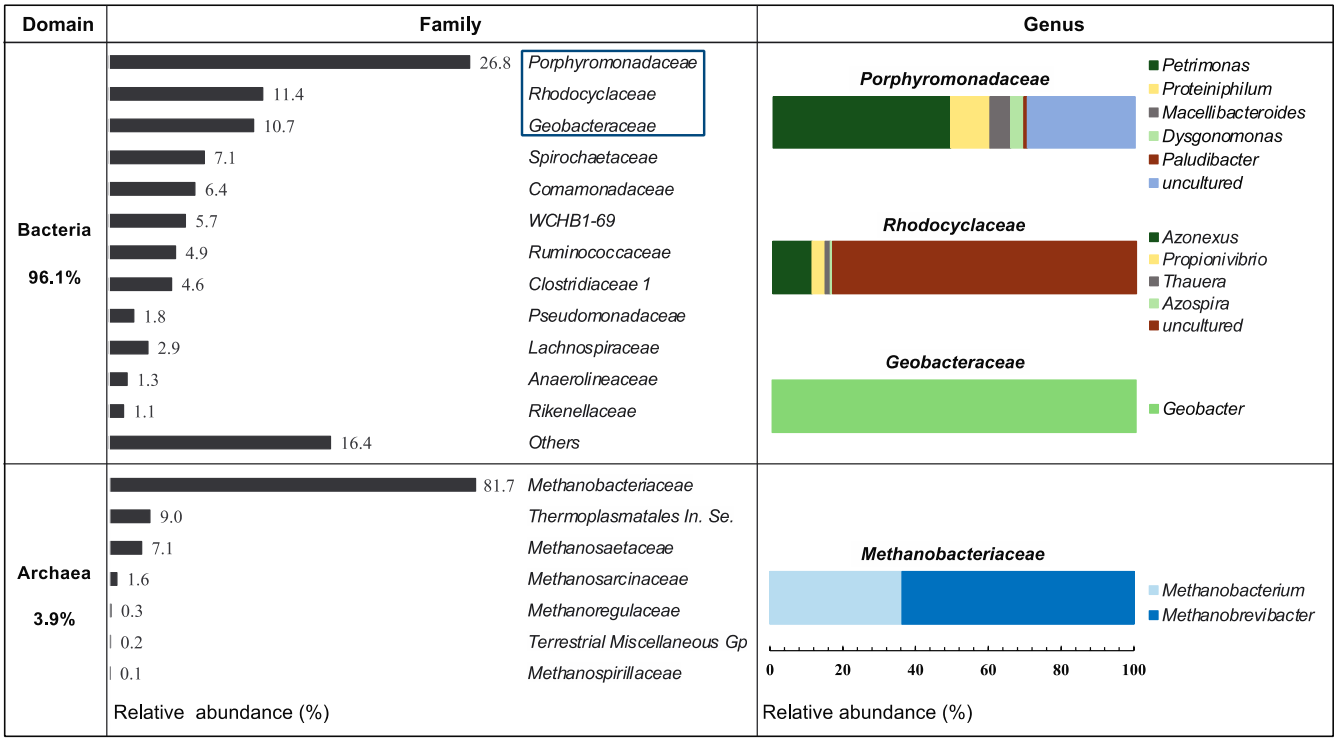

Fig. 3. Microbial community of a biomass sample on day 110, based on the 16S rRNA gene.

duced in the biocathode chamber. Most bacteria belonging to *Rhodocyclaceae* exhibit denitrification activity (Zhao *et al.*, 2013; Wang *et al.*, 2017). The predominant *Azonexus* genus detected, which may grow on molecular hydrogen as an electron donor (Zhao *et al.*, 2011; Liang *et al.*, 2021), plays an important role in the denitrification process to produce nitrogen gas. Only *Geobacter* was detected within the *Geobacterceae* family. The presence of electrically conductive pili or flagella on *Geobacter* species is reportedly linked to electron transfer in the MFC (Cabezas *et al.*, 2015; Yan *et al.*, 2020). In the present study, *Geobacter* appeared to be responsible for electron transfer to yield biogas.

Regarding archaea, all OTUs were *Euryarchaeota*. The majority of *Euryarchaeota* detected were methanogens, with the dominant family (81.7%) being *Methanobacteriaceae*, a hydrogen-utilizing methanogen (Fig. 3). Two genera, *Methanobrevibacter* and *Methanobacterium*, were detected at concentrations of 63.8 and 36.3%, respectively (Fig. 3). They played a major role in CH_4 production in the biocathode chamber. In addition, *Methanosaetaceae*, an obligate acetoclastic methanogen, was detected, albeit at a low concentration (7.1%); therefore, acetate may be produced and converted to CH_4. However, its contribution appears to have been insignificant.

The biological contributors to denitrification and methane production were identified; the produced gas containing CH_4 and N_2 may be explained by the presence of these microbes. Therefore, we demonstrated the biological production of CH_4 through the provision of electricity, even at very low voltages, and in the absence of organic substances in the MES.

Discussion

NH_4^+ oxidation was observed in the anode chamber, although at insignificant amounts, indicating that NH_4^+ was oxidized by donating electrons to the biocathode. Platinum is commonly accepted as the most promising catalyst in the electrochemical oxidation of ammonia (*e.g.*, De Vooys *et al.*, 2001; Li *et al.*, 2017). Müller and Spitzer (1905) reported that the anodic products of electrolyzing ammonia at a platinum anode were mainly NO_3^- and N_2 (25%–35%). With over-oxidation, NO_2^- and NO_3^- products were observed at applied voltages of higher than +0.6 V (vs Ag/AgCl) (Endo *et al.*, 2005; Bunce and Bejan, 2011). NO_3^- was also reportedly formed from NH_4^+ by catalytic oxidation with PtO_x (Fóti and Comninellis, 2004; Panizza and Cerisola, 2009). Since platinum powder was coated on the surface of the anode with a carbon cloth electrode in the present study, similar reactions to the electrolysis of water occurred; however, neither N_2 nor NO_2^- production was observed.

The oxidation of NH_4^+ at the anode may be represented as follows:

$$1/8\ NH_4^+ + 3/8\ H_2O \rightarrow 1/8\ NO_3^- + 5/4\ H^+ + e^- \quad (1)$$

The NO_3^- produced was transferred to the biocathode chamber through the salt bridge by diffusion, resulting in a decrease in the concentration of NO_3^- in the anode chamber (Fig. S3) because of N_2 production in the biocathode chamber.

CH_4 and N_2 production in the biocathode chamber suggest that the reduction reactions of NO_3^- and CO_2, respectively, are represented as follows:

$$1/8\ CO_2 + H^+ + e^- \rightarrow 1/8\ CH_4 + 1/4\ H_2O \quad (2)$$
$$1/5\ NO_3^- + 6/5\ H^+ + e^- \rightarrow 1/10\ N_2 + 3/5\ H_2O \quad (3)$$

Based on Faraday's laws of electrolysis, the number of donated electrons, *Ne* [mol], may be calculated from the measured current using the following equation:

$$Ne = \frac{\int I dt}{F} \quad (4)$$

where I is current (A), t is time (s), and F is Faraday's constant (C mol^{-1}).

Assuming that all yield electrons *Ne*, calculated as per Eq. (4), are used for the reduction of only CO_2 or NO_3^-, the amounts of CH_4 and N_2 produced versus the electron yield were calculated using Eqs. (2) and (3), respectively. Measured CH_4 production was markedly less than the calculated value, while measured N_2 production was also smaller than the theoretical value under this assumption (Fig. S4). Therefore, the two reductions were simultaneously performed, and *Ne* was distributed in both reductions. The required electrons for measured CH_4 production from CO_2 reduction were estimated using Eq. (2), with the ratio of required electrons to total measured electrons *Ne* shown in Fig. 4. The electron ratio slightly decreased with the applied voltage, rather than remaining constant. At very low voltages of 0.05 and 0.1 V, approximately 40% of the current was used for CO_2 reduction to CH_4, while only approximately 5% was utilized at 3 V. Assuming that the current to electron ratio was used for CO_2 reduction and that the remaining electrons were used for NO_3^- reduction to N_2, as per Eq. (3), it is possible to estimate CH_4 and N_2 production from *Ne*. Fig. 5 compares measured and estimated CH_4 and N_2 production, with the curve showing the relationship between the electron ratio and voltage in Fig. 4 used in the calculation. A good agreement was observed for both CH_4 and N_2 production, meaning that the electron balance was almost maintained in this experiment, and the production of CH_4 and N_2

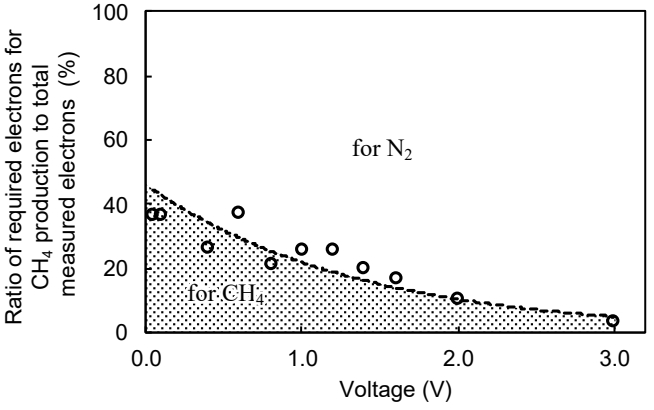

Fig. 4. Relationship between the ratio of required electrons for CH_4 production to total measured electrons *Ne* and applied voltage.

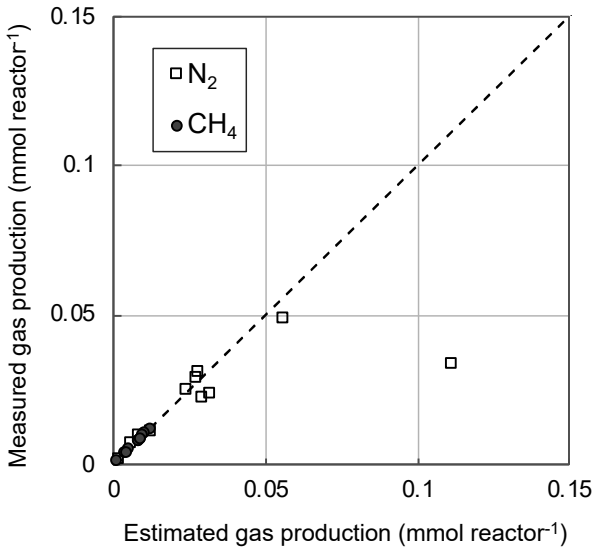

Fig. 5. Comparison between measured and estimated gas production. An estimation of produced CH_4 and N_2 was performed assuming that all electrons *Ne* were used for the reduction of both CO_2 and NO_3^-, while electrons from the ratio in Fig. 4 were used for CH_4 production.

may theoretically be performed in the biocathode chamber according to the reduction reactions of Eqs. (2) and (3). However, at a high voltage of 3.0 V, the calculated value of produced N_2 was markedly greater than the measured value (Fig. 5), indicating that some electrons were used for other reductions by chemical and/or microbial reactions. If NO_3^- reduction to NH_4^+ instead of N_2, which is the reverse reaction at the anode, is performed at the biocathode at high voltages, the reversible reactions will lead to a waste of electrons yielded in the MES. A previous study reported that a high imposing voltage exerted a negative effect on methanogens (Ding *et al.*, 2016) and nitrate-reducing bacteria (Li *et al.*, 2001; Ding *et al.*, 2016), and excessive voltage not only inhibited microbial activity, but also induced chemical reactions.

Hydrogen was not detected. However, hydrogen was expected to be produced in the biocathode chamber because of the presence of hydrogenotrophic methanogens, such as *Methanobacterium* and *Methanobrevibacter*, and the hydrogenotrophic denitrifiers of *Rhodocyclaceae (Azonexus)*. Furthermore, the hydrogen-producing bacteria *Petrimonas* were present. Previous studies on MESs also detected hydrogenotrophic methanogens, such as *Methanobrevibacter*, *Methanocorpusculum*, and *Methanoculleus sp.* (Sasaki *et al.*, 2011; Van Eerten-Jansen *et al.*, 2013; Jiang *et al.*, 2014; Siegert *et al.*, 2015). Cheng *et al.* (2019) reported that *Methanobacterium palustre* methanogens directly use electrons to produce methane without organic substances. However, this study did not provide sufficient evidence of electron utilization. Although *Geobacter* species are well-known to have the ability to transfer electrons, it was surprising that the dominant genus identified in this study was *Petrimonas* due to the lack of available information on the electron transfer ability of this genus. However, *Petrimonas* may accept electrons to produce hydrogen, which may be provided to the detected hydrogenotrophic methanogens and denitrifiers in the absence of an organic substrate in the reactor. During the bio-electrochemical production of hydrogen, it is reasonable to assume that a very small amount of hydrogen is electrochemically formed and biologically consumed. However, this electrochemical pathway may only negligibly contribute to production because hydrogen-producing *Petrimonas* was dominant in the microbial community.

Hydrogenotrophic methanogens and denitrifiers compete for the shared substrate of H_2 produced at the biocathode. Denitrifiers are dominant in wastewater treatments under anoxic conditions in the presence of nitrate; this phenomenon may be explained by Gibbs free energy. The energy obtained in the denitrification reaction of Eq. (3) is markedly larger than that in the methane production reaction of Eq. (2). However, under hydrogenotrophic conditions, methanogens and denitrifiers were both enriched even though denitrification dominated throughout the experiment. At the lowest applied voltage of 0.05 V, approximately 40% of the H_2 produced was utilized for methane production by the methanogens. However, with an increase in the applied voltage, the utilization ratio decreased (Fig. 4), indicating that the applied voltage affected the utilization of H_2 by methanogens and denitrifiers. H_2 production and concentrations are expected to increase at higher voltages. Microbes with a high affinity for substrates generally consume substrates faster than those with low affinity. The Monod constant K_m for H_2 uptake was reportedly 1 and 2 μM for *Methanobacterium ruminatium* (Lovley and Goodwin, 1988) and *Methanobrevibacter formicium* (Schauer and Ferry, 1980), respectively. In contrast, Smith *et al.* (1994) reported that the K_m of hydrogenotrophic denitrifiers ranged between 0.3 and 3.32 μM. If methanogens had lower K_m than the denitrifiers at the biocathode, indicating a higher affinity for H_2 and lower maximum H_2 uptake rate, the phenomenon of a decreasing current ratio in methane production with an increasing applied voltage, as shown in Fig. 4, may be explained by this difference in K_m between methanogens and denitrifiers.

Based on the experimental results obtained, Fig. 6 proposes a scheme for the process of electronic methane production used in the present study, without organic substances in the MES. Ammonium is oxidized to nitrate by a Pt catalyst at the anode with electron release. The nitrate formed is transferred into the biocathode chamber through the salt bridge. At the biocathode, the hydrogen-producing bacteria *Petrimonas* biochemically produce H_2 by accepting electrons and protons. The H_2 produced is biologically consumed by hydrogenotrophic methanogens of *Methanobacterium* and *Methanobrevibacter* coupled with CO_2 uptake, and by the hydrogenotrophic denitrifiers of *Rhodocyclaceae (Azonexus)*, with transferred nitrate reduction resulting in the production of methane and N_2, respectively. Consequently, the overall reaction at the anode and biocathode in the MES is as follows:

$$1/8\ CO_2+1/3\ NH_4^+ \rightarrow 1/8\ CH_4+1/6\ N_2+1/3\ H^++1/4\ H_2O$$
$$\Delta G^{0\prime}=-3.134\ \text{kJ mol}^{-1}\ e^- \quad (5)$$

Thermodynamically, this reaction proceeds under the standard condition even without the provision of external

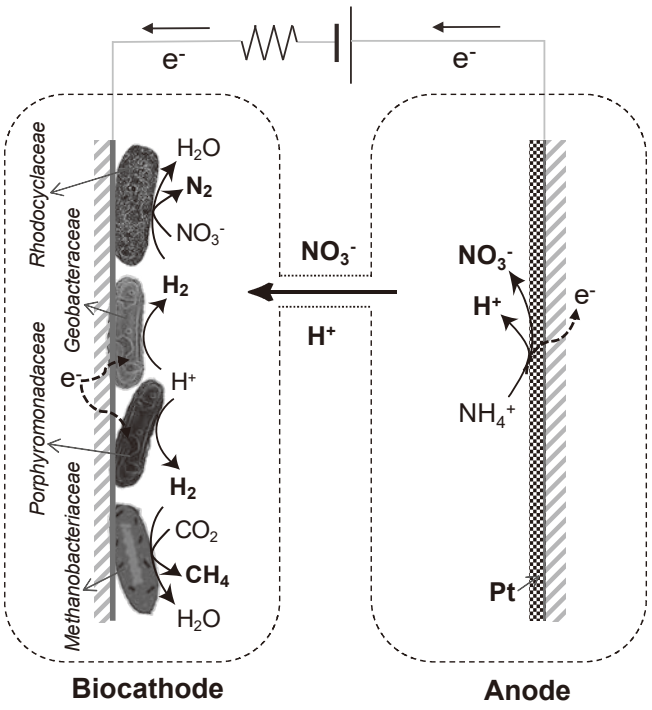

Fig. 6. Scheme of electronic methane and nitrogen production in MES without organic substances.

energy, such as electricity, because of the negative Gibbs free energy $\Delta G^{0'}$ value. The actual condition, for example, at an applied voltage of 0.1 V was as follows: p_{CH4}=0.36 atm, p_{N2}=0.65 atm, p_{CO2}=0.03 atm, $[H^+]=15.1\times10^{-5}$ M, and $[NH_4^+]=5.38\times10^{-3}$ M. In this case, the actual Gibbs free energy ΔG (=$\Delta G^{0'}$+RT ln[K]) was estimated to have a value of –5.18 kJ mol^{-1} e$^-$, suggesting that the production of methane and N_2 is expected. Therefore, the present study revealed that even in an inorganic environment, biological methane production coupled with denitrification is possible in combination with catalytic ammonium oxidation, even at very low applied voltages <0.1 V, through the three key players of hydrogenotrophic methanogens, denitrifiers, and hydrogen-producing bacteria.

Acknowledgements

This research was supported by the Japan Society for the Promotion of Science (JSPS) as a Grant-in-Aid for scientific research (grant numbers 17H01300). We would like to thank Editage (www.editage.jp) for English language editing.

References

Bunce, N.J., and Bejan, D. (2011) Mechanism of electrochemical oxidation of ammonia. *Electrochim Acta* **56**: 8085–8093.

Cabezas, A., Pommerenke, B., Boon, N., and Friedrich, M.W. (2015) *Geobacter*, *Anaeromyxobacter* and *Anaerolineae* populations are enriched on anodes of root exudate-driven microbial fuel cells in rice field soil. *Environ Microbiol Rep* **7**: 489–497.

Caporaso, J.G., Kuczynski, J., Stombaugh, J., Bittinger, K., Bushman, F.D., Costello, E.K., *et al.* (2010) QIIME allows analysis of high-throughput community sequencing data. *Nat Methods* **7**: 335–336.

Cecconet, D., Bolognesi, S., Callegari, A., and Capodaglio, A.G. (2019) Controlled sequential biocathodic denitrification for contaminated groundwater bioremediation. *Sci Total Environ* **651**: 3107–3116.

Cheng, S., Xing, D., Call, D.F., and Logan, B.E. (2009) Direct biological conversion of electrical current into methane by electromethanogenesis. *Environ Sci Technol* **43**: 3953–3958.

Clauwaert, P., Tolêdo, R., van der Ha, D., Crab, R., Verstraete, W., Hu, H., *et al.* (2008) Combining biocatalyzed electrolysis with anaerobic digestion. *Water Sci Technol* **57**: 575–579.

Clauwaert, P., and Verstraete, W. (2009) Methanogenesis in membraneless microbial electrolysis cells. *Appl Microbiol Biotechnol* **82**: 829–836.

De Vooys, A.C.A., Koper, M.T.M., Van Santen, R.A., and Van Veen, J.A.R. (2001) The role of adsorbates in the electrochemical oxidation of ammonia on noble and transition metal electrodes. *J Electroanal Chem* **506**: 127–137.

Ding, A., Yang, Y., Sun, G., and Wu, D. (2016) Impact of applied voltage on methane generation and microbial activities in an anaerobic microbial electrolysis cell (MEC). *Chem Eng J (Amsterdam, Neth)* **283**: 260–265.

Edgar, R.C. (2010) Search and clustering orders of magnitude faster than BLAST. *Bioinformatics* **26**: 2460–2461.

Eerten-Jansen, M.C.A.A.V., Heijne, A.T., Buisman, C.J.N., and Hamelers, H.V.M. (2012) Microbial electrolysis cells for production of methane from CO_2: long-term performance and perspectives. *Int J Energy Res* **36**: 809–819.

Endo, K., Katayama, Y., and Miura, T. (2005) A rotating disk electrode study on the ammonia oxidation. *Electrochim Acta* **50**: 2181–2185.

Fóti, G., and Comninellis, C. (2004) Electrochemical oxidation of organics on iridium oxide and synthetic diamond based electrodes. In *Mod Aspects Electrochem*. White, R.E., Conway, B.E., Vayenas, C.G., and Gamboa-Adelco, M.E. (eds). Boston, MA: Springer, pp. 87–130.

Holmes, D.E., Shrestha, P.M., Walker, D.J.F., Dang, Y., Nevin, K.P., Woodard, T.L., and Lovley, D.R. (2017) Metatranscriptomic evidence for direct interspecies electron transfer between *Geobacter* and *Methanothrix* species in methanogenic rice paddy soils. *Appl Environ Microbiol* **83**: e00223–17.

Jiang, Y., Su, M., and Li, D. (2014) Removal of sulfide and production of methane from carbon dioxide in Microbial Fuel Cells–Microbial Electrolysis Cell (MFCs–MEC) coupled system. *Appl Biochem Biotechnol* **172**: 2720–2731.

Lee, J.-Y., Park, J.-H., and Park, H.-D. (2017) Effects of an applied voltage on direct interspecies electron transfer via conductive materials for methane production. *Waste Manage (Oxford, U K)* **68**: 165–172.

Li, X.-G., Cao, H.-B., Wu, J.-C., and Yu, K.-T. (2001) Inhibition of the metabolism of nitrifying bacteria by direct electric current. *Biotechnol Lett* **23**: 705–709.

Li, Z.-F., Wang, Y., and Botte, G.G. (2017) Revisiting the electrochemical oxidation of ammonia on carbon-supported metal nanoparticle catalysts. *Electrochim Acta* **228**: 351–360.

Liang, D., He, W., Li, C., Wang, F., Crittenden, J.C., and Feng, Y. (2021) Remediation of nitrate contamination by membrane hydrogenotrophic denitrifying biofilm integrated in microbial electrolysis cell. *Water Res* **188**: 116498.

Liu, Q., Ren, Z.J., Huang, C., Liu, B., Ren, N., and Xing, D. (2016) Multiple syntrophic interactions drive biohythane production from waste sludge in microbial electrolysis cells. *Biotechnol Biofuels* **9**: 162.

Logan, B.E., Hamelers, B., Rozendal, R., Schröder, U., Keller, J., Freguia, S., *et al.* (2006) Microbial fuel cells: Methodology and technology. *Environ Sci Technol* **40**: 5181–5192.

Lohner, S.T., Deutzmann, J.S., Logan, B.E., Leigh, J., and Spormann, A.M. (2014) Hydrogenase-independent uptake and metabolism of electrons by the archaeon *Methanococcus maripaludis*. *ISME J* **8**: 1673–1681.

Lovley, D.R., and Goodwin, S. (1988) Hydrogen concentrations as an indicator of the predominant terminal electron-accepting reactions in aquatic sediments. *Geochim Cosmochim Acta* **52**: 2993–3003.

Lu, L., Xing, D., and Ren, N. (2012) Pyrosequencing reveals highly diverse microbial communities in microbial electrolysis cells involved in enhanced H_2 production from waste activated sludge. *Water Res* **46**: 2425–2434.

McDonald, D., Price, M.N., Goodrich, J., Nawrocki, E.P., DeSantis, T.Z., Probst, A., *et al.* (2012) An improved Greengenes taxonomy with explicit ranks for ecological and evolutionary analyses of bacteria and archaea. *ISME J* **6**: 610–618.

Müller, E., and Spitzer, F. (1905) Über die Elektrolytische Oxydation des Ammoniaks und Ihre Abhängigkeit vom Anodenmaterial. *Z Elektrochem Angew Physik Chem* **11**: 917–931 (in German).

Nutt, C.W., and Kapur, S. (1968) Mechanism of oxidation of ammonia on platinum. *Nature* **220**: 697–698.

Onodera, I. (2013) Development of methane fermentation technology for wastewater treatment. *Tappi J* **67**: 82–85.

Panizza, M., and Cerisola, G. (2009) Direct and mediated anodic oxidation of organic pollutants. *Chem Rev* **109**: 6541–6569.

Park, J., Lee, B., Tian, D., and Jun, H. (2018) Bioelectrochemical enhancement of methane production from highly concentrated food waste in a combined anaerobic digester and microbial electrolysis cell. *Bioresour Technol* **247**: 226–233.

Peng, H., Zhao, Z., Xiao, H., Yang, Y., Zhao, H., and Zhang, Y. (2019) A strategy for enhancing anaerobic digestion of waste activated sludge: Driving anodic oxidation by adding nitrate into microbial electrolysis cell. *J Environ Sci (Beijing, China)* **81**: 34–42.

Rabaey, K., and Rozendal, R. (2010) Microbial electrosynthesis—Revisiting the electrical route for microbial production. *Nat Rev Microbiol* **8**: 706–716.

Rice, D.D., and Claypool, G.E. (1981) Generation, accumulation, and resource potential of biogenic gas. *AAPG Bull* **65**: 5–25.

Rotaru, A.-E., Shrestha, P.M., Liu, F., Shrestha, M., Shrestha, D., Embree, M., *et al.* (2013) A new model for electron flow during anaerobic digestion: direct interspecies electron transfer to *Methanosaeta* for the reduction of carbon dioxide to methane. *Energy Environ Sci* **7**: 408–415.

Sarmin, S., Ethiraj, B., Islam, M.A., Ideris, A., Yee, C.S., and Khan, M.M.R. (2019) Bio-electrochemical power generation in petrochemical wastewater fed microbial fuel cell. *Sci Total Environ* **695**: 133820.

Sasaki, K., Morita, M., Sasaki, D., Hirano, S., Matsumoto, N., Ohmura, N., and Igarashi, Y. (2011) Methanogenic communities on the electrodes of bioelectrochemical reactors without membranes. *J Biosci Bioeng* **111**: 47–49.

Schauer, N.L., and Ferry, J.G. (1980) Metabolism of formate in *Methanobacterium formicicum*. *J Bacteriol* **142**: 800–807.

Schoell, M. (1988) Multiple origins of methane in the Earth. *Chem Geol* **71**: 1–10.

Siegert, M., Li, X.-F., Yates, M.D., and Logan, B.E. (2015) The presence of hydrogenotrophic methanogens in the inoculum improves methane gas production in microbial electrolysis cells. *Front Microbiol* **5**: 778.

Smith, R.L., Ceazan, M.L., and Brooks, M.H. (1994) Autotrophic, hydrogen-oxidizing, denitrifying bacteria in groundwater, potential agents for bioremediation of nitrate contamination. *Appl Environ Microbiol* **60**: 1949–1955.

Sun, R., Zhou, A., Jia, J., Liang, Q., Liu, Q., Xing, D., and Ren, N. (2015) Characterization of methane production and microbial community shifts during waste activated sludge degradation in microbial electrolysis cells. *Bioresour Technol* **175**: 68–74.

Townsend-Small, A., Disbennett, D., Fernandez, J.M., Ransohoff, R.W., Mackay, R., and Bourbonniere, R.A. (2016) Quantifying emissions of methane derived from anaerobic organic matter respiration and natural gas extraction in Lake Erie. *Limnol Oceanogr* **61**: S356–S366.

Van Eerten-Jansen, M.C.A.A., Veldhoen, A.B., Plugge, C.M., Stams, A.J.M., Buisman, C.J.N., and Ter Heijne, A. (2013) Microbial community analysis of a methane-producing biocathode in a bioelectrochemical system. *Archaea* **2013**: 481784.

Villano, M., Aulenta, F., Ciucci, C., Ferri, T., Giuliano, A., and Majone, M. (2010) Bioelectrochemical reduction of CO_2 to CH_4 via direct and indirect extracellular electron transfer by a hydrogenophilic methanogenic culture. *Bioresour Technol* **101**: 3085–3090.

Wagner, R.C., Regan, J.M., Oh, S.-E., Zuo, Y., and Logan, B.E. (2009) Hydrogen and methane production from swine wastewater using microbial electrolysis cells. *Water Res* **43**: 1480–1488.

Wang, W., Zhang, Y., Li, M., Wei, X., Wang, Y., Liu, L., *et al.* (2020) Operation mechanism of constructed wetland-microbial fuel cells for wastewater treatment and electricity generation: A review. *Bioresour Technol* **314**: 123808.

Wang, Y., Tian, H., Huang, F., Long, W., Zhang, Q., Wang, J., *et al.* (2017) Time-resolved analysis of a denitrifying bacterial community revealed a core microbiome responsible for the anaerobic degradation of quinoline. *Sci Rep* **7**: 14778.

Werner, J.J., Koren, O., Hugenholtz, P., DeSantis, T.Z., Walters, W.A., Caporaso, J.G., *et al.* (2012) Impact of training sets on classification of high-throughput bacterial 16s rRNA gene surveys. *ISME J* **6**: 94–103.

Whiticar, M.J., Faber, E., and Schoell, M. (1986) Biogenic methane formation in marine and freshwater environments: CO_2 reduction vs. acetate fermentation—Isotope evidence. *Geochim Cosmochim Acta* **50**: 693–709.

Whiticar, M.J. (1999) Carbon and hydrogen isotope systematics of bacterial formation and oxidation of methane. *Chem Geol* **161**: 291–314.

Yan, Y., Li, T., Zhou, L., Tian, L., Yan, X., Liao, C., *et al.* (2020) Spatially heterogeneous propionate conversion towards electricity in bioelectrochemical systems. *J Power Sources* **449**: 227557.

Zhao, H.-P., Van Ginkel, S., Tang, Y., Kang, D.-W., Rittmann, B., and Krajmalnik-Brown, R. (2011) Interactions between perchlorate and nitrate reductions in the biofilm of a hydrogen-based membrane biofilm reactor. *Environ Sci Technol* **45**: 10155–10162.

Zhao, H.-P., Ontiveros-Valencia, A., Tang, Y., Kim, B., Ilhan, Z.E., Krajmalnik-Brown, R., and Rittmann, B. (2013) Using a two-stage hydrogen-based membrane biofilm reactor (MBfR) to achieve complete perchlorate reduction in the presence of nitrate and sulfate. *Environ Sci Technol* **47**: 1565–1572.

Zhao, Z., Zhang, Y., Yu, Q., Ma, W., Sun, J., and Quan, X. (2016) Enhanced decomposition of waste activated sludge via anodic oxidation for methane production and bioenergy recovery. *Int Biodeterior Biodegrad* **106**: 161–169.

Zhen, G., Kobayashi, T., Lu, X., and Xu, K. (2015) Understanding methane bioelectrosynthesis from carbon dioxide in a two-chamber microbial electrolysis cells (MECs) containing a carbon biocathode. *Bioresour Technol* **186**: 141–148.

Microbes Environ. Vol. 34, No. 3, 278-292, 2019
https://www.jstage.jst.go.jp/browse/jsme2 doi:10.1264/jsme2.ME19017

MOST CITED ORIGINAL PAPER PUBLISHED
IN THIS THREE YEARS [2019-2021] (18 citations)

Geochemical and Metagenomic Characterization of Jinata Onsen, a Proterozoic-Analog Hot Spring, Reveals Novel Microbial Diversity including Iron-Tolerant Phototrophs and Thermophilic Lithotrophs

Lewis M. Ward[1,2,3]*, Airi Idei[4], Mayuko Nakagawa[2], Yuichiro Ueno[2,5,6], Woodward W. Fischer[3], and Shawn E. McGlynn[2]*

[1]*Department of Earth and Planetary Sciences, Harvard University, Cambridge, MA 02138 USA;* [2]*Earth-Life Science Institute, Tokyo Institute of Technology, Meguro, Tokyo, 152–8550, Japan;* [3]*Division of Geological and Planetary Sciences, California Institute of Technology, Pasadena, CA 91125 USA;* [4]*Department of Biological Sciences, Tokyo Metropolitan University, Hachioji, Tokyo 192–0397, Japan;* [5]*Department of Earth and Planetary Sciences, Tokyo Institute of Technology, Meguro, Tokyo, 152–8551, Japan; and* [6]*Department of Subsurface Geobiological Analysis and Research, Japan Agency for Marine-Earth Science and Technology, Natsushima-cho, Yokosuka 237–0061, Japan*

(Received February 1, 2019—Accepted May 22, 2019—Published online August 14, 2019)

Hydrothermal systems, including terrestrial hot springs, contain diverse geochemical conditions that vary over short spatial scales due to progressive interactions between reducing hydrothermal fluids, the oxygenated atmosphere, and, in some cases, seawater. At Jinata Onsen on Shikinejima Island, Japan, an intertidal, anoxic, iron-rich hot spring mixes with the oxygenated atmosphere and seawater over short spatial scales, creating diverse chemical potentials and redox pairs over a distance of ~10 m. We characterized geochemical conditions along the outflow of Jinata Onsen as well as the microbial communities present in biofilms, mats, and mineral crusts along its traverse using 16S rRNA gene amplicon and genome-resolved shotgun metagenomic sequencing. Microbial communities significantly changed downstream as temperatures and dissolved iron concentrations decreased and dissolved oxygen increased. Biomass was more limited near the spring source than downstream, and primary productivity appeared to be fueled by the oxidation of ferrous iron and molecular hydrogen by members of *Zetaproteobacteria* and *Aquificae*. The microbial community downstream was dominated by oxygenic *Cyanobacteria*. *Cyanobacteria* are abundant and active even at ferrous iron concentrations of ~150 μM, which challenges the idea that iron toxicity limited cyanobacterial expansion in Precambrian oceans. Several novel lineages of Bacteria are also present at Jinata Onsen, including previously uncharacterized members of the phyla *Chloroflexi* and *Calditrichaeota*, positioning Jinata Onsen as a valuable site for the future characterization of these clades.

Key words: geomicrobiology, Proterozoic, microaerobic, astrobiology, ferruginous, thermophiles

A major theme of environmental microbiology has been the enumeration of microbial groups with the capacity to exploit the diverse chemical potentials (*i.e.* chemical disequilibria) that occur in nature (*e.g.* 7, 25, 111). Hot springs, with their varied chemical compositions, provide reservoirs of novel microbial diversity; environmental and geochemical conditions in these environments select lineages and metabolic pathways that are distinct from other Earth-surface environments (*e.g.* 3, 9, 26, 126, 127). In addition to their value as sources of microbial diversity, hot springs are valuable test beds for understanding microbial community processes driven by different suites of metabolism (*e.g.* 50). This in turn allows these systems to serve as process analogs and also to provide a window into biosphere functions during early times in Earth history, for example when the O_2 content of surface waters was low or non-existent. Most surface ecosystems today are fueled entirely by oxygenic photosynthesis by plants, algae, and *Cyanobacteria*; in contrast, hot spring microbial communities are commonly supported by lithotrophic or anoxygenic phototrophic organisms that derive energy and electrons for carbon fixation by oxidizing geologically sourced electron donors such as Fe^{2+}, sulfide, arsenite, and molecular hydrogen (*e.g.* 34, 63, 69, 105, 126). These communities may therefore provide insight into the flow of energy and mass that characterized microbial communities on the early Earth or even other planets, in which oxygenic photosynthesis may be absent or less significant and anoxygenic photosynthetic or lithotrophic metabolisms may play a larger role, resulting in lower overall rates of primary productivity (*e.g.* 12, 63, 97, 131–133).

Here, we present a geomicrobiological characterization of a novel Precambrian Earth process analog site: Jinata Onsen on Shikinejima Island, Tokyo Prefecture, Japan. While a small number of metagenome-assembled genomes have previously been recovered from Jinata (125, 127), we describe here the first overall characterization of the geochemistry and microbial community of this site. This site supports sharp gradients in geochemistry that in some ways recapitulate spatially environmental transitions that occurred temporally during Proterozoic time. The modern, sulfate-rich, well-oxygenated ocean that we see today is a relatively recent state, typical of only the last few hundred million years (*e.g.* 76). For the first half of Earth history, until ~2.3 billion years ago (Ga), the atmosphere and oceans were anoxic (52), and the oceans were

* Corresponding authors.
Lewis M. Ward: E-mail: lewis_ward@fas.harvard.edu;
Tel: +1–617–998–1750; Fax: +1–617–384–7396.
Shawn E. McGlynn: E-mail: mcglynn@elsi.jp;
Tel: +81–3–5734–3414; Fax: +81–3–5734–3416.

rich in dissolved iron but poor in sulfur (120). Following the Great Oxygenation Event ~2.3 Ga, the atmosphere and surface waters accumulated oxygen, and the oceans became more strongly redox stratified with oxygenated surface waters and anoxic deeper waters, rich in either dissolved iron or sulfide (88). At Jinata Onsen, this range of geochemical conditions is recapitulated over just a few meters, providing an ideal space-for-time analog to test hypotheses of how microbial diversity and productivity may have varied as environmental conditions changed through Earth history.

At Jinata hot spring, anoxic, iron-rich hydrothermal fluids feed a subaerial spring that flows into a small bay, and mixes with seawater over the course of a few meters. Over its course, the waters transition from low-oxygen, iron-rich conditions analogous to some aspects of early Proterozoic oceans, toward iron-poor and oxygen-rich conditions typical of modern coastal oceans. In upstream regions of the stream where oxygenic *Cyanobacteria* are at very low abundance, biomass is visibly sparse; however, downstream, biomass accumulates in the form of thick microbial mats containing abundant *Cyanobacteria*. Visible differences in accumulation and appearance of biomass across the temperature and redox gradient establish the hypothesis that microbial community composition, as well as the magnitude and metabolic drivers of primary productivity, varies along the spring flow. To begin testing this hypothesis and to provide a baseline description of the geochemistry and microbiology of this site in support of future investigation, we performed geochemical measurements, 16S rRNA gene amplicon sequencing, and genome-resolved metagenomic sequencing to recover draft genomes of diverse novel microbial lineages that inhabit Jinata Onsen.

Materials and Methods

Geological context and sedimentology of Jinata

Jinata Onsen is located at 34.318 N, 139.216 E on the island of Shikinejima, Tokyo Prefecture, Japan. Shikinejima is part of the Izu Islands, a chain of volcanic islands that formed in the last few million years along the northern edge of the Izu-Bonin-Mariana Arc (56). Shikinejima is formed of Late Paleopleistocene- to-Holocene non-alkaline felsic volcanics and Late-Miocene to Pleistocene non-alkaline pyroclastic volcanic flows, with Jinata Onsen located on a small bay on the southern side of the island (Fig. 1).

Sample collections

Five sites were sampled at Jinata Onsen: the Source Pool, Pool 1, Pool 2, Pool 3, and the Outflow (Fig. 1 and 2). During the first sampling trip in January 2016, two whole community DNA samples were collected from each site for 16S rRNA gene amplicon sequencing. During the second sampling trip, additional DNA was collected from the Source Pool and Pool 2 for shotgun metagenomic sequencing along with gas samples for qualitative analysis. Samples for quantitative gas analysis were collected in October 2017 and April 2018.

Samples were collected as mineral scrapings of loosely attached, fluffy iron oxide coatings from surfaces and clasts upstream (Source Pool and Pool 1) and as samples of microbial mats downstream (Pools 2 and 3 and Outflow) using sterile forceps and spatulas (~0.25 cm^3 of material). Immediately after sampling, cells were lysed and DNA was preserved with a Zymo Terralyzer BashingBead Matrix and Xpedition Lysis Buffer. Lysis was achieved by attaching tubes to the blade of a cordless reciprocating saw (Black & Decker, Towson, MD, USA) and operating for 1 min. Aqueous geochemistry samples consisted of water collected with sterile syringes and filtered through a 0.2-µm filter. Gas samples were collected near sites of ebullition emerging from the bottom of the Source Pool; collection was performed into serum vials by water substitution that were then sealed underwater to prevent contamination by air.

Geochemical analysis

Dissolved oxygen (DO), pH, and temperature measurements were performed *in situ* using an Extech DO700 8-in-1 Portable Dissolved Oxygen Meter (FLIR Commercial Systems, Nashua, NH, USA). In upstream regions at which water temperatures were higher than the operating temperature of the oxygen probe (50°C), DO concentrations were estimated by filling a 50-mL Falcon tube with spring water, sealing the tube to prevent gas exchange, and allowing the water to cool to acceptable temperatures before reopening the tube and immediately measuring oxygen concentrations, thereby

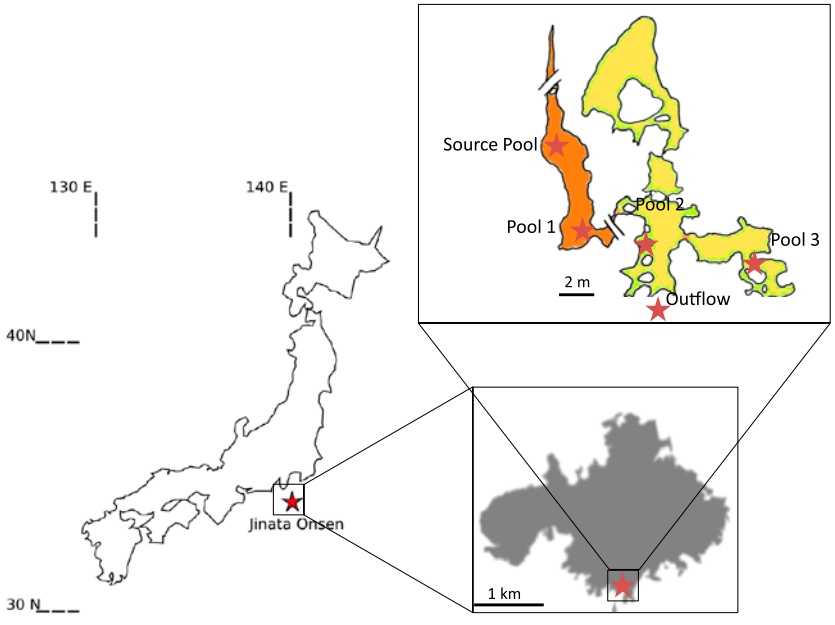

Fig. 1. Location of Jinata Onsen on Shikinejima Island, Japan, and inset overview sketch of the field site with sampling localities marked.

Fig. 2. Representative photos of Jinata. A) Panorama of the field site, with the Source Pool on the left (Pool 1 below), Pools 2 and 3 in the center, and the Outflow to the bay on the right. B) Undistorted view north up the canyon. C) Undistorted view south towards the bay, overlooking Pool 2. D) The Source Pool, coated in floc-y iron oxides and bubbling with a gas mixture containing CO_2, CH_4 and trace, potentially variable, H_2. E) Pool 2, with a mixture of red iron oxides and green from *Cyanobacteria*-rich microbial mats. F) Close up of textured microbial mats in Pool 3. G) Close up of the Outflow, at which hot spring water mixes with ocean water. Reprinted with permission from (127).

minimizing the dissolution of atmospheric O_2. Iron concentrations were measured using the ferrozine assay (110) following acidification with 40 mM sulfamic acid to inhibit iron oxidation by O_2 or oxidized nitrogen species (67). Ammonia/ammonium concentrations were measured using a TetraTest NH_3/NH_4^+ Kit (TetraPond, Blacksburg, VA, USA) following the manufacturer's instructions, but with the colorimetry of samples and NH_4Cl standards quantified with a Thermo Scientific Nanodrop 2000c spectrophotometer (Thermo Fisher Scientific, Waltham, MA, USA) at 700 nm to improve sensitivity and accuracy. Anion concentrations were measured via ion chromatography on a Shimadzu Ion Chromatograph (Shimadzu, Kyoto, Japan) equipped with a Shodex SI-90 4E anion column (Showa Denko, Tokyo, Japan).

The presence of H_2 and CH_4 in gas samples was initially qualitatively assessed by comparison to standards with a Shimadzu GC-14A gas chromatograph within 12 h of collection in order to minimize the oxidation of reduced gases. Subsequent gas samples were analyzed according to previously described methods (112). In brief, samples were analyzed using a gas chromatograph (GC-4000; GL Sciences, Tokyo, Japan) equipped with both a pulsed discharge detector (PDD) and thermal conductivity detector (TCD). The GC was equipped with a ShinCarbon ST packed column (2 m×2.2 mm ID, 50/80 mesh) connected to a HayeSepo Q packed column (2 m×2.2 mm ID, 60/80 mesh) to separate O_2, N_2, CO_2, and light hydrocarbons. Temperature was maintained at 40°C for 6 min before ramping up to 200°C at 20°C min^{-1}. This temperature was held for 6 min before ramping up to 250°C at 50°C min^{-1} before a final hold for 15 min. The values of standard errors (SE) were obtained by replicate measurements of samples. The detection limit was on the order of 1 nmol cc^{-1} for H_2 and CH_4.

Water samples for dissolved inorganic carbon (DIC) and dissolved organic carbon (DOC) concentration measurements were collected with sterile syringes and transferred after filtering through a 0.2-µm filter to pre-vacuumed 30-mL serum vials that were sealed with butyl rubber septa and aluminum crimps.

DIC and DOC concentrations in water samples were analyzed by measuring CO_2 in the headspace of the sampled vials after the reaction of samples with either phosphoric acid for DIC or potassium persulfate for DOC with a Shimadzu GC-14A gas chromatograph. Sodium bicarbonate standards and glucose standards were used to make calibration curves for quantifying DIC and DOC concentrations, respectively.

16S rRNA gene amplicon and metagenomic sequencing and analyses

The sequencing and analysis of 16S rRNA gene amplicon data followed previously described methods (126). After returning to the lab, bulk environmental DNA was extracted and purified with a Zymo Soil/Fecal DNA extraction kit. The V4–V5 region of the 16S rRNA gene was PCR amplified using the archaeal and bacterial primers 515F (GTGCCAGCMGCCGCGGTAA) and 926R (CCGY CAATTYMTTTRAGTTT) (14). DNA was quantified with a Qubit 3.0 fluorimeter (Life Technologies, Carlsbad, CA, USA) following the manufacturer's instructions after the DNA extraction and PCR steps. The successful amplification of all samples was verified by viewing on a gel after initial pre-barcoding PCR (30 cycles). Duplicate PCR reactions were pooled and reconditioned for five cycles with barcoded primers. Samples for sequencing were submitted to Laragen (Culver City, CA, USA) for analysis on an Illumina MiSeq platform. Sequence data were processed using QIIME version 1.9.1 (13). Raw sequence pairs were joined and quality-trimmed using the default parameters in QIIME. Sequences were clustered into *de novo* operational taxonomic units (OTUs) with 99% similarity using the UCLUST open reference clustering protocol (24). The most abundant sequence was selected as the representative for each *de novo* OTU (121). Taxonomic identification for each representative sequence was assigned using the Silva-132 database (90) clustered

separately at 99 and 97% similarities. Singletons and contaminants (OTUs appearing in negative control datasets) were removed. 16S rRNA gene sequences were aligned using MAFFT (60) and a phylogeny constructed using FastTree (89). Alpha diversity was estimated using the Shannon Index (96) and Inverse Simpson metric (1/D) (46, 100). Sampling depths were estimated using Good's Coverage (35). All statistics were calculated using scripts in QIIME and reported at the 99 and 97% OTU similarity levels. Multidimensional scaling (MDS) analyses and plots to evaluate similarities between different samples and environments were produced in R using the vegan and ggplot2 packages (91, 135) (Oksanen, J., F.G. Blanchet, M. Friendly, *et al.* 2016. Vegan: community ecology package. R package version 2.3-5. R Foundation, Vienna, Austria).

Following initial characterization via 16S rRNA gene sequencing, four samples were selected for shotgun metagenomic sequencing: JP1-A and JP3-A from the first sampling trip, and JP1L-1 and JP2-1 from the second sampling trip. Purified DNA was submitted to SeqMatic LLC (Fremont, CA, USA) for library preparation and 2×100-bp paired-end sequencing via Illumina HiSeq 4000 technology. Samples JP1-A and JP3-A shared a single lane with two samples from another project, while JP1L-1 and JP2-1 shared a lane with one sample from another project.

Raw sequence reads from all four samples were co-assembled with MegaHit v. 1.02 (75) and genome bins constructed based on nucleotide composition and differential coverage using MetaBAT (57), MaxBin (136), and CONCOCT (Alneberg, J., B.S. Bjarnason, I. de Bruijn, M. Schirmer, J. Quick, U.Z. Ijaz, N.J. Loman, A.F. Andersson, and C. Quince. 2013. CONCOCT: clustering contigs on coverage and composition. arXiv preprint arXiv:1312.4038.) prior to dereplication and refinement with DAS Tool (99) to produce the final bin set. Genome bins were assessed for completeness, contamination, and strain-level heterogeneity using CheckM (85), tRNA sequences found with Aragorn (71), and the presence of metabolic pathways of interest predicted with MetaPOAP (130). Coverage was extracted using bbmap (Bushnell, B. 2016. BBMap short read aligner. University of California, Berkeley, California. URL: http://sourceforge.net/projects/bbmap.) and samtools (74). Genes of interest (*e.g.* coding for ribosomal, photosynthesis, iron oxidation, and electron transport proteins) were identified from assembled metagenomic data locally with BLAST+ (10) and were screened against outlier (*e.g.* likely contaminant) contigs as identified by CheckM using tetranucleotide, GC, and coding density contents. Translated protein sequences of genes of interest were aligned with MUSCLE (23), and alignments were manually curated in Jalview (134). Phylogenetic trees were calculated using RAxML (106) on the Cipres science gateway (80). Node support for phylogenies was calculated with transfer bootstraps by BOOSTER (72). Trees were visualized with the Interactive Tree of Life viewer (73). Since the sequencing depth of each sample in the full metagenome was uneven, the relative abundance of genes of interest between metagenomic datasets was normalized to the coverage of *rpoB* genes in each raw dataset as mapped onto the co-assembly. Similar to the 16S rRNA gene, *rpoB* is a highly conserved, vertically-inherited gene that is useful for the taxonomic identification of organisms, but has the added advantage that it is only known to occur as a single copy per genome (15) and is more readily assembled in metagenomic datasets (*e.g.* 127). The presence and classification of hydrogenase genes was performed with HydDB (103). The taxonomic assignment of MAGs was made based on placement in a reference phylogeny built with concatenated ribosomal protein sequences following methods from Hug *et al.* (48), and confirmed using GTDB-Tk (86). The optimal growth temperatures of MAGs were predicted based on proteome-wide 2-mer amino acid compositions following previously described methods (Li, G., K.S. Rabe, J. Nielsen, and M.K. Engqvist. 2019. Machine learning applied to predicting microorganism growth temperatures and enzyme catalytic optima. BioRxiv. doi: https://doi.org/10.1101/522342).

Results

Site description

The source water of Jinata Onsen emerges with low DO concentrations near our limit of detection, is iron-rich, and gently bubbles gas from the spring source (Fig. 1 and 2, and Table 1). Temperatures at the source are ~63°C. Water emerges into the Source Pool, which has no visible microbial mats or biofilms (Fig. 2D). Surfaces are instead coated with a fluffy red precipitate, likely a poorly ordered or short range-ordered ferric iron oxide phase such as ferrihydrite. Flow from the source is, at least partially, tidally charged, with the highest water levels and flow rates occurring at high tide. At low tide, flow rates drop and the water level of the Source Pool may decrease by decimeters, with portions of the Source Pool potentially draining during spring low tides. Spring water collects downstream into a series of pools (Pools 1-3) (Fig. 2C, E, and F), which cool sequentially (Fig. 3 and Table S1). Pool 1 contains iron oxides, similar to the Source Pool, but also develops macroscopic microbial streamers that are coated in iron oxides and thin veil-like layers of microorganisms overlaying iron oxide sediments—structures similar to those typically made by marine iron-oxidizing *Zetaproteobacteria* (*e.g.* 33). Streamers are very fine (mm-scale) and delicate (break apart on contact with forceps) but can reach several centimeters in length. *Cyanobacteria* in Pools 2 and 3 display high levels of photosynthetic activity as revealed by high DO concentrations (~234 μM), low DIC concentrations, and the accumulation of visible O_2 bubbles on the surface and within the fabric of the mat. Downstream pools (Pools 2 and 3) mix with seawater during high tide due to wave action; however, this seawater influence does not appear to influence the Source Pool or Pool 1. Samples were collected and temperatures were measured at high tide, reflecting the lowest temperatures experienced by microbes in the pools; at low tide, hot spring input is dominant and temperatures rise (observed range at each site in Table S1). Subaqueous surfaces in Pools 2 and 3 are covered in thick microbial mats. In Pool 2, the mat is coated in a layer of fluffy iron oxide similar to that in the Source Pool, with a dense microbial mat below (Fig. 2E). Pool 3 contains only patchy iron oxides, with mostly exposed microbial mats displaying a finger-like morphology. These "fingers" were 0.5–1 cm in diameter, up to ~5 cm long and were closely packed and carpeting surfaces of Pool 3 below the high tide line, potentially related to turbulent mixing from wave action during high tide (Fig. 2F). The Outflow is the outlet of a channel connecting Pool 2 to the bay. Its hydrology is dominantly marine with small admixtures of inflowing spring water (Fig. 2G).

Table 1. Geochemistry of source water at Jinata Onsen.

T	63°C
pH	5.4
DO	4.7 μM
Fe^{2+}	261 μM
NH_3/NH_4^+	87 μM
Cl^-	654 mM
SO_4^-	17 mM
NO_3^-	<1.6 μM
NO_2^-	<2.2 μM
HPO_4^-	<1 μM

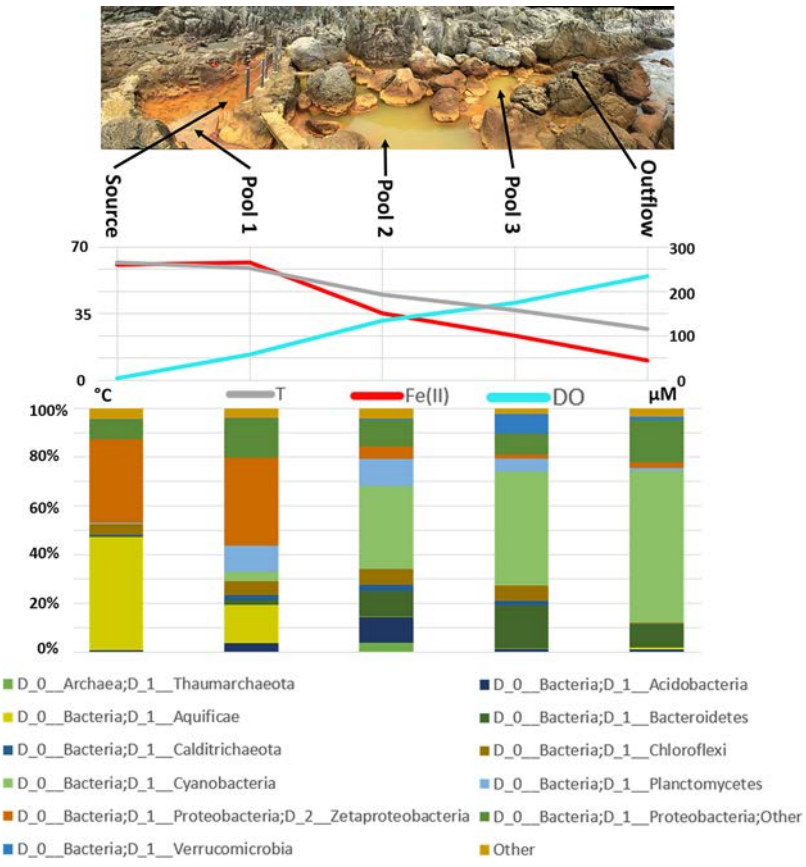

Fig. 3. Summary of geochemical and microbiological trends along the flow path of Jinata Onsen. Top: Panoramic view of Jinata Onsen, with the Source Pool at the left and the flow of spring water toward the bay at the right, with sampling locations indicated. Middle: Geochemical transect across the spring, showing temperature (°C, left axis) and dissolved Fe(II) and O_2 (µM, right axis). Bottom: Stacked bar chart of the relative community abundance of dominant microbial phyla as assessed by 16S rRNA amplicon sequencing. Sequence data were binned at the phylum level and duplicate samples at each site were averaged. Reads that could not be assigned to a phylum were discarded; all phyla that do not make up more than 2% of the community at any one site have been collapsed to "Other". Near the source, the community is predominantly made up of iron- and/or hydrogen-oxidizing organisms in the phyla *Proteobacteria* and *Aquificae*. As hot spring water flows downstream, it equilibrates with the atmosphere and eventually mixes with seawater, resulting in downstream cooling, the accumulation of oxygen, and loss of dissolved iron due to biological and abiotic processes. Oxygenic *Cyanobacteria* become progressively more abundant downstream. Putative hydrogen- and iron-oxidizing lithotrophs dominate near the source, whereas phototrophic *Cyanobacteria* dominate downstream. Additional community diversity is found in Table S4.

Jinata hot spring was visited twice for observations and community DNA sampling in 2016 (January and September), and again for observations and gas sampling in October 2017 and April 2018. These visits corresponded to a range of tidal conditions, including a spring low and high tide in September 2016. The general features of the spring were consistent across this period (including the abundance and distribution of iron minerals and microbial mats), differing primarily in apparent tidal dependence in the flow rate and water level of the spring and the extent of the seawater influence on Pool 3. These differences in flow and mixing led to variations in water temperatures of 3–10°C (Table S1). At high tide, the flow rate of the spring increases, as does seawater influx to Pool 3. During the spring low tide, the spring flow stagnated and the water level of Source Pool and Pool 1 dropped by decimeters, with some portions draining entirely. During less extreme low tides observed on other dates, the spring flow was low but nonzero and the water level of the Source Pool did not significantly drop. While marked variability was observed in the flow rate from the spring based on tides (and resulting shifts in water level and temperature), the overall geochemistry of the source water and microbial community mostly appeared to be similar between expeditions.

Geochemistry

Geochemical measurements along the flow path of Jinata Onsen revealed a major shift from hot, low-oxygen, high-iron source water to cooler, more oxygen-rich water with less dissolved iron downstream. Geochemistry measurements of Jinata source water are summarized in Table 1, while geochemical gradients along the stream outflow are shown in Fig. 3 and Table S1. Source waters were slightly enriched in chloride relative to seawater (~23.2 g L^{-1} in Jinata source water versus ~19.4 g L^{-1} in typical seawater) and depleted in sulfate (~1.6 g L^{-1} in Jinata versus ~2.7 g L^{-1} in seawater), but approached seawater concentrations downstream as mixing increased. Water emerging from the source was 63°C, very low in DO (~4.7 µM), at pH 5.4, and contained substantial concentrations of dissolved iron (~250 µM Fe^{2+}). DOC in the water of Pool 1 was high (~1.31 mM). It is unknown whether this is produced *in situ* or if the source water emerges with high DOC. DOC and DIC both decreased along the outflow

of the spring (Table S1). After emerging from the source, the spring water exchanges gases with the air due to mixing associated with water flow and gas ebullition, and DO increased to 39 μM at the surface of the Source Pool. As water flows downstream from the Source Pool, it cools slightly, exchanges gases with the atmosphere, and intermittently mixes with seawater below Pool 1.

H_2 and CH_4 were both qualitatively detected in bubbles from the Source Pool following initial sampling in September 2016. However, during subsequent analyses to quantify the gas composition in October 2017 and April 2018, the gas was found to contain CO_2, CH_4, and N_2 (Table S2). This subsequent non-detection of H_2 may be related to temporal variability in the gas composition at Jinata (*e.g.* following tidal influence; significant variability was observed in the CO_2:N_2 ratio between two sampling dates, Table S2) or may reflect oxidation of H_2 between sampling and analysis. The detection limit of H_2 for these later measurements was ~1 nmol cc^{-1} (in the gas phase of our quantitative gas analyses, or ~1 nM in the aqueous phase [2]), well above the energetic and ecological limits for hydrogenotrophic metabolisms (*e.g.* 51) leaving open the possibility of biologically significant H_2 fluxes at Jinata around the time of sampling. The oxidation of H_2 coupled to O_2 reduction is a thermodynamically favorable process even at very low substrate concentrations (*e.g.* $\Delta_rG' < -375$ kJ mol^{-1} with substrate concentrations of 0.1 nM $H_{2(aq)}$ and 0.1 μM $O_{2(aq)}$, below our limit of detection) (30). Consistent with this thermodynamic favorability, biology has been shown to make use of this metabolism in environments such as hot springs with H_2 concentrations near our detection limits (19) and in Antarctic soils where microbes rely on uptake of trace atmospheric H_2 at concentrations of ~190 ppbv (51). Therefore, the trace amounts of H_2 that may be present in the source water at Jinata may be sufficient to support lithoautotrophy near the hot spring source in organisms possessing the genetic capacity for hydrogen oxidation, as discussed below. Metagenomic data suggest that organisms with the genetic capacity for hydrogenotrophic metabolisms are abundant in upstream regions of Jinata (discussed below), and so it is also possible that low dissolved H_2 concentrations may be due to active biological consumption near the hot spring source. Improved quantification of H_2 concentrations, measurements of hydrogenase activity, and the productivity of hydrogenotrophic microbes will be necessary to determine the relative contribution of hydrogen oxidation to productivity at Jinata.

16S rRNA gene amplicon and genome-resolved metagenomic sequencing

16S rRNA gene amplicon and metagenomic sequencing of microbial communities at Jinata Onsen revealed a highly diverse community. In total, 16S rRNA gene amplicon sequencing recovered 456,737 sequences from the 10 samples at Jinata (Tables S3, 4, and 5). Reads per sample following filtering for quality and the removal of chimeras ranged between 2,076 for Pool 3 Sample B and 96,268 for Pool 1 Sample A (median 32,222, mean 35,479, and standard deviation 26,014). On average, 65% of the microbial community was recovered from Jinata samples at the 99% OTU level based on the Good's Coverage statistic of the 16S rRNA gene (ranging between 50% coverage in Outflow Sample A and 80% in Pool 1 Sample A) and 82% at the 97% OTU level (between 69% for Pool 2 Sample B and 93% for Pool 1 Sample B). MDS analysis (Fig. S1) demonstrates that samples from the same site were highly similar, and adjacent sites (*e.g.* Source Pool and Pool 1, Outflow and Pool 3) also showed a high degree of similarity. However, a substantial transition was observed in microbial community diversity between the most distant samples (*e.g.* Source Pool and Outflow).

Shotgun metagenomic sequencing of four samples from Jinata Onsen recovered 121 GB of data, forming a 1.48-Gb co-assembly consisting of 1,531,443 contigs with an N50 of 1,494 bp. Nucleotide composition and differential coverage-based binning of the co-assembly via multiple methods followed by dereplication and refinement resulted in a final set of 161 medium- or high-quality metagenome-assembled genomes (MAGs) following current standards (*i.e.* completeness >50% and contamination <10%) (6). These MAGs are from diverse phyla of Bacteria and Archaea (Fig. 4); metagenome and MAG statistics with tentative taxonomic assignments for recovered MAGs are shown in Table S6, while MAGs of particular interest due to their potential contribution to primary productivity at this site or due to substantial genetic or metabolic novelty are discussed in depth below and shown in phylogenetic trees alongside reference strains in Fig. 5, 6, and 7.

Discussion

As Jinata spring water flows from its source to the ocean, it transitions from hot, low-oxygen, high-iron water to cooler, iron-depleted, oxygen-rich water in downstream regions (Fig. 3). Following this geochemical transition is a major shift in the composition of the microbial community—from a high-temperature, putatively lithotrophic community which produces little visible biomass upstream, to a lower temperature community with well-developed, thick microbial mats downstream. This shift in community composition is summarized in Fig. 3, with complete diversity data in the Supplemental Information (including OTU counts per sample in Table S4 and relative abundance binned at the class level in Table S5). Below, we discuss the overall physiological and taxonomic trends across the spring sites as inferred from diversity and genomic analysis.

Potential for lithotrophic iron and hydrogen oxidation

The hot spring water emerging at the Source Pool at Jinata contains abundant dissolved Fe^{2+} and trace H_2 (though measurements of gas content varied, as discussed above) (Table 1). Although rates of carbon fixation were not measured, the appearance of (presumed) zetaproteobacterial veils and streamers together with molecular evidence for lithoautotrophic microbes suggest that these electron donors may fuel productivity and determine the microbial community upstream at the Source Pool and Pool 1, where microbial mats were not well developed. The low accumulation of visible biomass in upstream regions of Jinata is similar to other microbial ecosystems fueled by iron oxidation (*e.g.* Oku-Okuhachikurou Onsen [126], Fuschna Spring [43], and Jackson Creek [92]), in which lithotrophic communities appear capable of accumulating less organic carbon than communities fueled by oxygenic photosynthesis (including those in downstream regions at Jinata).

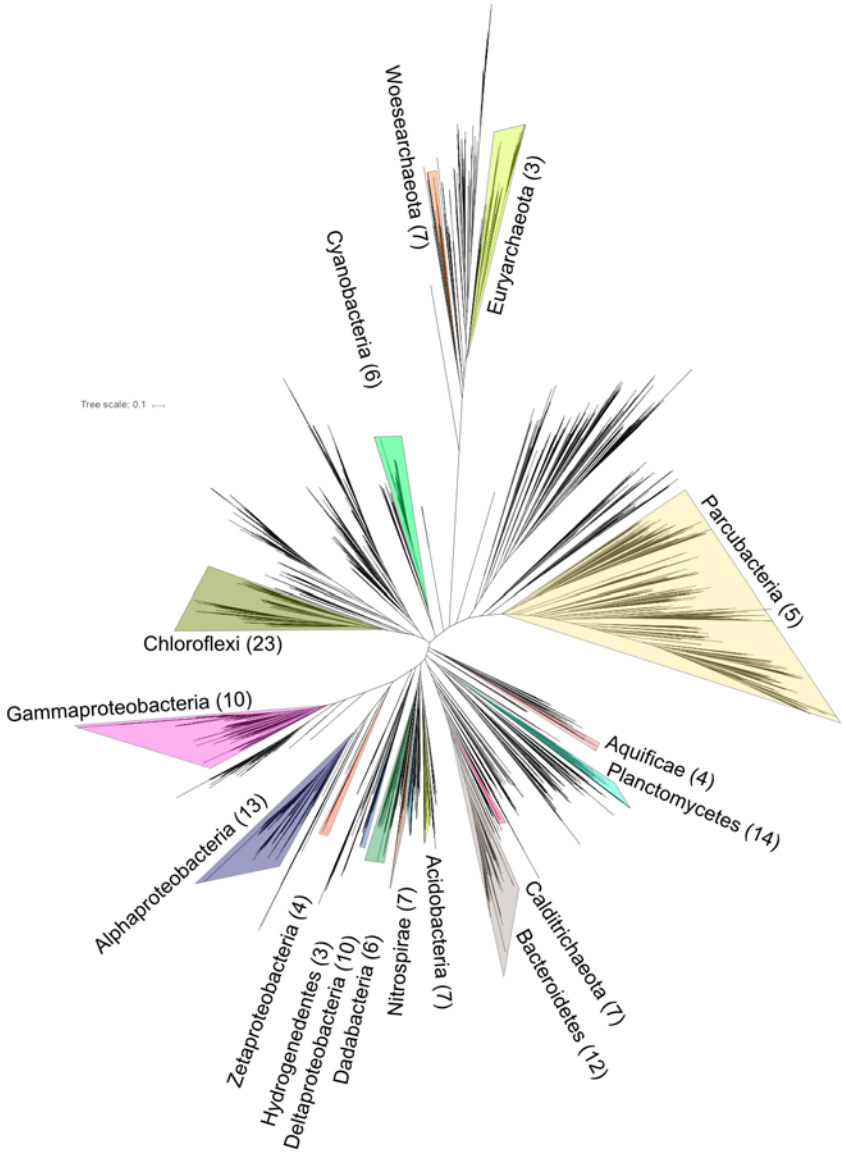

Fig. 4. Phylogeny of Bacteria and Archaea based on concatenated ribosomal proteins. Numbers in parentheses next to phylum labels refer to the number of MAGs recovered from Jinata Onsen. Labels for phyla with two or fewer MAGs recovered from Jinata were omitted for clarity. The reference alignment was modified from Hug *et al.* (48). A full list of MAGs recovered is available in Table S6.

The results of 16S rRNA gene amplicon sequencing indicate that the most abundant organisms in the Source Pool are members of the *Aquificae* family *Hydrogenothermaceae* (32% of reads in the Source Pool and 11.5% of reads in Pool 1). Members of this family are typically marine thermophilic lithotrophs capable of iron and hydrogen oxidation as well as heterotrophy (114); at Jinata, they may be utilizing Fe^{2+}, H_2, or DOC. The seventh most abundant OTU in the Source Pool samples was a novel sequence that was 89% similar to a strain of *Persephonella* observed in an alkaline hot spring in Papua New Guinea. *Persephonella* is a genus of thermophilic, microaerophilic hydrogen-oxidizing bacteria within *Hydrogenothermaceae* (36). Despite their abundance as assessed by 16S rRNA gene amplicon sequencing (Fig. 3), only four partial *Aquificae* MAGs were recovered from Jinata, of which only one (J026) was reasonably complete (~94%). Two *Aquificae* MAGs recovered Group 1 NiFe hydrogenase genes, which could support hydrogenotrophy; the absence of hydrogenases from the other MAGs may be related to their low completeness or could reflect a utilization of iron or other electron donors and not H_2 in these organisms.

The other most abundant organisms near the source are members of *Zetaproteobacteria*, a group typified by the neutrophilic, aerobic iron-oxidizing genus *Mariprofundus* common in marine systems (27). *Zetaproteobacteria* accounted for 24% of 16S rRNA gene sequences in the Source Pool and 26.5% in Pool 1. All *Zetaproteobacteria* characterized to date are obligate iron- and/or hydrogen-oxidizing lithoautotrophs (82), suggesting that these organisms play a substantial role in driving carbon fixation in the Source Pool and Pool 1.

Members of *Mariprofundaceae* have been observed to have an upper temperature limit for growth of 30°C (28), while *Zetaproteobacteria* at Jinata are found at temperatures up to 63°C. This currently represents a unique high-temperature environment for these organisms. In particular, the third most abundant OTU in the Source Pool and Pool 1 sample A is an

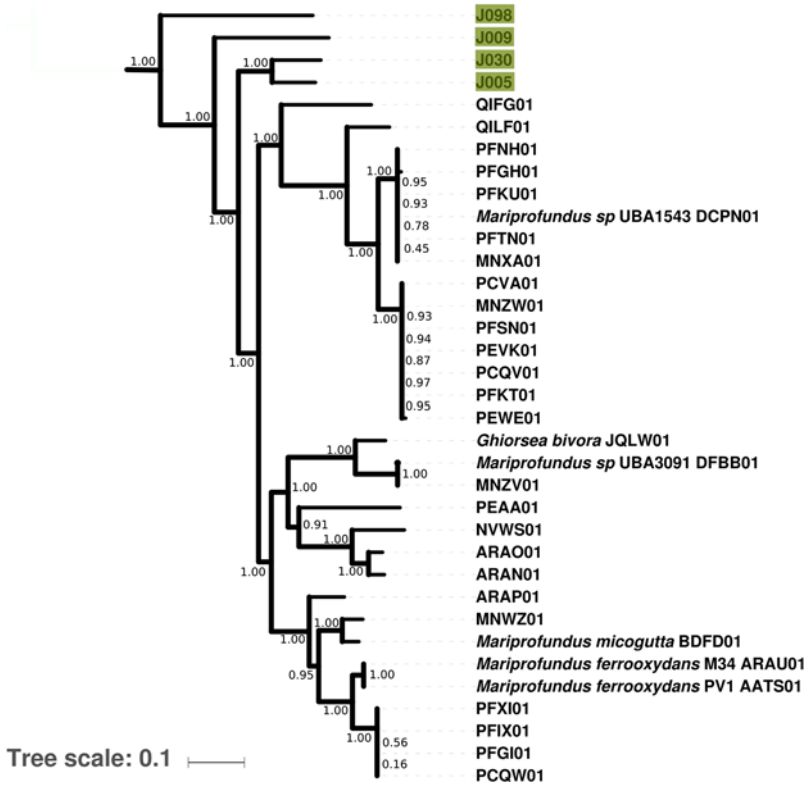

Fig. 5. Phylogeny of *Zetaproteobacteria*, rooted with *Alphaproteobacteria*, built with concatenated ribosomal protein sequences. Data from (77), (82), (101), and other draft genomes available on Genbank. Transfer bootstrap expectation (TBE) support values as calculated by BOOSTER (72) shown for internal nodes. In cases for which reference genomes have a unique strain name or identifier, this is included; otherwise Genbank WGS genome prefixes are used.

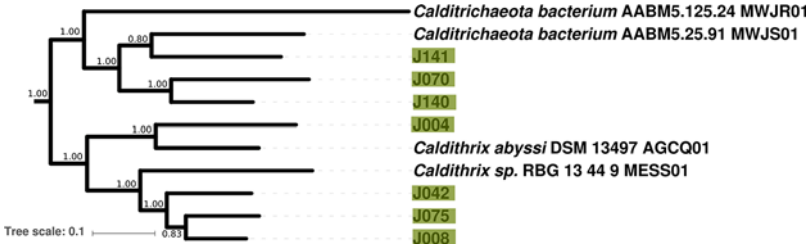

Fig. 6. Phylogeny of *Calditrichaeota*, rooted with *Bacteroidetes*, built with concatenated ribosomal protein sequences. Transfer bootstrap expectation (TBE) support values as calculated by BOOSTER (72) shown for internal nodes. Data from (68) and other draft genomes available on Genbank. In cases where reference genomes have a unique strain name or identifier, this is included; otherwise Genbank WGS genome prefixes are used.

unknown sequence that is 92% identical to a sequence from an uncultured zetaproteobacterium from a shallow hydrothermal vent in Papua New Guinea (79). This sequence likely marks a novel lineage of high-temperature iron-oxidizing *Zetaproteobacteria*.

The relative abundance of *Hydrogenothermaceae* decreases to less than 1% of sequences in areas where microbial mats are well developed downstream of Pool 1; however, *Zetaproteobacteria* continue to account for ~1–4% of reads in Pools 2 and 3 in which dissolved iron concentrations are still significant (Fig. 3). This relative abundance change may be due more to the increased abundance of other organisms rather than a decrease in the number of *Zetaproteobacteria* or their ability to make a living oxidizing iron. This hypothesis awaits confirmation by a technique such as qPCR. In contrast, the absence of *Hydrogenothermaceae* downstream may be a real signal driven by the rapid disappearance of trace H_2 as an electron donor. However, in both cases, a drop in relative abundance is likely related to the increasing total biomass (*i.e.* number of cells) downstream as *Cyanobacteria* become more productive, leading to sequences from *Hydrogenothermaceae* and *Zetaproteobacteria* being diluted out by increased numbers of *Cyanobacteria*, *Chloroflexi*, and other sequences.

Four MAGs affiliated with *Zetaproteobacteria* were recovered from Jinata with completeness estimates by CheckM ranging between ~80 and ~97% (J005, J009, J030, and J098). While these MAGs did not recover 16S rRNA genes, RpoB- and concatenated ribosomal protein-based phylogenies illustrated that members of this group at Jinata Onsen do not belong to the characterized genera *Mariprofundus* or *Ghiorsea*, but instead form separate basal lineages within *Zetaproteobacteria* (Fig. 5). Despite their phylogenetic distinctness, these MAGs largely recovered genes associated with aerobic iron oxidation as expected based on the physiology of other *Zetaproteobacteria*. These include a terminal O_2 reductase

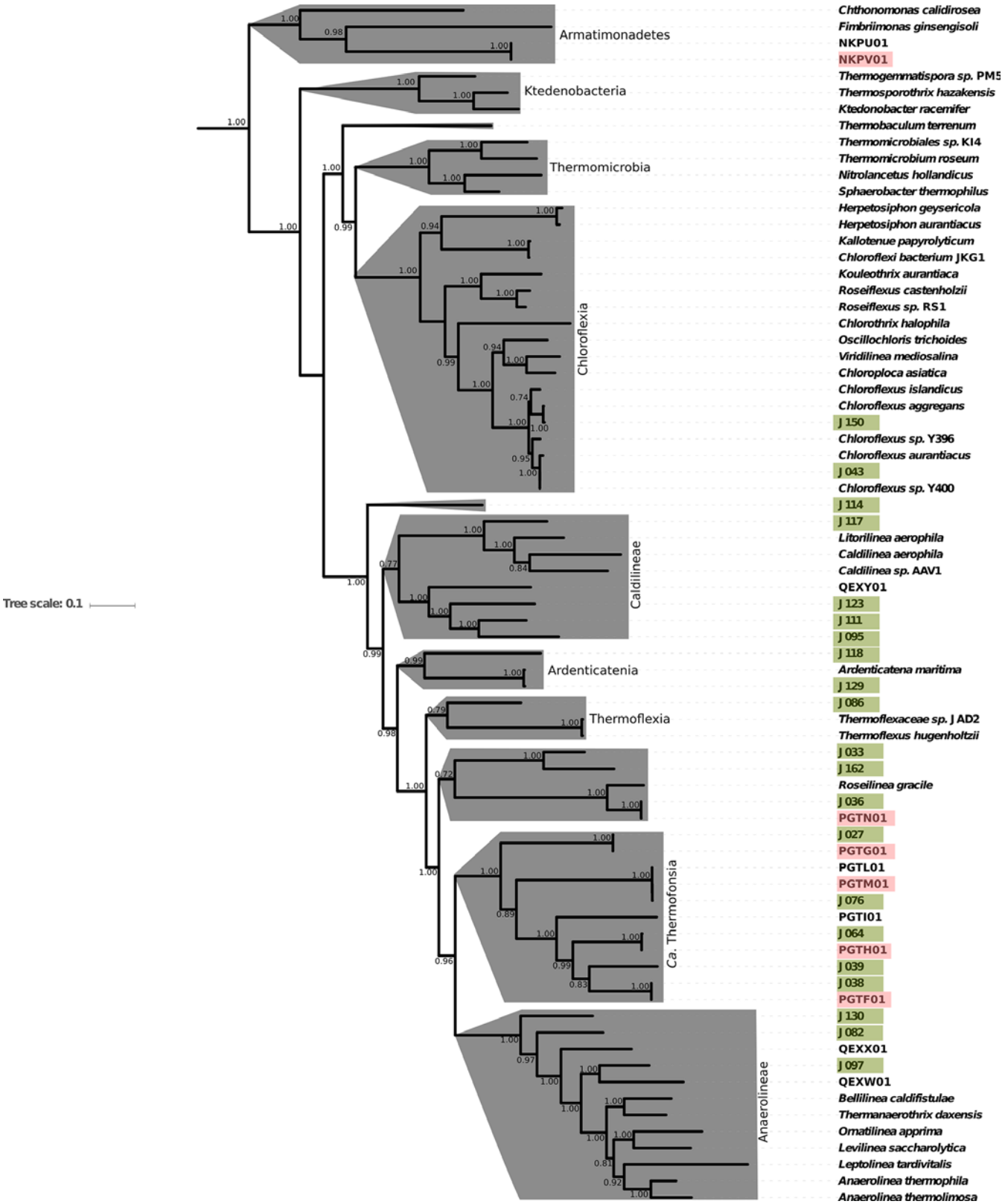

Fig. 7. Detailed phylogeny of the phylum *Chloroflexi*, with class-level clades highlighted in gray, built with concatenated ribosomal protein sequences. The large basal class *Dehalococcoidia*, which was not observed in 16S rRNA or metagenome data from Jinata, is omitted for clarity. The phylogeny contains MAGs reported here, members of the phylum *Chloroflexi* previously described (16, 20, 38, 41, 43–45, 62, 70, 83, 104, 122, 123, 127–129), and members of the closely related phylum *Armatimonadetes* as an outgroup (21, 125). MAGs described here are highlighted in green, and MAGs previously reported from Jinata Onsen are highlighted in pink. Transfer bootstrap expectation (TBE) support values as calculated by BOOSTER (72) shown for internal nodes. In cases for which reference genomes have a unique strain name or identifier, this is included; otherwise Genbank WGS genome prefixes are used.

from the C-family of heme copper oxidoreductases for respiration at low O_2 concentrations and *Cyc2* cytochrome genes implicated in ferrous iron oxidation in *Zetaproteobacteria* and other taxa (*e.g. Chlorobi*) (39, 40, 59). Hydrogenase catalytic subunit genes (neither [NiFe] nor [FeFe]) were not recovered in zetaproteobacterial MAGs even at high completeness, suggesting that these organisms are not hydrogenotrophic. Consistent with the obligately autotrophic lifestyle of previously characterized *Zetaproteobacteria*, J009 and J098 encode carbon fixation via the Calvin cycle. However, J005 and J030 did not recover genes for carbon fixation via the Calvin cycle such as the large and small subunits of rubisco, phosphoribulose kinase, or carboxysome proteins. The high completeness of these MAGs (~94–97%) makes it unlikely that these genes would all fail to be recovered (MetaPOAP False Negative estimates 10^{-5}–10^{-7}). The absence of carbon fixation pathways from these genomes together with the availability of abundant DOC in Pool 1 (~1.3 mM) suggest that these organisms may be heterotrophic, a lifestyle not previously observed for members of *Zetaproteobacteria*.

Seven MAGs were recovered from the enigmatic bacterial phylum *Calditrichaeota* (J004, J008, J042, J070, J075, J140, and J141) (Fig. 6). While few members of *Calditrichaeota* have been isolated or sequenced, the best known of these is *Caldithrix abyssi* (81); this taxon was characterized as an anaerobic thermophile capable of lithoheterotrophic H_2 oxidation coupled to denitrification and organoheterotrophic fermentation (1, 78). The *Calditrichaeota* MAGs reported here are up to 97% complete (J004) and contain members with variable putative metabolic capabilities, potentially including aerobic hydrogen- or iron-oxidizing lithoautotrophy. In the *Calditrichaeota* MAGs recovered from Jinata Onsen, aerobic respiration via A-family heme copper oxidoreductases could potentially be coupled to autotrophic hydrogen oxidation (via the Group 1d NiFe hydrogenase in J042) or iron oxidation (via the *pioA* gene in J075); however, *C. abyssi* appears incapable of aerobic respiration despite encoding an A-family heme copper oxidoreductase (68). A MAG from a member of *Calditrichaeota* has previously been recovered from Chocolate Pots hot spring in Yellowstone National Park (32); together with the data presented here this suggests that this phylum may be a common member of microbial communities in iron-rich hot springs. Unlike previously described *Calditrichaeota* which are all heterotrophic (78), most of the *Calditrichaeota* MAGs reported here possess a putative capacity for carbon fixation via the Calvin cycle. J004 is closely related to *C. abyssi*, while the other MAGs form two distinct but related clades (Fig. 6).

Oxygenic photosynthesis

Cyanobacteria are nearly absent from the Source Pool (<0.15% relative abundance), but are observed at low numbers in Pool 1 and become abundant starting in Pool 2. The most abundant *Cyanobacteria* present are predominantly members of *Nostocales*. This group includes *Leptolyngbya* and *Phormidium*, genera of filamentous non-heterocystous *Cyanobacteria* that are present in other hot springs of similar temperatures (*e.g.* 5, 94, 126). Diverse cyanobacterial MAGs were recovered, including members of the orders *Pleurocapsales* (J083), *Chroococcales* (J003 and J149), and *Oscillatoriales* (J007, J055, and J069). In Outflow samples, chloroplast sequences related to the diatom *Melosira* were abundant.

Cyanobacteria are sometimes underrepresented in 16S rRNA gene amplicon sequencing datasets as a result of a poor DNA yield or amplification biases (*e.g.* 84, 118); however, the low abundance of *Cyanobacteria* near the Source Pool was confirmed by fluorescent microscopy, in which cells displaying cyanobacterial autofluorescence were abundant in downstream samples, but not in samples from the Source Pool (Fig. S2). Thick microbial mats initially appear in Pool 2 when *Cyanobacteria* become abundant, suggesting that oxygenic photosynthesis fuels more net carbon fixation than lithotrophy in these environments.

It has been suggested that high ferrous iron concentrations are toxic to *Cyanobacteria*, and that this would have greatly reduced their productivity under ferruginous ocean conditions such as those that may have persisted through much of the Archean era (113). The abundant *Cyanobacteria* observed to be active at Jinata under high iron concentrations suggest that *Cyanobacteria* can adapt to ferruginous conditions, and therefore iron toxicity might not inhibit *Cyanobacteria* over geological timescales. Indeed, the soluble iron concentrations observed at Jinata are higher (150–250 μM) than predicted for the Archean oceans (<120 μM, 47) or observed at other iron-rich hot springs (~100–200 μM, 87, 126), making Jinata an excellent test case for determining the ability of *Cyanobacteria* to adapt to high iron concentrations. Culture-based physiological experiments may be useful to determine whether Jinata *Cyanobacteria* utilize similar strategies to other iron-tolerant strains (e.g. by those in Chocolate Pots Hot Spring, 87, or the ferric iron-tolerant *Leptolyngbya*-relative *Marsacia ferruginose*, 8) or whether Jinata strains possess unique adaptations that allow them to grow at higher iron concentrations than known for other environmental *Cyanobacteria* strains. This will in turn provide insight into whether iron tolerance is due to evolutionarily conserved strategies or whether this is a trait that has evolved convergently multiple times.

Diverse novel Chloroflexi *from Jinata Onsen*

In addition to the primary phototrophic and lithotrophic carbon fixers at Jinata, 16S rRNA gene and metagenomic data sets revealed diverse novel lineages within the phylum *Chloroflexi*. Twenty-three *Chloroflexi* MAGs were recovered, introducing substantial genetic and metabolic diversity that expands our understanding of this group. While the best known members of this phylum are Type 2 Reaction Center-containing lineages such as *Chloroflexus* and *Roseiflexus* within the class *Chloroflexia* (*e.g.* 117), phototrophy is not a synapomorphy of the phylum *Chloroflexi* or even the class *Chloroflexia* (*e.g.* 122) and most of the diversity of the phylum belongs to several other classes primarily made up of non-phototrophic lineages (127). The bulk of *Chloroflexi* diversity recovered from Jinata belongs to "subphlyum I", a broad group of predominantly non-phototrophic lineages that was originally described based on the class- or order-level lineages *Anaerolineae* and *Caldilineae* (137), but also encompasses the related groups *Ardenticatenia*, *Thermoflexia*, and *Candidatus* Thermofonsia (20, 61, 127).

16S rRNA gene analysis indicated that members of *Anaerolineae* and *Ca.* Thermofonsia (annotated by Silva and

GTDB-Tk as the order SBR1031) were fairly abundant at Jinata, with *Anaerolineae* at ~3% relative abundance in the Source Pool and Pool 1 and *Ca.* Thermofonsia at ~3.5% relative abundance in Pools 2 and 3. Three MAGs recovered from Jinata (J082, J097, and J130) are associated with the *Anaerolineae* class, as determined by RpoB and concatenated ribosomal protein phylogenies, along with seven associated with *Ca.* Thermofonsia (J027, J033, J036, J038, J039, J064, and J076). Of particular interest among these is J036, a close relative of the phototrophic *Ca.* Roseilinea gracile (66, 115, 116). J036 contains a 16S rRNA gene that is 96% similar to that of *Ca.* Roseilinea gracile, and two-way AAI estimates (93) showed 73.6% similarity between the two strains, indicating that these strains are probably best classified as distinct species within the same genus. Unlike other phototrophs in the phylum *Chloroflexi* that are capable of photoautotrophy via the 3-hydroxypropionate bicycle or the Calvin cycle (65, 98), J036 and *Ca.* Roseilinea gracile do not encode carbon fixation and are likely photoheterotrophic. Previous studies suggested that the *Roseilinea* lineage belongs to *Anaerolineae* (66) or *Thermofonsia* (127). However, our updated phylogeny presented here places J036 and *Roseilinea* in a separate lineage along with J033 and J162, diverging just outside of the *Anaerolineae*+ *Thermofonsia* clade. This suggests that these strains may instead be yet another class- or order-level lineage within the broader "subphylum I" of *Chloroflexi* (Fig. 7), an interpretation supported by analysis via GTDB-Tk that places these genomes outside of characterized clades (Table S6).

The *Chloroflexi* class *Ardenticatenia* was first described from an isolate from an iron-rich Japanese hydrothermal field (61) and has since also been recovered from sulfidic hot springs (128). Members of *Ardenticatenia* were present at up to 1.2% relative abundance in Pool 3 in 16S amplicon data. One MAG recovered from Jinata Onsen, J129, was closely related to *Ardenticatena maritima*. While *A. maritima 110S* contains a complete denitrification pathway (45), MAG J129 did not recover any denitrification genes. This may be related to the relatively low completeness of this MAG (~70%); however, MetaPOAP (131) False Negative estimates for the probability that all four steps in the canonical denitrification pathway would fail to be recovered in J129 given their presence in the source genome is less than 0.8%. This suggests that most, if not all denitrification genes are absent from the J129 genome and that the capacity for denitrification is not universal within members of *Ardenticatena*. This would be consistent with broad trends in the apparently frequent modular horizontal gene transfer of partial denitrification pathways between disparate microbial lineages to drive rapid adaption and metabolic flexibility of aerobic organisms in microoxic and anoxic environments, for reasons that are still not well established (17, 109).

Members of the *Chloroflexi* class *Caldilineae* were present at up to 0.5% abundance at Jinata in the 16S rRNA gene dataset. Members of *Caldilineae* have previously been isolated from intertidal hot springs in Iceland (55) and Japanese hot springs (95). Characterized organisms in this class are filamentous, anaerobic, or facultatively aerobic heterotrophs (37, 55, 95); therefore, these taxa may play a role in degrading biomass within low-oxygen regions of microbial mats at Jinata. Three MAGs were recovered that form a deeply branching lineage within the *Caldilineae* class (J095, J111, and J123), sister to the previously characterized genera *Caldilinea* and *Litorilinea*. Like other members of *Caldilineae*, these strains encode aerobic respiration via A-family heme copper oxidoreductases and both a *bc* complex III and alternative complex III, and are therefore likely at least facultatively aerobic. J095 also encodes carbon fixation via the Calvin cycle as well as a Group 1f NiFe hydrogenase, suggesting a potential capability for hydrogenotrophic lithoautotrophy, expanding the known metabolic diversity of this class and the *Chloroflexi* phylum as a whole.

MAG J114 branches at the base of subphylum I of *Chloroflexi*, potentially the first member of a novel class-level lineage. The divergence between *Anaerolineae* and *Caldilineae* has been estimated to have occurred on the order of 1.7 Ga (98). The phylogenetic placement of J114 suggests that it diverged from other members of subphylum I even earlier, and it may be a good target for future investigation to assess aspects of the early evolution of the phylum *Chloroflexi*. J114 encodes aerobic respiration via an A-family heme copper oxidoreductase and an alternative complex III like many other non-phototrophic *Chloroflexi* lineages (*e.g.* 122, 127) as well as a Group 1f NiFe hydrogenase and carbon fixation via the Calvin cycle, suggesting the capacity for aerobic hydrogen-oxidizing autotrophy—a lifestyle not previously described for members of *Chloroflexi*.

Conclusions

To our knowledge, this is the first overall geomicrobiological characterization of Jinata Onsen, providing baseline descriptions of geochemistry and microbial diversity in order to establish a series of testable hypotheses that can be addressed by future studies. We have also provided genome-resolved metagenomic sequencing of this site focusing on members of the microbial community predicted to be responsible for the bulk of primary productivity in this system along with other organisms belonging to novel or under-characterized lineages. However, this is just a subset of the diverse microbial populations at Jinata Onsen; many more MAGs from across the tree of life were recovered than are discussed in detail here but which may be of use to others (Fig. 4 and Table S6).

The diversity of iron-oxidizing bacteria at Jinata is different than in other Fe^{2+}-rich springs and environments. For example, in freshwater systems such as Oku-Okuhachikurou Onsen in Akita Prefecture (126) and Budo Pond in Hiroshima Prefecture, Japan (58), iron oxidation is primarily driven by the activity of chemoautotrophs such as members of *Gallionellaceae*. In contrast, at Chocolate Pots hot spring in Yellowstone National Park, USA, iron oxidation is primarily abiotic, driven by O_2 produced by *Cyanobacteria*, with only a small contribution from iron-oxidizing bacteria (32, 119). The distinct iron-oxidizing community at Jinata Onsen may be related to the salinity of the spring water, or biogeographically by access to the ocean, as *Zetaproteobacteria* are typically found in marine settings, particularly in deep ocean basins associated with hydrothermal iron sources (28). Despite the taxonomically distinct iron oxidizer communities between Jinata and Oku-Okuhachikurou Onsen, both communities support only limited visible biomass in regions dominated by iron oxidizers (126), perhaps reflecting the shared biochemical and bioenergetic

challenges of iron oxidation incurred by diverse iron-oxidizing bacteria including *Gallionellaceae* and *Zetaproteobacteria* (4, 28, 126). Future work focused on isolation and physiological characterization of these microbes, quantification of rates and determination of microbial drivers of carbon fixation and aerobic and anaerobic heterotrophy, and carbon isotope profiling of organic and inorganic species along the flow path of the hot spring will be necessary to fully characterize the activity of microbes at Jinata and to fully compare this system to other areas with high dissolved ferrous iron concentrations (*e.g.* Oku-Okuhachikurou Onsen [126], Fuschna Spring [42], Jackson Creek [92], and Chocolate Pots Hot Spring [32, 119]).

Future work aimed at a more complete understanding of the geochemistry of Jinata and its impact on microbial communities will be valuable. For example, a quantitative determination of budgets and variability of gas chemistry and DOC will be beneficial. DOC may stimulate heterotrophic activity by the microbial community at Jinata, coupled to aerobic or anaerobic respiration (such as dissimilatory iron reduction, as observed in other iron-rich hot springs, *e.g.* 31), resulting in the drawdown of DOC downstream. Since the source of this DOC is unclear, future work will be necessary to determine whether DOC is present in the source water or if it is produced *in situ* by the microbial community in the Source Pool and Pool 1. Future work is also needed to evaluate the potential for dissimilatory iron reduction and other anaerobic metabolisms including sulfate reduction and methanogenesis.

Throughout Earth history, the metabolic opportunities available to life, and the resulting organisms and metabolisms responsible for driving primary productivity, have been shaped by the geochemical conditions of the atmosphere and oceans. The modern, sulfate-rich, well-oxygenated oceans we see today reflect a relatively recent state—one typical of only the last few hundred million years (*e.g.* 76). For the first half of Earth history, until ~2.3 Ga, the atmosphere and oceans were anoxic (52), and seawater was rich in dissolved iron but poor in sulfur (120). At this time, productivity was low and fueled by metabolisms such as methanogenesis and anoxygenic photosynthesis (12, 64, 131). Following the expansion of oxygenic photosynthesis by *Cyanobacteria* and higher primary productivity around the Great Oxygenation Event ~2.3 Ga (18, 29, 124, 133), the atmosphere and surface ocean accumulated some oxygen, and the ocean transitioned into a state with oxygenated surface waters but often anoxic deeper waters, rich in either dissolved iron or sulfide (11, 53, 54, 88). At Jinata Onsen, this range of geochemical conditions is recapitulated over just a few meters, providing a useful test case for probing the shifts in microbial productivity over the course of Earth history. In particular, the concomitant increase in visible biomass at Jinata as the community shifts from lithotrophy toward water-oxidizing phototrophy (*i.e.* oxygenic photosynthesis) is consistent with estimates for greatly increased primary production following the evolution and expansion of *Cyanobacteria* around the GOE (18, 97, 102, 124, 131, 133).

The dynamic abundances of redox-active compounds including oxygen, iron, and hydrogen at Jinata may not only be analogous to conditions on the early Earth, but may have relevance for potentially habitable environments on Mars as well. Early Mars is thought to have supported environments with metabolic opportunities provided by the redox gradient between the oxidizing atmosphere and abundant electron donors such as ferrous iron and molecular hydrogen sourced from water/rock interactions (*e.g.* 49), and production of these substrates may continue today (22, 107), potentially supporting past or present life in the Martian subsurface (108). Understanding the potential productivity of microbial communities fueled by lithotrophic metabolisms is critical for setting expectations for the presence and size of potential biospheres on other worlds and early in Earth history (*e.g.* 131–133). Uncovering the range of microbial metabolisms present under the environmental conditions at Jinata, and their relative contributions to primary productivity, may therefore find application to predicting environments on Mars most able to support productive microbial communities.

Data availability

Raw 16S rRNA gene amplicon data, raw metagenomic sequence data, and MAGs have been uploaded and made publicly available on NCBI under Project Number PRJNA392119 (genome accession numbers are found in Table S6).

Acknowledgements

LMW acknowledges support from NASA NESSF (#NNX16AP39H), NSF (#OISE 1639454), NSF GROW (#DGE 1144469), the Lewis and Clark Fund for Exploration and Field Research in Astrobiology, the ELSI Origins Network, and an Agouron Institute postdoctoral fellowship. WWF acknowledges the support of NASA Exobiology award #NNX16AJ57G and the Simons Foundation Collaboration on the Origins of Life. MN and YU acknowledge the support of the Japan Society for the Promotion of Science (JP17K14412, JP17H06105)

References

1. Alauzet, C., and E. Jumas-Bilak. 2014. The phylum Deferribacteres and the genus Caldithrix, p. 595–611. *In* E. Rosenberg, E.F. Delong, S. Lory, E. Stackebrandt, and F. Thompson (ed.), The Prokaryotes. Springer, Berlin, Heidelberg.
2. Amend, J.P., and E.L. Shock. 2001. Energetics of overall metabolic reactions of thermophilic and hyperthermophilic Archaea and Bacteria. FEMS Microbiol. Rev. 25:175–243.
3. Beam, J.P., Z.J. Jay, M.C. Schmid, D.B. Rusch, M.F. Romine, R. de M Jennings, M.A. Kozubal, S.G. Tringe, M. Wagner, and W.P. Inskeep. 2016. Ecophysiology of an uncultivated lineage of Aigarchaeota from an oxic, hot spring filamentous 'streamer' community. ISME J. 10:210.
4. Bird, L.J., V. Bonnefoy, and D.K. Newman. 2011. Bioenergetic challenges of microbial iron metabolisms. Trends Microbiol. 19:330–340.
5. Bosak, T., B. Liang, T.D. Wu, S.P. Templer, A. Evans, H. Vali, J.L. Guerquin-Kern, V. Klepac-Ceraj, M.S. Sim, and J. Mui. 2012. Cyanobacterial diversity and activity in modern conical microbialites. Geobiology 10:384–401.
6. Bowers, R.M., N.C. Kyrpides, R. Stepanauskas, *et al.* 2017. Minimum information about a single amplified genome (MISAG) and a metagenome-assembled genome (MIMAG) of bacteria and archaea. Nat. Biotechnol. 35:725.
7. Broda, E. 1977. Two kinds of lithotrophs missing in nature. Z. Allg. Mikrobiol. 17:491–493.
8. Brown, I.I., D.A. Bryant, D. Casamatta, *et al.* 2010. Polyphasic characterization of a thermotolerant siderophilic filamentous cyanobacterium that produces intracellular iron deposits. Appl. Environ. Microbiol. 76:6664–6672.
9. Bryant, D.A., A.M.G. Costas, J.A. Maresca, *et al.* 2007. Candidatus Chloracidobacterium thermophilum: an aerobic phototrophic acidobacterium. Science 317:523–526.

10. Camacho, C., G. Coulouris, V. Avagyan, N. Ma, J. Papadopoulos, K. Bealer, and T.L. Madden. 2009. BLAST+: architecture and applications. BMC Bioinf. 10:421.
11. Canfield, D.E. 1998. A new model for Proterozoic ocean chemistry. Nature 396:450.
12. Canfield, D.E., M.T. Rosing, and C. Bjerrum. 2006. Early anaerobic metabolisms. Philos. Trans. R. Soc. Lond., B, Biol. Sci. 361:1819–1836.
13. Caporaso, J.G., J. Kuczynski, J. Stombaugh, *et al.* 2010. QIIME allows analysis of high-throughput community sequencing data. Nat. Methods 7:335.
14. Caporaso, J.G., C.L. Lauber, W.A. Walters, *et al.* 2012. Ultra-high-throughput microbial community analysis on the Illumina HiSeq and MiSeq platforms. ISME J. 6:1621.
15. Case, R.J., Y. Boucher, I Dahllöf, C. Holmström, W.F. Doolittle, and S. Kjelleberg. 2007. Use of 16S rRNA and rpoB genes as molecular markers for microbial ecology studies. Appl. Environ. Microbiol. 73:278–288.
16. Chang, Y.J., M. Land, L. Hauser, *et al.* 2011. Non-contiguous finished genome sequence and contextual data of the filamentous soil bacterium Ktedonobacter racemifer type strain (SOSP1-21 T). Stand. Genomic Sci. 5:97.
17. Chen, J., and M. Strous. 2013. Denitrification and aerobic respiration, hybrid electron transport chains and co-evolution. Biochim. Biophys. Acta 1827:136–144.
18. Crockford, P.W., J.A. Hayles, H. Bao, N.J. Planavsky, A. Bekker, P.W. Fralick, G.P. Halverson, T.H. Bui, Y. Peng, and B.A. Wing. 2018. Triple oxygen isotope evidence for limited mid-Proterozoic primary productivity. Nature 559:613.
19. D'Imperio, S., C.R. Lehr, H. Oduro, G. Druschel, M. Kühl, and T.R. McDermott. 2008. Relative importance of H2 and H2S as energy sources for primary production in geothermal springs. Appl. Environ. Microbiol. 74:5802–5808.
20. Dodsworth, J.A., J. Gevorkian, F. Despujos, J.K. Cole, S.K. Murugapiran, H. Ming, W.J. Li, G. Zhang, A. Dohnalkova, and B.P. Hedlund. 2014. Thermoflexus hugenholtzii gen. nov., sp. nov., a thermophilic, microaerophilic, filamentous bacterium representing a novel class in the Chloroflexi, Thermoflexia classis nov., and description of Thermoflexaceae fam. nov. and Thermoflexales ord. nov. Int. J. Syst. Evol. Microbiol. 64:2119–2127.
21. Dunfield, P.F., I. Tamas, K.C. Lee, X.C. Morgan, I.R. McDonald, and M.B. Stott. 2012. Electing a candidate: a speculative history of the bacterial phylum OP10. Environ. Microbiol. 14:3069–3080.
22. Dzaugis, M., A.J. Spivack, and S. D'Hondt. 2018. Radiolytic H2 production in martian environments. Astrobiology 18:1137–1146.
23. Edgar, R.C. 2004. MUSCLE: multiple sequence alignment with high accuracy and high throughput. Nucleic Acids Res. 32:1792–1797.
24. Edgar, R.C. 2010. Search and clustering orders of magnitude faster than BLAST. Bioinformatics 26:2460–2461.
25. Ehrenreich, A., and F. Widdel. 1994. Anaerobic oxidation of ferrous iron by purple bacteria, a new type of phototrophic metabolism. Appl. Environ. Microbiol. 60:4517–4526.
26. Eloe-Fadrosh, E.A., D. Paez-Espino, J. Jarett, *et al.*, 2016. Global metagenomic survey reveals a new bacterial candidate phylum in geothermal springs. Nat. Commun. 7:10476.
27. Emerson, D., J.A. Rentz, T.G. Lilburn, R.E. Davis, H. Aldrich, C. Chan, and C.L. Moyer. 2007. A novel lineage of proteobacteria involved in formation of marine Fe-oxidizing microbial mat communities. PLoS One 2:e667.
28. Emerson, D., E.J. Fleming, and J.M. McBeth. 2010. Iron-oxidizing bacteria: an environmental and genomic perspective. Annu. Rev. Microbiol. 64:561–583.
29. Fischer, W.W., J. Hemp, and J.E. Johnson. 2016. Evolution of oxygenic photosynthesis. Annu. Rev. Earth Planet. Sci. 44:647–683.
30. Flamholz, A., E. Noor, A. Bar-Even, and R. Milo. 2011. eQuilibrator—the biochemical thermodynamics calculator. Nucleic Acids Res. 40:D770–D775.
31. Fortney, N.W., S. He, B.J. Converse, B.L. Beard, C.M. Johnson, E.S. Boyd, and E.E. Roden. 2016. Microbial Fe (III) oxide reduction potential in Chocolate Pots hot spring, Yellowstone National Park. Geobiology 14:255–275.
32. Fortney, N.W., S. He, B.J. Converse, E.S. Boyd, and E.E. Roden. 2018. Investigating the composition and metabolic potential of microbial communities in Chocolate Pots hot springs. Front. Microbiol. 9.
33. Fullerton, H., K.W. Hager, S.M. McAllister, and C.L. Moyer. 2017. Hidden diversity revealed by genome-resolved metagenomics of iron-oxidizing microbial mats from Lō'ihi Seamount, Hawai'i. ISME J. 11:1900.
34. Giovannoni, S.J., N.P. Revsbech, D.M. Ward, and R.W. Castenholz. 1987. Obligately phototrophic Chloroflexus: primary production in anaerobic hot spring microbial mats. Arch. Microbiol. 147:80–87.
35. Good, I.J. 1953. The population frequencies of species and the estimation of population parameters. Biometrika 40:237–264.
36. Götz, D., A. Banta, T.J. Beveridge, A.I. Rushdi, B.R.T. Simoneit, and A.L. Reysenbach. 2002. Persephonella marina gen. nov., sp. nov. and Persephonella guaymasensis sp. nov., two novel, thermophilic, hydrogen-oxidizing microaerophiles from deep-sea hydrothermal vents. Int. J. Syst. Evol. Microbiol. 52:1349–1359.
37. Grégoire, P., M. Bohli, J.L. Cayol, *et al.* 2011. Caldilinea tarbellica sp. nov., a filamentous, thermophilic, anaerobic bacterium isolated from a deep hot aquifer in the Aquitaine Basin. Int. J. Syst. Evol. Microbiol. 61:1436–1441.
38. Grouzdev, D.S., M.S. Rysina, I.A. Bryantseva, V.M. Gorlenko, and V.A. Gaisin. 2018. Draft genome sequences of 'Candidatus Chloroploca asiatica' and 'Candidatus Viridilinea mediisalina', candidate representatives of the Chloroflexales order: phylogenetic and taxonomic implications. Stand. Genomic Sci. 13:24.
39. Han, H., J. Hemp, L.A. Pace, H. Ouyang, K. Ganesan, J.H. Roh, F. Daldal, S.R. Blanke, and R.B. Gennis. 2011. Adaptation of aerobic respiration to low O2 environments. Proc. Natl. Acad. Sci. U.S.A. 108:14109–14114.
40. He, S., R.A. Barco, D. Emerson, and E.E. Roden. 2017. Comparative genomic analysis of neutrophilic iron (II) oxidizer genomes for candidate genes in extracellular electron transfer. Front. Microbiol. 8:1584.
41. Hedlund, B.P., S.K. Murugapiran, M. Huntemann, *et al.* 2015. High-quality draft genome sequence of Kallotenue papyrolyticum JKG1T reveals broad heterotrophic capacity focused on carbohydrate and amino acid metabolism. Genome Announc. 3:e01410-15.
42. Hegler, F., T. Lösekann-Behrens, K. Hanselmann, S. Behrens, and A. Kappler. 2012. Influence of seasonal and geochemical changes on iron geomicrobiology of an iron-carbonate mineral water spring. Appl. Environ. Microbiol. 78:7185–7196.
43. Hemp, J., L.M. Ward, L.A. Pace, and W.W. Fischer. 2015. Draft genome sequence of Levilinea saccharolytica KIBI-1, a member of the Chloroflexi class Anaerolineae. Genome Announc. 3:e01357-15.
44. Hemp, J., L.M. Ward, L.A. Pace, and W.W. Fischer. 2015. Draft genome sequence of Ornatilinea apprima P3M-1, an anaerobic member of the Chloroflexi class Anaerolineae. Genome Announc. 3:e01353-15.
45. Hemp, J., L.M. Ward, L.A. Pace, and W.W. Fischer. 2015. Draft genome sequence of Ardenticatena maritima 110S, a thermophilic nitrate-and iron-reducing member of the Chloroflexi class Ardenticatenia. Genome Announc. 3:e01347-15.
46. Hill, M.O. 1973. Diversity and evenness: a unifying notation and its consequences. Ecology 54:427–432.
47. Holland, H.D. 1984. The Chemical Evolution of the Atmosphere and Oceans. Princeton University Press, Princeton, New Jersey.
48. Hug, L.A., B.J. Baker, K. Anantharaman, *et al.* 2016. A new view of the tree of life. Nat. Microbiol. 1:16048.
49. Hurowitz, J.A., W.W. Fischer, N.J. Tosca, and R.E. Milliken. 2010. Origin of acidic surface waters and the evolution of atmospheric chemistry on early Mars. Nat. Geosci. 3:323.
50. Inskeep, W.P., G.G. Ackerman, W.P. Taylor, M. Kozubal, S. Korf, and R.E. Macur. 2005. On the energetics of chemolithotrophy in nonequilibrium systems: case studies of geothermal springs in Yellowstone National Park. Geobiology 3:297–317.
51. Ji, M., C. Greening, I. Vanwonterghem, *et al.* 2017. Atmospheric trace gases support primary production in Antarctic desert surface soil. Nature 552:400.
52. Johnson, J.E., A. Gerpheide, M.P. Lamb, and W.W. Fischer. 2014. O2 constraints from Paleoproterozoic detrital pyrite and uraninite. Geol. Soc. Am. Bull. 126:813–830.
53. Johnston, D.T., F. Wolfe-Simon, A. Pearson, and A.H. Knoll. 2009. Anoxygenic photosynthesis modulated Proterozoic oxygen and sustained Earth's middle age. Proc. Natl. Acad. Sci. U.S.A. 106:16925–16929.
54. Johnston, D.T., S.W. Poulton, C. Dehler, S. Porter, J. Husson, D.E. Canfield, and A.H. Knoll. 2010. An emerging picture of Neoproterozoic ocean chemistry: Insights from the Chuar Group, Grand Canyon, USA. Earth Planet. Sci. Lett. 290:64–73.

55. Kale, V., S.H. Björnsdóttir, Ó.H. Friðjónsson, S.K. Pétursdóttir, S. Ómarsdóttir, and G.Ó. Hreggviðsson. 2013. Litorilinea aerophila gen. nov., sp. nov., an aerobic member of the class Caldilineae, phylum Chloroflexi, isolated from an intertidal hot spring. Int. J. Syst. Evol. Microbiol. 63:1149–1154.
56. Kaneoka, I., N. Isshiki, and S. Zashu. 1970. K-Ar ages of the Izu-Bonin islands. Geochem. J. 4:53–60.
57. Kang, D.D., J. Froula, R. Egan, and Z. Wang. 2015. MetaBAT, an efficient tool for accurately reconstructing single genomes from complex microbial communities. PeerJ. 3:e1165.
58. Kato, S., S. Kikuchi, T. Kashiwabara, Y. Takahashi, K. Suzuki, T. Itoh, M. Ohkuma, and A. Yamagishi. 2012. Prokaryotic abundance and community composition in a freshwater iron-rich microbial mat at circumneutral pH. Geomicrobiol. J. 29:896–905.
59. Kato, S., M. Ohkuma, D.H. Powell, S.T. Krepski, K. Oshima, M. Hattori, N. Shapiro, T. Woyke, and C.S. Chan. 2015. Comparative genomic insights into ecophysiology of neutrophilic, microaerophilic iron oxidizing bacteria. Front. Microbiol. 6:1265.
60. Katoh, K., K. Misawa, K.I. Kuma, and T. Miyata. 2002. MAFFT: a novel method for rapid multiple sequence alignment based on fast Fourier transform. Nucleic Acids Res. 30:3059–3066.
61. Kawaichi, S., N. Ito, R. Kamikawa, T. Sugawara, T. Yoshida, and Y. Sako. 2013. Ardenticatena maritima gen. nov., sp. nov., a ferric iron- and nitrate-reducing bacterium of the phylum 'Chloroflexi' isolated from an iron-rich coastal hydrothermal field, and description of Ardenticatenia classis nov. Int. J. Syst. Evol. Microbiol. 63:2992–3002.
62. Kawaichi, S., T. Yoshida, Y. Sako, and R. Nakamura. 2015. Draft genome sequence of a heterotrophic facultative anaerobic thermophilic bacterium, Ardenticatena maritima strain 110ST. Genome Announc. 3:e01145-15.
63. Kawasumi, T., Y. Igarashi, T. Kodama, and Y. Minoda. 1980. Isolation of strictly thermophilic and obligately autotrophic hydrogen bacteria. Agric. Biol. Chem. 44:1985–1986.
64. Kharecha, P., J. Kasting, and J. Siefert. 2005. A coupled atmosphere–ecosystem model of the early Archean Earth. Geobiology 3:53–76.
65. Klatt, C.G., D.A. Bryant, and D.M. Ward. 2007. Comparative genomics provides evidence for the 3-hydroxypropionate autotrophic pathway in filamentous anoxygenic phototrophic bacteria and in hot spring microbial mats. Environ. Microbiol. 9:2067–2078.
66. Klatt, C.G., J.M. Wood, D.B. Rusch, *et al.* 2011. Community ecology of hot spring cyanobacterial mats: predominant populations and their functional potential. ISME J. 5:1262.
67. Klueglein, N., and A. Kappler. 2013. Abiotic oxidation of Fe (II) by reactive nitrogen species in cultures of the nitrate-reducing Fe (II) oxidizer Acidovorax sp. BoFeN1–questioning the existence of enzymatic Fe (II) oxidation. Geobiology 11:180–190.
68. Kublanov, I.V., O.M. Sigalova, S.N. Gavrilov, *et al.* 2017. Genomic analysis of Caldithrix abyssi, the thermophilic anaerobic bacterium of the novel bacterial phylum Calditrichaeota. Front. Microbiol. 8:195.
69. Kulp, T.R., S.E. Hoeft, M. Asao, M.T. Madigan, J.T. Hollibaugh, J.C. Fisher, J.F. Stolz, C.W. Culbertson, L.G. Miller, and R.S. Oremland. 2008. Arsenic (III) fuels anoxygenic photosynthesis in hot spring biofilms from Mono Lake, California. Science 321:967–970.
70. Kuznetsov, B.B., R.N. Ivanovsky, O.I. Keppen, *et al.* 2011. Draft genome sequence of the anoxygenic filamentous phototrophic bacterium Oscillochloris trichoides subsp. DG-6. J. Bacteriol. 193:321–322.
71. Laslett, D., and B. Canback. 2004. ARAGORN, a program to detect tRNA genes and tmRNA genes in nucleotide sequences. Nucleic Acids Res. 32:11–16.
72. Lemoine, F., J.B.D. Entfellner, E. Wilkinson, D. Correia, M.D. Felipe, T. Oliveira, and O. Gascuel. 2018. Renewing Felsenstein's phylogenetic bootstrap in the era of big data. Nature 556:452.
73. Letunic, I., and P. Bork. 2016. Interactive tree of life (iTOL) v3: an online tool for the display and annotation of phylogenetic and other trees. Nucleic Acids Res. 44:W242–W245.
74. Li, H., B. Handsaker, A. Wysoker, T. Fennell, J. Ruan, N. Homer, G. Marth, G. Abecasis, and R. Durbin. 2009. The sequence alignment/map format and SAMtools. Bioinformatics 25:2078–2079.
75. Li, D., C.M. Liu, R. Luo, K. Sadakane, and T.W. Lam. 2015. MEGAHIT: an ultra-fast single-node solution for large and complex metagenomics assembly via succinct de Bruijn graph. Bioinformatics 31:1674–1676.
76. Lyons, T.W., C.T. Reinhard, and N.J. Planavsky. 2014. The rise of oxygen in Earth's early ocean and atmosphere. Nature 506:307.
77. Makita, H., E. Tanaka, S. Mitsunobu, M. Miyazaki, T. Nunoura, K. Uematsu, Y. Takaki, S. Nishi, S. Shimamura, and K. Takai. 2017. Mariprofundus micogutta sp. nov., a novel iron-oxidizing zetaproteobacterium isolated from a deep-sea hydrothermal field at the Bayonnaise knoll of the Izu-Ogasawara arc, and a description of Mariprofundales ord. nov. and Zetaproteobacteria classis nov. Arch. Microbiol. 199:335–346.
78. Marshall, I.P., P. Starnawski, C. Cupit, E. Fernández Cáceres, T.J. Ettema, A. Schramm, and K.U. Kjeldsen. 2017. The novel bacterial phylum Calditrichaeota is diverse, widespread and abundant in marine sediments and has the capacity to degrade detrital proteins. Environ. Microbiol. Rep. 9:397–403.
79. Meyer-Dombard, D., J.P. Amend, and M.R. Osburn. 2013. Microbial diversity and potential for arsenic and iron biogeochemical cycling at an arsenic rich, shallow-sea hydrothermal vent (Tutum Bay, Papua New Guinea). Chem. Geol. 348:37–47.
80. Miller, M.A., W. Pfeiffer, and T. Schwartz. 2010. Creating the CIPRES Science Gateway for inference of large phylogenetic trees, p. 1–8. *In* 2010 Gateway Computing Environments Workshop. (GCE), IEEE, Piscataway.
81. Miroshnichenko, M.L., N.A. Kostrikina, N.A. Chernyh, N.V. Pimenov, T.P. Tourova, A.N. Antipov, S. Spring, E. Stackebrandt, and E.A. Bonch-Osmolovskaya. 2003. Caldithrix abyssi gen. nov., sp. nov., a nitrate-reducing, thermophilic, anaerobic bacterium isolated from a Mid-Atlantic Ridge hydrothermal vent, represents a novel bacterial lineage. Int. J. Syst. Evol. Microbiol. 53:323–329.
82. Mori, J.F., J.J. Scott, K.W. Hager, C.L. Moyer, K. Küsel, and D. Emerson. 2017. Physiological and ecological implications of an iron-or hydrogen-oxidizing member of the Zetaproteobacteria, Ghiorsea bivora, gen. nov., sp. nov. ISME J. 11:2624.
83. Pace, L.A., J. Hemp, L.M. Ward, and W.W. Fischer. 2015. Draft genome of Thermanaerothrix daxensis GNS-1, a thermophilic facultative anaerobe from the Chloroflexi class Anaerolineae. Genome Announc. 3:e01354-15.
84. Parada, A.E., D.M. Needham, and J.A. Fuhrman. 2016. Every base matters: assessing small subunit rRNA primers for marine microbiomes with mock communities, time series and global field samples. Environ. Microbiol. 18:1403–1414.
85. Parks, D.H., M. Imelfort, C.T. Skennerton, P. Hugenholtz, and G.W. Tyson. 2015. CheckM: assessing the quality of microbial genomes recovered from isolates, single cells, and metagenomes. Genome Res. 25:1043–1055.
86. Parks, D.H., M. Chuvochina, D.W. Waite, C. Rinke, A. Skarshewski, P.A. Chaumeil, and P. Hugenholtz. 2018. A standardized bacterial taxonomy based on genome phylogeny substantially revises the tree of life. Nat. Biotechnol. 36:996–1004.
87. Pierson, B.K., M.N. Parenteau, and B.M. Griffin. 1999. Phototrophs in high-iron-concentration microbial mats: physiological ecology of phototrophs in an iron-depositing hot spring. Appl. Environ. Microbiol. 65:5474–5483.
88. Poulton, S.W., P.W. Fralick, and D.E. Canfield. 2010. Spatial variability in oceanic redox structure 1.8 billion years ago. Nat. Geosci. 3:486.
89. Price, M.N., P.S. Dehal, and A.P. Arkin. 2010. FastTree 2–approximately maximum-likelihood trees for large alignments. PLoS One 5:e9490.
90. Quast, C., E. Pruesse, P. Yilmaz, J. Gerken, T. Schweer, P. Yarza, J. Peplies, and F.O. Glöckner. 2012. The SILVA ribosomal RNA gene database project: improved data processing and web-based tools. Nucleic Acids Res. 41:D590–D596.
91. R Core Team. 2014. R: A Language and Environment for Statistical Computing. R Foundation for Statistical Computing, Vienna, Austria.
92. Roden, E., J.M. McBeth, M. Blothe, E.M. Percak-Dennett, E.J. Fleming, R.R. Holyoke, G.W. Luther III, and D. Emerson. 2012. The microbial ferrous wheel in a neutral pH groundwater seep. Front. Microbiol. 3:172.
93. Rodriguez-R, L.M., and K.T. Konstantinidis. 2014. Bypassing cultivation to identify bacterial species. Microbe 9:111–118.
94. Roeselers, G., T.B. Norris, R.W. Castenholz, S. Rysgaard, R.N. Glud, M. Kühl, and G. Muyzer. 2007. Diversity of phototrophic bacteria in microbial mats from Arctic hot springs (Greenland). Environ. Microbiol. 9:26–38.
95. Sekiguchi, Y., T. Yamada, S. Hanada, A. Ohashi, H. Harada, and Y. Kamagata. 2003. Anaerolinea thermophila gen. nov., sp. nov. and Caldilinea aerophila gen. nov., sp. nov., novel filamentous thermophiles that represent a previously uncultured lineage of the domain Bacteria at the subphylum level. Int. J. Syst. Evol. Microbiol. 53:1843–1851.

96. Shannon, C. 1948. A mathematical theory of communication, p. 379–423, 623–656. *In* The Bell System Technical Journal, vol. 27. University of Illinois Press, Champaign.
97. Shih, P.M., J. Hemp, L.M. Ward, N.J. Matzke, and W.W. Fischer. 2017. Crown group Oxyphotobacteria postdate the rise of oxygen. Geobiology 15:19–29.
98. Shih, P.M., L.M. Ward, and W.W. Fischer. 2017. Evolution of the 3-hydroxypropionate bicycle and recent transfer of anoxygenic photosynthesis into the Chloroflexi. Proc. Natl. Acad. Sci. U.S.A. 114:10749–10754.
99. Sieber, C.M., A.J. Probst, A. Sharrar, B.C. Thomas, M. Hess, S.G. Tringe, and J.F. Banfield. 2018. Recovery of genomes from metagenomes via a dereplication, aggregation and scoring strategy. Nat. Microbiol. 3:836–843.
100. Simpson, E.H. 1949. Measurement of diversity. Nature 63:688.
101. Singer, E., D. Emerson, E.A. Webb, *et al.* 2011. Mariprofundus ferrooxydans PV-1 the first genome of a marine Fe (II) oxidizing Zetaproteobacterium. PLoS One 6:e25386.
102. Sleep, N.H., and D.K. Bird. 2007. Niches of the pre-photosynthetic biosphere and geologic preservation of Earth's earliest ecology. Geobiology 5:101–117.
103. Søndergaard, D., C.N. Pedersen, and C. Greening. 2016. HydDB: a web tool for hydrogenase classification and analysis. Sci. Rep. 6:34212.
104. Sorokin, D.Y., S. Lücker, D. Vejmelkova, *et al.* 2012. Nitrification expanded: discovery, physiology and genomics of a nitrite-oxidizing bacterium from the phylum Chloroflexi. ISME J. 6:2245.
105. Spear, J.R., J.J. Walker, T.M. McCollom, and N.R. Pace. 2005. Hydrogen and bioenergetics in the Yellowstone geothermal ecosystem. Proc. Natl. Acad. Sci. U.S.A. 102:2555–2560.
106. Stamatakis, A. 2014. RAxML version 8: a tool for phylogenetic analysis and post-analysis of large phylogenies. Bioinformatics 30:1312–1313.
107. Stamenković, V., L.M. Ward, M. Mischna, and W.W. Fischer. 2018. O 2 solubility in Martian near-surface environments and implications for aerobic life. Nat. Geosci. 11:905–909.
108. Stamenković, V., L.W. Beegle, K. Zacny, *et al.* 2019. The next frontier for planetary and human exploration. Nat. Astron. 3:116–120.
109. Stein, L.Y., and M.G. Klotz. 2016. The nitrogen cycle. Curr. Biol. 26:R94–R98.
110. Stookey, L.L. 1970. Ferrozine—a new spectrophotometric reagent for iron. Anal. Chem. 42:779–781.
111. Strous, M., J.A. Fuerst, E.H. Kramer, S. Logemann, G. Muyzer, K.T. van de Pas-Schoonen, R. Webb, J.G. Kuenen, and M.S. Jetten. 1999. Missing lithotroph identified as new planctomycete. Nature 400:446.
112. Suda, K., A. Gilbert, K. Yamada, N. Yoshida, and Y. Ueno. 2017. Compound–and position–specific carbon isotopic signatures of abiogenic hydrocarbons from on–land serpentinite–hosted Hakuba Happo hot spring in Japan. Geochim. Cosmochim. Acta 206:201–215.
113. Swanner, E.D., A.M. Mloszewska, O.A. Cirpka, R. Schoenberg, K.O. Konhauser, and A. Kappler. 2015. Modulation of oxygen production in Archaean oceans by episodes of Fe (II) toxicity. Nat. Geosci. 8:126–130.
114. Takai, K., and S. Nakagawa. 2014. The family Hydrogenothermaceae, p. 689–699. *In* E. Rosenberg, E.F. Delong, S. Lory, E. Stackebrandt, and F. Thompson (ed.), The Prokaryotes. Springer, Berlin, Heidelberg.
115. Tank, M., V. Thiel, D.M. Ward, and D.A. Bryant. 2017. A panoply of phototrophs: an overview of the thermophilic chlorophototrophs of the microbial mats of alkaline siliceous hot springs in Yellowstone National Park, WY, USA, p. 87–137. *In* M. Tank, V. Thiel, D.M. Ward, and D.A. Bryant (ed.), Modern Topics in the Phototrophic Prokaryotes. Springer International Publishing, New York.
116. Thiel, V., M. Hügler, D.M. Ward, and D.A. Bryant. 2017. The dark side of the mushroom spring microbial mat: life in the shadow of chlorophototrophs. II. Metabolic functions of abundant community members predicted from metagenomic analyses. Front. Microbiol. 8:943.
117. Thiel, V., M. Tank, and D.A. Bryant. 2018. Diversity of chlorophototrophic bacteria revealed in the omics era. Annu. Rev. Plant Biol. 69:21–49.
118. Trembath-Reichert, E., L.M. Ward, S.P. Slotznick, S.L. Bachtel, C. Kerans, J.P. Grotzinger, and W.W. Fischer. 2016. Gene sequencing-based analysis of microbial-mat morphotypes, caicos platform, British West Indies. J. Sediment. Res. 86:629–636.
119. Trouwborst, R.E., A. Johnston, G. Koch, G.W. Luther III, and B.K. Pierson. 2007. Biogeochemistry of Fe (II) oxidation in a photosynthetic microbial mat: implications for Precambrian Fe (II) oxidation. Geochim. Cosmochim. Acta 71:4629–4643.
120. Walker, J.C. and P. Brimblecombe. 1985. Iron and sulfur in the pre-biologic ocean. Precambrian Res. 28:205–222.
121. Wang, Q., G.M. Garrity, J.M. Tiedje, and J.R. Cole. 2007. Naive Bayesian classifier for rapid assignment of rRNA sequences into the new bacterial taxonomy. Appl. Environ. Microbiol. 73:5261–5267.
122. Ward, L.M., J. Hemp, L.A. Pace, and W.W. Fischer. 2015. Draft genome sequence of Herpetosiphon geysericola GC-42, a nonphototrophic member of the Chloroflexi class Chloroflexia. Genome Announc. 3:e01352-15.
123. Ward, L.M., J. Hemp, L.A. Pace, and W.W. Fischer. 2015. Draft genome sequence of Leptolinea tardivitalis YMTK-2, a mesophilic anaerobe from the Chloroflexi class Anaerolineae. Genome Announc. 3:e01356-15.
124. Ward, L.M., J.L. Kirschvink, and W.W. Fischer. 2016. Timescales of oxygenation following the evolution of oxygenic photosynthesis. Origins Life Evol. Biospheres 46:51–65.
125. Ward, L.M., S.E. McGlynn, and W.W. Fischer. 2017. Draft genome sequences of a novel lineage of armatimonadetes recovered from Japanese hot springs. Genome Announc. 5:e00820-17.
126. Ward, L.M., A. Idei, S. Terajima, T. Kakegawa, W.W. Fischer, and S.E. McGlynn. 2017. Microbial diversity and iron oxidation at Okuoku—hachikurou Onsen, a Japanese hot spring analog of Precambrian iron formations. Geobiology 15:817–835.
127. Ward, L.M., J. Hemp, P.M. Shih, S.E. McGlynn, and W.W. Fischer. 2018. Evolution of phototrophy in the Chloroflexi phylum driven by horizontal gene transfer. Front. Microbiol. 9:260.
128. Ward, L.M., S.E. McGlynn, and W.W. Fischer. 2018. Draft genome sequence of a divergent anaerobic member of the chloroflexi class ardenticatenia from a sulfidic hot spring. Genome Announc. 6:e00571-18.
129. Ward, L.M., S.E. McGlynn, and W.W. Fischer. 2018. Draft genome sequences of two basal members of the anaerolineae class of chloroflexi from a sulfidic hot spring. Genome Announc. 6:e00570-18.
130. Ward, L.M., P.M. Shih, and W.W. Fischer. 2018. MetaPOAP: Presence or absence of metabolic pathways in metagenome-assembled genomes. Bioinformatics 34:4284–4286.
131. Ward, L.M., B. Rasmussen, and W.W. Fischer. 2019. Primary productivity was limited by electron donors prior to the advent of oxygenic photosynthesis. J. Geophys. Res.: Biogeosci. 124:211–226.
132. Ward, L.M., V. Stamenković, K. Hand, and W.W. Fischer. 2019. Follow the oxygen: Comparative histories of planetary oxygenation and opportunities for aerobic life. Astrobiology 19:811–824.
133. Ward, L.M., and P.M. Shih. 2019. The evolution and productivity of carbon fixation pathways in response to changes in oxygen concentration over geological time. Free Radical Biol. Med. https://doi.org/10.1016/j.freeradbiomed.2019.01.049
134. Waterhouse, A.M., J.B. Procter, D.M. Martin, M. Clamp, and G.J. Barton. 2009. Jalview Version 2—a multiple sequence alignment editor and analysis workbench. Bioinformatics 25:1189–1191.
135. Wickham, H. 2010. ggplot2: elegant graphics for data analysis. J. Stat. Softw. 35:65–88.
136. Wu, Y.W., Y.H. Tang, S.G. Tringe, B.A. Simmons, and S.W. Singer. 2014. MaxBin: an automated binning method to recover individual genomes from metagenomes using an expectation-maximization algorithm. Microbiome 2:26.
137. Yamada, T., and Y. Sekiguchi. 2009. Cultivation of uncultured chloroflexi subphyla: significance and ecophysiology of formerly uncultured Chloroflexi 'subphylum I' with natural and biotechnological relevance. Microbes Environ. 24:205–216.

Microbes Environ. Vol. 29, No. 4, 427-430, 2014
https://www.jstage.jst.go.jp/browse/jsme2 doi:10.1264/jsme2.ME14054

MOST CITED ORIGINAL PAPER PUBLISHED
IN THIS TEN YEARS [2012-2021] (201 citations)
MOST CITED ORIGINAL PAPER IN 2021 (59 citations)

Short Communication

Intestinal Colonization by a *Lachnospiraceae* Bacterium Contributes to the Development of Diabetes in Obese Mice

Keishi Kameyama[1]*, and Kikuji Itoh[2]

[1]*Institute for Innovation, Ajinomoto Co., Inc., Kawasaki 210–8681, Japan; and* [2]*Department of Veterinary Public Health, Graduate School of Agricultural and Life Sciences, The University of Tokyo, Tokyo 113–8657, Japan*

(Received April 4, 2014—Accepted July 17, 2014—Published online October 4, 2014)

The aim of the present study was to identify bacteria that may contribute to the onset of metabolic dysfunctions. We isolated and identified a candidate bacterium belonging to *Lachnospiraceae* (strain AJ110941) in the feces of hyperglycemic obese mice. The colonization of germ-free *ob/ob* mice by AJ110941 induced significant increases in fasting blood glucose levels as well as liver and mesenteric adipose tissue weights, and decreases in plasma insulin levels and HOMA-β values. These results indicated that the specific gut commensal bacterium AJ110941 influenced the development of obesity and diabetes in *ob/ob* mice with genetic susceptibility for obesity.

Key words: gut microbiota, diabetes, T-RFLP, gnotobiotic mouse, *Lachnospiraceae*

The gut microbiota has been shown to influence host energy homeostasis, metabolism, and inflammation; thus, microbial communities within the gut are now recognized as an important environmental factor in the onset of obesity and type 2 diabetes (T2D) (5, 7, 12, 14, 23). As a consequence, interest in the development of methods to target gut microbiota as a therapy for T2D is increasing (2, 12, 18, 21).

Several studies have conducted metagenomic analyses in an attempt to identify members of the gut microbial community that contribute most significantly to the progression of T2D. Qin *et al.* performed a metagenomic analysis on fecal samples obtained from 345 Chinese men and women with or without T2D (19). Karlsson *et al.* also conducted a metagenomic analysis to compare microbial communities in fecal samples collected from 145 European women who had either T2D, impaired glucose metabolism, or were healthy (13). Both of these studies reported that butyrate-producing *Roseburia* species and *Faecalibacterium prauznitzii* were rarer in subjects with T2D; however, the identified bacteria that existed in high population in T2D subjects differed between these studies (8). Cani *et al.* proposed that lipopolysaccharide (LPS), a cell wall component of almost all Gram-negative bacteria, may be a key substance responsible for metabolic endotoxemia, low-grade systemic inflammation, and insulin resistance in mouse models (1, 3). In support of this, a previous study reported that experimental endotoxemia induced adipose inflammation and insulin resistance in human subjects (17).

We herein searched for the specific gut commensal bacterium related to metabolic syndrome using the terminal restriction fragment length polymorphism (T-RFLP) analysis of fecal samples from a mouse model of T2D. In this study, a comparison of homozygous *db/db* (diabetic) with heterozygous *db/+* (non-diabetic) mice revealed that a specific fragment of the T-RFLP analysis was present at significantly higher levels in *db/db* mice than in *db/+* mice. Even though *ob/ob* obese mice gain weight rapidly and show the symptoms of insulin resistance, most of the obese mice do not develop severe hyperglycemia compared with *db/db* mice (22). However, one of the *ob/ob* mice in the present study showed an abnormally high fasting blood glucose (FBG) level similar to *db/db* mice. The specific fragment observed in *db/db* mice was also the most prominent in the abnormally hyperglycemic *ob/ob* mouse. We hypothesized that the specific bacterium harboring the fragment may have contributed to the progression of T2D; therefore, we isolated and cultured the bacterium (strain AJ110941). We then determined that colonization by the isolate with the LPS producer *E. coli* induced hyperglycemia and the accumulation of adipose tissue in the gnotobiotic *ob/ob* mouse model.

All experimental procedures were reviewed and approved by the Animal Care Committee of Ajinomoto Co., Inc. Male 5-week-old homozygous BKS.Cg-Dock7^{m} +/+Lepr^{db}/J (*db/db*, diabetic) mice, heterozygous control (*db/+*, non-diabetic) mice, and homozygous B6.V-Lep^{ob}/J (*ob/ob*, obese) mice were obtained from Charles River Japan (Yokohama, Japan). Male 5-week-old germ-free *ob/ob* mice were obtained from Sankyo Lab Service (Tokyo, Japan). These mice were housed in a controlled environment (on a 12-h light/dark cycle with lights turning off at 19:00) with free access to standard chow CRF-1 (Oriental Yeast, Tokyo, Japan) and water and kept in specific pathogen-free (SPF) or germ-free/gnotobiotic conditions throughout the experimental period. Fresh feces and blood were collected from 5- and 11-week-old mice after fasting for 16 h.

Blood glucose (FBG) levels were determined using DRI-CHEM 7000V (Fujifilm, Tokyo, Japan). Plasma insulin levels were determined using an ultrasensitive mouse insulin kit (Morinaga Institute of Biological Science, Yokohama, Japan). Plasma glucagon levels were determined using the

* Corresponding author. E-mail: keishi_kameyama@ajinomoto.com

Glucagon ELISA Kit Wako (Wako Pure Chemical Industries, Osaka, Japan). Insulin resistance (HOMA-IR) and β-cell function (HOMA-β) were both calculated on the basis of the fasting levels of plasma glucose and insulin according to the homeostasis model assessment (HOMA) method (16).

Fresh fecal samples were collected from mice, added to 99% ethanol, and stored at −30°C. Bacterial DNA was extracted from the fecal samples using the FastDNA spin kit for soil (MP Biomedicals, Santa Ana, CA) using the FastPrep instrument (MP Biomedicals). T-RFLP analyses of the mouse gut microbiota were performed as previously described (10). Two universal primers, 27F labeled with 6-carboxyfluorescein (FAM): 5'-FAM-AGAGTTTGATCCTGGCTCAG-3' and 1492R: 5'-GGTTACCTTGTTACGACTT-3' were used in PCR to amplify the 16S rRNA gene coding region. Purified PCR products of the 16S rRNA gene were digested with *Msp*I (Takara Bio, Otsu, Japan).

To isolate and culture the bacterium, fresh feces were collected and immediately weighed and transferred to an anaerobic chamber. The feces were homogenized with a 50-fold volume (v/w) of an anaerobic diluent, serially diluted, and then plated on Eggerth-Gagnon (EG) agar plates (11). The agar plates were incubated at 37°C for 4 d in the anaerobic chamber. All of the colonies were identified by their fragment size, and a target colony with a fragment size of 282 bp was then selected. The colony was passaged onto new EG agar plates, and the bacterial purity of the isolate was ensured by re-streaking and microscopic observations. The 16S rRNA gene sequence of the isolated bacterium was determined as previously described (15). The sequence was assembled using GENETYX version 7 (GENETYX, Tokyo, Japan). The identification and phylogenic tree analysis of the 16S rRNA gene sequence were carried out using the Ribosomal Database Project (RDP) (6).

When the mice were 8 weeks old, germ-free *ob/ob* mice were separated into 3 groups for the germ-free/gnotobiotic experiment: Group-1 (n=4), germ-free; Group-2 (n=4), colonization by the non-pathogenic *Escherichia coli* strain E-17, which had been isolated from SPF mice; Group-3 (n=4), colonization by AJ110941 with *E. coli* E-17. Groups-2 and -3 were then orally inoculated with *E. coli* E-17 or AJ110941 with *E. coli* E-17 (approximately 1×10^8 cells suspended in anaerobic PBS, respectively). Group-1 was orally administered PBS only. These mice were maintained under the germ-free or gnotobiotic conditions for 8 weeks.

We compared differences in gut microbiota patterns between *db/+* and *db/db* mice. Hyperglycemia was observed in 11-week-old, but not in 5-week-old mice (Fig. S1). The 282 bp fragment was significantly higher in *db/db* than *db/+* mice at both 5 and 11 weeks old (Fig. S2). We then evaluated the presence of the 282 bp fragment in another metabolic syndrome model, the *ob/ob* mouse. The highest FBG level observed among all *ob/ob* mice was in Mouse Number 4 (Fig. S3). The 282 bp fragment was also more prominent in hyperglycemic Mouse Number 4 than in the normal glycemic *ob/ob* mouse at both 5 and 11 weeks old (Fig. S4). Based on these *db/db* and *ob/ob* mice results, we focused on this 282 bp fragment bacteria.

We isolated a colony harboring the 282 bp fragment and established an axenic strain (strain AJ110941). The isolate was determined to be closely related to the genus *Anaerostipes* in the family *Lachnospiraceae* (Fig. 1).

We then generated gnotobiotic *ob/ob* mice colonized by AJ110941 with *E. coli*. Eight weeks after the inoculation, the cecum, liver, adipose tissue, and blood were collected after a 16-h fast. The gut microbiota of the cecal contents from the three groups was determined by T-RFLP analysis. No PCR amplicon was detected in Group-1. Only a single fragment (488 bp) that corresponded to *E. coli* was detected in Group-2. Only two fragments (282 bp and 488 bp) were detected in Group-3. These results clearly indicated that germ-free or gnotobiotic conditions were maintained during the experimental period. The weights of the liver and mesenteric adipose tissue significantly increased in Group-3, whereas no significant difference was observed in body weights between the three groups. FBG and plasma glucagon levels were significantly higher in Group-3, while plasma insulin levels were significantly lower. On the other hand, no significant differences were observed in these parameters between Groups-1 and -2. The homeostasis model assessment was calculated from FBG and plasma insulin levels as an index of insulin resistance (HOMA-IR) and pancreatic β cell function (HOMA-β). HOMA-β was significantly lower in Group-3, whereas no significant differences were noted in HOMA-IR between the three groups (Table 1). These results suggested that colonization by AJ110941 may have promoted the dysfunction of pancreatic β-cells.

Therefore, AJ110941 should be regarded as one of the important causative gut bacteria for the induction of T2D. A previous study reported that the relative abundance of the

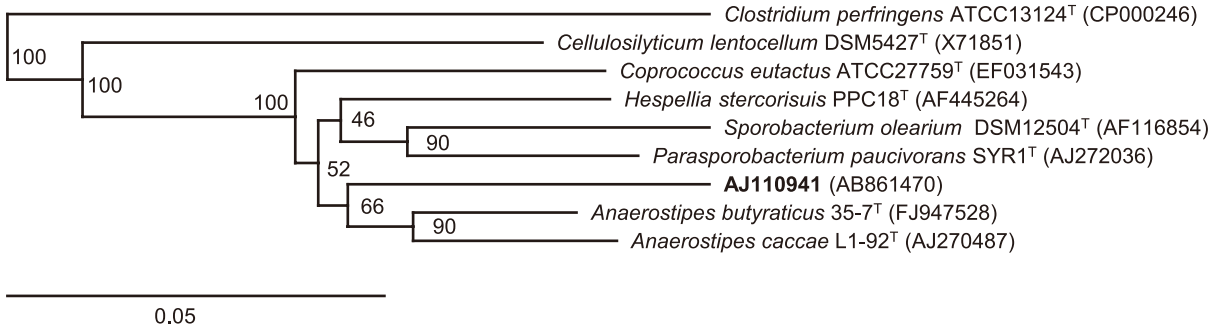

Fig. 1. Phylogenetic tree based on the 16S rRNA gene constructed by Weighbor, the weighted neighbor-joining tree building algorithm, showing AJ110941 and other strains of the family *Lachnospiraceae*. *Clostridium perfringens* ATCC13124^T was used as an outgroup. The numbers close to the nodes represent bootstrap values (n=100 replicates). The scale bar represents 0.05 substitutions per nucleotide position.

Table 1. Phenotypes of germ-free and gnotobiotic *ob/ob* mice

	Group-1	Group-2	Group-3
Body weight without the caecum (g)	58.10 ± 5.98^{a}	61.75 ± 4.29^{a}	63.48 ± 10.37^{a}
Cecum (% of body weight)	11.63 ± 4.89^{a}	12.88 ± 1.94^{a}	4.47 ± 0.93^{b}
Liver (% of body weight without the cecum)	6.91 ± 0.66^{a}	7.29 ± 1.83^{a}	9.70 ± 0.46^{b}
Mesenteric adipose tissue (% of body weight without the cecum)	1.64 ± 0.46^{a}	1.81 ± 0.39^{a}	2.63 ± 0.30^{b}
Fasting blood glucose (mg dL^{-1})	216.5 ± 113.6^{a}	286.5 ± 54.1^{ab}	433.25 ± 65.4^{b}
Fasting plasma insulin (μU mL^{-1})	339.7 ± 46.44^{a}	299.8 ± 105.0^{a}	159.4 ± 50.9^{b}
Fasting plasma glucagon (pg mL^{-1})	179.9 ± 43.0^{a}	324.2 ± 42.4^{a}	529.0 ± 18.3^{b}
HOMA-IR	132.5 ± 23.3^{a}	187.5 ± 70.6^{a}	184.4 ± 64.1^{a}
HOMA-β	1350.4 ± 468.9^{a}	638.5 ± 411.9^{ab}	141.7 ± 40.7^{b}

Group-1: germ-free, Group-2: colonization by *E. coli*, Group-3: colonization by AJ110941 with *E. coli*. Data are expressed as means±SD. Values not sharing a common letter are significantly different at $p<0.05$ by the Tukey–Kramer multiple comparisons test ($n=4$ per group) using the JMP 10.0.0 statistical software package (SAS Institute, Cary, NC).

taxonomic family *Lachnospiraceae* was increased by early-life subtherapeutic antibiotic treatments in an obese mouse model (4). Additionally, a metagenomic study indicated that the taxonomic family *Lachnospiraceae* may be associated with T2D (19). However, it remains unclear whether bacteria belonging to the family *Lachnospiraceae* actually affect obesity and FBG levels *in vivo*. Therefore, we generated gnotobiotic *ob/ob* mice colonized by AJ110941 with *E. coli* to reveal a possible causal relationship. In a preliminary examination, we microscopically observed that AJ110941 did not singly colonize the intestinal tract of *ob/ob* germ-free mice. *E. coli*, which is a facultative anaerobe, may be needed to maintain an oxygen-free environment in the intestinal tract because AJ110941 needs strict anaerobic conditions for growth. In our study, a mono-association with the LPS producer *E. coli* induced neither hyperglycemia nor the accumulation of adipose tissues. In contrast, LPS derived from Gram-negative bacteria in the gastrointestinal tract was previously identified as one of the most important factors inducing the development of T2D (1, 3). Our results indicated that the presence of LPS in the intestinal tract was necessary, but not sufficient for the pathogenesis of diabetes. We speculated that AJ110941 may have assisted with the translocation of LPS into the blood from the intestinal tract. We are currently investigating the effects of AJ110941 on LPS translocation in *in vitro*/*vivo* models.

Regarding the particular gut bacterium involved in metabolic syndrome, *Methanobrevibacter smithii* and *Bacteroides thetaiotaomicron* were previously shown to enhance host energy storage in di-associated mice (20). Furthermore, Fei and Zhao reported that the strain *Enterobacter cloacae* B29, which was isolated from an obese human subject, induced obesity and insulin resistance accompanied by serum endotoxemia in mono-associated mice (9).

This is the first study to have successfully identified a specific *Lachnospiraceae* bacterium involved in metabolic disorders. Future studies are needed to elucidate the molecular mechanisms underlying the adverse effects of AJ110941 on glucose and lipid metabolism in mouse models. It remains unclear whether AJ110941 or its closely-related species inhabits the human intestinal tract. We intend to perform a preliminary epidemiological study on obese and diabetic subjects to address this question.

The 16S rRNA gene sequence of the isolated bacterium (strain AJ110941) is available in the DDBJ/EMBL/GenBank databases under the accession number AB861470.

Acknowledgements

We thank Ranko Nishi and Mizuki Kobayashi for their research assistance.

References

1. Cani, P.D., J. Amar, M.A. Iglesias, *et al.* 2007. Metabolic endotoxemia initiates obesity and insulin resistance. Diabetes 56:1761–1772.
2. Cani, P.D., and N.M. Delzenne. 2012. The gut microbiome as therapeutic target. Pharmacol. Ther. 130:202–212.
3. Cani, P.D., S. Possemiers, T. Van de Wiele, *et al.* 2009. Changes in gut microbiota control inflammation in obese mice through a mechanism involving GLP-2-driven improvement of gut permeability. Gut 58:1091–1103.
4. Cho, I., S. Yamanishi, L. Cox, *et al.* 2012. Antibiotics in early life alter the murine colonic microbiome and adiposity. Nature 488:621–626.
5. Clemente, J.C., L.K. Ursell, L.W. Parfrey, and R. Knight. 2012. The impact of the gut microbiota on human health: an integrative view. Cell 148:1258–1270.
6. Cole, J.R., Q. Wang, J.A. Fish, *et al.* 2014. Ribosomal Database Project: data and tools for high throughput rRNA analysis. Nucleic Acids Res. 42:D633–642.
7. Cox, L.M., and M.J. Blaser. 2013. Pathways in microbe-induced obesity. Cell Metab. 17:883–894.
8. de Vos, W.M., and M. Nieuwdorp. 2013. Genomics: A gut prediction. Nature 498:48–49.
9. Fei, N., and L. Zhao. 2013. An opportunistic pathogen isolated from the gut of an obese human causes obesity in germfree mice. ISME J. 7:880–884.
10. Hayashi, H., M. Sakamoto, M. Kitahara, and Y. Benno. 2003. Molecular analysis of fecal microbiota in elderly individuals using 16S rDNA library and T-RFLP. Microbiol. Immunol. 47:557–570.
11. Itoh, K., and T. Mitsuoka. 1985. Characterization of clostridia isolated from faeces of limited flora mice and their effect on caecal size when associated with germ-free mice. Lab. Anim. 19:111–118.
12. Johnson, A.M., and J.M. Olefsky. 2013. The origins and drivers of insulin resistance. Cell 152:673–684.
13. Karlsson, F.H., V. Tremaroli, I. Nookaew, G. Bergström, C.J. Behre, B. Fagerberg, J. Nielsen, and F. Bäckhed. 2013. Gut metagenome in European women with normal, impaired and diabetic glucose control. Nature 498:99–103.
14. Le Chatelier, E., T. Nielsen, J. Qin, *et al.* 2013. Richness of human gut microbiome correlates with metabolic markers. Nature 500:541–546.
15. Liu, W.T., T.L. Marsh, H. Cheng, and L.J. Forney. 1997. Characterization of microbial diversity by determining terminal restriction fragment length polymorphisms of genes encoding 16S rRNA. Appl. Environ. Microbiol. 63:4516–4522.
16. Matthews, D.R., J.P. Hosker, A.S. Rudenski, B.A. Naylor, D.F. Treacher, and R.C. Turner. 1985. Homeostasis model assessment: insulin resistance and beta-cell function from fasting plasma glucose and insulin concentrations in man. Diabetologia 28:412–419.
17. Mehta, N.N., F.C. McGillicuddy, P.D. Anderson, *et al.* 2010. Experimental endotoxemia induces adipose inflammation and insulin resistance in humans. Diabetes 59:172–181.

18. Panwar, H., H.M. Rashmi, V.K. Batish, and S. Grover. 2013. Probiotics as potential biotherapeutics in the management of type 2 diabetes—prospects and perspectives. Diabetes Metab. Res. Rev. 29:103–112.
19. Qin, J., Y. Li, Z. Cai, *et al.* 2012. A metagenome-wide association study of gut microbiota in type 2 diabetes. Nature 490:55–60.
20. Samuel, B.S., and J.I. Gordon. 2006. A humanized gnotobiotic mouse model of host-archaeal-bacterial mutualism. Proc. Natl. Acad. Sci. U.S.A. 103:10011–10016.
21. Sanz, Y., A. Santacruz, and P. Gauffin. 2010. Gut microbiota in obesity and metabolic disorders. Proc. Nutr. Soc. 69:434–441.
22. Shafrir, E., E. Ziv, and L. Mosthaf. 1999. Nutritionally induced insulin resistance and receptor defect leading to beta-cell failure in animal models. Ann. N. Y. Acad. Sci. 892:223–246.
23. Tremaroli, V., and F. Bäckhed. 2012. Functional interactions between the gut microbiota and host metabolism. Nature 489:242–249.

Microbes Environ. 35(2), 2020
https://www.jstage.jst.go.jp/browse/jsme2 doi:10.1264/jsme2.ME20025

MOST CITED REVIEW PAPER PUBLISHED
IN THIS THREE YEARS [2019-2021] (11 citations)

Minireview

Size Matters: Ultra-small and Filterable Microorganisms in the Environment

Ryosuke Nakai[1]*†

[1]*Applied Molecular Microbiology Research Group, Bioproduction Research Institute, National Institute of Advanced Industrial Science and Technology (AIST), 2–17–2–1, Tsukisamu-Higashi, Sapporo, 062–8517, Japan*

(Received February 29, 2020—Accepted April 17, 2020—Published online June 3, 2020)

Ultra-small microorganisms are ubiquitous in Earth's environments. Ultramicrobacteria, which are defined as having a cell volume of <0.1 μm^3, are often numerically dominant in aqueous environments. Cultivated representatives among these bacteria, such as members of the marine SAR11 clade (*e.g.*, "*Candidatus* Pelagibacter ubique") and freshwater *Actinobacteria* and *Betaproteobacteria*, possess highly streamlined, small genomes and unique ecophysiological traits. Many ultramicrobacteria may pass through a 0.2-μm-pore-sized filter, which is commonly used for filter sterilization in various fields and processes. Cultivation efforts focusing on filterable small microorganisms revealed that filtered fractions contained not only ultramicrocells (*i.e.*, miniaturized cells because of external factors) and ultramicrobacteria, but also slender filamentous bacteria sometimes with pleomorphic cells, including a special reference to members of *Oligoflexia*, the eighth class of the phylum *Proteobacteria*. Furthermore, the advent of culture-independent "omics" approaches to filterable microorganisms yielded the existence of candidate phyla radiation (CPR) bacteria (also referred to as "*Ca.* Patescibacteria") and ultra-small members of DPANN (an acronym of the names of the first phyla included in this superphyla) archaea. Notably, certain groups in CPR and DPANN are predicted to have minimal or few biosynthetic capacities, as reflected by their extremely small genome sizes, or possess no known function. Therefore, filtered fractions contain a greater variety and complexity of microorganisms than previously expected. This review summarizes the broad diversity of overlooked filterable agents remaining in "sterile" (<0.2-μm filtered) environmental samples.

Key words: filterable microorganisms, ultramicrocells, ultramicrobacteria, candidate phyla radiation, minimal cell

How small may actual organisms be? This question has long fascinated scientists in various fields. Prokaryotic microorganisms (*Archaea* and *Bacteria*) constitute the smallest life forms. Bacterial cells range in volume from ultramicrobacteria (UMB; <0.1 μm^3; Duda *et al.*, 2012) to the typical bacterium *Escherichia coli* (1.6 μm^3; Moore, 1999) and the giant bacterium *Epulopiscium fishelsoni* (3.0×10^6 μm^3; Schulz and Jørgensen, 2001; note that the cells of *Thiomargarita namibiensis* are larger [2.2×10^8 μm^3], but are occupied by a liquid vacuole, that is, they do not have large cytoplasmic bodies; Schulz *et al.*, 1999). Thus, bacteria exhibit cell-size plasticity by varying cell volume by more than seven orders of magnitude in different species. UMB may pass through membrane filters down to 0.2-μm-pore-size, which is commonly used for filter sterilization in research laboratories as well as in medical, food, and industrial processes (Levy and Jornitz, 2006). In fact, efforts to culture microorganisms remaining in the 0.2-μm filtrate (hereafter called filterable microorganisms) of environmental samples have yielded diverse UMB members. The several isolates were affiliated with unique lineages, such as cosmopolitan freshwater *Actinobacteria* and *Betaproteobacteria* (Hahn, 2003; Hahn *et al.*, 2003) as well as the candidate phylum termite group 1 (TG1) described as *Elusimicrobia* (Geissinger *et al.*, 2009). The existence of UMB has expanded our knowledge of microbial life at the lower size limit.

In the last five years, filterable microorganisms have been attracting increasing interest with the discovery of other ultra-small members: the candidate phyla radiation (CPR) bacteria, also referred to as "*Candidatus* Patescibacteria" (hereafter described as CPR/Patescibacteria; Rinke *et al.*, 2013; Brown *et al.*, 2015), and some members of DPANN (an acronym of the names of the first phyla included in this superphyla, "*Ca.* Diapherotrites", "*Ca.* Parvarchaeota", "*Ca.* Aenigmarchaeota", *Nanoarchaeota*, and "*Ca.* Nanohalorchaeota"; Rinke *et al.*, 2013; Dombrowski *et al.*, 2019). Several CPR members have an extremely small cell volume (approximately 0.01 μm^3) that was unveiled by cryo-transmission electron microscopy imaging (Luef *et al.*, 2015). Moreover, the emergence of these ultra-small prokaryotes has re-opened debate on the tree of life (Hug *et al.*, 2016; Parks *et al.*, 2018; Zhu *et al.*, 2019). These members are ubiquitous in the environment and recent studies have provided insights into their contribution to the material cycle (*e.g.*, carbon and nitrogen cycles; Danczak *et al.*, 2017; Lannes *et al.*, 2019). This review focuses on the phylogenetic diversity and complexity of filterable microorganisms in natural systems, with specific references to UMB and pleomorphic bacteria. Other reviews presented aspects of ultra-small microorganisms including CPR/Patescibacteria and DPANN members (*e.g.*, terminology, biogeography,

* Corresponding author. E-mail: nakai-ryosuke@aist.go.jp;
Tel: +81–11–857–8408; Fax: +81–11–857–8980.
† Present address: Microbial Ecology and Technology Research Group, Bioproduction Research Institute, National Institute of Advanced Industrial Science and Technology (AIST), 2–17–2–1, Tsukisamu-Higashi, Sapporo, 062–8517, Japan.

Citation: Nakai, R. (2020) Size Matters: Ultra-small and Filterable Microorganisms in the Environment. *Microbes Environ* **35:** ME20025. https://doi.org/10.1264/jsme2.ME20025

genomic diversity, and metabolic variety; Duda *et al.*, 2012; Castelle *et al.*, 2018; Ghuneim *et al.*, 2018; Dombrowski *et al.*, 2019). In this review, archaea with a cell volume of <0.1 μm^3 are specifically referred to as ultramicroarchaea (UMA) to distinguish them from UMB.

Filterable microorganisms

To date, many studies have reported the presence of filterable microorganisms in various environments (mainly aqueous environments) including seawater (Haller *et al.*, 2000; Elsaied *et al.*, 2001; Lannes *et al.*, 2019; Obayashi and Suzuki, 2019), lake water (Hahn, 2003; Hahn *et al.*, 2003; Watanabe *et al.*, 2009; Fedotova *et al.*, 2012; Maejima *et al.*, 2018; Vigneron *et al.*, 2019), terrestrial aquifers (Miyoshi *et al.*, 2005; Luef *et al.*, 2015), glacier ice and the ice cover of lakes (Miteva and Brenchley, 2005; Kuhn *et al.*, 2014), deep-sea hydrothermal fluids (Naganuma *et al.*, 2007; Nakai *et al.*, 2011), and soil and sand (Nakai *et al.*, 2013). However, the use of membrane filters with a small pore size (approximately 0.2 μm) was traditionally recommended for the retention of bacteria in the field of marine microbial ecology in the 1960s (*e.g.*, Anderson and Heffernan, 1965) and is still widely practiced today in various fields. The existence of very small microorganisms has been well recognized since the 1980s. The term "ultramicrobacteria" was first used by Torrella and Morita (1981) to describe very small coccoid cell forms of <0.3 μm in diameter from seawater. MacDonell and Hood (1982) subsequently isolated and characterized viable filterable microorganisms potentially belonging to the genera *Vibrio*, *Aeromonas*, *Pseudomonas*, and *Alcaligenes* from estuarine waters. They concluded that these filterable microorganisms represented a state of dormancy for adaptation to low nutrient conditions and were not completely novel bacteria. Other studies also reported that external factors reduced cell sizes, such as *Staphylococcus aureus* and *Pseudomonas syringae* (~50% reduction in size as described in Table 1; Watson *et al.*, 1998; Monier and Lindow, 2003). Therefore, the cells of miniaturized microorganisms need to be distinguished from true UMB and are described in this review as "ultramicrocells", which has the synonyms dwarf cells and midget cells, according to Duda *et al.* (2012). Schut *et al.* (1997) and Duda *et al.* (2012) subsequently defined a cell volume index of <0.1 μm^3 as being characteristic of true UMB.

Based on previous studies, filterable microorganisms have been classified into five groups (Fig. 1): (I) ultramicrocells that are miniaturized microorganisms because of external factors (*e.g.*, environmental stress) as described above; (II) obligate UMB that maintain small cell volumes (<0.1 μm^3) regardless of their growth conditions; (III) facultative UMB that contain a small proportion of larger cells with a cell volume >0.1 μm^3 (note that the definitions of the terms "obligate" and "facultative" UMB follow those of Duda *et al.* [2012]); (IV) slender filamentous bacteria; and (V) ultra-small members among CPR/Patescibacteria bacteria and DPANN archaea. In contrast to UMB strains, the cell shapes and morphological characteristics of members in group V are largely unknown under different environmental or culture conditions because all of the members of CPR and DPANN are uncultivated, with a few exceptions of members belonging to the phyla "*Ca.* Saccharibacteria" (former TM7) and *Nanoarchaeota* (*e.g.*, Huber *et al.*, 2002; He *et al.*, 2015). Incidentally, the groups presented in this review do not include filterable cell-wall-less mycoplasmas as well as "nanobacteria" or "nannobacteria" as microfossils, which are often referred to in geological literature (Folk, 1999), or as calcium carbonate nanoparticles in the human body, as reported in medical literature (Martel and Young, 2008). Representative cases of groups II to V are described below and Table 1 shows a summarized list.

Obligate UMB

Obligate UMB are often reported from aqueous environments. One of the most prominent representatives is "*Candidatus* Pelagibacter ubique" HTCC1062, which is a SAR11 clade bacterium that is ubiquitous in marine environments. Previous studies found that SAR11 members consistently dominated ribosomal RNA gene clone libraries derived from seawater DNA and estimated their global population size as 2.4×10^{28} cells—approximately 25% of all prokaryotic cells—in oceans (Giovannoni *et al.*, 1990; Morris *et al.*, 2002). Despite their ubiquitous and abundant presence, it was not possible to isolate them. However, the first cultivated strain HTCC1062 was established in 2002 using a high-throughput dilution-to-extinction culturing (HTC) technique (Rappé *et al.*, 2002). This HTC technique involves cultivation with serial dilutions of natural seawater samples into very low nutrient media (Connon and Giovannoni, 2002). The cell volume (approximately 0.01 μm^3) of "*Ca.* P. ubique" was reported as one of the smallest free-living cells known. Subsequent studies characterized the SAR11 clade with the small, streamlined genomes (<1.5 Mbp) described below, an unusual mode of glycine auxotrophy, a light-dependent proton pump known as proteorhodopsin, and the ability to utilize various one-carbon compounds (reviewed in Tripp, 2013; Giovannoni, 2017). The SAR11 clade is highly divergent with multiple ecotypes and has freshwater members known as LD12 classified in SAR11 subclade IIIb (Grote *et al.*, 2012). An LD12 cultivated representative, "*Ca.* Fonsibacter ubiquis" strain LSUCC0530, was subsequently established (Henson *et al.*, 2018), and its genomic characteristics promoted the hypothesis that gene losses for osmolyte uptake were related to the evolutionary transition, or metabolic tuning, of freshwater SAR11 (LD12) from a salt to freshwater habitat.

Another marine ultramicrobacterium, *Sphingopyxis alaskensis* (formerly known as *Sphingomonas alaskensis*) RB2256 was intensively investigated before the study of the SAR11 clade (*e.g.*, Eguchi *et al.*, 1996; Schut *et al.*, 1997). This strain was also characterized as an obligate UMB (Duda *et al.*, 2012). When the cultivation of this strain transitioned from low-carbon to highly-enriched media, the cell volume of *S. alaskensis* remained at <0.1 μm^3 in most media; however, larger elongated cells, not UMB cells, were observed in trypticase soy agar medium (Vancanneyt *et al.*, 2001). Furthermore, this strain possesses a larger genome of 3.3 Mb (DDBJ/ENA/GenBank accession no. CP000356) than other UMB (Table 1).

Table 1. An overview of ultra-small and filterable microorganisms in the environment

Taxa	Phylum (and class for *Proteobacteria*)	Isolation source	Cell shape	Cell size (length×width and/or volume)	Genome size (Mbp)	Physiological and ecological trait(s) or its potential	Reference
Ultramicrocells							
Staphylococcus aureus 8325-4	*Firmicutes*	derivative of *S. aureus* NCTC8325 (patient's strain)	cocci	cell size reduction from 0.69±0.08 to 0.41±0.08 μm	n.d.	host cell invasion, starvation-associated cell size reduction	Watson *et al.* (1998)
Pseudomonas syringae pv. *syringae* B728a	*Proteobacteria* (*γ-proteobacteria*)	snap bean leaflet	rods	cell length reduction from ~2.5 to ~1.2 μm	6.09	host cell invasion, leaf environment-induced cell size reduction	Monier and Lindow (2003); Feil *et al.* (2005)
Obligate ultramicrobacteria and related candidates							
"*Candidatus* Pelagibacter ubique" HTCC1062	*Proteobacteria* (*α-proteobacteria*)	coastal sea	curved rods	0.01 μm^3	1.31	glycine auxotrophy, rhodopsin-based photometabolism, utilization of one-carbon compounds	Rappé *et al.* (2002); Tripp (2013); Giovannoni (2017)
"*Candidatus* Fonsibacter ubiquis" LSUCC0530	*Proteobacteria* (*α-proteobacteria*)	coastal lagoon	curved rods	1.0×0.1 μm	1.16	glycine auxotrophy, rhodopsin-based photometabolism, tetrahydrofolate metabolism**	Henson *et al.* (2018)
Sphingopyxis alaskensis RB2256	*Proteobacteria* (*α-proteobacteria*)	fjord estuary	short rods	0.05–0.09 μm^3	3.35	utilization of various amino acids, resistance to heat shock, H_2O_2, and ethanol	Eguchi *et al.* (1996); Schut *et al.* (1997)
Aurantimicrobium minutum KNC^T	*Actinobacteria*	freshwater river	curved rods	0.7–0.8×0.3 μm; 0.04–0.05 μm^3	1.62	rhodopsin-based photometabolism**	Nakai *et al.* (2015, 2016b)
Rhodoluna lacicola MWH-Ta8^T	*Actinobacteria*	freshwater lake	curved rods	0.85×0.30 μm; 0.053 μm^3	1.43	rhodopsin-based photometabolism	Hahn *et al.* (2014); Keffer *et al.* (2015)
Rhodoluna limnophila 27D-LEPI^T	*Actinobacteria*	freshwater pond	short rods	0.49×0.28 μm	1.40	nitrate uptake and nitrite excretion system**	Pitt *et al.* (2019)
"*Candidatus* Planktophila rubra" IMCC25003	*Actinobacteria*	freshwater lake	curved rods	0.041 μm^3	1.35	catalase-dependent growth	Kim *et al.* (2019)
"*Candidatus* Planktophila aquatilis" IMCC26103	*Actinobacteria*	freshwater lake	curved rods	0.061 μm^3	1.46	catalase-dependent growth	Kim *et al.* (2019)
Polynucleobacter necessarius subsp. *asymbioticus* QLW-P1DMWA-1^T	*Proteobacteria* (*β-proteobacteria*)	freshwater pond	straight rods	0.7–1.2×0.4–0.5 μm	2.16	utilization of low-molecular-weight substrates	Hahn *et al.* (2012); Meincke *et al.* (2012)
Opitutus sp. VeCb1	*Verrucomicrobia*	rice paddy soil	ellipsoids	0.49×0.33 μm; 0.030 μm^3	n.d.	utilization of sugars and sugar polymers, strict fermentative metabolism, oxygen tolerance	Janssen *et al.* (1997); Chin *et al.* (2001)
Facultative ultramicrobacteria							
Endomicrobium proavitum Rsa215	*Elusimicrobia*	gut homogenate of *Reticulitermes santonensis*	cocci, rods showing budding cell division	0.3–0.5 μm (for cocci); 0.5–3.5×0.15–0.30 μm (for rods)	1.59	nitrogen fixation	Zheng and Brune (2015); Zheng *et al.* (2016)
Chryseobacterium solincola NF4	*Bacteroidetes*	lake sediment	cocci, rods showing budding cell division or cell septation	0.004–0.04 μm^3 (for cocci); 0.1–0.3 μm^3 (for rods)	~1.7	ectoparasite of *Bacillus subtilis*	Suzina *et al.* (2011); Duda *et al.* (2012)
Slender filamentous bacteria							
Hylemonella gracilis CB	*Proteobacteria* (*β-proteobacteria*)	freshwater	spirals	0.12 μm^3 (smallest width=0.2 μm)	n.d.	n.d.	Wang *et al.* (2007, 2008)
Oligoflexus tunisiensis Shr3^T	*Proteobacteria* (*Oligoflexia*)*	desert sand	pleomorphic (rods, filaments, spirals, and spherical [or curled] cells)	various lengths×0.4–0.8 μm (for filaments)	7.57	multidrug resistance, incomplete denitrification**	Nakai *et al.* (2014, 2016a)
Silvanigrella aquatica MWH-Nonnen-W8red^T	*Proteobacteria* (*Oligoflexia*)*	freshwater lake	pleomorphic (rods, filaments, and spirals)	3.6×0.6 μm (for rods)	3.51	antimicrobial peptides, plasmid-encoded type IV secretion systems**	Hahn *et al.* (2017)
Silvanigrella paludirubra SP-Ram-0.45-NSY-1^T	*Proteobacteria* (*Oligoflexia*)*	freshwater pond	pleomorphic (rods and filaments)	various lengths	3.94	utilization of limited substrates	Pitt *et al.* (2020)
Fluviispira multicolorata 33A1-SZDP^T	*Proteobacteria* (*Oligoflexia*)*	freshwater creek	pleomorphic (rods and filaments)	various lengths	3.39	violacein-like production	Pitt *et al.* (2020)
CPR/Patescibacteria bacteria							
WWE3-OP11-OD1 bacteria	candidate division WWE3, "*Candidatus* Microgenomates" (OP11), "*Candidatus* Parcubacteria" (OD1)	deep aquifer	cocci or oval-shaped	0.009±0.002 μm^3	0.69–1.05	potential interaction with other bacterial cells via pili-like structures	Luef *et al.* (2015)
"*Candidatus* Sonnebornia yantaiensis"	"*Candidatus* Parcubacteria" (OD1)	ciliated protist *Paramecium bursaria*	straight rods	1.6–1.9×0.5–0.6 μm	n.d.	endoplasmic symbiont of the ciliate *P. bursaria*	Gong *et al.* (2014)
TM7x bacterium	"*Candidatus* Saccharibacteria" (TM7)	human oral cavity	cocci	0.2–0.3 μm	0.71	ectosymbiont of *Actinomyces odontolyticus*	He *et al.* (2015)
DPANN archaea							
Nanoarchaeum equitans	*Nanoarchaeota*	submarine hot vent	cocci	0.4 μm	~0.5	ectosymbiont of *Ignicoccus hospitalis*	Huber *et al.* (2002)
"*Candidatus* Nanopusillus acidilobi"	*Nanoarchaeota*	hot spring	cocci	0.1–0.3 μm	0.61	ectosymbiont of *Acidilobus* species	Wurch *et al.* (2016)
"*Candidatus* Nanoclepta minutus" Ncl-1	*Nanoarchaeota*	hot spring	flagellated cocci	~0.2 μm	0.58	ectosymbiont of *Zestosphaera tikiterensis*	John *et al.* (2019)
"*Candidatus* Nanosalina" sp. J07AB43	"*Candidatus* Nanohaloarchaeota"	hypersaline lake	cocci-like	0.6 μm	1.23	possible free-living lifestyle	Narasingarao *et al.* (2012)
"*Candidatus* Nanosalinarum" sp. J07AB56	"*Candidatus* Nanohaloarchaeota"	hypersaline lake	cocci-like	0.6 μm	1.22	possible free-living lifestyle	Narasingarao *et al.* (2012)
ARMAN-2, -4, and -5	"*Candidatus* Micrarchaeota"	acid mine drainage	cocci	~0.5 μm	~1.0	potential interaction with *Thermoplasmatales* cells via pili-like structures	Baker *et al.* (2010)
"*Candidatus* Mancarchaeum acidiphilum" Mia14	"*Candidatus* Micrarchaeota"	acid mine drainage	n.d.	n.d.	0.95	ectoparasite of *Cuniculiplasma divulgatum*	Golyshina *et al.* (2017)

n.d.: no data.
* The proteobacterial class *Oligoflexia* is classified in the candidate phylum "Bdellovibrionota" in the Genome Taxonomy Database (GTDB).
** Putative physiological traits are inferred from their genomic and plasmid annotation.

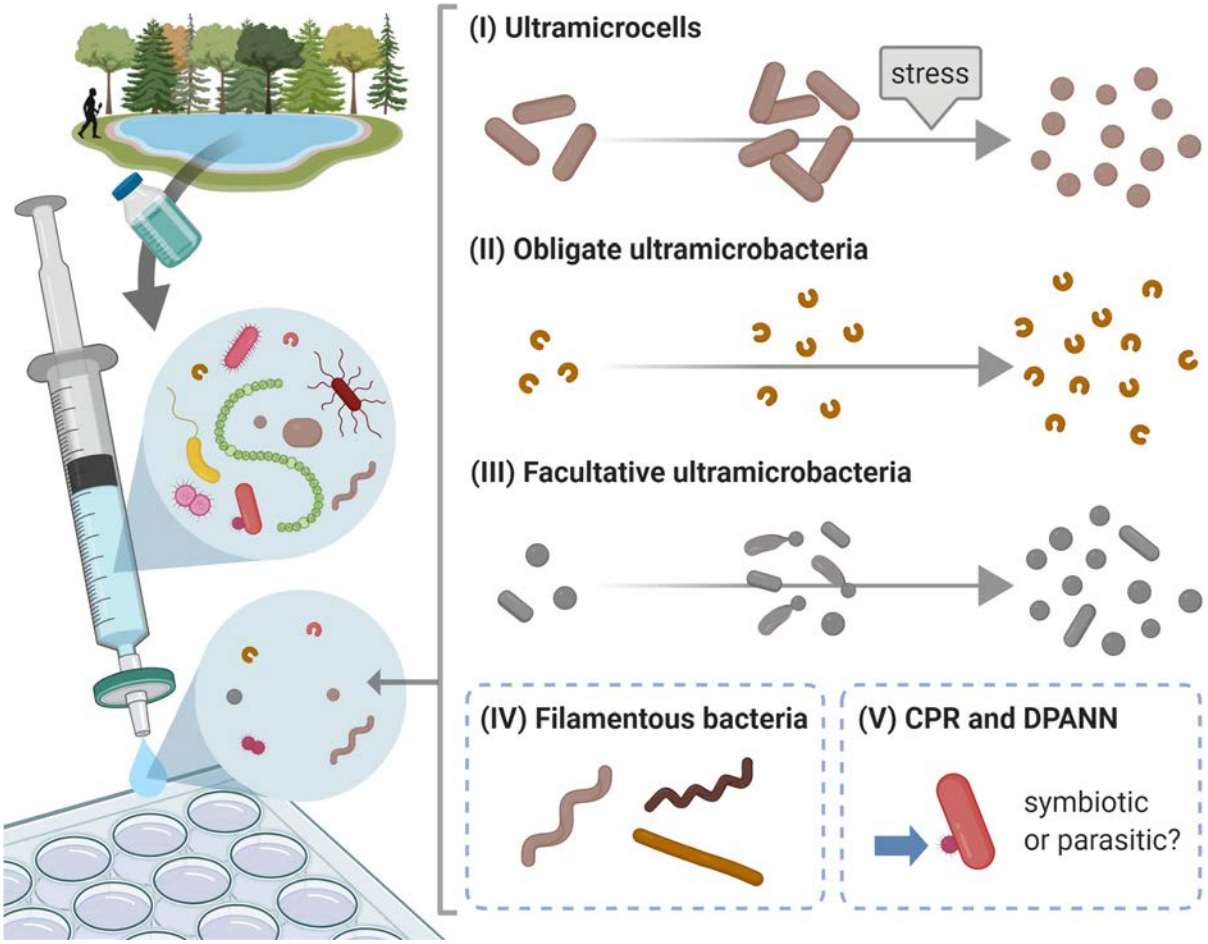

Fig. 1. Diagram showing filterable microorganisms in the environment. (I) ultramicrocells; (II) obligate ultramicrobacteria; (III) facultative ultramicrobacteria; (IV) slender filamentous bacteria; (V) ultra-small members of CPR bacteria (also referred to as "*Candidatus* Patescibacteria") and DPANN archaea indicated by the arrow in this Figure. See details in the text. This figure was created with BioRender (https://biorender.com/).

Other prominent representatives of obligate UMB are freshwater actinobacterial strains. Typically, actinobacteria are among the numerically dominant groups in freshwater and their cells are found in smaller size fractions (Glöckner *et al.*, 2000; Sekar *et al.*, 2003). Hahn *et al.* (2003) first isolated nine filterable UMB of the class *Actinobacteria* from freshwater habitats and newly described a novel phylogenetic cluster (Luna cluster). This isolation was achieved by the "filtration-acclimatization" method of filter separation combined with an acclimatization procedure, which is a stepwise transition from low substrate conditions to artificial culture conditions. The important features of Luna cluster strains are their wide distribution in freshwater systems (Hahn and Pöckl, 2005) and their small cell sizes are stable and maintained in nutrient-rich media (Hahn *et al.*, 2003). Our group also isolated an ultamicrosize actinobacterium related to Luna strains from river water in Japan and named it *Aurantimicrobium minutum* KNC^{T} (Fig. 2; Nakai *et al.*, 2015). This strain showed high 16S rRNA gene sequence similarity (>99%) to strains isolated from freshwater systems in other places in Japan as well as in Austria, Australia, China, Nicaragua, and Uganda (accession nos. AB278121, AB599783, AJ507461, AJ507467, AJ565412, AJ565413, and AJ630367), suggesting its cosmopolitan distribution in freshwater.

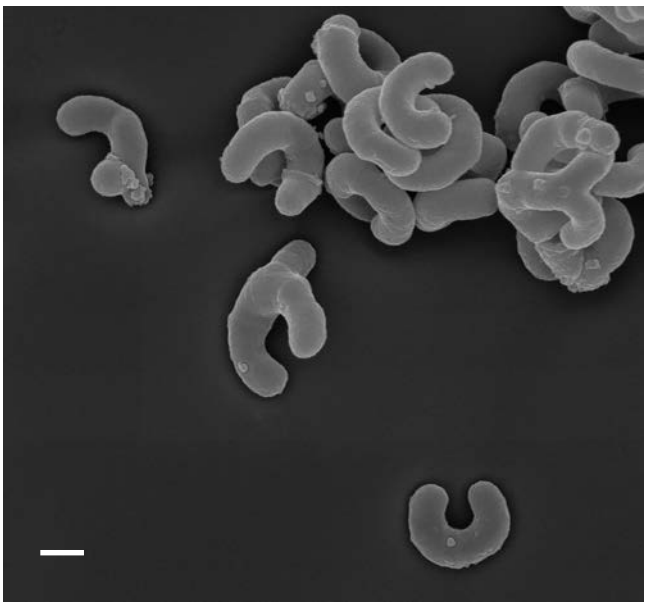

Fig. 2. Scanning electron micrograph of c-shaped cells of *Aurantimicrobium minutum* KNC^{T}. Cells were cultured in organic NSY (nutrient broth, soytone, and yeast extract; Hahn *et al.*, 2004) medium for two weeks. Scale bar: 200 nm. This micrograph is an unpublished figure from the author; other micrographs of this species are shown in Nakai *et al.* (2013, 2015).

The other freshwater bacterium belonging to the Luna cluster, *Rhodoluna lacicola* MWH-Ta8^T, was also described as an obligate UMB (Hahn *et al.*, 2014); an additional three *Rhodoluna* strains smaller than *R. lacicola* were subsequently reported (Pitt *et al.*, 2019). From an ecophysiological point of view, the genomes of freshwater actinobacteria possess rhodopsin photosystems (Neuenschwander *et al.*, 2018), while *R. lacicola* has an unconventional proton-pumping rhodopsin that requires external supplementation with the cofactor retinal (Keffer *et al.*, 2015). The underlying cause is considered to be an inability to biosynthesize the cofactor (Neuenschwander *et al.*, 2018), suggesting that *R. lacicola* obtains retinal from the surrounding environment. One potential source in freshwater appears to be retinoids produced and released by cyanobacteria (Ruch *et al.*, 2005; Wu *et al.*, 2013).

Freshwater actinobacteria, including UMB strains, were previously shown to be phylogenetically diverse and subsequent studies yielded nine lineages (acI, acTH1, acSTL, Luna1, acIII, Luna3, acTH2, acIV, and acV; Newton *et al.*, 2011). Among these lineages, acI containing multiple tribes is considered to be the most successful and ubiquitous group in the environment (Zwart *et al.*, 2002; Warnecke *et al.*, 2004; Kang *et al.*, 2017), although pure cultures had not been established despite various cultivation trials. However, Kim *et al.* (2019) recently reported the first two pure acI cultures with very small sizes (volume, 0.04–0.06 μm^3; Table 1), which are assumed to be obligate UMB. A key factor for their growth was the supplementation of a "helper" catalase, an enzyme that degrades hydrogen peroxide (H_2O_2), to the culture medium. Previous studies showed that H_2O_2 generated in medium affected the culture efficiency of microorganisms sensitive to oxidative stress (Kawasaki and Kamagata, 2017) and that the growth of the cyanobacterium *Prochlorococcus* was promoted by the presence of H_2O_2-scavenging microbes (Morris *et al.*, 2011). These findings demonstrated that a catalase-supplemented cultivation strategy may facilitate the successful isolation of previously uncultured freshwater UMB.

Freshwater habitats also harbor another obligate UMB belonging to the genus *Polynucleobacter* in the class *Betaproteobacteria*. Similar to some actinobacteria described earlier, UMB members of this genus also showed a cosmopolitan distribution in freshwater systems (Hahn, 2003). The relative abundance of the subspecies named PnecC was high, ranging between <1% and 67% (average 14.5%) of total bacterial numbers, in more than 130 lakes studied in Central Europe, as assessed by fluorescent *in situ* hybridization (Jezberová *et al.*, 2010). Culture experiments and genomic characterization suggested that PnecC bacteria in nature can utilize low-molecular-weight products derived from photooxidation and/or the direct enzymatic cleavage of high-molecular-weight substrates, such as humic substances (Watanabe *et al.*, 2009; Hahn *et al.*, 2012). Certain PnecC strains sharing ≥99% similarity in 16S rRNA gene sequences differed in their ecophysiological and genomic features (*e.g.*, the presence/absence of iron transporter genes), suggesting cryptic diversity among the abundant lineage not covered by 16S rRNA gene-based typing (Hahn *et al.*, 2016).

The obligate UMB inhabiting sea and freshwaters described above were characterized by minute cell sizes, but also small genome sizes (<2 Mbp) with a low genomic guanine-cytosine (GC) content: this genome "streamlining" is considered to reflect an adaptation to nutrient-limited conditions (*e.g.*, SAR11 members; 1.16–1.46 Mb; Giovannoni *et al.*, 2005; Grote *et al.*, 2012; Henson *et al.*, 2018) (Table 1). This phenomenon of a reduced genome size with gene loss also indicates metabolic dependencies on co-existing microorganisms in nature, as described by the "Black Queen Hypothesis" (Morris *et al.*, 2012). As another example, the reconstructed genomes of ultra-small and uncultivated marine actinobacteria ("*Candidatus* Actinomarinidae") were very small (<1 Mb) and had a very low GC content of 33% (Ghai *et al.*, 2013). In addition, known obligate UMB of different lineages, such as "*Ca.* P. ubique" (*Alphaproteobacteria*), *Polynucleobacter* strains (*Betaproteobacteria*), and *A. minutum* and *R. lacicola* (*Actinobacteria*), showed similar "c-shaped" (curved-rod) cells (Table 1; *A. minutum* for Fig. 2; Hahn, 2003). This unique shape may be advantageous for the efficient acquisition of substances because of their increased surface-to-volume ratio of cells or grazing resistance against bacteriovorus protists for planktonic life in waters.

In contrast to aquatic environments, limited information is currently available on UMB, including the obligate type, from soil habitats. Janssen *et al.* (1997) previously reported anaerobic obligate UMB with very small ellipsoid to nearly spherical shapes (*e.g.*, *Opitutus* sp. VeCb1 with a cell volume of 0.030 μm^3) belonging to the *Verrucomicrobiales* lineage from rice paddy soil using dilution culture techniques. Nakai *et al.* (2013) isolated and cultivated filterable strains from soil and sand suspensions; however, obligate UMB were not found among these strains. High-throughput sequencing of the 16S rRNA gene revealed that the smaller size fractions in soils were more likely to harbor rare or poorly characterized bacterial and archaeal taxa, such as *Acidobacteria*, *Gemmatimonadetes*, *Elusimicrobia*, *Verrucomicrobia*, and *Crenarchaeota* (Portillo *et al.*, 2013). However, further studies are needed to clarify whether the members detected in the small fractions contain UMB.

Facultative UMB

Facultative UMB that contain a small proportion of larger cells with a cell volume >0.1 μm^3 have not yet been characterized in detail (Table 1) because morphological changes throughout the growth cycle have only been examined in a limited number of UMB. *Endomicrobium proavitum* Rsa215 (now deposited as DSM29378^T=JCM32103^T) belonging to the phylum *Elusimicrobia* appears to be a well-studied example of facultative UMB. The phylum *Elusimicrobia* (former termite group 1 candidate phylum) was initially established with the cultivated ultramicrobacterium of *Elusimicrobium minutum* strain Pei191^T from the 0.2 μm-filtered filtrate—originally prepared as a growth promoting supplement for gut bacteria—of the gut homogenates of a scarab beetle larva (Geissinger *et al.*, 2009; Herlemann *et al.*, 2009). *E. proavitum* Rsa215 was isolated from the filtrate of the gut homogenate and was identified as a free-

living bacterium of a novel class-level lineage in *Elusimicrobia* (Zheng *et al.*, 2016). *E. proavitum* has an unusual cell cycle that involves different cell forms, *i.e.*, cocci, rods, and budding-like cells, during the cell cycle. Under laboratory cultivation conditions, before growth commences, the cell population is comprised of a large population of UMB coccoid cells with a few rod-shaped cells (~3.5 μm in length); small cocci are formed from a bud-like swelling at one pole of the rod-shaped cells during growth. Although its morphological variation in the host gut currently remains unclear, cell characteristics as observed in the laboratory result in the classification of facultative UMB. Another important trait for *E. proavitum* is the ability to fix nitrogen gas with a group IV nitrogenase, which was considered to harbor functions other than nitrogen fixation (Dos Santos *et al.*, 2012).

Slender filamentous bacteria

In addition to ultramicrocells and UMB, slender filamentous bacteria have frequently been found in 0.2 μm-filtered fractions of environmental samples. Slender spirillum-shaped *Hylemonella gracilis* was isolated from filtrates of freshwater samples (*e.g.*, Hahn *et al.*, 2004; Nakai *et al.*, 2013) and passes through membrane filters with small pore sizes of not only 0.22–0.45 μm, but also 0.1 μm (Wang *et al.*, 2007). The smallest widths of *H. gracilis* cells are approximately 0.2 μm and close to filter pore sizes, which may allow its slender cells to "squeeze" through these pores. Regarding the quality control and assessment of filter sterilization, Wang *et al.* (2008) proposed that filterable slender bacteria, such as *H. gracilis* with small cell widths, may be used for the microbiological validation of membrane filters instead of *Brevundimonas diminuta*, which is the current standard strain tested.

During a screening of UMB, our group isolated a slender filamentous bacterium from the filtrate of a suspension of desert sands collected in Tunisia, and described *Oligoflexus tunisiensis* Shr3^T, which represents the eighth novel class named *Oligoflexia* within the phylum *Proteobacteria* (Nakai *et al.*, 2014; 2016a). The cell shape of this species is mainly slender, filamentous, and of variable lengths, but shows a pleomorphism with other shapes, such as a spiral, spherical (or curled), or curved rod morphology (Fig. 3; Nakai and Naganuma, 2015). This polymorphic flexibility of cells with small widths down to 0.4 μm appears to be related to their ability to pass through membrane filters; however, it has not yet been clarified whether each morphological shape is associated with a resting state or other states. Regarding filamentous formation, this shape may be related to resistance to protozoan grazing, as reported in previous studies (*e.g.*, Jürgens *et al.*, 1999; Suzuki *et al.*, 2017a). The environmental sequences closely related (>97%) to the 16S rRNA gene sequence of *O. tunisiensis* were recovered from paddy soil, cyanobacterial bloom in lake water, bioreactors, and human skin using culture-independent approaches; however, their detection frequency was low, with at most ~0.6% (Nakai and Naganuma, 2015). Thus, *O. tunisiensis* and its relatives appear to be rare species, and their ecological roles are currently unclear; one possible role for *O. tunisiensis* may be incomplete denitrification to nitrous oxide, as inferred from its genome sequence (Nakai *et al.*, 2016a).

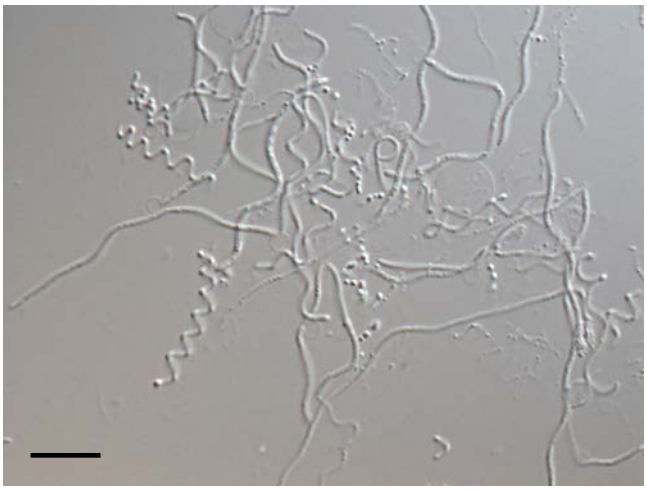

Fig. 3. Micrograph of pleomorphic cells of *Oligoflexus tunisiensis* Shr3^T. Cells were cultured in R2A medium for more than two weeks. This micrograph is slightly modified from the figure originally published in Nakai and Naganuma (2015). Scale bar: 10 μm.

Despite the potential rarity of its occurrence, the size filtration method led to the isolation of an additional slender filamentous strain, *Silvanigrella aquatica* MWH-Nonnen-W8red^T, with a pleomorphic morphology in the class (Hahn *et al.*, 2017). Hahn *et al.* (2017) reclassified the order *Bdellovibrionales*, including *Bdellovibrio* spp. known as small "bacteria-eating" bacteria (reviewed in Sockett, 2009), from the class *Deltaproteobacteria* to the class *Oligoflexia* based on in-depth phylogenetic analyses. Incidentally, 0.45-μm filtrates of environmental samples are frequently used for the enrichment culture of *Bdellovibrio* predatory bacteria. In the Genome Taxonomy Database (GTDB) based on genome phylogeny (https://gtdb.ecogenomic.org/; Parks *et al.*, 2018), the class *Oligoflexia* belongs to the candidate phylum "Bdellovibrionota", named after the genus *Bdellovibrio*, and not the phylum *Proteobacteria*; its taxonomic assignment will be discussed in future studies. *Oligoflexia* very recently gained two more species, *Fluviispira multicolorata* 33A1-SZDP^T and *Silvanigrella paludirubra* SP-Ram-0.45-NSY-1^T, from freshwater habitats (Pitt *et al.*, 2020). *Silvanigrella* spp. are phylogenetically closely aligned with "*Candidatus* Spirobacillus cienkowskii" (Pitt *et al.*, 2020), which is an uncultured pathogen of water fleas (*Daphnia* spp.) described morphologically almost 130 years ago (Metchnikoff, 1889). Since *Silvanigrella* spp. are isolated from the filtrates of micropore filtration, size fractionation may be an effective method for isolating the uncultivated pathogen as well as additionally overlooked agents in *Oligoflexia*. A detailed comparison within members of this class will also be important for pursuing the evolutionary acquisition and divergence of predatory and pathogenic behaviors.

Diverse ultra-small members and their potentials

Metagenomic investigations on microbial communities have generated genomes for an astounding diversity of bac-

teria and archaea; CPR/Patescibacteria inhabiting groundwater has attracted increasing attention in recent years. Traditionally, certain types of groundwater bacteria were known to pass through a micropore filter (*e.g.*, Shirey and Bissonnette, 1991). Additionally, Miyoshi *et al.* (2005) phylogenetically characterized filterable microorganisms captured by 0.1-μm-pore-sized filters from deep aquifers of the Tono uranium mine, Japan and then discovered candidate divisions OD1 and OP11 (now recognized as candidate phyla "*Ca.* Parcubacteria" and "*Ca.* Microgenomates", respectively) enriched by approximately 44% in 16S rRNA gene clones from the filtered fraction. The specific occurrence of "*Ca.* Parcubacteria" (OD1) in the 0.2-μm filtrate was also detected in deep-sea hydrothermal fluid (Naganuma *et al.*, 2007). It was previously unclear whether members of these candidate divisions were UMB. In subsequent studies using cryo-imaging, ultra-small cells (approximately 0.009±0.002 μm^3) were reported in the filtrate of an aquifer water near Colorado, USA, which were enriched with the candidate divisions WWE3, OD1, and OP11, all recently belonging to CPR/Patescibacteria (Luef *et al.*, 2015).

Metagenomics was then used to reconstruct the genomes of filterable members in the aquifer system, representing >35 candidate phyla named CPR (Brown *et al.*, 2015). This highly diversified group of uncultivated bacteria may subdivide the domain *Bacteria* (Hug *et al.*, 2016); however, this scenario remains controversial (*e.g.*, Parks *et al.*, 2018; Zhu *et al.*, 2019). Importantly, measurements of replication rates (Brown *et al.*, 2016; Suzuki *et al.*, 2017b) and cryo-transmission electron microscopy images showing a dividing cell (Luef *et al.*, 2015) indicated that the extremely small cells of CPR/Patescibacteria are metabolically active and not simply ultramicrocells during starvation. Moreover, CPR/Patescibacteria genomes have been recovered from other environments, such as highly alkaline groundwater (Suzuki *et al.*, 2017b; Sato *et al.*, 2019), lakes (Vigneron *et al.*, 2019), soil (Starr *et al.*, 2018), and marine sediment (Orsi *et al.*, 2018) as well as the human microbiome (He *et al.*, 2015) and dolphin mouse (Dudek *et al.*, 2017), suggesting a wide distribution across environments. Besides describing ultra-small life forms with high phylogenetic novelty, genomic analyses of CPR/Patescibacteria members have provided information on their small genomes, fermentative metabolism, and other unusual features (*e.g.*, self-splicing introns varying in length and proteins encoded within their 16S rRNA genes; Brown *et al.*, 2015; Castelle *et al.*, 2018). Divergent 16S rRNA gene sequences prevent many specific phyla (*e.g.*, ~50% of "*Ca.* Microgenomates" [OP11] and 60% of candidate division WWE3) from being detected by typical PCR surveys with the universal bacterial primer set 515F and 806R (Brown *et al.*, 2016). The small genome sizes observed (often <1 Mb) appear to be a reflection of a symbiotic lifestyle and/or high *in situ* selection pressure in a stable environment, rather than the genome streamlining of free-living obligate UMB, as described earlier, assuming streamlining characteristics (*e.g.*, highly conserved core genomes with few pseudogenes; Giovannoni *et al.*, 2014). Although the CPR/Patescibacteria genomes studied to date possess incomplete biosynthetic pathways for their cellular building blocks (*e.g.*, nucleotides and fatty acids; Castelle *et al.*, 2018), the possibility of their ability to *de novo* synthesize them by unknown pathways cannot be ruled out. Furthermore, their host-associated distribution was reported: "*Candidatus* Sonnebornia yantaiensis" of "*Ca.* Parcubacteria" (OD1) as an endoplasmic symbiont of the protist (Gong *et al.*, 2014) and TM7x bacterium of "*Ca.* Saccharibacteria" (TM7) attached to *Actinomyces odontolyticus* (He *et al.*, 2015), as shown in Table 1.

The features of small cell sizes and small genomes observed in CPR/Patescibacteria are shared by some members of the DPANN archaea, particularly *Nanoarchaeota* (Huber *et al.*, 2002), "*Ca.* Nanohalorchaeota" (Narasingarao *et al.*, 2012), and so-called ARMAN (archaeal Richmond Mine acidophilic nano-organisms; Baker *et al.*, 2010). DPANN including these UMA has been expanded by the addition of novel phylum-level groups, and, at the time of writing, encompasses at least ten different lineages (reviewed in Dombrowski *et al.*, 2019). In several cases, except for the members of "*Ca.* Nanohalorchaeota", as with CPR/Patescibacteria, DPANN-affiliated UMA showed an ectosymbiotic localization: *Nanoarchaeum equitans* attached to *Ignicoccus hospitalis* (Huber *et al.*, 2002), "*Ca.* Nanopusillus acidilobi" and its host *Acidilobus* species (Wurch *et al.*, 2016), and "*Ca.* Mancarchaeum acidiphilum" Mia14 (ARMAN-2-related organism) and its host *Cuniculiplasma divulgatum* (Golyshina *et al.*, 2017) (other data in Table 1). Additionally, DPANN organisms lack the ability to biosynthesize their building blocks (Castelle *et al.*, 2018). Although it is still unclear whether these symbiotic or parasitic lifestyles represent a way of life for the CPR/Patescibacteria and DPANN groups, the cases described above indicate that several members of these groups appear to be important in organism-organism interactions.

The characterization of ultra-small life forms may provide a new perspective for minimal cells and synthetic cells. In the field of synthetic biology, the top-down approach has been employed to reduce and simplify the genomes of microbial cells by genetic engineering, and then to identify essential genes for living systems; the bottom-up approach, which is the opposite of the top-down approach, has been used to examine what is sufficient for living systems by assembling non-living components, such as nucleic acids, proteins, and lipids (*e.g.*, Matsuura *et al.*, 2011; Xu *et al.*, 2016). In this context, DeWall and Cheng (2011) pointed out that the small genomes of microorganisms in nature may be models for the identification of a minimal genome. Since the ultra-small members described here as well as free-living obligate UMB already harbor small and sometimes streamlined genome structures (<2 Mb) through the loss of unnecessary components, the "middle-out" approach, referring to the metabolic pathway of these members (Fig. 4), which effectively combines traditional top-down and bottom-up approaches, will be useful for the rational design of artificial cells.

Conclusions

Numerous cultivation efforts have clearly shown that some previously uncultured members remain viable in

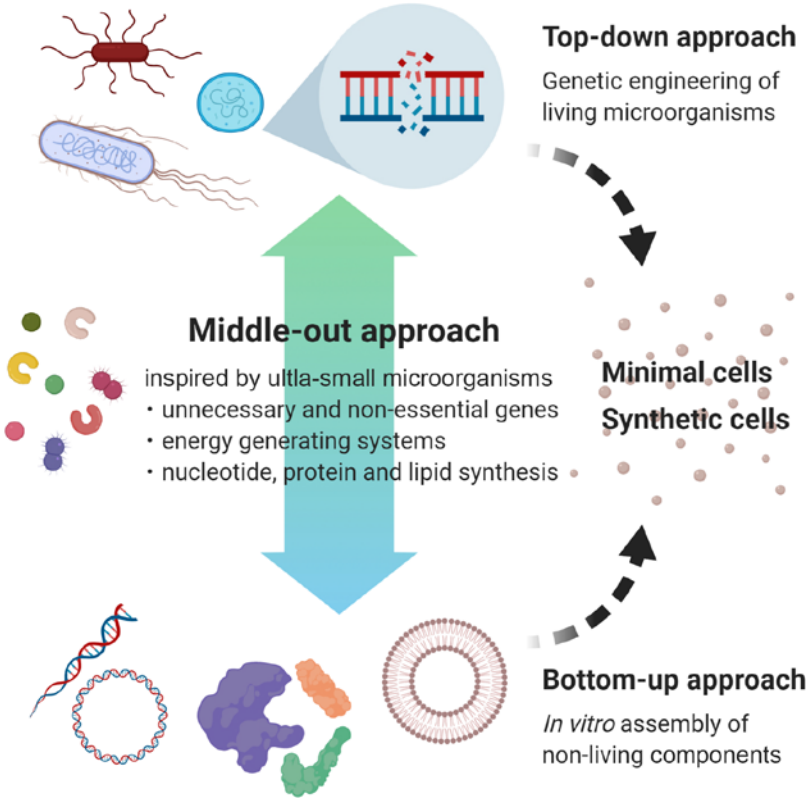

Fig. 4. A schematic diagram of the "middle-out" approach toward the development of minimal cells or synthetic cells. This approach, inspired by the unusual biology of ultra-small life forms, may provide a new perspective to traditional top-down or bottom-up approaches. This figure was created with BioRender (https://biorender.com/).

small-size fractions. Some obligate UMB are ubiquitous and dominant in water systems and may play important roles in natural microbiome functions. In parallel, the advent of high-throughput sequencing technology has greatly expanded our knowledge of ultra-small microbial diversity. Future studies are required to shed light on small microorganisms hidden in various environmental samples (*e.g.*, soils and sediments) other than aqueous environments, and on the ecophysiological traits and biogeochemical roles of these members, including CPR/Patescibacteria and DPANN. Further studies on "extreme" microorganisms at the lower size limit will undoubtedly lead to new conundrums about life on Earth.

Acknowledgement

I would like to thank Dr. K. Takai (JAMSTEC) and one anonymous reviewer for their helpful comments and suggestions on an earlier draft of this review.

References

Anderson, J.I.W., and Heffernan, W.P. (1965) Isolation and characterization of filterable marine bacteria1. *J Bacteriol* **90**: 1713–1718.

Baker, B.J., Comolli, L.R., Dick, G.J., Hauser, L.J., Hyatt, D., Dill, B.D., *et al.* (2010) Enigmatic, ultrasmall, uncultivated Archaea. *Proc Natl Acad Sci U S A* **107**: 8806–8811.

Brown, C.T., Hug, L.A., Thomas, B.C., Sharon, I., Castelle, C.J., Singh, A., *et al.* (2015) Unusual biology across a group comprising more than 15% of domain Bacteria. *Nature* **523**: 208–211.

Brown, C.T., Olm, M.R., Thomas, B.C., and Banfield, J.F. (2016) Measurement of bacterial replication rates in microbial communities. *Nat Biotechnol* **34**: 1256–1263.

Castelle, C.J., Brown, C.T., Anantharaman, K., Probst, A.J., Huang, R.H., and Banfield, J.F. (2018) Biosynthetic capacity, metabolic variety and unusual biology in the CPR and DPANN radiations. *Nat Rev Microbiol* **16**: 629–645.

Chin, K.J., Liesack, W., and Janssen, P.H. (2001) *Opitutus terrae* gen. nov., sp. nov., to accommodate novel strains of the division '*Verrucomicrobia*' isolated from rice paddy soil. *Int J Syst Evol Microbiol* **51**: 1965–1968.

Connon, S.A., and Giovannoni, S.J. (2002) High-throughput methods for culturing microorganisms in very-low-nutrient media yield diverse new marine isolates. *Appl Environ Microbiol* **68**: 3878.

Danczak, R.E., Johnston, M.D., Kenah, C., Slattery, M., Wrighton, K.C., and Wilkins, M.J. (2017) Members of the Candidate Phyla Radiation are functionally differentiated by carbon- and nitrogen-cycling capabilities. *Microbiome* **5**: 112.

DeWall, M.T., and Cheng, D.W. (2011) The minimal genome—a metabolic and environmental comparison. *Briefings Funct Genomics* **10**: 312–315.

Dombrowski, N., Lee, J.-H., Williams, T.A., Offre, P., and Spang, A. (2019) Genomic diversity, lifestyles and evolutionary origins of DPANN archaea. *FEMS Microbiol Lett* **366**: fnz008.

Dos Santos, P.C., Fang, Z., Mason, S.W., Setubal, J.C., and Dixon, R. (2012) Distribution of nitrogen fixation and nitrogenase-like sequences amongst microbial genomes. *BMC Genomics* **13**: 162.

Duda, V.I., Suzina, N.E., Polivtseva, V.N., and Boronin, A.M. (2012) Ultramicrobacteria: formation of the concept and contribution of ultramicrobacteria to biology. *Microbiology* **81**: 379–390.

Dudek, N.K., Sun, C.L., Burstein, D., Kantor, R.S., Aliaga Goltsman, D.S., Bik, E.M., *et al.* (2017) Novel microbial diversity and functional potential in the marine mammal oral microbiome. *Curr Biol* **27**: 3752–3762.e6.

Eguchi, M., Nishikawa, T., Macdonald, K., Cavicchioli, R., Gottschal, J.C., and Kjelleberg, S. (1996) Responses to stress and nutrient availability by the marine ultramicrobacterium *Sphingomonas* sp. strain RB2256. *Appl Environ Microbiol* **62**: 1287.

Elsaied, H.E., Sato, M., and Naganuma, T. (2001) Viable *Cytophaga*-like bacterium in the 0.2 μm-filtrate seawater. *Syst Appl Microbiol* **24**: 618–622.

Fedotova, A.V., Belova, S.E., Kulichevskaya, I.S., and Dedysh, S.N. (2012) Molecular identification of filterable bacteria and archaea in the water of acidic lakes of northern Russia. *Microbiology* **81**: 281–287.

Feil, H., Feil, W.S., Chain, P., Larimer, F., DiBartolo, G., Copeland, A., *et al.* (2005). Comparison of the complete genome sequences of *Pseudomonas syringae* pv. *syringae* B728a and pv. tomato DC3000. *Proc Natl Acad Sci U S A* **102**: 11064–11069.

Folk, R.L. (1999) Nannobacteria and the precipitation of carbonate in unusual environments. *Sediment Geol* **126**: 47–55.

Geissinger, O., Herlemann, D.P.R., Mörschel, E., Maier, U.G., and Brune, A. (2009) The ultramicrobacterium "*Elusimicrobium minutum*" gen. nov., sp. nov., the first cultivated representative of the termite group 1 phylum. *Appl Environ Microbiol* **75**: 2831.

Ghai, R., Mizuno, C.M., Picazo, A., Camacho, A., and Rodriguez-Valera, F. (2013) Metagenomics uncovers a new group of low GC and ultra-small marine Actinobacteria. *Sci Rep* **3**: 2471.

Ghuneim, L.-A.J., Jones, D.L., Golyshin, P.N., and Golyshina, O.V. (2018) Nano-sized and filterable bacteria and archaea: biodiversity and function. *Front Microbiol* **9**: 1971.

Giovannoni, S.J., Britschgi, T.B., Moyer, C.L., and Field, K.G. (1990) Genetic diversity in Sargasso Sea bacterioplankton. *Nature* **345**: 60–63.

Giovannoni, S.J., Tripp, H.J., Givan, S., Podar, M., Vergin, K.L., Baptista, D., *et al.* (2005) Genome streamlining in a cosmopolitan oceanic bacterium. *Science* **309**: 1242.

Giovannoni, S.J., Cameron Thrash, J., and Temperton, B. (2014) Implications of streamlining theory for microbial ecology. *ISME J* **8**: 1553–1565.

Giovannoni, S.J. (2017) SAR11 bacteria: the most abundant plankton in the oceans. *Ann Rev Mar Sci* **9**: 231–255.

Glöckner, F.O., Zaichikov, E., Belkova, N., Denissova, L., Pernthaler, J., Pernthaler, A., and Amann, R. (2000) Comparative 16S rRNA analysis of lake bacterioplankton reveals globally distributed phylogenetic clusters including an abundant group of actinobacteria. *Appl Environ Microbiol* **66**: 5053.

Golyshina, O.V., Toshchakov, S.V., Makarova, K.S., Gavrilov, S.N., Korzhenkov, A.A., La Cono, V., *et al.* (2017) 'ARMAN' archaea depend on association with euryarchaeal host in culture and in situ. *Nat Commun* **8**: 60.

Gong, J., Qing, Y., Guo, X., and Warren, A. (2014) "*Candidatus* Sonnebornia yantaiensis", a member of candidate division OD1, as intracellular bacteria of the ciliated protist *Paramecium bursaria* (Ciliophora, Oligohymenophorea). *Syst Appl Microbiol* **37**: 35–41.

Grote, J., Thrash, J.C., Huggett, M.J., Landry, Z.C., Carini, P., Giovannoni, S.J., and Rappé, M.S. (2012) Streamlining and core genome conservation among highly divergent members of the SAR11 clade. *mBio* **3**: e00252-12.

Hahn, M.W. (2003) Isolation of strains belonging to the cosmopolitan *Polynucleobacter necessarius* cluster from freshwater habitats located in three climatic zones. *Appl Environ Microbiol* **69**: 5248.

Hahn, M.W., Lünsdorf, H., Wu, Q., Schauer, M., Höfle, M.G., Boenigk, J., and Stadler, P. (2003) Isolation of novel ultramicrobacteria classified as actinobacteria from five freshwater habitats in Europe and Asia. *Appl Environ Microbiol* **69**: 1442.

Hahn, M.W., Stadler, P., Wu, Q.L., and Pöckl, M. (2004) The filtration–acclimatization method for isolation of an important fraction of the not readily cultivable bacteria. *J Microbiol Methods* **57**: 379–390.

Hahn, M.W., and Pöckl, M. (2005) Ecotypes of planktonic actinobacteria with identical 16S rRNA genes adapted to thermal niches in temperate, subtropical, and tropical freshwater habitats. *Appl Environ Microbiol* **71**: 766.

Hahn, M.W., Scheuerl, T., Jezberová, J., Koll, U., Jezbera, J., Šimek, K., *et al.* (2012) The passive yet successful way of planktonic life: genomic and experimental analysis of the ecology of a free-living polynucleobacter population. *PLoS One* **7**: e32772.

Hahn, M.W., Schmidt, J., Taipale, S.J., Doolittle, W.F., and Koll, U. (2014) *Rhodoluna lacicola* gen. nov., sp. nov., a planktonic freshwater bacterium with stream-lined genome. *Int J Syst Evol Microbiol* **64**: 3254–3263.

Hahn, M.W., Jezberová, J., Koll, U., Saueressig-Beck, T., and Schmidt, J. (2016) Complete ecological isolation and cryptic diversity in *Polynucleobacter* bacteria not resolved by 16S rRNA gene sequences. *ISME J* **10**: 1642–1655.

Hahn, M.W., Schmidt, J., Koll, U., Rohde, M., Verbarg, S., Pitt, A., *et al.* (2017) *Silvanigrella aquatica* gen. nov., sp. nov., isolated from a freshwater lake, description of *Silvanigrellaceae* fam. nov. and *Silvanigrellales* ord. nov., reclassification of the order *Bdellovibrionales* in the class *Oligoflexia*, reclassification of the families *Bacteriovoracaceae* and *Halobacteriovoraceae* in the new order *Bacteriovoracales* ord. nov., and reclassification of the family *Pseudobacteriovoracaceae* in the order *Oligoflexales*. *Int J Syst Evol Microbiol* **67**: 2555–2568.

Haller, C.M., Rölleke, S., Vybiral, D., Witte, A., and Velimirov, B. (2000) Investigation of 0.2 μm filterable bacteria from the Western Mediterranean Sea using a molecular approach: dominance of potential starvation forms. *FEMS Microbiol Ecol* **31**: 153–161.

He, X., McLean, J.S., Edlund, A., Yooseph, S., Hall, A.P., Liu, S.-Y., *et al.* (2015) Cultivation of a human-associated TM7 phylotype reveals a reduced genome and epibiotic parasitic lifestyle. *Proc Natl Acad Sci U S A* **112**: 244.

Henson, M.W., Lanclos, V.C., Faircloth, B.C., and Thrash, J.C. (2018) Cultivation and genomics of the first freshwater SAR11 (LD12) isolate. *ISME J* **12**: 1846–1860.

Herlemann, D.P.R., Geissinger, O., Ikeda-Ohtsubo, W., Kunin, V., Sun, H., Lapidus, A., *et al.* (2009) Genomic analysis of "*Elusimicrobium minutum*," the first cultivated representative of the phylum "*Elusimicrobia*" (formerly termite group 1). *Appl Environ Microbiol* **75**: 2841.

Huber, H., Hohn, M.J., Rachel, R., Fuchs, T., Wimmer, V.C., and Stetter, K.O. (2002) A new phylum of Archaea represented by a nanosized hyperthermophilic symbiont. *Nature* **417**: 63–67.

Hug, L.A., Baker, B.J., Anantharaman, K., Brown, C.T., Probst, A.J., Castelle, C.J., *et al.* (2016) A new view of the tree of life. *Nat Microbiol* **1**: 16048.

Janssen, P.H., Schuhmann, A., Mörschel, E., and Rainey, F.A. (1997) Novel anaerobic ultramicrobacteria belonging to the *Verrucomicrobiales* lineage of bacterial descent isolated by dilution culture from anoxic rice paddy soil. *Appl Environ Microbiol* **63**: 1382–1388.

Jezberová, J., Jezbera, J., Brandt, U., Lindström, E.S., Langenheder, S., and Hahn, M.W. (2010) Ubiquity of *Polynucleobacter necessarius* subsp. *asymbioticus* in lentic freshwater habitats of a heterogenous 2000 km^2 area. *Environ Microbiol* **12**: 658–669.

John, E.S., Liu, Y., Podar, M., Stott, M.B., Meneghin, J., Chen, Z., *et al.* (2019). A new symbiotic nanoarchaeote (*Candidatus* Nanoclepta minutus) and its host (*Zestosphaera tikiterensis* gen. nov., sp. nov.) from a New Zealand hot spring. *Syst Appl Microbiol* **42**: 94–106.

Jürgens, K., Pernthaler, J., Schalla, S., and Amann, R. (1999) Morphological and compositional changes in a planktonic bacterial community in response to enhanced protozoan grazing. *Appl Environ Microbiol* **65**: 1241–1250.

Kang, I., Kim, S., Islam, M.R., and Cho, J.C. (2017) The first complete genome sequences of the acI lineage, the most abundant freshwater *Actinobacteria*, obtained by whole-genome-amplification of dilution-to-extinction cultures. *Sci Rep* **7**: 42252.

Kawasaki, K., and Kamagata, Y. (2017) Phosphate-catalyzed hydrogen peroxide formation from agar, gellan, and κ-carrageenan and recovery of microbial cultivability via catalase and pyruvate. *Appl Environ Microbiol* **83**: e01366-17.

Keffer, J.L., Hahn, M.W., and Maresca, J.A. (2015) Characterization of an unconventional rhodopsin from the freshwater actinobacterium *Rhodoluna lacicola*. *J Bacteriol* **197**: 2704–2712.

Kim, S., Kang, I., Seo, J.-H., and Cho, J.-C. (2019) Culturing the ubiquitous freshwater actinobacterial acI lineage by supplying a biochemical 'helper' catalase. *ISME J* **13**: 2252–2263.

Kuhn, E., Ichimura, A.S., Peng, V., Fritsen, C.H., Trubl, G., Doran, P.T., and Murray, A.E. (2014) Brine assemblages of ultrasmall microbial cells within the ice cover of Lake Vida, Antarctica. *Appl Environ Microbiol* **80**: 3687.

Lannes, R., Olsson-Francis, K., Lopez, P., and Bapteste, E. (2019) Carbon fixation by marine ultrasmall prokaryotes. *Genome Biol Evol* **11**: 1166–1177.

Levy, R.V., and Jornitz, M.W. (2006) Types of filtration. In *Sterile Filtration*. Jornitz, M.W. (ed.) Berlin, Heidelberg: Springer, pp. 1–26.

Luef, B., Frischkorn, K.R., Wrighton, K.C., Holman, H.-Y.N., Birarda, G., Thomas, B.C., *et al.* (2015) Diverse uncultivated ultra-small bacterial cells in groundwater. *Nat Commun* **6**: 6372.

MacDonell, M.T., and Hood, M.A. (1982) Isolation and characterization of ultramicrobacteria from a Gulf Coast estuary. *Appl Environ Microbiol* **43**: 566.

Maejima, Y., Kushimoto, K., Muraguchi, Y., Fukuda, K., Miura, T., Yamazoe, A., *et al.* (2018) *Proteobacteria* and *Bacteroidetes* are major phyla of filterable bacteria passing through 0.22 μm pore size membrane filter, in Lake Sanaru, Hamamatsu, Japan. *Biosci Biotechnol Biochem* **82**: 1260–1263.

Martel, J., and Young, J.D.-E. (2008) Purported nanobacteria in human blood as calcium carbonate nanoparticles. *Proc Natl Acad Sci U S A* **105**: 5549.

Matsuura, T., Ichihashi, N., Sunami, T., Kita, H., Suzuki, H., and Yomo, T. (2011) Evolvability and self-replication of genetic information in liposomes. In *The Minimal Cell*. Luisi, P., and Stano, P. (eds). Dordrecht: Springer, pp. 275–287.

Meincke, L., Copeland, A., Lapidus, A., Lucas, S., Berry, K.W., Del Rio, T.G., *et al.* (2012) Complete genome sequence of *Polynucleobacter necessarius* subsp. *asymbioticus* type strain (QLW-P1DMWA-1^T). *Stand Genomic Sci* **6**: 74–83.

Metchnikoff, E. (1889) Contributions á l'etude du pleomorphisme des bacteriens. *Ann Inst Pasteur* **3**: 61–68.

Miteva, V.I., and Brenchley, J.E. (2005) Detection and isolation of ultrasmall microorganisms from a 120,000-year-old Greenland glacier ice core. *Appl Environ Microbiol* **71**: 7806.

Miyoshi, T., Iwatsuki, T., and Naganuma, T. (2005) Phylogenetic characterization of 16S rRNA gene clones from deep-groundwater microorganisms that pass through 0.2-micrometer-pore-size filters. *Appl Environ Microbiol* **71**: 1084.

Monier, J.-M., and Lindow, S.E. (2003) *Pseudomonas syringae* responds to the environment on leaves by cell size reduction. *Phytopathology* **93**: 1209–1216.

Moore, P.B. (1999) A biophysical chemist's thoughts on cell size. In *Size Limits of Very Small Microorganisms: Proceedings of a Workshop*. Washington, DC: National Academies Press, pp. 16–20.

Morris, J.J., Johnson, Z.I., Szul, M.J., Keller, M., and Zinser, E.R. (2011) Dependence of the cyanobacterium *Prochlorococcus* on hydrogen peroxide scavenging microbes for growth at the ocean's surface. *PLoS One* **6**: e16805.

Morris, J.J., Lenski, R.E., and Zinser, E.R. (2012) The Black Queen hypothesis: evolution of dependencies through adaptive gene loss. *mBio* **3**: e00036-12.

Morris, R.M., Rappé, M.S., Connon, S.A., Vergin, K.L., Siebold, W.A., Carlson, C.A., and Giovannoni, S.J. (2002) SAR11 clade dominates ocean surface bacterioplankton communities. *Nature* **420**: 806–810.

Naganuma, T., Miyoshi, T., and Kimura, H. (2007) Phylotype diversity of deep-sea hydrothermal vent prokaryotes trapped by 0.2- and 0.1-μm-pore-size filters. *Extremophiles* **11**: 637–646.

Nakai, R., Abe, T., Takeyama, H., and Naganuma, T. (2011) Metagenomic analysis of 0.2-μm-passable microorganisms in deep-sea hydrothermal fluid. *Mar Biotechnol* **13**: 900–908.

Nakai, R., Shibuya, E., Justel, A., Rico, E., Quesada, A., Kobayashi, F., *et al.* (2013) Phylogeographic analysis of filterable bacteria with special reference to *Rhizobiales* strains that occur in cryospheric habitats. *Antarct Sci* **25**: 219–228.

Nakai, R.*, Nishijima, M.*, Tazato, N., Handa, Y., Karray, F., Sayadi, S., *et al.* (*equal contribution) (2014) *Oligoflexus tunisiensis* gen. nov., sp. nov., a Gram-negative, aerobic, filamentous bacterium of a novel proteobacterial lineage, and description of *Oligoflexaceae* fam. nov., *Oligoflexales* ord. nov. and *Oligoflexia* classis nov. *Int J Syst Evol Microbiol* **64**: 3353–3359.

Nakai, R., Baba, T., Niki, H., Nishijima, M., and Naganuma, T. (2015) *Aurantimicrobium minutum* gen. nov., sp. nov., a novel ultramicrobacterium of the family *Microbacteriaceae*, isolated from river water. *Int J Syst Evol Microbiol* **65**: 4072–4079.

Nakai, R., and Naganuma, T. (2015) *Oligoflexia*, the newest class of the phylum *Proteobacteria*, consisting of only one cultured species and uncultured bacterial phylotypes from diverse habitats. *J Phylogenet Evol Biol* **3**: 141.

Nakai, R., Fujisawa, T., Nakamura, Y., Baba, T., Nishijima, M., Karray, F., *et al.* (2016a) Genome sequence and overview of *Oligoflexus tunisiensis* Shr3^T in the eighth class *Oligoflexia* of the phylum *Proteobacteria*. *Stand Genomic Sci* **11**: 90.

Nakai, R., Fujisawa, T., Nakamura, Y., Nishide, H., Uchiyama, I., Baba, T., *et al.* (2016b) Complete genome sequence of *Aurantimicrobium minutum* type Strain KNC^T, a planktonic ultramicrobacterium isolated from river water. *Genome Announc* **4**: e00616-16.

Narasingarao, P., Podell, S., Ugalde, J.A., Brochier-Armanet, C., Emerson, J.B., Brocks, J.J., *et al.* (2012) *De novo* metagenomic assembly reveals abundant novel major lineage of Archaea in hypersaline microbial communities. *ISME J* **6**: 81–93.

Neuenschwander, S.M., Ghai, R., Pernthaler, J., and Salcher, M.M. (2018) Microdiversification in genome-streamlined ubiquitous freshwater Actinobacteria. *ISME J* **12**: 185–198.

Newton, R.J., Jones, S.E., Eiler, A., McMahon, K.D., and Bertilsson, S. (2011) A guide to the natural history of freshwater lake bacteria. *Microbiol Mol Biol Rev* **75**: 14.

Obayashi, Y., and Suzuki, S. (2019) High growth potential of transiently 0.2-μm-filterable bacteria with extracellular protease activity in coastal seawater. *Plankton Benthos Res* **14**: 276–286.

Orsi, W.D., Richards, T.A., and Francis, W.R. (2018) Predicted microbial secretomes and their target substrates in marine sediment. *Nat Microbiol* **3**: 32–37.

Parks, D.H., Chuvochina, M., Waite, D.W., Rinke, C., Skarshewski, A., Chaumeil, P.-A., and Hugenholtz, P. (2018) A standardized bacterial taxonomy based on genome phylogeny substantially revises the tree of life. *Nat Biotechnol* **36**: 996–1004.

Pitt, A., Schmidt, J., Koll, U., and Hahn, M.W. (2019) *Rhodoluna limnophila* sp. nov., a bacterium with 1.4 Mbp genome size isolated from freshwater habitats located in Salzburg, Austria. *Int J Syst Evol Microbiol* **69**: 3946–3954.

Pitt, A., Koll, U., Schmidt, J., and Hahn, M.W. (2020) *Fluviispira multicolorata* gen. nov., sp. nov. and *Silvanigrella paludirubra* sp. nov., isolated from freshwater habitats. *Int J Syst Evol Microbiol* **70**: 1630–1638.

Portillo, M.C., Leff, J.W., Lauber, C.L., and Fierer, N. (2013) Cell size distributions of soil bacterial and archaeal taxa. *Appl Environ Microbiol* **79**: 7610.

Rappé, M.S., Connon, S.A., Vergin, K.L., and Giovannoni, S.J. (2002) Cultivation of the ubiquitous SAR11 marine bacterioplankton clade. *Nature* **418**: 630–633.

Rinke, C., Schwientek, P., Sczyrba, A., Ivanova, N.N., Anderson, I.J., Cheng, J.-F., *et al.* (2013) Insights into the phylogeny and coding potential of microbial dark matter. *Nature* **499**: 431–437.

Ruch, S., Beyer, P., Ernst, H., and Al-Babili, S. (2005) Retinal biosynthesis in Eubacteria: *in vitro* characterization of a novel carotenoid oxygenase from *Synechocystis* sp. PCC 6803. *Mol Microbiol* **55**: 1015–1024.

Sato, T., Yoshiya, K., and Maruyama, S. (2019) History of the Hadean "Living Microfossil" OD1 and ultra-reducing environments. *J Geogr (Tokyo, Japan)* **128**: 571–596.

Schulz, H.N., Brinkhoff, T., Ferdelman, T.G., Mariné, M.H., Teske, A., and Jørgensen, B.B. (1999) Dense populations of a giant sulfur bacterium in Namibian shelf sediments. *Science* **284**: 493.

Schulz, H.N., and Jørgensen, B.B. (2001) Big bacteria. *Annu Rev Microbiol* **55**: 105–137.

Schut, F., Gottschal, J.C., and Prins, R.A. (1997) Isolation and characterisation of the marine ultramicrobacterium *Sphingomonas* sp. strain RB2256. *FEMS Microbiol Rev* **20**: 363–369.

Sekar, R., Pernthaler, A., Pernthaler, J., Warnecke, F., Posch, T., and Amann, R. (2003) An improved protocol for quantification of freshwater *Actinobacteria* by fluorescence in situ hybridization. *Appl Environ Microbiol* **69**: 2928.

Shirey, J.J., and Bissonnette, G.K. (1991) Detection and identification of groundwater bacteria capable of escaping entrapment on 0.45-micron-pore-size membrane filters. *Appl Environ Microbiol* **57**: 2251.

Sockett, R.E. (2009) Predatory lifestyle of *Bdellovibrio bacteriovorus*. *Annu Rev Microbiol* **63**: 523–539.

Starr, E.P., Shi, S., Blazewicz, S.J., Probst, A.J., Herman, D.J., Firestone, M.K., and Banfield, J.F. (2018) Stable isotope informed genome-resolved metagenomics reveals that *Saccharibacteria* utilize microbially-processed plant-derived carbon. *Microbiome* **6**: 122.

Suzina, N.E., Duda, V.I., Esikova, T.Z., Shorokhova, A.P., Gafarov, A.B., Oleinikov, R.R., *et al.* (2011) Novel ultramicrobacteria, strains NF4 and NF5, of the genus *Chryseobacterium*: Facultative epibionts of *Bacillus subtilis*. *Microbiology* **80**: 535.

Suzuki, K., Yamauchi, Y., and Yoshida, T. (2017a) Interplay between microbial trait dynamics and population dynamics revealed by the combination of laboratory experiment and computational approaches. *J Theor Biol* **419**: 201–210.

Suzuki, S., Ishii, S., Hoshino, T., Rietze, A., Tenney, A., Morrill, P.L., *et al.* (2017b) Unusual metabolic diversity of hyperalkaliphilic microbial communities associated with subterranean serpentinization at The Cedars. *ISME J* **11**: 2584–2598.

Torrella, F., and Morita, M.Y. (1981) Microcultural study of bacterial size changes and microcolony and ultramicrocolony formation by heterotrophic bacteria in seawater. *Appl Environ Microbiol* **41**: 518.

Tripp, H.J. (2013) The unique metabolism of SAR11 aquatic bacteria. *J Microbiol* **51**: 147–153.

Vancanneyt, M., Schut, F., Snauwaert, C., Goris, J., Swings, J., and Gottschal, J.C. (2001) *Sphingomonas alaskensis* sp. nov., a dominant bacterium from a marine oligotrophic environment. *Int J Syst Evol Microbiol* **51**: 73–79.

Vigneron, A., Cruaud, P., Langlois, V., Lovejoy, C., Culley, A.I., and Vincent, W.F. (2019) Ultra-small and abundant: Candidate phyla radiation bacteria are potential catalysts of carbon transformation in a thermokarst lake ecosystem. *Limnol Oceanogr Lett* **5**:212–220.

Wang, Y., Hammes, F., Boon, N., and Egli, T. (2007) Quantification of the filterability of freshwater bacteria through 0.45, 0.22, and 0.1 µm pore size filters and shape-dependent enrichment of filterable bacterial communities. *Environ Sci Technol* **41**: 7080–7086.

Wang, Y., Hammes, F., Düggelin, M., and Egli, T. (2008) Influence of size, shape, and flexibility on bacterial passage through micropore membrane filters. *Environ Sci Technol* **42**: 6749–6754.

Warnecke, F., Amann, R., and Pernthaler, J. (2004) Actinobacterial 16S rRNA genes from freshwater habitats cluster in four distinct lineages. *Environ Microbiol* **6**: 242–253.

Watanabe, K., Komatsu, N., Ishii, Y., and Negishi, M. (2009) Effective isolation of bacterioplankton genus *Polynucleobacter* from freshwater environments grown on photochemically degraded dissolved organic matter. *FEMS Microbiol Ecol* **67**: 57–68.

Watson, S.P., Clements, M.O., and Foster, S.J. (1998) Characterization of the starvation-survival response of *Staphylococcus aureus*. *J Bacteriol* **180**: 1750–1758.

Wu, X., Jiang, J., and Hu, J. (2013) Determination and occurrence of retinoids in a eutrophic lake (Taihu Lake, China): cyanobacteria blooms produce teratogenic retinal. *Environ Sci Technol* **47**: 807–814.

Wurch, L., Giannone, R.J., Belisle, B.S., Swift, C., Utturkar, S., Hettich, R.L., *et al.* (2016) Genomics-informed isolation and characterization of a symbiotic Nanoarchaeota system from a terrestrial geothermal environment. *Nat Commun* **7**: 12115.

Xu, C., Hu, S., and Chen, X. (2016) Artificial cells: from basic science to applications. *Mater Today (Oxford, U K)* **19**: 516–532.

Zheng, H., and Brune, A. (2015). Complete genome sequence of *Endomicrobium proavitum*, a free-living relative of the intracellular symbionts of termite gut flagellates (phylum *Elusimicrobia*). *Genome Announc* **3**: e00679-15.

Zheng, H., Dietrich, C., Radek, R., and Brune, A. (2016) *Endomicrobium proavitum*, the first isolate of *Endomicrobia* class. nov. (phylum *Elusimicrobia*)—an ultramicrobacterium with an unusual cell cycle that fixes nitrogen with a Group IV nitrogenase. *Environ Microbiol* **18**: 191–204.

Zhu, Q., Mai, U., Pfeiffer, W., Janssen, S., Asnicar, F., Sanders, J.G., *et al.* (2019) Phylogenomics of 10,575 genomes reveals evolutionary proximity between domains Bacteria and Archaea. *Nat Commun* **10**: 5477.

Zwart, G., Crump, B.C., Kamst-van Agterveld, M.P., Hagen, F., and Han, S.-K. (2002) Typical freshwater bacteria: an analysis of available 16S rRNA gene sequences from plankton of lakes and rivers. *Aquat Microb Ecol* **28**: 141–155.

Microbes Environ. Vol. 32, No. 4, 300-313, 2017
https://www.jstage.jst.go.jp/browse/jsme2 doi:10.1264/jsme2.ME17017

MOST CITED REVIEW PAPERS PUBLISHED
IN THIS TEN YEARS [2012-2021] (191 citations)
MOST CITED REVIEW PAPER in 2021 (66 citations)

Minireview

Microbial Ecology along the Gastrointestinal Tract

Ethan T. Hillman[1], Hang Lu[2], Tianming Yao[3], and Cindy H. Nakatsu[4]*

[1]*Department of Agricultural and Biological Engineering, Purdue University, West Lafayette, Indiana 47907, USA;* [2]*Department of Animal Science, Purdue University, West Lafayette, Indiana 47907, USA;* [3]*Department of Food Science, Purdue University, West Lafayette, Indiana 47907, USA; and* [4]*Department of Agronomy, Purdue University, West Lafayette, Indiana 47907, USA*

(Received January 31, 2017—Accepted August 19, 2017—Published online November 10, 2017)

The ecosystem of the human gastrointestinal (GI) tract traverses a number of environmental, chemical, and physical conditions because it runs from the oral cavity to the anus. These differences in conditions along with food or other ingested substrates affect the composition and density of the microbiota as well as their functional roles by selecting those that are the most suitable for that environment. Previous studies have mostly focused on *Bacteria*, with the number of studies conducted on *Archaea*, *Eukarya*, and *Viruses* being limited despite their important roles in this ecosystem. Furthermore, due to the challenges associated with collecting samples directly from the inside of humans, many studies are still exploratory, with a primary focus on the composition of microbiomes. Thus, mechanistic studies to investigate functions are conducted using animal models. However, differences in physiology and microbiomes need to be clarified in order to aid in the translation of animal model findings into the context of humans. This review will highlight *Bacteria*, *Archaea*, *Fungi*, and *Viruses*, discuss differences along the GI tract of healthy humans, and perform comparisons with three common animal models: rats, mice, and pigs.

Key words: Microbiome, mycobiome, virome, human gastrointestinal (GI) tract, animal models, diet

Researchers have been investigating the ecology of the intestinal microbiota for decades (120, 165) in order to identify, characterize, and count their numbers. These extensive efforts are due to the important roles the intestinal microbiota play in digestion, the production of essential vitamins, and protection of the gastrointestinal (GI) tract from pathogen colonization (141). In the past few decades, molecular techniques targeting the 16S rRNA gene and other genetic markers have been developed to characterize and analyze bacterial communities. These methods have been used to reveal the important roles played by microbes in the GI tract (23, 180, 183, 184, 189, 212). In healthy individuals, the microbiome (microbial community) and host have a mutualistic relationship in which both partners benefit; however, pathogens may invade and cause disease under certain conditions. The initial aim of most studies was to elucidate the role of the microbiome in disease. More recently, surveys have been performed on healthy individuals in order to assess the contribution of the microbiota to health, particularly in response to dietary changes/supplementation with probiotics and/or prebiotics.

The human GI tract is a complex system that starts from the oral cavity, continues through the stomach and intestines, and finally ends at the anus (Fig. 1). The density and composition of the microbiome change along the GI tract, with major populations being selected by the functions performed at the various locations. Bacteria along the GI tract have several possible functions, many of which are beneficial for health including vitamin production, the absorption of ions (Ca, Mg, and Fe), protection against pathogens, histological development, enhancement of the immune system, and the fermentation of "non-digestible foods" to short chain fatty acids (SCFA) and other metabolites (19, 58, 63, 77, 138). The roles of fungi and viruses have not been examined in as much detail; however, they are known to play important roles in microbiota dynamics and host physiology/immunity related to health and disease (45, 94, 133).

Food passes through the GI tract and the absorption rate of nutrients is largely dependent on the activities of various enzymes in the digestive system, such as amylase in saliva, pepsin in the stomach, and pancreatic enzymes in the small intestine. These mechanisms have been extensively examined (61, 62), particularly in the stomach. However, many food components cannot be digested in the upper GI tract and are passed into the lower intestinal tract, in which they are fermented by microbes. Functional studies commonly use animal models in order to obtain a better understanding of the processes in the GI tract that may lead to better health or decrease disease. However, information from animal models may not be directly translatable to humans. Therefore, researchers need to consider the limitations of the selected animal model when extrapolating findings to humans.

Although microbiome studies often include an ecological component, most of the research performed to date has focused on *Bacteria* and not all of the biota. This represents a logical approach because *Bacteria* comprise most of the microbiome. However, even biota representing a small proportion of the microbiome may play important roles in the ecosystem (133). Therefore, researchers need to start shifting their approach to include eukaryotic, prokaryotic, and viral (33, 133) interactions in efforts to elucidate the roles of all components of the microbiome.

In recent years, a number of reviews have summarized findings from the increasing number of studies being performed in this field (36, 73, 176, 188). While most studies have focused on disease, the microbiome is also important for maintaining

* Corresponding author. E-mail: cnakatsu@purdue.edu;
Tel: +1 (765) 496–2997; Fax: +1 (765) 496–2926.

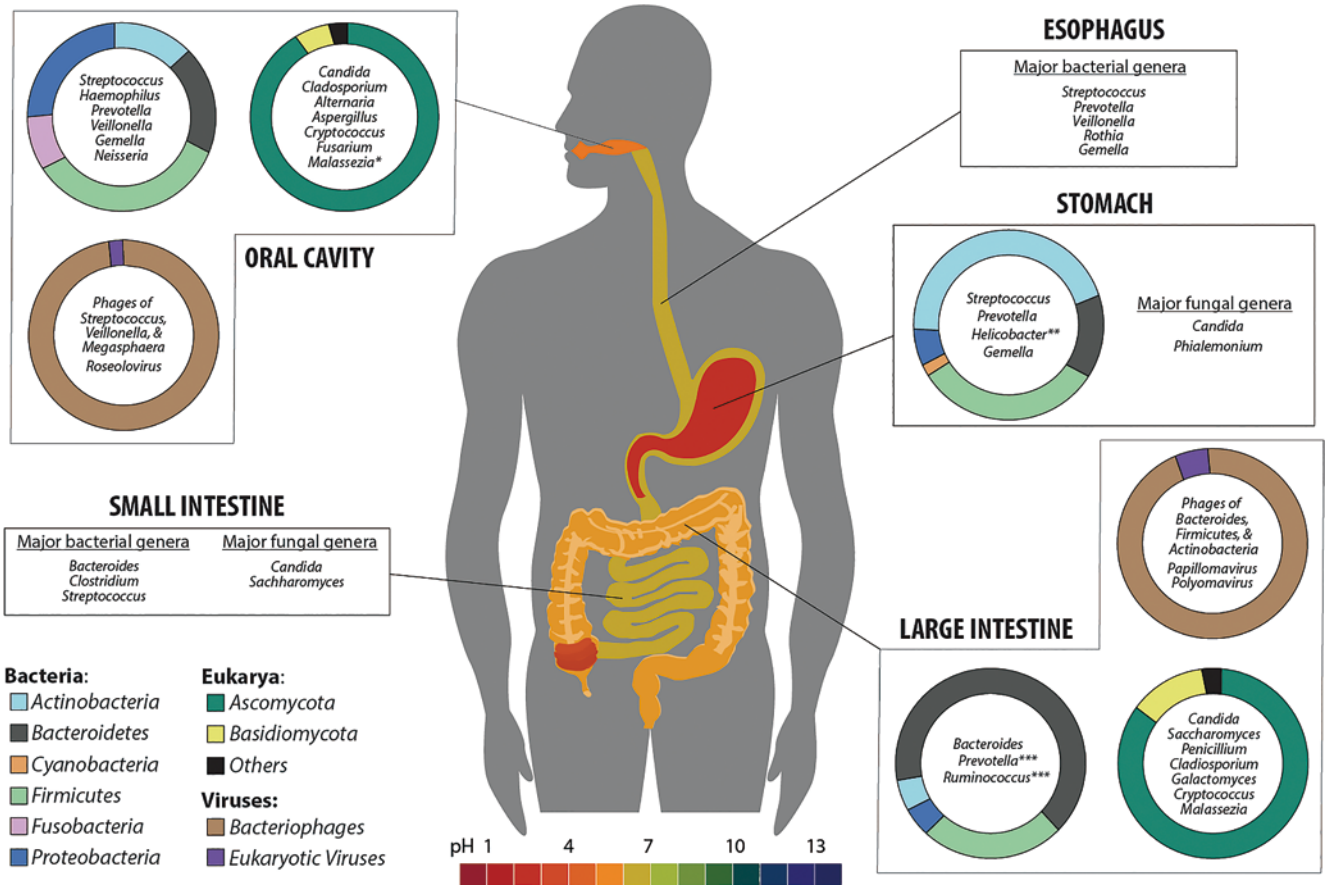

Fig. 1. Microbiome composition of *Bacteria* (1, 5, 20, 21, 43, 147, 156, 223), *Eukarya* (52, 85, 114, 126, 182, 197), and *Viruses* (45, 134, 151, 215) among the physiological niches of the human gastrointestinal (GI) tract. Phylum level compositional data are presented where available along with the most common genera in each GI tract location. The colors on the doughnut plots correspond to the legend in the lower left corner; the GI tract is colored according to the pH scale shown at the bottom of Fig. 1. (* *Malassezia* was very abundant in one study and was not detected in another study. ** The abundance of *Helicobacter* may vary greatly between individuals. *** Proportions of these and other colon genera vary with age, diet, & geographical location.)

health. We herein highlight differences in the microbiome (*Bacteria*, *Archaea*, *Fungi*, and *Viruses*) along the GI tract of healthy humans, and how it compares to those of typical animal models used in research. One finding that is consistent to most studies is that the microbiome of healthy individuals is unique; however, there are still some generalities that will be discussed in this review.

Microbiome diversity

Many factors contribute to the diversity of microbiomes, and most studies have demonstrated the individuality of microbiomes among subjects. Previous findings support microbial communities being more similar in subjects that are genetically related (191), of a similar age (135, 213), or with common diets (including the influences of ethnicity and geography) (63). Diseases will also have an impact on microbiome diversity, including autoimmune and neoplastic diseases, such as inflammatory bowel disease, diabetes, obesity, cardiovascular diseases, allergies, and cancer (37, 121). Treatments for diseases may also affect a patient's gut microbiota, and the consequences of antibiotic use have been intensively investigated (22, 95).

The host genotype has been shown to influence the development of the gut microbiota, and the immune system has been identified as a contributing factor (188). Crosstalk between the microbiome and human immune system occurs in response to a number of environmental factors, such as diet, xenobiotics, and pathogens. Microbial host interactions occur in the gut, mainly in the epithelial cell layer, myeloid cells, and innate lymphoid cells, in which crosstalk and feedback loops contribute to the microbiome composition, host physiology, and disease susceptibility. These interactions contribute not only to the bacterial community along the GI tract, but also to the other microbiota (*Fungi*, *Archaea*, and *Viruses*). Our understanding of the immunology associated with *Fungi* (150) and *Archaea* is currently limited. Transkingdom commensal relationships among microbiota (including *Viruses*) are considered to form from infancy (29, 30, 106, 200) and several co-occurring relationships have been identified (35, 75, 76, 85, 214).

Bacteria. A more complete picture of human-associated bacterial communities obtained using molecular techniques has revealed that their diversity is greater than initially considered through cultivation (9, 20, 56, 90, 113). Using almost full-length 16S rRNA gene sequences, predicted taxa numbers range from 100–300 (20, 56), while pyrosequencing suggests there are 1000s of phylotypes (38, 49). Most of the

gut bacteria identified by 16S rRNA gene sequencing belong to the five phyla originally identified by cultivation, namely, *Bacteroidetes*, *Firmicutes*, *Actinobacteria*, *Proteobacteria*, and *Verrucomicrobia* (90), and, at lower proportions, *Fusobacteria*, *Tenericutes*, *Spirochaetes*, *Cyanobacteria*, and TM7 (189). At lower levels of the taxonomic classification, microbiome compositions vary with each individual. Attempts have been made to identify a single core microbiome of *Bacteria* in the GI tract. Although this has not been possible in the lower GI tract (mainly using fecal samples) based on taxonomy, it appears there are core microbial functions (152, 189, 191). It is possible to identify some core microbiota in the oral cavity, esophagus, and stomach (148). Although extensive efforts have been made to cultivate representative gut microbiota in an attempt to gain a better understanding of the relationship between taxa and function (156), there are still many undescribed taxa with unknown functional roles in the gut.

As the price of sequencing decreases, it is becoming more common to use a metagenomic approach that provides information on all microbiota and potential functions (3, 70, 167, 189). This provides a means to go beyond *Bacteria* and obtain information on eukaryotic microbes (mainly fungi) and viruses. Although *Fungi*, *Archaea*, and *Viruses* in the microbiome are a part of the 'rare biosphere' (organisms that comprise <0.1% of the microbiome) (173), they still have a significant impact on host health.

Fungi

Fungi are considered to comprise approximately 0.03% of the fecal microbiome (143); making them approximately 3,300-fold less abundant than *Bacteria*. Fungal diversity in the human gut is also lower than that of *Bacteria* (143, 166), although more taxa are being found as the number of individuals being studied using next generation sequencing is increasing (44, 126, 166, 182). In 2015, a review of 36 fungal gut microbiome studies revealed that there have been at least 267 distinct fungi identified in the human gut (181), while another study reported 221 (72). Despite the number of taxa that have been reported, most fungi are highly variable among individuals, with few appearing to be common to all.

Cultivation-based analyses have typically identified *Candida* as the most common fungal genus (166), and it is also frequently identified using non-cultivation-based methods, whereas the other taxa identified have been variable, which may be because of the analytical method used and/or subject variability. For example, 66 genera of fungi were found using pyrosequencing when 98 individuals were examined, with the genera *Saccharomyces*, *Candida*, and *Cladosporium* being the most prevalent (85). *Mucor* was common in Spanish individuals (126) and the most common fungi in 16 vegetarians were *Fusarium*, *Malassezia*, *Penicillium*, and *Aspergillus* (182). These studies suggested that some taxa, *e.g.*, *Penicillium* and *Aspergillus*, are not resident in the gut and enter through environmental sources, such as food and water, in which they are commonly found. This may account for some of the variability in taxa reported in various studies and for the increasing number of fungi being identified as more studies are being performed, even those based on cultivation (71). Under certain conditions, some fungi may flourish and become pathogenic including *Candida*, *Aspergillus*, *Fusarium*, and *Cryptococcus* (44, 84, 140, 143). More information on fungal interactions and diseases is available in a review by Wang *et al.* (204).

Despite their low abundance, fungi appear to have developed in mammalian guts along with the rest of the body from infancy (106, 169). Although there is no consensus of a core mycobiome, *Candida*, *Saccharomyces*, and *Malassezia* have been commonly reported (72). Most of the fungal species detected appear to be either transient or environmental fungi that cannot colonize the gut and are often found in a single study and/or one host only. A previous study indicated that the fungal community is unstable; only 20% of the initially identified fungi were detected again 4 months later (78). More studies on the stability of the mycobiome are needed in order to establish the ecological roles of the components of the mycobiome. Many non-bacterial organisms have been found in numerous mammalian systems, which indicates that they play an important role that has been largely overlooked and may lead to important discoveries and understanding in the coming years.

Archaea

The most commonly reported genus of *Archaea* that has been found in the GI tract is *Methanobrevibacter* (51, 55, 66, 85, 109). Other genera that have also been detected are *Methanosphaera* (51), *Nitrososphaera*, *Thermogynomonas*, and *Thermoplasma* (85) and the new candidate species, *Methanomethylophilus alvus* (27, 131). Although *Archaea* comprise a very small proportion of the microbiota, *Methanobrevibacter* species are important contributors to methanogenesis (66). Differences in *Archaea* in microbiome samples may be due to the method used (51) and/or complex relationships with other microbiota. For example, *Methanobrevibacter* and *Nitrososphaera* were previously shown to be mutually exclusive and potentially related to carbohydrate intake (85). More studies are needed in order to clarify the interaction between *Archaea* and other microbiota groups, which may contribute to our understanding of their fitness and function (beyond methanogenesis) in the microbiome.

Viruses

Viruses in the human microbiome have also been understudied and available information is limited (161); the majority of data are related primarily to disease and do not address the commensal virome (34, 40). The majority of viral reads in studies that have been performed cannot be assigned to a known group; this has contributed to the difficulties associated with assessing their roles in the GI tract (124, 160). A number of teams have made extensive efforts in order to advance human virome studies (157, 161). In the last ten years, the number of identified polyomaviruses has increased from 4 to 13 species (some that cause disease and some that do not) (47), and the accuracy of identification techniques has been improved to identify taxa at the genus level (199) and use metagenomic information for viral taxonomy (172). Viral communities are mainly comprised of bacteria-infecting phage families (~90%), while eukaryotic viruses (~10%) are

in lower abundance (157, 161). Metagenomic analyses have suggested that the new bacteriophage, crAssphage associated with *Bacteroides*, is potentially common in humans (53). The greatest diversity of phages is considered to occur in infants and decreases with age, in contrast to increases in bacterial diversity (116, 117, 162). With the availability of methods to enrich viruses in samples (41), and with more metagenomic sequences and bioinformatics tools to identify viral sequences (53, 139), more information will be obtained on viral diversity and associated physiological factors in humans.

Similar to the microbiota, considerable variability appears to exist in the viral taxa found among subjects (133). Limited information is currently available on the functional roles of most viruses in the human GI tract. However, some possible functions are: to increase bacterial fitness as sources of genetic information (*e.g.*, the source of antibiotic resistance genes), to increase the immunity of bacteria or the human host, and to protect against pathogens (40, 64, 157). The general consensus is that the presence of bacteria is beneficial for viruses that are increasingly trying to evade the immune system. This relationship may also be beneficial to bacteria as viruses may be sources of potentially advantageous genes (resistance or tolerance to stress environments). Researchers are now examining the ecological and evolutionary influences of phages on bacterial ecosystems (102), and the findings obtained may provide insights into the important roles played by phages in the gut microbiome.

The GI tract

Many challenges are associated with studying the microbial ecology of the GI tract because it is composed of chemically and physically diverse microhabitats stretching from the esophagus to the rectum, providing a surface area of 150–200 m^2 for colonization or transient occupation by microbes (16). The adult GI tract was initially estimated to harbor 10^{14} bacteria, 10 times more cells than the human body (16, 120); however, a more recent calculation estimates there to be 10^{13} bacteria, which is equivalent to the number of human cells (170). Lower bacterial numbers (10^3 to 10^4 bacteria mL^{-1} of intestinal content) are found in the upper end of the GI tract, stomach, and small intestine, in which pH is low and the transit time is short (16). The highest biodiversity (richness and evenness) of bacteria (10^{10}–10^{11} bacteria g^{-1} of intestinal content) is in the colon, in which cell turnover rate is low, redox potential is low, and the transit time is long. This section highlights the different functions and associated microbiota along the human GI tract starting from the oral cavity, then the esophagus, stomach, and intestines (Fig. 1).

The oral cavity. Activity in the mouth may have a large impact on the further digestion of food in the lower GI tract. Food is mechanically ground into small particles, typically 0.1 mm, which increases the surface area. The oral microbiome is composed of transient and commensal populations that often form biofilms on soft and hard surfaces in the mouth (8). The most up-to-date information on taxa of the oral microbiome may be found in the Human Oral Microbiome Database (HOMD, http://www.homd.org/) (50). Information in this database is limited to *Bacteria* and one *Archaea*. Cultivation-independent analyses indicate that the most common genus is *Streptococcus*, while other genera include *Neisseria*, *Gemella*, *Granulicatella*, and *Veillonella*, but not in all individuals examined (1, 91, 92, 107). The taxa present appear to be dependent on interactions between microbes within the community. For example, using a graph theory-based algorithm of an organism's nutritional profile, the species *Streptococcus oralis* and *S. gordonii* have low metabolic complementarity and high metabolic competition, indicating they are antagonistic to each other (110). In contrast, *Porphyromonas gingivalis* was shown to have high metabolic complementarity, indicating its ability to grow symbiotically with diverse oral microbiota taxa. This computational method was tested and confirmed with growth assays, making it a viable means to assess the ability of species to inhabit the same environment. This has also been shown using an *in situ* spectral analysis of microbiota in biofilm plaques. Biofilms were shown to be composed of a number of taxa with *Corynebacterium* at the foundation (209). The other taxa are considered to play complementary roles driven by the environmental and chemical gradients formed in biofilms that control nutrient availability. These findings indicate that, despite the large number of taxa identified in oral microbiome studies, the core taxa of all microbiota may be identified in the future based on spatial locations and functional roles (10).

Similar to *Bacteria*, large variations have been noted in viruses found in the oral cavity among subjects (151). Most viruses are bacteriophages (approx. 99% of known sequences). Viral communities are reproducible across time points within a subject, suggesting that they are stable; however, the human and bacterial host significantly influence compositions (2, 151, 163). In addition to interactions among oral bacteria, many may associate with phages (57). Depending on the host range of the oral virome, this may make phages very common inhabitants of the oral cavity. Furthermore, in addition to survival within bacterial hosts, phages may also survive in the oral mucosa and contribute to host immunity (11). These are all new avenues of oral virome research that will likely be investigated in greater depth in the future.

In addition to the bacterial microbiome, two cultivation-independent studies have been conducted on oral fungi. Approximately 100 fungal species (20 genera) were detected in one study of the oral mycobiome of healthy individuals (68). Among the fungi detected, *Candida* species were the most common and abundant, while the other genera consisted of *Cladosporium*, *Aureobasidium*, *Saccharomycetales*, *Aspergillus*, *Fusarium*, and *Cryptococcus*. Most of these genera were also detected in a recent study on three subjects; however, *Malassezia*, a skin pathogen, accounted for the most sequence reads (52). Most of the other studies conducted on the oral mycobiome have focused on the role of fungi in disease (69, 136). Since the oral microbial community is directly exposed to the environment, the presence of a dynamic and transient community is expected, but warrants further study.

Esophagus. After swallowing, food is transported down the esophagus by peristalsis to the stomach. Limited information is available on microbes inhabiting the esophagus (5, 91, 147), and this may be due to the difficulties associated with obtaining samples because biopsies have typically been used. However, a less invasive method using an esophageal string has recently been demonstrated to be a feasible alternative

and yields similar findings to non-cultivation-based analyses of biopsies (60). Similar to the oral cavity, the most common genus found in the esophagus is *Streptococcus*; however, an overall comparison of the two communities has indicated that the number of taxa significantly differ between the two locations (15, 60). Among the few studies conducted on the viral and fungal microbiota of the esophagus, the focus has been on association with disease (204) and none of the pathogenic taxa inhabit healthy individuals.

Stomach. The stomach is the first digestive organ in the body (89). It holds food and mechanically mixes it with proteolytic enzymes and gastric acids that aid in the breakdown and subsequent absorption of nutrients. The growth of many common bacteria is inhibited by these acidic conditions (pH<4), making this a unique community with the lowest number of microbes, ranging between 10^1 and 10^3 CFU g^{-1}. In addition to digestion, the acidic conditions of the stomach are considered to have evolved as a means of protection from pathogens. This hypothesis is supported by the recent finding of a lower pH in the stomachs of scavengers and higher pH in herbivores, which are less likely to encounter pathogens in their food (13). Caution is needed when comparing the findings of various studies throughout the GI tract because gastric juice has a lower pH than the mucosal layer, resulting in differences in the microbiota present (89).

Despite the low pH, non-cultivation-based analyses on stomach biopsies revealed a more diverse microbiota than expected (5, 20, 115). Regardless of variations among subjects, there appears to be two major groups of individuals: those with and without *Helicobacter pylori* (20). There is a third subset in which *H. pylori* is present in lower proportions in some individuals that were negative using conventional testing. Microbiomes dominated by *H. pylori* had significantly greater proportions of the phylum *Proteobacteria*, of which it is a member, and lower alpha diversity (5, 20). Other common genera are *Streptococcus* and *Prevotella*, both of which are also found in the oral and esophageal communities; however, the communities at these locations appear to differ (5). Limited information is available on fungi analyzed in biopsy samples; although a cultivation study detected *Candida* species, this appeared to be associated more with disease (224). The major interaction currently studied in the stomach microbiota is with *Helicobacter* because of its association with gastritis, peptic ulcers, and gastric cancer. However, this taxon has been suggested to be beneficial for health, leading some to question whether the complete eradication of this microbe is the best option (67, 89).

In contrast, less information is available on the microbiome of stomach fluids; it appears to harbor fewer *Helicobacter* and an analysis of transcripts indicated that *Actinobacteria* are the most active phylum; however, the other major phyla, *Firmicutes*, *Bacteroidetes*, and *Proteobacteria*, are also present (197). In the same study, it also appeared to harbor novel fungi; 77.5% of the ITS reads were not identified at the phylum level or lower. *Candida* and *Phialemonium* were the only two identifiable fungal genera in all subjects tested, whereas an additional 66 genera were present in at least one of the nine subjects examined. Based on the infrequency and number of reads in this analysis, most of the taxa identified in stomach fluids appear to be transient, and those playing an active role are limited in this location.

Intestines. After mixing in the stomach, chime slowly passes through the pyloric sphincter and enters the intestines, in which the major digestion and absorption of nutrients begin (12). Humans have a small and large intestine. The small intestine, the main location in which food digestion and absorption occurs, is further divided into three parts, the duodenum, jejunum, and ileum. The duodenum, in which food chime enters from the stomach, is directly associated with digestion and is linked to the pancreas and gallbladder. Bile salts from the gallbladder and enzymes from the pancreas enter the duodenum and mix with stomach chime in order to start the digestion process. The epithelium in the jejunum and ileum is responsible for glucose absorption into the bloodstream via glucose transporters and sodium ions. The small intestine is followed by the large intestine (colon), which has a larger diameter, but shorter length and is divided into four sections: the ascending colon (cecum), transverse colon, descending colon, and sigmoid colon (123). Water and minerals are continuously absorbed along the colon before excretion. Furthermore, complex foods that cannot be digested by the host are used as growth substrates for the colonic microbiota (25, 178).

Spatial and temporal variabilities have been noted in the microbial composition among the different intestinal structures based on their functional roles and timing of food intake (18, 129, 186). Although spatial variability exists along the intestinal tract, the bacterial microbiome at the phylum level is considered to remain fairly stable over time (43, 155); however, many factors may affect its stability (119). Undigested food and most of the microbiota are found in the lumen, the central space surrounded by the mucosal layer of the tubular intestinal structure. The main absorption of growth substrates occurs through the epithelial cells of the mucosa, which also prevents the entry of the microbiota into host cells (174). A number of important host-microbe interactions occur within the mucosa. Energy from microbially produced metabolites, such as butyrate, contributes to epithelial metabolism (97). Most of the gut is anaerobic, but there is an oxygen gradient in the mucosa that provides a competitive advantage for facultative anaerobes (174). Recent studies have also shown the importance of metabolites produced by transkingdom microbiota to host physiology (185, 187, 188). Microbiota, such as *Akkermansia mucinophila*, are commonly found residing in the mucus layer and feed on mucin (39, 48). Therefore, the effects of host interactions with the gut microbiota, particularly those in the large intestine, have a prominent impact on overall human health, including energy reabsorption and immune system development.

Due to the difficulties associated with collecting multiple samples along a healthy human GI tract in order to capture the spatial heterogeneity of microbes in this environment, most studies use fecal samples as a surrogate. However, this limits the availability of regio-specific community information on the GI tract, resulting in portions, such as the small intestine, remaining poorly characterized. The few studies conducted on the small intestine have limited subject numbers because they used biopsy samples (4, 201, 203) or ileotomy patients (108, 195, 222). The bacterial genera most commonly found among these studies were *Clostridium*, *Streptococcus*, and *Bacteroides*. The number of studies that include fungi are

Table 1. Comparison of the anatomy of the intestinal tract in humans and animal models

	Human	Mouse	Rat	Pig
Stomach	Four regions: cardia, fundus, body, and pylorus	Three regions: forestomach, body, and pylorus	Three regions: forestomach, body, and pylorus	Four regions: esophagus, cardia, fundus, and pylorus
	pH 1.5 to 3.5	pH 3.0 to 4.0	pH 3.0 to 4.0	pH 1.5 to 2.5
Small intestine	5.5–6.4 m in length	350 mm in length	1,485 mm in length	1.2–2.1 m in length
	pH 6.4 to 7.3	pH 4.7 to 5.2	pH 5.0 to 6.1	pH 6.1 to 6.7
Cecum	Smaller than the colon	Larger than the colon	Larger than the colon	Smaller than the colon
	No fermentation	Main fermentation	Main fermentation	Some fermentation
	pH 5.7	pH 4.4 to 4.6	pH 5.9 to 6.6	pH 6.0 to 6.4
Appendix	Present	Absent	Absent	Absent
Colon	Divided into the ascending, transcending, and descending colon	Not divided	Not divided	Divided into the ascending, transcending, and descending colon
	Main fermentation	No fermentation	No fermentation	Main fermentation
	Thick mucosa	Thinner mucosa	Thinner mucosa	Thick mucosa
	pH 6.7	pH 4.4 to 5.0	pH 5.5 to 6.2	pH 6.1 to 6.6

Adapted from (59, 96, 128, 130, 137, 196)

even more limited, with the genera *Candida* and *Saccharomyces* being the most frequently detected (108, 114). Caution is also needed when extrapolating these findings to all individuals because the health of some subjects was compromised when samples were obtained.

Bacteria in the colon account for approximately 70% of all bacteria in the human body because it is the main site for the bacterial fermentation of non-digestible food components such as soluble fiber. The small number of studies that have examined microbial communities directly in the colon suggests that the bacterial composition is similar to that found in feces (86). However, fecal communities do not represent a single colonic environment, such as the mucosa (223), but a mixture of indigenous and transient microbes from the entire GI tract. In studies in which a global view of the GI tract microbial community is of interest, fecal material represents a good surrogate and is easily obtained, allowing for multiple samples to be obtained over short and long time periods from healthy individuals. The majority of microbiome reviews have extensively covered colonic communities using feces (74, 92, 121, 148, 189); therefore, we will not describe its composition in detail. However, later in this review, the impact of diet on the microbiome composition will be discussed. Furthermore, the above sections on fungi and viruses provide information on the taxa of these groups in the intestines.

Summary of the GI tract. The use of non-cultivation-based methods to investigate the microbiota in the GI tract has increased our knowledge of their diversity. One group that we neglected to mention in this review was *Protozoans*/*Protists*; however, recent reviews are available (79, 145). Despite representing a smaller biomass than fungi, they also appear to be important to the ecological structure of the gut microbiome. The predator-prey relationship they have with other microbiota (145) may, in some cases, lead to disease prevention (7). Difficulties are associated with elucidating the functional roles played by these various taxa at different points along the GI tract. Therefore, it is still important to obtain cultivated representatives to investigate their role and ecological significance along the GI tract. This consideration is important for all microbiota; however, it represents a larger issue for low diversity groups, such as fungi, which may not be numerically abundant, but still play a significant role (17).

Use of animal models

Animal models have been widely adopted in human gut microbiome research (28, 98, 220) to reduce confounding experimental factors such as genetics, age, and diet, which may be more easily controlled in laboratory animals. Additionally, animal models with modified genetic backgrounds are available for investigating potential mechanisms (137). Ideally, animal models with relatively similar genetic information (217), gut structures, metabolism (142), and diets and behavior patterns (202) to humans need to be selected. Comprehensive comparisons of mice (137) and pigs (217) to humans were recently conducted in order to aid in translating information from animal models to humans. In this section, we will highlight some of their findings and compare GI tract structures and microbial community compositions. Furthermore, some advantages and limitations associated with the use of animal models in human microbiome research will be discussed.

Similarities exist in the anatomy of the GI tract between humans and most animal models (Table 1). However, differences in anatomical structures and pH at different locations along the GI tract may contribute to differences in the microbiota found in humans versus animal models (26). The human colon also has a thicker mucosal layer than those of mice and rats (137), which may have an effect on the diversity of the microbiota colonizing the colon. Human gut bacteria are dominated by two phyla: *Firmicutes* and *Bacteroidetes* (189), which also dominate the GI tract of commonly used model animals (112). However, at lower taxonomic levels, some differences have been reported in microbiome compositions in the gut between humans and animal models (Table 2). The dominant taxa reported have varied as the number of comparisons performed has increased (137, 152); therefore, the findings shown in Table 2 need to be used cautiously.

A pig gut gene catalogue of metabolic function was recently developed and compared to catalogues available for humans and mice (217). They found that 96% of the KEGG orthologs in humans were also present in pigs, whereas the overlap at the gene level was markedly lower (9.46%). However, there was a greater overlap between humans and pigs than between humans and mice. Microbial activity also differs along the GI tract, with the most relevant being fermentation occurring in the ceca of most animal models, but

Table 2. Major taxa of the gut microbiota in humans and animal models

	Human	Mouse	Rat	Pig
Bacteria	*Firmicutes* *Bacteroidetes* *Actinobacteria* *Proteobacteria*	*Firmicutes* *Bacteroidetes*	*Firmicutes* *Bacteroidetes*	*Firmicutes* *Bacteroidetes*
Archaea	*Methanobrevibacter* *Nitrososphaera*	*Methanobrevibacter*	*Methanobrevibacter*	*Methanomicrobia*, *Methanosphaera*
Viruses	*Herpesviridae* *Papillomaviridae* *Polyomaviridae* *Adenoviridae*	Variable	Variable	*Picornaviridae* *Astroviridae* *Coronaviridae* *Caliciviridae*
Eukarya	*Candida* *Malassezia* *Saccharomyces* *Cladosporium*	*Ascomycota* *Basidiomycota* *Chytridiomycota* *Zygomycota*	*Ascomycota* *Basidiomycota* *Chytridiomycota* *Zygomycota*	*Kazachstania* *Candida* *Galactomyces* *Issatchenkia*

Adapted from (85, 103, 105, 112, 125, 137, 153, 154, 171, 179, 193, 194, 215, 216, 221)

not in humans (137). Strengths and weaknesses are associated with the major animal models being used, and these need to be taken into consideration when conducting translational research.

Rats. The use of rats as lab animals dates back to the 1850s. They were considered to be a good candidate for human microbiome research because the rat contains the same four dominant bacteria phyla in the GI tract (31), with *Firmicutes* (74%) and *Bacteroidetes* (23%) representing the largest proportions (221). The advantages of using rats in human microbiome research include quick reproduction, a fully sequenced genome, and easy handling and maintenance due to their relatively small size. The limitation of this model is that the diet used in rats differs from that for humans, and their behavior and living environment are also different, which will affect the gut microbiota. The diet used in rat studies is normal chow that is rich in fiber (205), and diet may rapidly alter gut microbiota diversity (46). Although most studies emphasize the impact of diet on the microbiota in the cecum and/or colon (feces), the oral cavity of rats has been used to clarify the impact of diet on the microbiome (93).

Mice. Many of the strengths and weaknesses associated with using rats are also applicable to mice. Similar to humans, the microbiota in the GI tract of mice is dominated by *Firmicutes* (74%) and *Bacteroidetes* (23%) at the phylum level (217). However, there are differences at the genus level, and this has led to the use of "humanized" mice. This is achieved by inoculating human gut microbiota into germ-free (GF) mice (192) or mice treated with antibiotics to eliminate their gut microbiome (83). The microbiome of these mice after fecal transplants may have a composition at the phyla level that is 100% similar to humans and 88% at the genus level (137). A recent study (175) used humanized mice to test microbiome diversity after feeding with poorly accessible carbohydrates, and found a similar reduction in OTU numbers to a human study (219). However, there are also some limitations to using these animals, including the diet and environmental living conditions. Furthermore, gnotobiotic mice may not reflect the human-microbe relationship due to their weaker immune system (6).

Approximately 10 years ago, Scupham (168) showed that all four major fungal phyla, *Ascomycota*, *Basidiomycota*, *Chytridiomycota*, and *Zygomycota*, were present in the murine gut. Additionally, many genera were identified, including *Acremonium*, *Monilinia*, *Fusarium*, *Cryptococcus*, *Filobasidium*, *Scleroderma*, *Catenomyces*, *Spizellomyces*, *Neocallimastix*, *Powellomyces*, *Entophlyctis*, *Mortierella*, and *Smittium*. When comparing these studies to the human gut, it is important to note that this study indicated a more diverse fungal community than those found in humans; the eukaryotic diversity of the human gut is low (143).

Pigs. Pigs have been used as surrogates for human microbiome research due to their highly similar genetics, physiological structures, behavior, metabolism, and immune functions to those of humans (81, 202). The greater similarities in the omnivorous diet and GI tract structure between pigs and humans are more advantageous than the murine model. The microbiome of pigs is dominated by two phyla: *Firmicutes* and *Bacteroidetes* (104); however, there are some notable differences at the genus level. The genus *Prevotella* was found to be common in two pig metagenomic studies (104, 118). Since the number of pigs used in most studies is less than humans, the pig core microbiome at the genus level may change as more pigs are studied. Another contributing factor to shaping the microbiome composition is diet. Most studies have found that the number of *Bifidobacteria* in pigs, even those on high fiber diets, is lower than that in humans (132, 218), while that of *Lactobacillus* is higher (149). In nutrition studies, humans and pigs are both dependent on the quality of the nutrient load; however, the pig cecum has a larger capacity to ferment indigestible compounds than the human cecum (54). The microbiota composition in pigs may differ from that in humans due in part to differences in diet (81). Similar to mice, humanized GF pigs have been developed and the microbiome after human fecal transplantation more closely resembles that of the donor than conventional pigs (144). However, the same disadvantages associated with using GF mice are also true for GF pigs.

The genome of pigs may be mutated to study human diseases; this is typically performed using miniature pigs such as those from the Ossabaw and Gottingen islands (146). Genetic mutations for metabolic syndrome and insulin resistance have successfully been performed using Ossabaw pigs to study human diseases such as type 2 diabetes (14, 177) and obesity (101). The ratio of *Firmicutes* to *Bacteroidetes* is higher in obese Ossabaw pigs than in lean pigs (146), similar to some

obese humans (111, 190). This finding suggests that Ossabaw pigs are a good model for researching the role of the microbiota in human obesity. However, disadvantages are associated with using miniature pigs, mainly the higher cost for maintenance and longer reproductive period than rodents (146).

Although more extensive efforts have been made to investigate fungi in pigs than in other animal models, many of these studies were cultivation-based or for use as probiotics. Fungi in pigs have been recently studied using a non-cultivation approach and up to 17 species of yeast (belonging to the genera *Kazachstania*, *Galactomyces*, *Candida*, *Issatchenkia*, *Pichia*, *Rhodotorula*, and *Trichosporon*) were common in the gut (194). The number of studies on viruses is limited, but the composition appears to be highly variable among samples (164, 171) and affected by disease (24). These groups need to be examined in more detail in order to establish whether pigs are good models for use in understanding fungi and viruses in humans.

Animal model summary. The convenience and cost of using animal models for human research are appealing. However, researchers need be very careful when selecting animal models appropriate for their objectives, particularly when the objective is to directly extrapolate findings from animals to humans, due to the significant differences in GI tract physiology and microbiome composition (65, 137, 217).

Diet in health

Many studies have found that diet is one of the main factors shaping the composition of gut microbial populations. Dietary approaches, such as the ingestion of non-digestible carbohydrates (prebiotics) and fermented food products containing live cultures (probiotics), have been suggested to confer health benefits by enhancing the growth of beneficial intestinal bacteria (100, 158). As described earlier, the microbiota may break down food components, such as non-digestible carbohydrates, which are indigestible by the host in order to aid in maximizing available nutrients (9) and produce metabolites that contribute to host health. Probiotics have been used as a means to replenish the gut with "beneficial" microbiota after antibiotic treatments or to treat diseases (82, 159). This section will highlight some studies that demonstrated the health benefits of prebiotics and probiotics and possible roles played by the microbiota.

Dietary prebiotics and probiotics. Non-digestible and fermentable food components are often consumed as prebiotics to selectively stimulate the growth and/or activity of endogenous colonic bacteria that may be beneficial to host health. The increased consumption of prebiotics often correlates with enhancements in certain bacterial genera (a common example is *Bifidobacterium* sp.); however, the reason they are beneficial remains unclear (208). Challenges are associated with elucidating the role being played by specific bacterial phylotypes because many of their processes are interactive (207). For example, SCFA produced by bacterial fermentation may lower intestinal pH, thereby increasing the solubility of essential minerals, such as calcium, iron, and magnesium, and consequently enhancing their absorption and improving health. Metabolites produced by microbes may also play an important role in cellular differentiation and proliferation in the colonic mucosa by inducing apoptosis and may confer protection against colitis and colorectal cancer by modulating oncogene expression. These functions do not appear to be performed by a single species; a number of different species may be acting independently or in combination. Research is leading to an understanding of microbial community structure and composition dynamics with respect to diet aids in establishing testable hypotheses for future research in health and beneficial microbes (32). Most research has been performed on the influence of beneficial intestinal bacteria such as *Bifidobacterium* spp. and *Lactobacillus* spp. on host health monitored using a cultivation approach. Cultivation-independent approaches have now become more popular, leading to the identification of new beneficial microbiota taxa and their potential functional roles in the gut as they relate to diet.

Dietary fibers and oligosaccharides are carbohydrate ingredients that vary in composition and structure, but are considered to be non-digestible because of the lack of appropriate intestinal enzymes to hydrolyze them or structural hindrances that prevent enzyme access in the gut. Although bacteria in the lower gut may ferment these carbohydrates, the rate and degree of fermentation vary with the polysaccharide (80). The range of fermentation in the colon for various fibers is broad, from approximately 5% for cellulose to nearly 100% for pectin (42). The resulting SCFA, including butyrate and propionate, are considered to reduce pH and solubilize minerals, thereby improving their absorption and subsequent utilization. Inulin, a long chain fructooligosaccharide (FOS) often obtained from chicory root, and FOS from other sources are the fibers that have been studied in the most detail (206). Several novel fibers have been tested in an *in vitro* large intestine model for their effects on the microbial stimulation and production of SCFA (122). All these novel fibers stimulated the growth of beneficial *Bifidobacteria* and some *Lactobacillus* species along with increases in SCFA production. Only a few studies have examined the effects of fibers and resistant starches on the human microbiome (87, 127, 198, 210, 211). A soluble corn fiber product has been demonstrated to increase Ca absorption in a number of different studies (210, 211). More benefits to human health may be attributed to the consumption of prebiotics and fermentation by the gut microbiome.

The number of studies that include diet effects on *Archaea*, *Fungi*, and/or *Viruses* are limited; however, some examples are included herein. Examinations of *Archaea*, *Fungi*, and *Bacteria* correlations in response to diet revealed a syntrophic model involving *Candida*, *Prevotella*, *Ruminococcus*, and *Methanobrevibacter* (85). *Candida* was considered to break down carbohydrates into metabolites used by *Prevotella* and *Ruminococcus* that produce CO_2 for *Methanobrevibacter* (85). However, shifts in carbon sources or breaking down starches via amylases from the human mouth may alter this relationship because *Prevotella* may no longer be dependent on *Candida*. This is a good example of how *Archaea*, which represent a very small portion of the microbiome, are a key contributor to methanogenesis and waste decomposition. The absence of *Archaea* may have severe effects on the surrounding community as hydrogen, glucose metabolites, and other carbon sources accumulate. Other organisms will eventually fill this niche, but may diminish or accumulate new metabolites that

ultimately shift the surrounding community based on their fitness for using these substrates.

A recent study investigated rapid changes in the microbiome composition when diets were either high in animal-based or plant-based fat and protein (46). The fungus *Candida* was found to increase in subjects placed on a plant-based diet, whereas *Penicillium* increased on animal-based diets. The most commonly found fungi in vegetarians were *Fusarium*, *Malassezia*, *Penicillium*, *Aspergillus*, and *Candida* (182). Caution is needed when interpreting findings because some of these fungi may be found on food prior to ingestion (46, 78, 182)

Phages assembled in the gut may also be modified by diet. A recent study examined changes in the fecal viral community over an 8-d period in six subjects supplied different diets (134). Shotgun sequencing of virus-like particles revealed that interpersonal differences in the virome were the largest source of variations in this study. However, the virome of subjects whose diets were changed differed more than in those who maintained their normal diet. Although this is only one study with a few human subjects, studies using a mouse model and different dietary fats support these findings (88, 99). Collectively, these findings indicate that diet plays a key role in shaping the gut virome, and further research is needed in order to investigate interactions between diet and the virome.

Summary

Advances have been made in the last decade in our understanding of the role of the GI tract microbiome in human health. This review has highlighted changes and differences in the microbiome along the GI tract that are due to changes in physical, chemical, and biological interactions. Although extensive research has been conducted on *Bacteria* in fecal samples, the main kingdom inhabiting the gut, our knowledge is still insufficient, particularly in other regions of the GI tract. Furthermore, other groups (*Archaea*, *Fungi*, and *Viruses*) have not yet been investigated in adequate detail, demonstrating a real void in knowledge. This highlights that the basic ecology of microbiomes is important for gaining a greater understanding to improve human health and decrease disease. In order to achieve this goal, it is important to include all microbiota in studies and remain cognizant of the limitations associated with understanding the entire GI tract of humans despite challenges in sampling and cultivation. Furthermore, the use of appropriate animal models in mechanistic studies requires careful consideration.

References

1. Aas, J.A., B.J. Paster, L.N. Stokes, I. Olsen, and F.E. Dewhirst. 2005. Defining the normal bacterial flora of the oral cavity. J. Clin. Microbiol. 43:5721–5732.
2. Abeles, S.R., R. Robles-Sikisaka, M. Ly, A.G. Lum, J. Salzman, T.K. Boehm, and D.T. Pride. 2014. Human oral viruses are personal, persistent and gender-consistent. ISME J. 8:1753–1767.
3. Abubucker, S., N. Segata, J. Goll, *et al.* 2012. Metabolic reconstruction for metagenomic data and Its application to the human microbiome. PLoS Comput. Biol. 8:e1002358.
4. Ahmed, S., G.T. Macfarlane, A. Fite, A.J. McBain, P. Gilbert, and S. Macfarlane. 2007. Mucosa-associated bacterial diversity in relation to human terminal ileum and colonic biopsy samples. Appl. Environ. Microbiol. 73:7435–7442.
5. Andersson, A.F., M. Lindberg, H. Jakobsson, F. Bäckhed, P. Nyrén, and L. Engstrand. 2008. Comparative analysis of human gut microbiota by barcoded pyrosequencing. PLoS One 3:e2836.
6. Atarashi, K., T. Tanoue, K. Oshima, *et al.* 2013. T-reg induction by a rationally selected mixture of Clostridia strains from the human microbiota. Nature 500:232–236.
7. Audebert, C., G. Even, A. Cian, A. Loywick, S. Merlin, E. Viscogliosi, and M. Chabe. 2016. Colonization with the enteric protozoa *Blastocystis* is associated with increased diversity of human gut bacterial microbiota. Sci. Rep. 6:25255.
8. Avila, M., D.M. Ojcius, and Ö. Yilmaz. 2009. The oral microbiota: Living with a permanent guest. DNA Cell Biol. 28:405–411.
9. Backhed, F., R.E. Ley, J.L. Sonnenburg, D.A. Peterson, and J.I. Gordon. 2005. Host-bacterial mutualism in the human intestine. Science 307:1915–1920.
10. Baker, J.L., B. Bor, M. Agnello, W.Y. Shi, and X.S. He. 2017. Ecology of the oral microbiome: Beyond bacteria. Trends Microbiol. 25:362–374.
11. Barr, J.J., R. Auro, M. Furlan, *et al.* 2013. Bacteriophage adhering to mucus provide a non-host-derived immunity. Proc. Natl. Acad. Sci. U.S.A. 110:10771–10776.
12. Barrett, K.E. 2014. Gastrointestinal Physiology, 2nd ed. Lange Medical Books/McGraw-Hill.
13. Beasley, D.E., A.M. Koltz, J.E. Lambert, N. Fierer, and R.R. Dunn. 2015. The evolution of stomach acidity and is relevance to the human microbiome. PLoS One 10:e.0134116.
14. Bellinger, D.A., E.P. Merricks, and T.C. Nichols. 2006. Swine models of type 2 diabetes mellitus: Insulin resistance, glucose tolerance, and cardiovascular complications. ILAR J. 47:243–258.
15. Benitez, A.J., C. Hoffmann, A.B. Muir, K.K. Dods, J.M. Spergel, F.D. Bushman, and M.-L. Wang. 2015. Inflammation-associated microbiota in pediatric eosinophilic esophagitis. Microbiome 3:23.
16. Berg, R.D. 1996. The indigenous gastrointestinal microflora. Trends Microbiol. 4:430–435.
17. Berrilli, F., D. Di Cave, S. Cavallero, and S. D'Amelio. 2012. Interactions between parasites and microbial communities in the human gut. Front. Cell. Infect. Microbiol. 2:141.
18. Biggs, M.B., G.L. Medlock, T.J. Moutinho, H.J. Lees, J.R. Swann, G.L. Kolling, and J.A. Papin. 2017. Systems-level metabolism of the altered Schaedler flora, a complete gut microbiota. ISME J. 11:426–438.
19. Bik, E.M. 2009. Composition and function of the human-associated microbiota. Nutr. Rev. 67:S164–S171.
20. Bik, E.M., P.B. Eckburg, S.R. Gill, K.E. Nelson, E.A. Purdom, F. Francois, G. Perez-Perez, M.J. Blaser, and D.A. Relman. 2006. Molecular analysis of the bacterial microbiota in the human stomach. Proc. Natl. Acad. Sci. U.S.A. 103:732–737.
21. Bik, E.M., C.D. Long, G.C. Armitage, *et al.* 2010. Bacterial diversity in the oral cavity of 10 healthy individuals. ISME J. 4:962–974.
22. Blaser, M.J. 2016. Antibiotic use and its consequences for the normal microbiome. Science 352:544–545.
23. Blaut, M., M.D. Collins, G.W. Welling, J. Dore, J. van Loo, and W. de Vos. 2002. Molecular biological methods for studying the gut microbiota: the EU human gut flora project. Brit. J. Nutr. 87:S203–S211.
24. Blomstrom, A.L., C. Fossum, P. Wallgren, and M. Berg. 2016. Viral metagenomic analysis displays the co-infection situation in healthy and PMWS affected pigs. PLoS One 11:e0166863.
25. Bolam, D.N., and J.L. Sonnenburg. 2011. Mechanistic insight into polysaccharide use within the intestinal microbiota. Gut microbes 2:86–90.
26. Booijink, C., E.G. Zoetendal, M. Kleerebezem, and W.M. de Vos. 2007. Microbial communities in the human small intestine: coupling diversity to metagenomics. Fut. Microbiol. 2:285–295.
27. Borrel, G., H.M. Harris, W. Tottey, *et al.* 2012. Genome sequence of "Candidatus *Methanomethylophilus alvus*" Mx1201, a methanogenic archaeon from the human gut belonging to a seventh order of methanogens. J. Bacteriol. 194:6944–6945.
28. Bowey, E., H. Adlercreutz, and I. Rowland. 2003. Metabolism of isoflavones and lignans by the gut microflora: a study in germ-free and human flora associated rats. Food Chem. Toxicol. 41:631–636.
29. Breitbart, M., I. Hewson, B. Felts, J.M. Mahaffy, J. Nulton, P. Salamon, and F. Rohwer. 2003. Metagenomic analyses of an uncultured viral community from human feces. J. Bacteriol. 185:6220–6223.

30. Breitbart, M., M. Haynes, S. Kelley, *et al.* 2008. Viral diversity and dynamics in an infant gut. Res. Microbiol. 159:367–373.
31. Brooks, S.P.J., M. McAllister, M. Sandoz, and M.L. Kalmokoff. 2003. Culture-independent phylogenetic analysis of the faecal flora of the rat. Can. J. Microbiol. 49:589–601.
32. Brownawell, A.M., W. Caers, G.R. Gibson, C.W.C. Kendall, K.D. Lewis, Y. Ringel, and J.L. Slavin. 2012. Prebiotics and the health benefits of fiber: Current regulatory status, future research, and goals. J. Nutr. 142:962–974.
33. Cadwell, K. 2015. Expanding the role of the virome: Commensalism in the gut. J. Virol. 89:1951–1953.
34. Cadwell, K. 2015. The virome in host health and disease. Immunity 42:805–813.
35. Cavalcanti, I.M.G., A.H. Nobbs, A.P. Ricomini, H.F. Jenkinson, and A.A.D. Cury. 2016. Interkingdom cooperation between *Candida albicans*, *Streptococcus oralis* and *Actinomyces oris* modulates early biofilm development on denture material. Pathog. Dis. 74:ftw002.
36. Charbonneau, M.R., L.V. Blanton, D.B. DiGiulio, D.A. Relman, C.B. Lebrilla, D.A. Mills, and J.I. Gordon. 2016. A microbial perspective of human developmental biology. Nature 535:48–55.
37. Cho, I., and M.J. Blaser. 2012. The human microbiome: at the interface of health and disease. Nat. Rev. Genet. 13.
38. Claesson, M.J., O. O'Sullivan, Q. Wang, J. Nikkilä, J.R. Marchesi, H. Smidt, W.M. de Vos, R.P. Ross, and P.W. O'Toole. 2009. Comparative analysis of pyrosequencing and a phylogenetic microarray for exploring microbial community structures in the human distal intestine. PLoS ONE 4:e6669.
39. Collado, M.C., M. Derrien, E. Isolauri, W.M. de Vos, and S. Salminen. 2007. Intestinal Integrity and *Akkermansia muciniphila*, a mucin-degrading member of the intestinal microbiota present in infants, adults, and the elderly. Appl. Environ. Microbiol. 73:7767–7770.
40. Columpsi, P., P. Sacchi, V. Zuccaro, S. Cima, C. Sarda, M. Mariani, A. Gori, and R. Bruno. 2016. Beyond the gut bacterial microbiota: The gut virome. J. Med. Virol. 88:1467–1472.
41. Conceição-Neto, N., M. Zeller, H. Lefrère, *et al.* 2015. Modular approach to customise sample preparation procedures for viral metagenomics: a reproducible protocol for virome analysis. Sci. Rep. 5:16532.
42. Cook, S.I., and J.H. Sellin. 1998. Review article: short chain fatty acids in health and disease. Ailment Pharmacol. Ther. 12:499–507.
43. Costello, E.K., C.L. Lauber, M. Hamady, N. Fierer, J.I. Gordon, and R. Knight. 2009. Bacterial community variation in human body habitats across space and time. Science 326:1694–1697.
44. Cui, L., A. Morris, and E. Ghedin. 2013. The human mycobiome in health and disease. Genome Med. 5:63.
45. Dalmasso, M., C. Hill, and R.P. Ross. 2014. Exploiting gut bacteriophages for human health. Trends Microbiol. 22:399–405.
46. David, L.A., C.F. Maurice, R.N. Carmody, *et al.* 2014. Diet rapidly and reproducibly alters the human gut microbiome. Nature 505:559–563.
47. DeCaprio, J.A., and R.L. Garcea. 2013. A cornucopia of human polyomaviruses. Nat. Rev. Microbiol. 11:264–276.
48. Derrien, M., E.E. Vaughan, C.M. Plugge, and W.M. de Vos. 2004. *Akkermansia muciniphila* gen. nov., sp nov., a human intestinal mucin-degrading bacterium. Internat. J. Syst. Evol. Microbiol. 54:1469–1476.
49. Dethlefsen, L., S. Huse, M.L. Sogin, and D.A. Relman. 2008. The pervasive effects of an antibiotic on the human gut microbiota, as revealed by deep 16S rRNA sequencing. PLoS Biol. 6:e280.
50. Dewhirst, F.E., T. Chen, J. Izard, B.J. Paster, A.C.R. Tanner, W.-H. Yu, A. Lakshmanan, and W.G. Wade. 2010. The human oral microbiome. J. Bacteriol. 192:5002–5017.
51. Dridi, B., D. Raoult, and M. Drancourt. 2011. Archaea as emerging organisms in complex human microbiomes. Anaerobe 17:56–63.
52. Dupuy, A.K., M.S. David, L. Li, T.N. Heider, J.D. Peterson, E.A. Montano, A. Dongari-Bagtzoglou, P.I. Diaz, and L.D. Strausbaugh. 2014. Redefining the human oral mycobiome with improved practices in amplicon-based taxonomy: Discovery of *Malassezia* as a prominent commensal. PLoS One 9:e90899.
53. Dutilh, B.E., C.W. Noriko, K. McNair, *et al.* 2014. A highly abundant bacteriophage discovered in the unknown sequences of human faecal metagenomes. Nat. Commun. 5:4498.
54. Eberhard, M., U. Hennig, S. Kuhla, R.M. Brunner, B. Kleessen, and C.C. Metges. 2007. Effect of inulin supplementation on selected gastric, duodenal, and caecal microbiota and short chain fatty acid pattern in growing piglets. Arch. Animal Nutr. 61:235–246.
55. Eckburg, P.B., P.W. Lepp, and D.A. Relman. 2003. Archaea and their potential role in human disease. Infect. Immun. 71:591–596.
56. Eckburg, P.B., E.M. Bik, C.N. Bernstein, E. Purdom, L. Dethlefsen, M. Sargent, S.R. Gill, K.E. Nelson, and D.A. Relman. 2005. Diversity of the human intestinal microbial flora. Science 308:1635–1638.
57. Edlund, A., T.M. Santiago-Rodriguez, T.K. Boehm, and D.T. Pride. 2015. Bacteriophage and their potential roles in the human oral cavity. J. Oral Microbiol. 7:27423.
58. Egert, M., A.A. de Graaf, H. Smidt, W.M. de Vos, and K. Venema. 2006. Beyond diversity: functional microbiomics of the human colon. Trends Microbiol. 14:86.
59. Fallingborg, J., L.A. Christensen, M. Ingeman-Nielsen, B.A. Jacobsen, K. Abildgaard, and H.H. Rasmussen. 1989. pH-profile and regional transit times of the normal gut measured by a radiotelemetry device. Aliment Pharmacol. Ther. 3:605–613.
60. Fillon, S.A., J.K. Harris, B.D. Wagner, *et al.* 2012. Novel device to sample the esophageal microbiome—The esophageal string test. PLoS One 7:e42938.
61. Fleet, J.C. 2006. Molecular regulation of calcium metabolism, p. 163–189. *In* C.M. Weaver and R.P. Heaney (ed.), Calcium in Human Health. Humana Press Inc., Totowa, NJ.
62. Fleet, J.C., and R.D. Schoch. 2010. Molecular mechanisms for regulation of intestinal calcium absorption by vitamin D and other factors. Crit. Rev. Clin.l Lab. Sci. 47:181–195.
63. Flint, H.J., S.H. Duncan, K.P. Scott, and P. Louis. 2007. Interactions and competition within the microbial community of the human colon: links between diet and health. Environ. Microbiol. 9:1101–1111.
64. Foca, A., M.C. Liberto, A. Quirino, N. Marascio, E. Zicca, and G. Pavia. 2015. Gut inflammation and immunity: What is the role of the human gut virome? Mediat. Inflamm. Article ID 326032.
65. Fritz, J.V., M.S. Desai, P. Shah, J.G. Schneider, and P. Wilmes. 2013. From meta-omics to causality: experimental models for human microbiome research. Microbiome 1:14.
66. Gaci, N., G. Borrel, W. Tottey, P.W. O'Toole, and J.-F. Brugère. 2014. Archaea and the human gut: New beginning of an old story. World J. Gastroenterol. 20:16062–16078.
67. Gagnaire, A., B. Nadel, D. Raoult, J. Neefjes, and J.-P. Gorvel. 2017. Collateral damage: insights into bacterial mechanisms that predispose host cells to cancer. Nat. Rev. Microbiol. 15:109–128.
68. Ghannoum, M.A., R.J. Jurevic, P.K. Mukherjee, F. Cui, M. Sikaroodi, A. Naqvi, and P.M. Gillevet. 2010. Characterization of the oral fungal microbiome (mycobiome) in healthy individuals. PLoS Pathog 6:e1000713.
69. Gholizadeh, P., H. Eslami, M. Yousefi, M. Asgharzadeh, M. Aghazadeh, and H.S. Kafil. 2016. Role of oral microbiome on oral cancers, a review. Biomed. Pharmacother. 84:552–558.
70. Gill, S.R., M. Pop, R.T. DeBoy, *et al.* 2006. Metagenomic analysis of the human distal gut microbiome. Science 312:1355–1359.
71. Gouba, N., D. Raoult, and M. Drancourt. 2014. Eukaryote culturomics of the gut reveals new species. PLoS One 9:e106994.
72. Gouba, N., and M. Drancourt. 2015. Digestive tract mycobiota: A source of infection. Med. Mal. Infect. 45:9–16.
73. Greenhalgh, K., K.M. Meyer, K.M. Aagaard, and P. Wilmes. 2016. The human gut microbiome in health: establishment and resilience of microbiota over a lifetime. Environ. Microbiol. 18:2103–2116.
74. Grice, E.A., and J.A. Segre. 2012. The human microbiome: Our second genome, p. 151–170. *In* A. Chakravarti and E. Green (ed.), Ann. Rev. Genom. Hum. Genet., vol. 13.
75. Grimaudo, N.J., W.E. Nesbitt, and W.B. Clark. 1996. Coaggregation of *Candida albicans* with oral Actinomyces species. Oral Microbiol. Immunol. 11:59–61.
76. Grimaudo, N.J., and W.E. Nesbitt. 1997. Coaggregation of *Candida albicans* with oral Fusobacterium species. Oral Microbiol. Immunol. 12:168–173.
77. Guarner, F., and J.-R. Malagelada. 2003. Gut flora in health and disease. The Lancet 361:512–519.
78. Hallen-Adams, H.E., S.D. Kachman, J. Kim, R.M. Legge, and I. Martínez. 2015. Fungi inhabiting the healthy human gastrointestinal tract: A diverse and dynamic community. Fung. Ecol. 15:9–17.

79. Hamad, I., D. Raoult, and F. Bittar. 2016. Repertory of eukaryotes (eukaryome) in the human gastrointestinal tract: Taxonomy and detection methods. Parasite Immunol. 38:12–36.
80. Hamaker, B.R., and Y.E. Tuncil. 2014. A perspective on the complexity of dietary fiber structures and their potential effect on the gut microbiota. J. Mol. Biol. 426:3838–3850.
81. Heinritz, S.N., R. Mosenthin, and E. Weiss. 2013. Use of pigs as a potential model for research into dietary modulation of the human gut microbiota. Nutr. Res. Rev. 26:191–209.
82. Hemarajata, P., and J. Versalovic. 2013. Effects of probiotics on gut microbiota: mechanisms of intestinal immunomodulation and neuromodulation. Therapeu. Adv. Gastroenterol. 6:39–51.
83. Hintze, K.J., J.E. Cox, G. Rompato, A.D. Benninghoff, R.E. Ward, J. Broadbent, and M. Lefevre. 2014. Broad scope method for creating humanized animal models for animal health and disease research through antibiotic treatment and human fecal transfer. Gut Microbes 5:183–191.
84. Hoarau, G., P.K. Mukherjee, C. Gower-Rousseau, *et al.* 2016. Bacteriome and mycobiome interactions underscore microbial dysbiosis in familial Crohn's disease. mBio 7:e01250-16.
85. Hoffmann, C., S. Dollive, S. Grunberg, J. Chen, H. Li, G.D. Wu, J.D. Lewis, and F.D. Bushman. 2013. Archaea and fungi of the human gut microbiome: Correlations with diet and bacterial residents. PLoS One 8:e66019.
86. Hold, G.L., S.E. Pryde, V.J. Russell, E. Furrie, and H.J. Flint. 2002. Assessment of microbial diversity in human colonic samples by 16S rDNA sequence analysis. FEMS Microbiol. Ecol. 39:33–39.
87. Hooda, S., B.M.V. Boler, M.C.R. Serao, J.M. Brulc, M.A. Staeger, T.W. Boileau, S.E. Dowd, G.C. Fahey, and K.S. Swanson. 2012. 454 Pyrosequencing reveals a shift in fecal microbiota of healthy adult men consuming polydextrose or soluble corn fiber. The J. Nutr. 142:1259–1265.
88. Howe, A., D.L. Ringus, R.J. Williams, Z.N. Choo, S.M. Greenwald, S.M. Owens, M.L. Coleman, F. Meyer, and E.B. Chang. 2016. Divergent responses of viral and bacterial communities in the gut microbiome to dietary disturbances in mice. ISME J. 10:1217–1227.
89. Hunt, R.H., M. Camilleri, S.E. Crowe, *et al.* 2015. The stomach in health and disease. Gut 64:1650–1668.
90. Huse, S.M., L. Dethlefsen, J.A. Huber, D. Mark Welch, D.A. Relman, and M.L. Sogin. 2008. Exploring microbial diversity and taxonomy using SSU rRNA hypervariable tag sequencing. PLoS Genet. 4:e1000255.
91. Huse, S.M., Y. Ye, Y. Zhou, and A.A. Fodor. 2012. A core human microbiome as viewed through 16S rRNA sequence clusters. PLoS ONE 7:e34242.
92. Huttenhower, C., D. Gevers, R. Knight, *et al.* 2012. Structure, function and diversity of the healthy human microbiome. Nature 486:207–214.
93. Hyde, E.R., B. Luk, S. Cron, *et al.* 2014. Characterization of the rat oral microbiome and the effects of dietary nitrate. Free Radic. Biol. Med. 77:249–257.
94. Iliev, I.D., V.A. Funari, K.D. Taylor, *et al.* 2012. Interactions between commensal fungi and the C-type lectin receptor dectin-1 Influence colitis. Science 336:1314–1317.
95. Jernberg, C., S. Lofmark, C. Edlund, and J.K. Jansson. 2010. Long-term impacts of antibiotic exposure on the human intestinal microbiota. Microbiol. 156:3216–3223.
96. Kararli, T.T. 1995. Comparison of the gastrointestinal anatomy, physiology, and biochemistry of humans and commonly used laboratory animals. Biopharm. Drug Dispos. 16:351–380.
97. Kelly, C.J., L. Zheng, E.L. Campbell, *et al.* 2015. Crosstalk between microbiota-derived short-chain fatty acids and intestinal epithelial HIF augments tissue barrier function. Cell Host Microbe 17:662–671.
98. Kibe, R., M. Sakamoto, H. Yokota, H. Ishikawa, Y. Aiba, Y. Koga, and Y. Benno. 2005. Movement and fixation of intestinal microbiota after administration of human feces to germfree mice. Appl. Environ. Microbiol. 71:3171–3178.
99. Kim, M.-S., and J.-W. Bae. 2016. Spatial disturbances in altered mucosal and luminal gut viromes of diet-induced obese mice. Environ. Microbiol. 18:1498–1510.
100. Kleerebezem, M., and E.E. Vaughan. 2009. Probiotic and gut Lactobacilli and Bifidobacteria: Molecular approaches to study diversity and activity. Ann. Rev. Microbiol. 63:269–290.
101. Koopmans, S.J., and T. Schuurman. 2015. Considerations on pig models for appetite, metabolic syndrome and obese type 2 diabetes: From food intake to metabolic disease. Eur. J. Pharmacol. 759:231–239.
102. Koskella, B., and M.A. Brockhurst. 2014. Bacteria–phage coevolution as a driver of ecological and evolutionary processes in microbial communities. FEMS Microbiol. Rev. 38:916–931.
103. Lam, V., J.D. Su, S. Koprowski, A.N. Hsu, J.S. Tweddell, P. Rafiee, G.J. Gross, N.H. Salzman, and J.E. Baker. 2012. Intestinal microbiota determine severity of myocardial infarction in rats. FASEB J. 26:1727–1735.
104. Lamendella, R., J.W.S. Domingo, S. Ghosh, J. Martinson, and D.B. Oerther. 2011. Comparative fecal metagenomics unveils unique functional capacity of the swine gut. BMC Microbiol. 11:103.
105. Lamendella, R., J.W. Santo Domingo, S. Ghosh, J. Martinson, and D.B. Oerther. 2011. Comparative fecal metagenomics unveils unique functional capacity of the swine gut. BMC Microbiol 11:103.
106. LaTuga, M.S., J.C. Ellis, C.M. Cotton, R.N. Goldberg, J.L. Wynn, R.B. Jackson, and P.C. Seed. 2011. Beyond bacteria: A study of the enteric microbial consortium in extremely low birth weight infants. PLoS ONE 6:e27858.
107. Lazarevic, V., K. Whiteson, S. Huse, D. Hernandez, L. Farinelli, M. Osteras, J. Schrenzel, and P. Francois. 2009. Metagenomic study of the oral microbiota by Illumina high-throughput sequencing. J. Microbiol. Meth. 79:266–271.
108. Leimena, M.M., J. Ramiro-Garcia, M. Davids, *et al.* 2013. A comprehensive metatranscriptome analysis pipeline and its validation using human small intestine microbiota datasets. BMC Genom. 14:530.
109. Lepp, P.W., M.M. Brinig, C.C. Ouverney, K. Palm, G.C. Armitage, and D.A. Relman. 2004. Methanogenic Archaea and human periodontal disease. Proc. Natl. Acad. Sci. U.S.A. 101:6176–6181.
110. Levy, R., and E. Borenstein. 2013. Metabolic modeling of species interaction in the human microbiome elucidates community-level assembly rules. Proc. Natl. Acad. Sci. U.S.A. 110:12804–12809.
111. Ley, R.E., P.J. Turnbaugh, S. Klein, and J.I. Gordon. 2006. Microbial ecology—Human gut microbes associated with obesity. Nature 444:1022–1023.
112. Ley, R.E., M. Hamady, C. Lozupone, *et al.* 2008. Evolution of mammals and their gut microbes. Science 320:1647–1651.
113. Li, M., B. Wang, M. Zhang, *et al.* 2008. Symbiotic gut microbes modulate human metabolic phenotypes. Proc. Natl. Acad. Sci. U.S.A. 105:2117–2122.
114. Li, Q., C. Wang, Q. Zhang, C. Tang, N. Li, B. Ruan, and J. Li. 2012. Use of 18S ribosomal DNA polymerase chain reaction–denaturing gradient gel electrophoresis to study composition of fungal community in 2 patients with intestinal transplants. Hum. Pathol. 43:1273–1281.
115. Li, X.-X., G.L.-H. Wong, K.-F. To, V.W.-S. Wong, L.H. Lai, D.K.-L. Chow, J.Y.-W. Lau, J.J.-Y. Sung, and C. Ding. 2009. Bacterial microbiota profiling in gastritis without *Helicobacter pylori* infection or non-steroidal anti-inflammatory drug use. PLoS One 4:e7985.
116. Lim, E.S., Y.J. Zhou, G.Y. Zhao, *et al.* 2015. Early life dynamics of the human gut virome and bacterial microbiome in infants. Nat. Med. 21:1228–1234.
117. Lim, E.S., D. Wang, and L.R. Holtz. 2016. The bacterial microbiome and virome milestones of infant development. Trends Microbiol. 24:801–810.
118. Looft, T., T.A. Johnson, H.K. Allen, *et al.* 2012. In-feed antibiotic effects on the swine intestinal microbiome. Proc. Natl. Acad. Sci. U.S.A. 109:1691–1696.
119. Lozupone, C.A., J.I. Stombaugh, J.I. Gordon, J.K. Jansson, and R. Knight. 2012. Diversity, stability and resilience of the human gut microbiota. Nature 489:220–230.
120. Luckey, T.D. 1972. Introduction to intestinal microecology Amer. J. Clin. Nutr. 25:1292–1294.
121. Lynch, S.V., and O. Pedersen. 2016. The human intestinal microbiome in health and disease. New Engl. J. Med. 375:2369–2379.
122. Maathuis, A., A. Hoffman, A. Evans, L. Sanders, and K. Venema. 2009. The effect of the undigested fraction of maize products on the activity and composition of the microbiota determined in a dynamic *in vitro* model of the human proximal large intestine. J. Am. Coll. Nutr. 28:657–666.

123. Macfarlane, G.T., and J.H. Cummings. 1991. The colonic flora, fermentation and large bowel digestive function. Raven Press, New York, N.Y.
124. Manrique, P., B. Bolduc, S.T. Walk, J. van der Oost, W.M. de Vos, and M.J. Young. 2016. Healthy human gut phageome. Proc. Natl. Acad. Sci. U.S.A. 113:10400–10405.
125. Mao, S.Y., C.F. Yang, and W.Y. Zhu. 2011. Phylogenetic analysis of methanogens in the pig feces. Curr. Microbiol. 62:1386–1389.
126. Mar Rodríguez, M., D. Pérez, F. Javier Chaves, *et al.* 2015. Obesity changes the human gut mycobiome. Sci. Rep. 5:14600.
127. Martinez, I., J. Kim, P.R. Duffy, V.L. Schlegel, and J. Walter. 2010. Resistant starches types 2 and 4 have differential effects on the composition of the fecal microbiota in human subjects. PLoS One 5:e15046.
128. McConnell, E.L., A.W. Basit, and S. Murdan. 2008. Measurements of rat and mouse gastrointestinal pH, fluid and lymphoid tissue, and implications for in-vivo experiments. J. Pharm. Pharmacol. 60:63–70.
129. McHardy, I.H., M. Goudarzi, M. Tong, *et al.* 2013. Integrative analysis of the microbiome and metabolome of the human intestinal mucosal surface reveals exquisite inter-relationships. Microbiome 1:17.
130. Merchant, H.A., E.L. McConnell, F. Liu, C. Ramaswamy, R.P. Kulkarni, A.W. Basit, and S. Murdan. 2011. Assessment of gastrointestinal pH, fluid and lymphoid tissue in the guinea pig, rabbit and pig, and implications for their use in drug development. Eur. J. Pharm. Sci. 42:3–10.
131. Mihajlovski, A., M. Alric, and J.-F. BrugËre. 2008. A putative new order of methanogenic Archaea inhabiting the human gut, as revealed by molecular analyses of the mcrA gene. Res. Microbiol. 159:516–521.
132. Mikkelsen, L.L., C. Bendixen, M. Jakobsen, and B.B. Jensen. 2003. Enumeration of bifidobacteria in gastrointestinal samples from piglets. Appl. Environ. Microbiol. 69:654–658.
133. Mills, S., F. Shanahan, C. Stanton, C. Hill, A. Coffey, and R.P. Ross. 2013. Movers and shakers: Influence of bacteriophages in shaping the mammalian gut microbiota. Gut Microbes 4:4–16.
134. Minot, S., R. Sinha, J. Chen, H.Z. Li, S.A. Keilbaugh, G.D. Wu, J.D. Lewis, and F.D. Bushman. 2011. The human gut virome: Inter-individual variation and dynamic response to diet. Genome Res. 21:1616–1625.
135. Mitsuoka, T. 1992. Intestinal flora and aging. Nutr. Rev. 50:438–446.
136. Mukherjee, P.K., J. Chandra, M. Retuerto, *et al.* 2014. Oral mycobiome analysis of HIV-infected patients: Identification of *Pichia* as an antagonist of opportunistic fungi. PLoS Pathog. 10:e1003996.
137. Nguyen, T.L.A., S. Vieira-Silva, A. Liston, and J. Raes. 2015. How informative is the mouse for human gut microbiota research? Dis. Mod. Mech. 8:1–16.
138. Nicholson, J.K., E. Holmes, and I.D. Wilson. 2005. Gut microorganisms, mammalian metabolism and personalized health care. Nat. Rev. Microbiol. 3:431–438.
139. Nielsen, H.B., M. Almeida, A.S. Juncker, *et al.* 2014. Identification and assembly of genomes and genetic elements in complex metagenomic samples without using reference genomes. Nat. Biotechnol. 32:822–828.
140. Noble, S.M., B.A. Gianetti, and J.N. Witchley. 2017. Candida albicans cell-type switching and functional plasticity in the mammalian host. Nat. Rev. Microbiol. 15:96–108.
141. O'Hara, A.M., and F. Shanahan. 2006. The gut flora as a forgotten organ. EMBO Rep. 7:688–693.
142. Odle, J., X. Lin, S.K. Jacobi, S.W. Kim, and C.H. Stahl. 2014. The suckling piglet as an agrimedical model for the study of pediatric nutrition and metabolism. Ann. Rev. Anim. Biosci. 2:419–444.
143. Ott, S.J., T. Kuhbacher, M. Musfeldt, *et al.* 2008. Fungi and inflammatory bowel diseases: Alterations of composition and diversity. Scand. J. Gastroenterol. 43:831–841.
144. Pang, X.Y., X.G. Hua, Q. Yang, D.H. Ding, C.Y. Che, L. Cui, W. Jia, P. Bucheli, and L.P. Zhao. 2007. Inter-species transplantation of gut microbiota from human to pigs. ISME J. 1:156–162.
145. Parfrey, L.W., W.A. Walters, and R. Knight. 2011. Microbial eukaryotes in the human microbiome: ecology, evolution, and future directions. Front. Microbiol. 2:153.
146. Pedersen, R., H.C. Ingerslev, M. Sturek, M. Alloosh, S. Cirera, B.O. Christoffersen, S.G. Moesgaard, N. Larsen, and M. Boye. 2013. Characterisation of gut microbiota in Ossabaw and Gottingen minipigs as models of obesity and metabolic syndrome. PLoS One 8:e 0056612.
147. Pei, Z.H., E.J. Bini, L.Y. Yang, M.S. Zhou, F. Francois, and M.J. Blaser. 2004. Bacterial biota in the human distal esophagus. Proc. Natl. Acad. Sci. U.S.A. 101:4250–4255.
148. Pflughoeft, K.J., and J. Versalovic. 2012. Human Microbiome in Health and Disease. Ann. Revi. Pathol. 7:99–122.
149. Pieper, R., P. Janczyk, A. Zeyner, H. Smidt, V. Guiard, and W.B. Souffrant. 2008. Ecophysiology of the developing total bacterial and *Lactobacillus* communities in the terminal small intestine of weaning piglets. Microb. Ecol. 56:474–483.
150. Pothoulakis, C. 2009. Review article: anti-inflammatory mechanisms of action of *Saccharomyces boulardii*. Alimen. Pharmacol. Therapeut. 30:826–833.
151. Pride, D.T., J. Salzman, M. Haynes, F. Rohwer, C. Davis-Long, R.A. White, III, P. Loomer, G.C. Armitage, and D.A. Relman. 2012. Evidence of a robust resident bacteriophage population revealed through analysis of the human salivary virome. ISME J. 6:915–926.
152. Qin, J., R. Li, J. Raes, *et al.* 2010. A human gut microbial gene catalogue established by metagenomic sequencing. Nature 464:59–65.
153. Qiu, X.Y., F. Zhang, X. Yang, N. Wu, W.W. Jiang, X. Li, X.X. Li, and Y.L. Liu. 2015. Changes in the composition of intestinal fungi and their role in mice with dextran sulfate sodium-induced colitis. Sci. Rep. 5:10416.
154. Queipo-Ortuno, M.I., L.M. Seoane, M. Murri, M. Pardo, J.M. Gomez-Zumaquero, F. Cardona, F. Casanueva, and F.J. Tinahones. 2013. Gut microbiota composition in male rat models under different nutritional status and physical activity and its association with serum leptin and ghrelin levels. PLoS One 8:e65465.
155. Rajilic-Stojanovic, M., H.G.H.J. Heilig, S. Tims, E.G. Zoetendal, and W.M. de Vos. 2013. Long-term monitoring of the human intestinal microbiota composition. Environ. Microbiol. 15:1146–1159.
156. Rajilic-Stojanovic, M., and W.M. de Vos. 2014. The first 1000 cultured species of the human gastrointestinal microbiota. FEMS Microbiol. Rev. 38:996–1047.
157. Rascovan, N., R. Duraisamy, and C. Desnues. 2016. Metagenomics and the human virome in asymptomatic individuals, p. 125–141. *In* S. Gottesman (ed.), Ann. Rev. Microbiol. 70:125–141.
158. Rastall, R.A., G.R. Gibson, H.S. Gill, F. Guarner, T.R. Klaenhammer, B. Pot, G. Reid, I.R. Rowland, and M.E. Sanders. 2005. Modulation of the microbial ecology of the human colon by probiotics, prebiotics and synbiotics to enhance human health: An overview of enabling science and potential applications. FEMS Microbiol. Ecol. 52:145.
159. Rauch, M., and S.V. Lynch. 2012. The potential for probiotic manipulation of the gastrointestinal microbiome. Curr. Opin. Biotechnol. 23:192–201.
160. Reyes, A., M. Haynes, N. Hanson, F.E. Angly, A.C. Heath, F. Rohwer, and J.I. Gordon. 2010. Viruses in the faecal microbiota of monozygotic twins and their mothers. Nature 466:334–338.
161. Reyes, A., N.P. Semenkovich, K. Whiteson, F. Rohwer, and J.I. Gordon. 2012. Going viral: next-generation sequencing applied to phage populations in the human gut. Nat. Rev. Microbiol. 10:607–617.
162. Reyes, A., L.V. Blanton, S. Cao, *et al.* 2015. Gut DNA viromes of Malawian twins discordant for severe acute malnutrition. Proc. Natl. Acad. Sci. U.S.A. 112:11941–11946.
163. Robles-Sikisaka, R., M. Ly, T. Boehm, M. Naidu, J. Salzman, and D.T. Pride. 2013. Association between living environment and human oral viral ecology. ISME J. 7:1710–1724.
164. Sachsenroder, J., S.O. Twardziok, M. Scheuch, and R. Johne. 2014. The general composition of the faecal virome of pigs depends on age, but not on feeding with a probiotic bacterium. PLoS One 9:e88888.
165. Savage, D.C. 1977. Microbial ecology of gastrointestinal-tract. Ann. Revi. Microbiol. 31:107–133.
166. Scanlan, P.D., F. Shanahan, C. O'Mahony, and J.R. Marchesi. 2006. Culture-independent analyses of temporal variation of the dominant fecal microbiota and targeted bacterial subgroups in Crohn's Disease. J. Clin. Microbiol. 44:3980–3988.
167. Schwartz, S., I. Friedberg, I.V. Ivanov, *et al.* 2012. A metagenomic study of diet-dependent interaction between gut microbiota and host in infants reveals differences in immune response. Genome Biol. 13:r32.
168. Scupham, A.J., L.L. Presley, B. Wei, *et al.* 2006. Abundant and diverse fungal microbiota in the murine intestine. Appl. Environ. Microbiol. 72:793–801.
169. Seed, P.C. 2015. The Human Mycobiome. Cold Spring Harbor Perspectives in Medicine 5.

170. Sender, R., S. Fuchs, and R. Milo. 2016. Revised estimates for the number of human and bacteria cells in the body. PLoS Biol. 14:e1002533.
171. Shan, T.L., L.L. Li, P. Simmonds, C.L. Wang, A. Moeser, and E. Delwart. 2011. The fecal virome of pigs on a high-density farm. J. Virol. 85:11697–11708.
172. Simmonds, P., M.J. Adams, M. Benko, *et al.* 2017. Virus taxonomy in the age of metagenomics. Nat. Rev. Microbiol. 15:161–168.
173. Sogin, M.L., H.G. Morrison, J.A. Huber, D.M. Welch, S.M. Huse, P.R. Neal, J.M. Arrieta, and G.J. Herndl. 2006. Microbial diversity in the deep sea and the underexplored "rare biosphere". Proc. Natl. Acad. Sci. U.S.A. 103:12115–12120.
174. Sommer, F., and F. Bäckhed. 2016. Know your neighbor: Microbiota and host epithelial cells interact locally to control intestinal function and physiology. BioEssays 38:455–464.
175. Sonnenburg, E.D., S.A. Smits, M. Tikhonov, S.K. Higginbottom, N.S. Wingreen, and J.L. Sonnenburg. 2016. Diet-induced extinctions in the gut microbiota compound over generations. Nature 529:212–215.
176. Sonnenburg, J.L., and F. Backhed. 2016. Diet-microbiota interactions as moderators of human metabolism. Nature 535:56–64.
177. Spurlock, M.E., and N.K. Gabler. 2008. The development of porcine models of obesity and the metabolic syndrome. J. Nutr. 138:397–402.
178. Stephen, A.M., and J.H. Cummings. 1980. Mechanism of action of dietary fibre in the human colon. Nature 284:283–284.
179. Su, Y., G.R. Bian, Z.G. Zhu, H. Smidt, and W.Y. Zhu. 2014. Early methanogenic colonisation in the faeces of Meishan and Yorkshire piglets as determined by pyrosequencing analysis. Archaea 2014:547908.
180. Suau, A., R. Bonnet, M. Sutren, J.J. Godon, G.R. Gibson, M.D. Collins, and J. Dore. 1999. Direct analysis of genes encoding 16S rRNA from complex communities reveals many novel molecular species within the human gut. Appl. Environ. Microbiol. 65:4799–4807.
181. Suhr, M.J., and H.E. Hallen-Adams. 2015. The human gut mycobiome: pitfalls and potentials—a mycologist's perspective. Mycologia 107:1057–1073.
182. Suhr, M.J., N. Banjara, and H.E. Hallen-Adams. 2016. Sequence-based methods for detecting and evaluating the human gut mycobiome. Lett. Appl. Microbiol. 62:209–215.
183. Tannock, G.W. 2002. Exploring the relationships between intestinal microflora and inflammatory conditions of the human bowel and spine. Anton. Leeuw. Int. J. G. 81:529–535.
184. Tannock, G.W. 2008. Molecular analysis of the intestinal microflora in IBD. Mucosal Immunol. 1:S15–S18.
185. Thaiss, C.A., D. Zeevi, M. Levy, *et al.* 2014. Transkingdom control of microbiota diurnal oscillations promotes metabolic homeostasis. Cell 159:514–529.
186. Thaiss, C.A., D. Zeevi, M. Levy, E. Segal, and E. Elinav. 2015. A day in the life of the meta-organism: diurnal rhythms of the intestinal microbiome and its host. Gut Microbes 6:137–142.
187. Thaiss, C.A., M. Levy, T. Korem, *et al.* 2016. Microbiota diurnal rhythmicity programs host transcriptome oscillations. Cell 167: 1495–1510.e12.
188. Thaiss, C.A., N. Zmora, M. Levy, and E. Elinav. 2016. The microbiome and innate immunity. Nature 535:65–74.
189. The Human Microbiome Project Consortium. 2012. Structure, function and diversity of the healthy human microbiome. Nature 486:207–214.
190. Turnbaugh, P., R. Ley, M.A. Mahowald, V. Magrini, E.R. Mardis, and J. Gordon. 2006. An obesity-associated gut microbiome with increased capacity for energy harvest. Nature 444:1027–1131.
191. Turnbaugh, P.J., and J.I. Gordon. 2009. The core gut microbiome, energy balance and obesity. J. Physiol. 587:4153–4158.
192. Turnbaugh, P.J., V.K. Ridaura, J.J. Faith, F.E. Rey, R. Knight, and J.I. Gordon. 2009. The effect of diet on the human gut microbiome: A metagenomic analysis in humanized gnotobiotic mice. Sci. Trans. Med. 1:6ra14–6ra14.
193. Underhill, D.M., and L.D. Lliev. 2014. The mycobiota: interactions between commensal fungi and the host immune system. Nat. Rev. Immunol. 14:405–416.
194. Urubschurov, V., P. Janczyk, W.B. Souffrant, G. Freyer, and A. Zeyner. 2011. Establishment of intestinal microbiota with focus on yeasts of unweaned and weaned piglets kept under different farm conditions. FEMS Microbiol. Ecol. 77:493–502.
195. van den Bogert, B., O. Erkus, J. Boekhorst, M. de Goffau, E.J. Smid, E.G. Zoetendal, and M. Kleerebezem. 2013. Diversity of human small intestinal *Streptococcus* and *Veillonella* populations. FEMS Microbiol. Ecol. 85:376–388.
196. Vdoviaková, K., E. Petrovová, M. Maloveská, L. Krešáková, J. Teleky, M.Z.J. Elias, and D. Petrášová. 2016. Surgical anatomy of the gastrointestinal tract and its vasculature in the laboratory rat. Gastroenterol. Res. Pract. 2016, Article ID 2632368.
197. von Rosenvinge, E.C., Y. Song, J.R. White, C. Maddox, T. Blanchard, and W.F. Fricke. 2013. Immune status, antibiotic medication and pH are associated with changes in the stomach fluid microbiota. ISME J. 7:1354–1366.
198. Walker, A.W., J. Ince, S.H. Duncan, *et al.* 2011. Dominant and diet-responsive groups of bacteria within the human colonic microbiota. ISME J. 5:220–230.
199. Waller, A.S., T. Yamada, D.M. Kristensen, J.R. Kultima, S. Sunagawa, E.V. Koonin, and P. Bork. 2014. Classification and quantification of bacteriophage taxa in human gut metagenomes. ISME J. 8:1391–1402.
200. Wampach, L., A. Heintz-Buschart, A. Hogan, *et al.* 2017. Colonization and succession within the human gut microbiome by Archaea, Bacteria, and Microeukaryotes during the first year of life. Front. Microbiol. 8:738.
201. Wang, M., S. Ahrn, B. Jeppsson, and G. Molin. 2005. Comparison of bacterial diversity along the human intestinal tract by direct cloning and sequencing of 16S rRNA genes. FEMS Microbiol. Ecol. 54:219.
202. Wang, M., and S.M. Donovan. 2015. Human microbiota-associated swine: Current progress and future opportunities. ILAR J. 56:63–73.
203. Wang, X., S.P. Heazlewood, D.O. Krause, and T.H.J. Florin. 2003. Molecular characterization of the microbial species that colonize human ileal and colonic mucosa by using 16S rDNA sequence analysis. J. Appl. Microbiol. 95:508–520.
204. Wang, Z.K., Y.S. Yang, A.T. Stefka, G. Sun, and L.H. Peng. 2014. Review article: fungal microbiota and digestive diseases. Alimen. Pharmacol. Therapeu. 39:751–766.
205. Warden, C.H., and J.S. Fisler. 2008. Comparisons of diets used in animal models of high fat feeding. Cell Metabol. 7:277.
206. Weaver, C.M., L.D. McCabe, G.M. McCabe, R. Novotny, M.D. Van Loan, S.B. Going, C. Boushey, D.A. Savaiano, and V. Matkovic. 2005. Bone mineral and predictors of whole body, total hip, and lumbar spine for 740 early pubertal white, Hispanic, and Asian girls. J. Bone Miner. Res. 20:S314–S314.
207. Weaver, C.M., B.R. Martin, J.A. Story, I. Hutchinson, and L. Sanders. 2010. Novel fibers Increase bone calcium content and strength beyond efficiency of large intestine fermentation. J. Ag. Food Chem. 58:8952–8957.
208. Weaver, C.M., B.R. Martin, C.H. Nakatsu, *et al.* 2011. Galactooligosaccharides improve mineral absorption and bone properties in growing rats through gut fermentation. J. Ag. Food Chem. 59:6501–6510.
209. Welch, J.L.M., B.J. Rossetti, C.W. Rieken, F.E. Dewhirst, and G.G. Borisy. 2016. Biogeography of a human oral microbiome at the micron scale. Proc. Natl. Acad. Sci. U.S.A. 113:E791–E800.
210. Whisner, C.M., B.R. Martin, C.H. Nakatsu, G.P. McCabe, L.D. McCabe, M. Peacock, and C.M. Weaver. 2014. Soluble maize fibre affects short-term calcium absorption in adolescent boys and girls: a randomised controlled trial using dual stable isotopic tracers. Brit. J. Nutr. 112:446–456.
211. Whisner, C.M., B.R. Martin, C.H. Nakatsu, J.A. Story, C.J. MacDonald-Clarke, L.D. McCabe, G.P. McCabe, and C.M. Weaver. 2016. Soluble corn fiber increases calcium absorption associated with shifts in the gut microbiome: A randomized dose-response trial in free-living pubertal girls. Nutr. J. 146:1298–1306
212. Wilson, K., and R. Blitchington. 1996. Human colonic biota studied by ribosomal DNA sequence analysis. Appl. Environ. Microbiol. 62:2273–2278.
213. Woodmansey, E.J. 2007. Intestinal bacteria and ageing. J. Appl. Microbiol. 102:1178–1186.
214. Wright, C.J., L.H. Burns, A.A. Jack, C.R. Back, L.C. Dutton, A.H. Nobbs, R.J. Lamont, and H.F. Jenkinson. 2013. Microbial interactions in building of communities. Mol. Oral Microbiol. 28:83–101.
215. Wylie, K.M., K.A. Mihindukulasuriya, Y. Zhou, E. Sodergren, G.A. Storch, and G.M. Weinstock. 2014. Metagenomic analysis of double-stranded DNA viruses in healthy adults. BMC Biol. 12:71.
216. Xiao, L., Q. Feng, S. Liang, *et al.* 2015. A catalog of the mouse gut metagenome. Nat Biotechnol. 33:1103–1108.

217. Xiao, L., J. Estellé, P. Kiilerich, *et al.* 2016. A reference gene catalogue of the pig gut microbiome. Nat. Microbiol. 1:16161.
218. Yan, H., R. Potu, H. Lu, *et al.* 2013. Dietary fat content and fiber type modulate hind gut microbial community and metabolic markers in the pig. PLoS One 8:e59581.
219. Yatsunenko, T., F.E. Rey, M.J. Manary, *et al.* 2012. Human gut microbiome viewed across age and geography. Nature 486:222–227.
220. Zhang, Q., G. Widmer, and S. Tzipori. 2013. A pig model of the human gastrointestinal tract. Gut Microbes 4:193–200.
221. Zhu, Y.Y., H. Li, X.L. Xu, C.B. Li, and G.H. Zhou. 2016. The gut microbiota in young and middle-aged rats showed different responses to chicken protein in their diet. BMC Microbiol. 16:281.
222. Zoetendal, E.G., A. von Wright, T. Vilpponen-Salmela, K. Ben-Amor, A.D.L. Akkermans, and W.M. de Vos. 2002. Mucosa-associated bacteria in the human gastrointestinal tract are uniformly distributed along the colon and differ from the community recovered from feces. Appl. Environ. Microbiol. 68:3401–3407.
223. Zoetendal, E.G., J. Raes, B. van den Bogert, *et al.* 2012. The human small intestinal microbiota is driven by rapid uptake and conversion of simple carbohydrates. ISME J. 6:1415–1426.
224. Zwolinska-Wcislo, M., A. Budak, D. Trojanowska, J. Bogdal, and J. Stachura. 1998. Fungal colonization of the stomach and its clinical relevance. Mycoses 41:327–334.

Microbes and Environments

EDITORIAL BOARD (2022)

Editor-in-Chief

Ken Takai, *Japan Agency for Marine-Earth Science and Technology (JAMSTEC), Yokosuka, Japan*

Senior Editors

Koki Toyota, *Tokyo University of Agriculture and Technology, Koganei, Japan*
Shin Haruta, *Tokyo Metropolitan University, Hachioji, Japan*
Hiroyuki Futamata, *Shizuoka University, Hamamatsu, Japan*
Kazuhiko Narisawa, *Ibaraki University, Ami, Japan*
Kiwamu Minamisawa, *Tohoku University, Sendai, Japan*
Nobuhiko Nomura, *University of Tsukuba, Tsukuba, Japan*
Takuro Nunoura, *Japan Agency for Marine-Earth Science and Technology (JAMSTEC), Yokosuka, Japan*
Satoshi Ishii, *University of Minnesota, St. Paul, MN, USA*
Sen-Lin Tang, *Academia Sinica, Taipei, Taiwan*

Managing Editors

Yoshihiro Takaki (Online Submission System), *Japan Agency for Marine-Earth Science and Technology (JAMSTEC), Yokosuka, Japan*
Satoshi Nakagawa (Online Submission System), *Kyoto University, Kyoto, Japan*
Shigeto Otsuka (Online Submission System), *The University of Tokyo, Tokyo, Japan*
Takuro Nunoura (Treasurer), *Japan Agency for Marine-Earth Science and Technology (JAMSTEC), Yokosuka, Japan*
Hiroyuki Imachi (Business affairs/Manuscript Reception), *Japan Agency for Marine-Earth Science and Technology (JAMSTEC), Yokosuka, Japan*
Yuki Morono (Manuscript Reception), *Japan Agency for Marine-Earth Science and Technology (JAMSTEC), Nankoku, Japan*
Michinari Sunamura (Manuscript Reception), *The University of Tokyo, Tokyo, Japan*
Takashi Narihiro (Manuscript Edition), *National Institute of Advanced Industrial Science and Technology (AIST), Sapporo,Japan*
Satoko Shinozaki-Yabana (Manuscript Edition/Manuscript Reception), *National Institutes for Cultural Heritage, Tokyo, Japan*

Associate Editors

Yoshiteru Aoi, *Hiroshima University, Higashi-Hiroshima, Japan*
Chih-Yu Chiu, *Academia Sinica, Taipei, Taiwan*
Jang-Cheon Cho, *Inha University, Incheon, Korea*
Peter Dunfield, *University of Calgary, Calgary, Canada*
Craig Everroad, *NASA Ames Research Center, Moffett Field, CA, USA*
Manabu Fukui, *Hokkaido University, Sapporo, Japan*
Natsuko Hamamura, *Kyushu University, Fukuoka, Japan*
Yasufumi Hikichi, *Kochi University, Nankoku, Japan*
Shir-Ly Huang, *National Central University, Jhongli City, Taiwan*
Yuichi Hongoh, *Tokyo Institute of Technology, Tokyo, Japan*
Hiroyuki Imachi, *Japan Agency for Marine-Earth Science and Technology (JAMSTEC), Yokosuka, Japan*
Shun'ichi Ishii, *Japan Agency for Marine-Earth Science and Technology (JAMSTEC), Yokosuka, Japan*
Tsukasa Ito, *Gunma University, Kiryu, Japan*
Elena P. Ivanova, *Swinburne University of Technology, Melbourne, Australia*
Wataru Iwasaki, *The University of Tokyo, Tokyo, Japan*
Yasuhiro Kasahara, *Hokkaido University, Sapporo, Japan*
Takafumi Kataoka, *Fukui Prefectural University, Obama, Japan*
Junichi Kato, *Hiroshima University, Higashi-Hiroshima, Japan*
Yoshitomo Kikuchi, *National Institute of Advanced Industrial Science and Technology (AIST), Sapporo, Japan*
Hiroyuki Kimura, *Shizuoka University, Shizuoka, Japan*
Tomonori Kindaichi, *Hiroshima University, Higashi-Hiroshima, Japan*
Staffan Kjelleberg, *The University of New South Wales, Sydney, Australia*
Ken Kurokawa, *National Institute of Genetics, Mishima, Japan*
Mei-Chin Lai, *National Chung Hsing University, Taichung, Taiwan*
Shuang-Jiang Liu, *Institute of Microbiology Chinese Academy of Sciences (IMCAS), Beijing, China*
Wen-Tso Liu, *University of Illinois at Urbana-Champaign, Champaign, IL, USA*
Fumito Maruyama, *Hiroshima University, Higashi-Hiroshima, Japan*
Shawn McGlynn, *Tokyo Institute of Technology, Tokyo, Japan*
Keisuke Miyauchi, *Tohoku Gakuin University, Tagajo, Japan*
Ryo Miyazaki, *National Institute of Advanced Industrial Science and Technology (AIST), Tsukuba, Japan*
Keizo Nagasaki, *Kochi University, Kochi, Japan*
Yuji Nagata, *Tohoku University, Sendai, Japan*
Atsushi Nakabachi, *Toyohashi University of Technology, Toyohashi, Japan*
Satoshi Nakagawa, *Kyoto University, Kyoto, Japan*
Tatsunori Nakagawa, *Nihon University, Fujisawa, Japan*
Shin-ichi Nakano, *Kyoto University, Otsu, Japan*
Naohiro Noda, *National Institute of Advanced Industrial Science and Technology (AIST), Tsukuba, Japan*

This journal is partly subsidized by the Grant-in-Aid for Publication of Scientific Research Results from the Japan Society for the Promotion of Science (JSPS).

c/o Nakanishi Printing Co.
Shimodachiuri Ogawa Higashi Kamikyoku, Kyoto 602-8048, Japan TEL: +81–75–441–3155, FAX: +81–75–417–2050

Satoko Noda, *Ibaraki University, Mito, Japan*
Hideaki Nojiri, *The University of Tokyo, Tokyo, Japan*
Ryo Ohtomo, *Hokkaido Agricultural Research Center (NARO), Sapporo, Hokkaido*
Shin Okazaki, *Tokyo University of Agriculture and Technology, Fuchu, Japan*
Shigeto Otsuka, *The University of Tokyo, Tokyo, Japan*
Joonhong Park, *Yonsei University, Seoul, Korea*
Michael J. Sadowsky, *University of Minnesota, St. Paul, MN, USA*
Keishi Senoo, *The University of Tokyo, Tokyo, Japan*
Toru Shigematsu, *Niigata University of Pharmacy and Applied Sciences, Niigata, Japan*
Masaki Shintani, *Shizuoka University, Hamamatsu, Japan*
Satoru Suzuki, *Ehime University, Matsuyama, Japan*
Shino Suzuki, *Japan Aerospace Exploration Agency (JAXA), Sagamihara, Japan*
Mio Takeuchi, *National Institute of Advanced Industrial Science and Technology (AIST), Osaka, Japan*
Hideyuki Tamaki, *National Institute of Advanced Industrial Science and Technology (AIST), Tsukuba, Japan*
Akinori Yabuki, *Japan Agency for Marine-Earth Science and Technology (JAMSTEC), Yokosuka, Japan*
Naoko Yoshida, *Nagoya Institute of Technology, Nagoya, Japan*
Takashi Yoshida, *Kyoto University, Kyoto, Japan*
Susumu Yoshizawa, *The University of Tokyo, Tokyo, Japan*
Lian-Hui Zhang, *Institute of Molecular and Cell Biology, Proteos, Singapore*
Kazuhiko Saeki, *Nara Women's University, Nara, Japan*
Katsuharu Saito, *Shinshu University, Kamiina, Japan*
Shusei Sato, *Tohoku University, Sendai, Japan*
Masaru Usui, *Rakuno Gakuen University, Ebetsu, Japan*
Torahiko Okubo, *Hokkaido University, Sapporo, Japan*
Takayuki Wada, *Osaka City University, Osaka, Japan*
Masafumi Shimizu, *Gifu University, Gifu, Japan*
Tomoyasu Nishizawa, *Ibaraki University, Ami, Japan*
Rie Yatsunami, *Tokyo Institute of Technology, Yokohama, Japan*
Masaaki Konishi, *Kitami Institute of Technology, Kitami, Japan*
Satoshi Wakai, *Japan Agency for Marine-Earth Science and Technology (JAMSTEC), Yokosuka, Japan*

JAPANESE SOCIETY OF MICROBIAL ECOLOGY

President (2021–2022): Satoshi OKABE, Hokkaido University
Secretary/Treasurer (2021–2022): Mamoru OSHIKI, Hokkaido University
Business affairs (2021–2022): Tomonori KINDAICHI, Hiroshima University
Business affairs (2021–2022): Takashi NARIHIRO, National Institute of Advanced Industrial Science and Technology (AIST)
Business affairs (2021–2022): Hideomi ITO, National Institute of Advanced Industrial Science and Technology (AIST)
Treasurer (2021–2022): Tsukasa ITO, Gunma University
Treasurer (2021–2022): Shigeyuki KAKIZAWA, National Institute of Advanced Industrial Science and Technology (AIST)

JAPANESE SOCIETY OF SOIL MICROBIOLOGY

President (2021–2023): Masahiro SHISHIDO, Chiba University
Vice President (2021–2023): Koki TOYOTA, Tokyo University of Agriculture and Technology
Secretary (2021–2023): Naoto OGAWA, Shizuoka University
Treasurer (2021–2023): Reiko SAMESHIMA, Shizuoka University

TAIWAN SOCIETY OF MICROBIAL ECOLOGY

President (2020–2022): Chang-Ping YU, National Taiwan University
Vice President (2020–2022): Pi-Han WANG, Tunghai University
International Business Affairs (2020–2022): Shiu-Mei LIU, National Taiwan Ocean University
International Business Affairs (2020–2022): Shir-Ly HUANG, National Yang Ming Chiao Tung University
Secretary-General (2020–2022): Chien-Sen LIAO, I-Shou University

JAPANESE SOCIETY OF PLANT MICROBE INTERACTIONS

Chair of Society: Kiwamu MINAMISAWA, Tohoku University
Secretary-General: Shusei SATO, Tohoku University
Treasurer: Hisayuki MITSUI, Tohoku University
General affairs: Masayuki SUGAWARA, Obihiro University of Agriculture and Veterinary Medicine

JAPANESE SOCIETY FOR EXTREMOPHILES

President (2022–2023): Tairo OSHIMA, Kyowa-kako Co., Ltd
Vice President (2022–2023): Satoshi NAKAMURA, Tokyo Institute of Technology
Vice President (2022–2023): Yoshizumi ISHINO, Kyushu University